UNIVERSITY OF SOUTHERN QUEENSLAND

AUSTRALIA

BEHAVIOUR OF FILLED PULTRUDED GLASS FIBRE REINFORCED POLYMER TUBES UNDER AXIAL LOADING

A Thesis submitted by

Ali Umran Kadhum Alsaadi, M Eng.

For the Award of

Doctor of Philosophy

2019

Abstract

The use of fibre reinforced polymer (FRP) materials in civil engineering applications has been broadened as an alternative construction material due to their features such as high strength, stiffness-to-weight ratio and excellent durability characteristics in aggressive environments. They act as a non-corrosive reinforcement for concrete structures and as a permanent formwork. Pultruded FRP (PFRP) profiles are made in shapes similar to those are made of steel. The usage of pultruded FRP tube sections for column applications in civil infrastructure is not widespread. This is because their full capacity is not utilised due to low stiffness and buckling issues. To overcome this shortage in their axial compressive behaviour, it is necessary to study effects of tube shape, wall thickness, fibre orientation and layup using different sections. Examining effects of filler materials having different stiffness and simulate the axial behaviour using finite element method to study impacts of change in different parameters on the axial behaviour of pultruded FRP tubes are provided a comprehensive understanding about improving the stiffness and load capacity of pultruded FRP tube columns.

Firstly, the mechanical properties of different pultruded FRP tubes were calculated by conducting material tests. The results show that the mechanical properties of the pultruded FRP tubes rely mainly on the percentage of the fibre content and fibre orientation. Moreover, it provides an enhancing approach to the axial behaviour of the FRP columns. The basis of this approach is selection the appropriate fibre orientation and layup for the targeted applications for the best structural performance.

Secondly, the effect on the axial behaviour of PFRP tube columns due to different types of fillers was experimentally investigated. The results revealed that the stiffness and load carrying capacity of filled columns is increased as the modulus of infill concrete increases. It further shows that the degree of improvement depends on the properties of PFRP tube and concrete. The other important output is the axial behaviour after the peak load. The strength of the filled columns does not decrease sharply after the point of the peak load instead it declines gradually. The properties of infill concrete and transverse modulus of PFRP tube govern the rate of strength

reduction in the post-peak region of the load deflection curves and capacity of the energy absorption.

Thirdly, finite element simulation was performed to study the axial behaviour of the hollow and filled pultruded FRP columns. The simulation accuracy level was checked against the experimental results. The load-deflection curves, based on the lamina method, give a better agreement compared with the curves of the full-scale column tests. The numerical values of the load capacity also coincide well with those of the experimental tests. The importance of obtaining finite element model with adequate level of accuracy is important to investigate the effects of other parameters.

Finally, the last part of this study is numerically examining the effect of different parameters using a parametric study. The parameters considered are wall thickness, fibre orientation and fibre concentration of the pultruded FRP tubes and properties of the infill concrete. The results show that the wall thickness impact positively on the stiffness and load capacity of the hollow square and circular columns. The stiffness of filled columns depends on the compressive strength of filler. The influence of fibre orientation on the performance of hollow circular columns is more significant than its influence on square columns.

The significant outcomes of this study are advancing the knowledge of axial compressive behaviour of hollow pultruded FRP columns and establishing the effect of infill concrete on enhancing stiffness, load capacity and energy absorption capacity of filled pultruded FRP columns. Moreover, impacts of various parameters related to shape, dimensions, fibre structure and properties of the concrete filler material are also determined. This study outlines the importance of properties of FRP tube and filler material to enhance the axial behaviour of filled FRP tubes towards broadening their utilisation in civil infrastructure.

Certification of thesis

This Thesis is the work of **Ali Al-saadi** except where otherwise acknowledged, with the majority of the authorship of the papers presented as a Thesis by Publication undertaken by the Student. The work is original and has not previously been submitted for any other award, except where acknowledged.

Ali Al-saadi	*19 April 2019*
Signature of Candidate	Date

Endorsement

Professor Thiru Aravinthan	*19 April 2019*
Signature of principle Supervisor	Date

Dr Weena Lokuge	*19 April2019*
Signature of Associate Supervisor	Date

Student and Supervisors signatures of endorsement are held at USQ.

Statements of contributions

The following papers were a joint contribution of the authors. The details of the author contributions are provided below:

- Al-saadi, AU, Aravinthan, T & Lokuge, W 2018, 'Structural applications of Fibre Reinforced Polymer (FRP) composite tubes: a review of columns members', *Composite Structures*. Vol. 204, pp. 513-524. (IF: 4.101, SNIP: 1.939).

  The overall contribution of Ali Umran Kadhum Al-saadi was 65% to the reviewed the literature, stated the usage fields of FRP in applications of civil engineering, prepared the initial draft and revised the final submission; Thiru Aravinthan and Weena Lokuge contributed 35% in the form of concept development, editing and providing technical advice.

- Al-saadi, AU, Aravinthan, T & Lokuge, W 2018, 'Effects of fibre orientation and layup on the mechanical properties of the pultruded glass fibre reinforced polymer tubes ', *Engineering Structures*, (Under review, IF: 2.755 , SNIP: 2.165, Manuscript No: ENGSTRUCT_2018_3907).

  The overall contribution of Ali Umran Kadhum Al-saadi was 70% to conduct the experimental work, analysis and interpretation of results, wrote the initial draft and revised the final submission; Thiru Aravinthan and Weena Lokuge contributed 30% to the analysis, editing, providing important technical discussion points.

- Al-saadi, AU, Aravinthan, T & Lokuge, W 2019, 'Experimental investigation on the compressive behaviour of filled pultruded glass fibre reinforced polymer tubes ', *Construction and Building Materials*, (Submitted, IF: 3.485, SNIP 2.309, Manuscript No: CONBUILDMAT-S-19-04342).

The overall contribution of Ali Umran Kadhum Al-saadi was 70% to conduct the experimental work, analysis and interpretation of results, wrote the initial draft and revised the final submission; Thiru Aravinthan and Weena Lokuge were contributed 30% to experimental work, analysis and editing, providing important technical discussion points.

- Al-saadi, AU, Aravinthan, T & Lokuge, W 2019, 'Finite element analyses of filled glass fibre reinforced polymer (GFRP) pultruded tubes under axial loading', *Engineering Structures*, (Under review, IF: 2.755, SNIP 2.165, Manuscript No: ENGSTRUCT_2019_940).

The overall contribution of Ali Umran Kadhum Al-saadi was 70% to perform the finite element analyses, interpretation of results, wrote the initial draft and revised the final submission; Thiru Aravinthan and Weena Lokuge contributed 30% in improving the model, editing, and providing important technical discussion points.

Acknowledgements

All praise is due to *ALLAH* for giving me the patience, the knowledge and the strength to complete this work.

Firstly, I would like to express my deepest gratitude to my supervisors, *Prof. Thiru Aravinthan* and *Dr Weena Lokuge* for their supervision, support and encouragement over the course of my PhD. I would particularly like to thank *Prof. Thiru Aravinthan* for his continuous eagerness, vision and determination for my research to succeed. I am also grateful to *Dr Weena Lokuge* for her constant motivation and scientific insight into my research.

Grateful thanks are extended to the all academics and technical staff who have helped me in this thesis. In particular, I thank *Mr Wayne Crowell*, *Mr Martin Geach, Mr Daniel Eising, Mrs Piumika Ariyadasa* and *all staff at the workshop* for providing their technical assistance during the preparation and testing of the specimens.

I am very grateful to the wonderful colleagues of postgraduate student at CFM for their help in fabrication and construction column specimens and for their friendship.

My appreciations and respect go to my father, my mother, my brother and sisters for their support, ineffable love and prayers.

I would like to show my great appreciation to my wife *Dalia* for her patient and continuous encouragement. She gave me the strength to overcome this challenge and at the same time, she looked after the family while I was doing this thesis. Presenting this work without statement of my love to my daughter *Rynaz* is not quite fair, because she is the happy memorial of the past, the joyful moments of the present and the hope and promise of the future.

I acknowledge the *Government of the Republic of Iraq* for their sponsoring this journey of my Ph.D., and special thanks goes to *Iraqi Cultural Attaché* (Canberra) for their support during the period of this study.

Finally, to those I failed to mention, thank you very much.

Table of content

List of Figures

List of Tables

Chapter 1:

Introduction

1.1 Introduction

Timber, masonry, steel and concrete are traditional construction materials, which dominate the construction industry. Environmental conditions such as sunlight, fire and water as well as wood pests like termites and wood ants have an effect on timber. Thus, not only the mechanical properties of the timber material reduces but also the cross-sectional area of a timber column could decrease (Chang 2015). Figure 1.1 shows the deterioration in a column due to insects.

Figure 1.1 Timber column damage due to insects (Chang 2015)

Brick columns have been subjected to damage due to environmental conditions (such as rain) and to construction errors such as using poor quality of materials. The failure of brick buildings in compression depends on the properties of brick and mortar (Hansen & Nielsen 2005). Depending on the compressive strength of the mortar f_m and brick f_b, the compressive failure modes of masonry are shear and splitting (Figure 1.2).
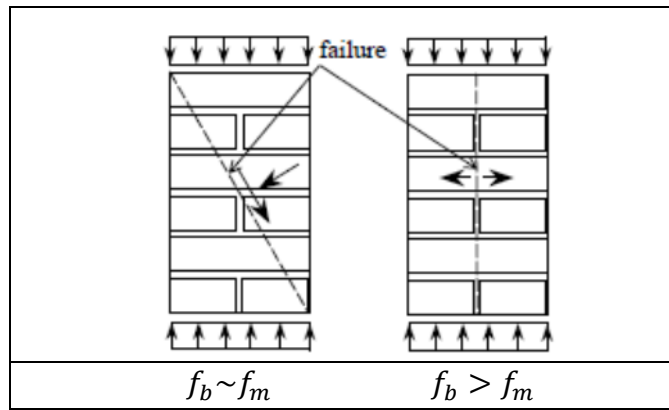
Figure 1.2 Compressive failure modes of masonry column (Hansen & Nielsen 2005)

Using steel as a structural material provides advantages such as ductile, reliability of the material properties and high quality of construction. Disadvantages of using steel are high cost, negative effects of temperature on steel strength, and its tendency to buckling and corrosion. The effects of environmental conditions on the deterioration of steel material due to corrosion (Figure 1.3) increase after years of exposure to air and water (Liu et al. 2005).

Figure 1.3 Corrosion of steel bridge column (Liu et al. 2005)

Reinforced concrete is a durable construction material. The corrosion of steel reinforcement of concrete is the main cause of degradation of concrete structures (Hansson et al. 2007). The corrosion occurs due to presence of moisture, lack of sufficient concrete cover, presence of soluble chlorides and due to carbonation of the concrete (Figure 1.4). As a result, the performance of the reinforced concrete structure is affected adversely by cracking of concrete due to expansion of corrosion products, reduction in steel cross-sectional area and changes in the bond strength of concrete-steel interface (Bossio et al. 2015).

Figure 1.4 Steel corrosion of concrete columns
(http:// www.cortecvci.com/publications/corrosion-protection-using-mci-2021-22/)

The demand for new materials to accommodate the improvement in all aspects of life motivates researchers to explore new materials. New materials that can provide an increase in the service life for existing structures, better resistance to aggressive environments and enable the design and construction of new structure are essential (Hollaway 2010). Fibre reinforced polymer composites material has low weight which reduces the cost of construction, speeds up the installation and reduces influences on the environment (Lee & Jain 2009). Another major benefits of FRP composites are non-corrosive material, high strength to weight ratio, high stiffness to weight ratio and easiness in construction (Friberg & Olsson 2014).

These properties have marked the FRP composites in the last decades as an innovative material for various civil engineering applications. The first development of polymer

composites was in 1940 (Gand et al. 2013). However, the use was limited to military and aerospace applications since the characterisation of FRP composites materials includes an ability to form various shapes, low density, good mechanical properties, non-magnetic qualities and good resistance to corrosion. Civil engineers started to consider FRP composites as a semi-load bearing and infill panels fabricated by the hand lay-up process in the 1970 (Hollaway 2010).

As a result, different techniques have been developed to increase the use of FRP composites in various applications. Pultrusion is the popular technique for producing FRP profiles (Figure 1.5). It is a continuous process to manufacture constant cross-section profiles at any length (Figure 1.6). The cost of pultrusion process is low because it involves pulling the raw fibres through injection chamber of resin and then through a heated die, which gives the shape of product (Barbero 2017).
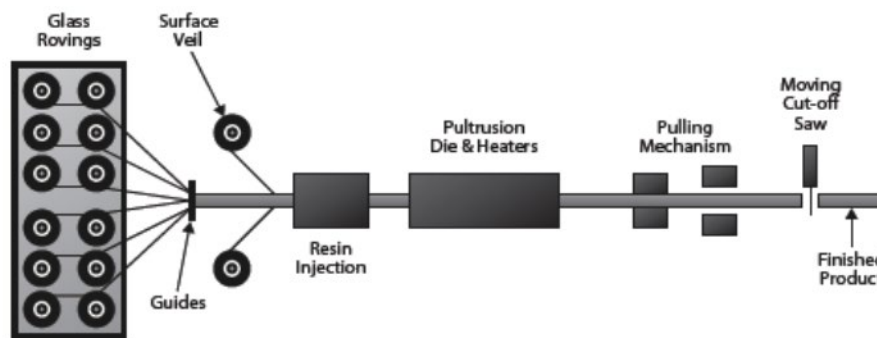
Figure 1.5 Pultrusion process (https://www.wagner.com.au/main/what-we-do/composite-fibre-technologies/downloads)
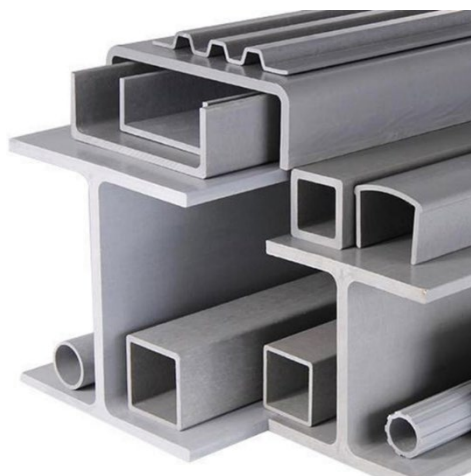
Figure 1.6 Pultruded FRP profiles
(https://www.indiamart.com/proddetail/pultruded-section-15875392355.html)

The test laboratories of the Electromagnetic Interference (EMI) was the first structure to be constructed from FRP profiles. The non-magnetic feature is the key of FRP profile in the use of computer and electronics industry. Similar structures were also used in Apple and IBM buildings (Bank 2006). In 1999, a multistorey building named Eyecatcher Building (Figure 1.7) was constructed for the Swissbau Fair in Basel, Switzerland.

Figure 1.7 Eyecatcher Building (Ascione et al. 2016)

The cooling towers are another type of structure that has been constructed by using FRP profiles as beam, column and panel components (Figure 1.8).

Figure 1.8 Colling tower made from pultruded

structural profiles in Russia (Ascione et al. 2016)

Bridge structures are another area of application of pultruded FRP profiles due to their low weight, corrosion resistance and ease in installation. The pedestrian and cycle bridge in Kolding, Denmark, as shown in Figure 1.9, is made from 100% pultruded GFRP shapes. The length of the bridge is 40 m and width is 3.2 m. The bridge was checked after 15 years and no damage was observed (Ascione et al. 2016).

Figure 1.9 All pultruded GFRP Kolding bridge

(Ascione et al. 2016)

The FRP bridge can be transported to the site in one piece or it can be assembled on site. Figure 1.10 shows the construction of bridge in Svenborg, Denmark. The length and width are 40 m and 3.2 m respectively. The installation of the bridge took only two hours (Ascione et al. 2016).

Figure 1.10 Construction of the pultruded FRP bridge

(Ascione et al. 2016)

In Australia, Wagner's Composite Technologies constructed the footbridge 40 m long over the Rifle Range Creek in Bargara, Queensland as shown on Figure 1.11(a). Another example of using FRP profiles in Australia is a footbridge at Ballin drive in Toowoomba, Queensland with span 25 m is shown on Figure 1.11 (b).

Figure 1.11 Pultruded FRP footbridges (a) Bargara Bridge and (b) Toowoomba
Bridge (https://www.wagner.com.au)

1.2 Problem statement

The trend of using Fibre Reinforced Polymer (FRP) materials in civil engineering
applications has increased during the last two decades due to the increasing demand in
the use of new construction materials to meet the requirements of modern and special
structures. FRP materials have better properties than the traditional construction
materials such as steel and timber. It is able to resist corrosion, and it is easy to use
either for strengthening existing concrete members or for building new structural
members (Becque et al. 2003). It provides an advantage for construction by decreasing
the required time and eventual maintenance cost as well. Bonding FRP sheets along
the tension side of a beam, wrapping in the transverse direction of a column and FRP
tube encased concrete columns are common techniques that were used to obtain
strength and strain enhancements. FRP structural members that are fabricated by
pultrusion method are another type of FRP composite materials. This method plays a
role in decreasing the cost of FRP production (Deskovic et al. 1995).

The main areas of using FRP tubes in columns applications are encased concrete columns to achieve strength and strain improvements, as structural column members and finally, in hybrid FRP column that consists of steel, concrete and FRP tube.

The concrete filled FRP tube (CFFT) and hybrid FRP of columns applications require to keep the orientation of fibre layers towards the transverse direction of the column to decrease or to delay the lateral dilation of concrete. The all FRP column has most of its fibre layers laying in the axial direction, which enables it to stand alone as a structural column member, carrying axial compressive load.

Previous studies focused mainly on two areas. Firstly, achieving improvements in the behaviour of concrete members by creating confining pressure by keeping the orientation of fibres in transverse direction. In this application, the concrete is used to fill FRP tubes to improve the axial behaviour of concrete member through utilisation the confining pressure of FRP tube. Secondly, the study of the axial behaviour of pultruded FRP column members and proposed models to predict axial strength with consideration of buckling effects (Figure 1.12). These purposes have been researched a lot in last two decades.

This study was designed to address the research question of how the axial behaviour of pultruded FRP tubes with fibres laid in multiple directions can be improved. The effects of potential variables on the stiffness, load carrying capacity and energy absorption capacity of pultruded FRP columns are the major research gaps required investigation. The research is designed to investigate the major research gaps by considering different variables such as cross-section of pultruded FRP tube, wall thickness, fibre layup and orientation as well as, diverse filler materials. Accordingly, it is important to conduct an extensive study on the factors affecting the performance of axial behaviour of pultruded FRP tubes. The results will enhance the broader utilisation of FRP tubes in structural applications.

(a) Local buckling (Godat et al. 2013)
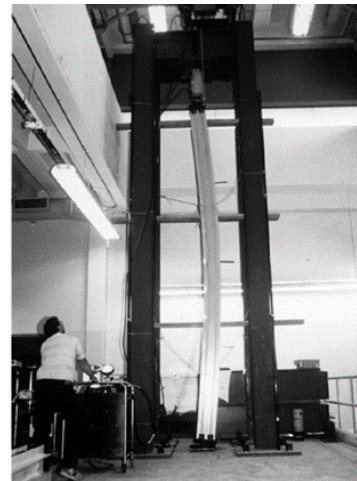
(b) Global buckling (Hashem and Yuan 2011)

Figure 1.12 Buckling issues of pultruded FRP columns

1.3 Research objectives

The aim of this research is to improve the axial behaviour of pultruded FRP tubes by using a suitable filler material. Different types of concrete and pultruded FRP tubes in shapes of square and circular with different fibre orientation and wall thickness available in the market were selected (Figure 1.13). The main objectives of this study are:

1- Investigate how fibre orientation and fibre layup affect the mechanical properties of different PFRP tubes

2- Study the axial behaviour of PFRP tube columns to investigate effects of wall thickness and cross-section shape of PFRP tube columns

3- Examine the effects on axial behaviour of filling PFRP tube with different types of fillers with varying modulus

4- Simulate axial behaviour of FRP structural member by using finite element method

5- Investigate the impacts of change in different parameters on the axial behaviour of hollow and filled pultruded FRP tubes through conduct a parametric study
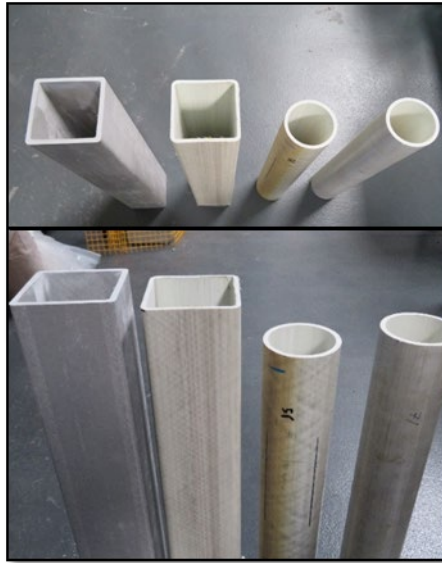
Figure 1.13 Square and circular pultruded FRP tubes

1.4 Scope of the thesis

This study focused on understanding the axial behaviour of pultruded FRP tubes, subjected to axial compression. An extensive experimental investigation, together with numerical and parametric studies were conducted to meet the above research objectives. Experimental investigations were conducted for material characterisation of different types of FRP tubes and various filler materials. These were followed with full-scale experimental investigation on FRP tubes under axial loading. A numerical model in finite element analysis software STRAND 7 is used to simulate specimen behaviour and compare the results with experimental observations to validate the developed model. Finally, a parametric study was performed to explore the effect of the variation of research parameters and design recommendations are made.

For this study, pultruded FRP tubes existing in the markets in shapes of square and circular with different wall thickness, fibre orientation and layup were considered in this study. To improve the stiffness, load capacity and energy absorption of pultruded FRP tubes, different types of filler were used.

The scope of this study can be summarised below:

1. Review the use of FRP material in column applications and recent approaches for developing the axial behaviour of pultruded FRP tubes;
2. Identify the research gaps and research aim and specify the research parameters which include the proposed approach to address the research gap;
3. Characterise the material properties of different types of pultruded tubes and concrete;
4. Test both hollow and filled square and circular pultruded FRP tubes and compare the experimental results with the numerical results from FEM;
5. Study the variation of the research parameters using a parametric study; and,
6. Summarise the positive effect of different parameters on the axial behaviour of pultruded FRP columns for wider usage in column application in civil infrastructure in a cost-effective way.

1.5 Thesis organisation

This thesis contains seven (7) Chapters including this introduction. The content of each Chapter is summarised below:

Chapter 2 presents background information on the use of FRP composite material in column applications. In addition, it provides a literature review of each type of FRP applications, showing the effects of different parameters. This chapter also presents Gaps in knowledge. This chapter is paper **I**.

Chapter 3 is paper **II**. It describes the material tests for mechanical properties for different square and circular pultruded FRP tubes. The results were explained in terms of fibre orientation and its layup. Furthermore, it contains the details of the concrete cylinder tests and results of different types of infill concrete.

Chapter 4 describes the experimental work carried out on four types of pultruded FRP tubes, both hollow and filled with different types of concrete, with the aim to assess the effects of filling, fibre orientation and fibre concentration. A comprehensive discussion is presented to indicate effects of different research parameters. This chapter is paper **III.**

Chapter 5 is paper **IV.** It presents the finite element simulation of pultruded FRP tube columns. The numerical study was completed for both hollow and filled columns in STRAND 7. The results of simulation in terms of load-axial deflection curves, peak load capacity and failure modes were explained and discussed against the results of the experimental work to indicate the accuracy level of finite element simulation.

Chapter 6 presents the use of the finite element model to implement a parametric study. Different parameters related to the dimensions of the FRP tubes, layers of fibre and strength of the concrete infill were considered in the study of axial behaviour of the hollow and filled pultruded GFRP tube columns.

Chapter 7 presents the conclusions of this research and suggests recommendations for future work.

References

Ascione, L, Caron, J-F, Godonou, P, van IJselmuijden, K, Knippers, J, Mottram, T, Oppe, M, Gantriis Sorensen, M, Taby, J & Tromp, L 2016, Prospect for new guidance in the design of FRP: Support to the implementation, harmonization and further development of the Eurocodes, Publications Office of the European Union.

Bank, LC 2006, Composites for construction: Structural design with FRP materials, John Wiley & Sons.

Barbero, EJ 2017, Introduction to composite materials design, Third edn, CRC Press, Boca Raton, Fla.

Becque, J, Patnaik, AK & Rizkalla, SH 2003, 'Analytical models for concrete confined with FRP tubes', Journal of Composites for Construction, vol. 7, no. 1, pp. 31-8.

Bossio, A, Monetta, T, Bellucci, F, Lignola, GP & Prota, A 2015, 'Modeling of concrete cracking due to corrosion process of reinforcement bars', Cement and Concrete Research, vol. 71, pp. 78-92.

Chang, W-S 2015, 'Repair and reinforcement of timber columns and shear walls–A review', Construction and Building Materials, vol. 97, pp. 14-24.

Deskovic, N, Triantafillou, TC & Meier, U 1995, 'Innovative design of FRP combined with concrete: short-term behavior', Journal of Structural Engineering, vol. 121, no. 7, pp. 1069-78.

Friberg, E & Olsson, J 2014, Application of fibre reinforced polymer materials in road bridges–General requirements and design considerations, Gothenburg: Chalmers University of Technology, Department of Civil and ….

Gand, AK, Chan, T-M & Mottram, JT 2013, 'Civil and structural engineering applications, recent trends, research and developments on pultruded fiber reinforced polymer closed sections: a review', Frontiers of Structural and Civil Engineering, vol. 7, no. 3, pp. 227-44.

Hansen, LZ & Nielsen, MP 2005, 'Stability of masonry columns'.

Hansson, C, Poursaee, A & Jaffer, S 2007, 'Corrosion of reinforcing bars in concrete', R&D Serial, no. 3013.

Hollaway, L 2010, 'A review of the present and future utilisation of FRP composites in the civil infrastructure with reference to their important in-service properties', Construction and Building Materials, vol. 24, no. 12, pp. 2419-45.

Lee, LS & Jain, R 2009, The role of FRP composites in a sustainable world, Springer, 1618-954X.

Liu, X, Nanni, A & Silva, PF 2005, 'Rehabilitation of compression steel members using FRP pipes filled with non-expansive and expansive light-weight concrete', Advances in Structural Engineering, vol. 8, no. 2, pp. 129-42.

Chapter 2:

Literature Review

This chapter is a review paper for the structural application of fibre reinforced polymers (FRP) in civil engineering. It shows the main categories of using FRP materials in column applications are FRP tube encased concrete, all FRP profiles and hybrid FRP columns. This is because the FRP material can be used as a confining material to the concrete, a reinforcement and a structural column. According to the fibre orientation and layup, the application of FRP tubes are stated. For confinement, fibres should be in the transverse direction while they should be in the axial direction when tubes are used as a column.

 The concrete columns confined by FRP and hybrid FRP columns categories are related to the confinement purpose to enhance the strength and strain capacities of the concrete. On the other hand, the purpose of the all FRP columns category is to provide light weight structural column members. The review paper identifies the research gaps related to these categories. The area of pultruded fibre reinforced polymer profiles that are being used as structural column members is the core of this study.

2.1 Paper 1

Structural applications of Fibre Reinforced Polymer (FRP) composite tubes: a review of columns members

Ali Umran Al-saadi, Thiru Aravinthan and Weena Lokuge

University of Southern Queensland, School of Civil Engineering and Surveying, Centre for Future Materials (CFM), Australia.

Review

Structural applications of fibre reinforced polymer (FRP) composite tubes: A review of columns members

Ali Umran Al-saadi[a,b], Thiru Aravinthan[a,*], Weena Lokuge[a]

[a] *Centre for Future Materials (CFM), School of Civil Engineering and Surveying, University of Southern Queensland, Toowoomba 4350, QLD, Australia*
[b] *University of Babylon, Babil, Iraq*

ABSTRACT

Use of fibre reinforced polymer (FRP) in column applications is increased because it can act as a confining material, a reinforcement and a structural column. The application of FRP tubes is correlated with the fibre orientation since tube stiffness is mainly attributed to the stiffness of fibres. Thus, for confinement, the fibres should align in the transverse direction of the tube while they should align in the axial direction when tubes are used as compression members. FRP tubes with fibres mainly in axial direction may reach failure because the stiffness in the perpendicular direction to fibres depends only on the stiffness of the matrix. In order to boost the stiffness in the secondary direction while supporting fibres in the main direction, fibres should be in multi-directions.

This paper reviews and identifies gaps in knowledge on the use of FRP materials in column applications in new or existing construction regimes.

1. Introduction

The use of Fibre Reinforced Polymer (FRP) materials in civil engineering applications gained increased popularity during the last three decades because they have better properties than the traditional construction materials such as steel. FRP materials have an ability to resist corrosion, and it is easy to use them either for strengthening existing concrete members or for building new composite members [1]. Reduced construction time and lower maintenance cost during the service life are some advantages of FRP members.

FRP profiles are mainly used in beam and column applications in a typical structure. Using FRP tubes in column applications can be classified into three categories; (a) FRP tube encased concrete to obtain strength and strain enhancements, (b) all FRP profiles and (c) hybrid columns that consist of steel, concrete and FRP tube. Main purpose of the first and the third categories is to utilize the strength of the FRP tube to produce confining pressure in the transverse direction of concrete columns or concrete–steel columns. On the other hand, the purpose of the second category of FRP profiles is to produce light weight structural column members. The use of pultruded FRP profiles which are similar to existing steel profiles has gained popularity because of the cost reduction in the fabrication process [2].

This paper reviews the recent research on the axial behavior of structural column members which are made by using FRP tubes and to point out the knowledge gaps for further studies. The review is presented using the three categories identified above.

2. Concrete columns with FRP confinement

Reinforced concrete column members fail when the lateral strain reaches a specific value and concrete cover starts spalling followed by the buckling of steel reinforcement [3]. Thus, a delay in reaching lateral strain in the concrete to its ultimate failure leads to performance enhancement of a concrete column. This goal can be met by providing lateral pressure around the column diameter through confinement by FRP materials. The concept of confinement depends on keeping fibre orientation in the transverse direction of the column [4–6]. This is because the concrete under axial load expands laterally. This expansion creates tensile stress in the confining material which turns into confining pressure on the lateral direction of concrete columns [7]. The following sections highlight the effect of FRP confinement on the compressive behavior of concrete columns by considering the influences of different parameters on the degree of confinement and present a summary of the available stress-strain models for FRP confined concrete.

2.1. Advantages of FRP confinement in concrete columns

The confinement of concrete columns results in mitigating the possible failure due to unexpected load due to an earthquake since the confinement with FRP material increases the ultimate strength and strain. Additionally, FRP confined material protects the concrete column against aggressive environments, acts as non-corrosive re-inforcement and as permanent formwork. Moreover, Qasrawi et al. [8] found out that the localised damage is decreased in FRP-confined concrete columns compared with conventional reinforced concrete columns under blast loading. This important feature provides the ability to save civilian and property against intentional or accidental explosions.

2.2. Effect of different parameters on the degree of confinement

The degree of improvement in the axial strength and strain capacities of concrete columns due to the confinement with FRP materials depends on many parameters such as slenderness ratio of columns, shape of cross–section, concrete strength, method used to manufacture the tube, fibre properties, fibre orientation and FRP thickness [9].

2.2.1. Slenderness ratio

The influence of slenderness on the axial performance of normal strength concrete filled [10] as well as high strength concrete filled [11] FRP circular tubes were studied in the past. Their studies concluded that the degree of enhancement of strength and strain capacities in concrete has been decreased when the slenderness ratio is increased. Similarly, it was found that FRP confinement of circular reinforced concrete columns was less significant for slender columns than short columns [12–14].

2.2.2. Shape of the concrete columns

Less effect of FRP confining material on the behavior of columns with non-circular cross-sections was reported by Pessiki et al. [15], Hong and Kim [4], Fam et al. [16] and Mirmiran et al. [17]. The results of their work verified that the confinement in non-circular sections is not as effective as circular columns due to the outward bending in the flat sides of the non-circular FRP tubes. The same view was reported by Ozbakkaloglu and Xie [18] after testing square and circular FRP tubes filled with geopolymer concrete under axial compression. Thus, researchers have followed two methods to overcome this problem to improve the confinement of square and rectangular concrete columns by modifying the cross section to circular and elliptical shapes respectively. In the first method, prefabricated FRP shells were placed around the existing concrete column to change the cross section and the gap between shells and original concrete column was filled with concrete (Fig. 1a). A wet lay-up process of FRP sheets or strips were used to fix FRP shells [19]. The second method (Fig. 1b) to modify the cross section was similar to the first one except the use of concrete segments without creating a gap with the original concrete section [20].

Beddiar et al. [9] improved the first method by assembling three GFRP sheets made from twill weave glass with structural bending to modify the cross section of square concrete columns and then, filled the gap with shrinkage compensating cement mortar (Fig. 2). The test results confirmed that strength and ductility capacities of non-circular concrete sections can be improved through cross section modifications.

The second method has also been evolved for rectangular columns with large aspect ratio by Bhowmik et al. [21]. They used the concrete segments to form a capsule-shaped column instead of an elliptical shaped column. The concrete segments in shape of either semi-circular or circular were added at the short ends of the rectangular columns to change the cross section of rectangular columns. The results showed that the shape modification techniques enhanced the confinement effects on the structural response of the rectangular columns.

In addition to the circularization modification method of the
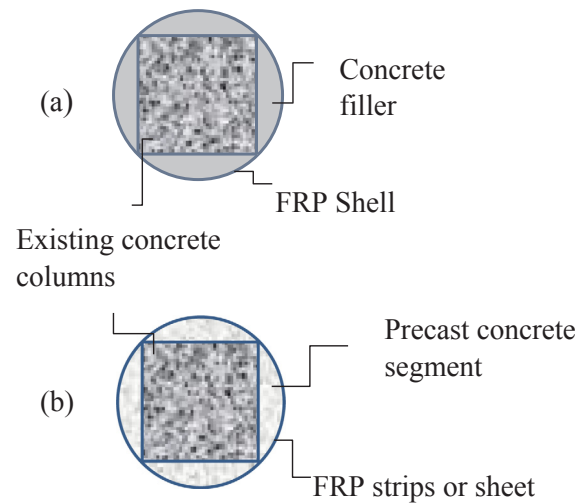
Fig. 1. Modification methods of non-circular sections (a) using prefabricated FRP shell and (b) using precast concrete segment.

conventional square concrete columns, Youssf et al. [22] followed two more methods; refined–corner section and rounded – corner angle section as shown in Fig. 3. They used crumb rubber aggregate in three different percentages to replace the fine aggregate in the concrete cross-sections modifiers. The external confinement was achieved by using unidirectional carbon sheets with a nominal thickness of 0.128 mm. Their test results showed that crumb rubber concrete is useful to replace the normal concrete in modification approaches of the non-circular columns.

Recently Zeng et al. [23] studied circularized concrete square columns that were confined partially and comprehensively with fibre reinforced materials. They tested 33 concrete columns divided into three groups; one for square columns and two groups for the circularized square columns. The difference between circularized groups is the strength of the concrete segments that were used to circularize the square column. Concrete segments of one group was made identical to the concrete strength of the core while it was higher for the other group. The width of the FRP strips was set to 90 mm. The fully FRP confined strengthening technique was used for all square columns and some circularized square columns while the remaining columns were confined partially. The partial FRP confinement was performed by creating space between the adjacent FRP strips. Four spacings (0, 30, 45 and 90 mm) of FRP strips were considered. The results reported in this study showed that the partial FRP confinement of the modified square column is an economical and unconventional method compared to the fully FRP confinement. This is because the consumption of FRP material is decreased by about 50% without a huge compromise on the strength and strain capacities compared with fully FRP confined square columns.

2.2.3. Concrete strength and concrete types

In order to identify the influence of concrete strength on the behavior of FRP–concrete columns under axial compression, Vincent and Ozbakkaloglu [24] used three different concrete strengths; 35 MPa, 65 MPa and 100 MPa. They tested 55 cylindrical specimens with 152 mm diameter and 305 mm height under axial loading. Carbon FRP (CFRP)-wrapping and CFRP tube–encased concrete were used. The research concluded that the ductility of the high and ultra-high strength concrete specimens can be improved when the FRP confinement is at adequate level. On the other hand, for the same confinement ratio, the strength and strain enhancements increase as the compressive strength of the concrete decreases. This is due to the increased brittleness in concrete with increased compressive strength which resulted in an increase in the hoop rupture strain of FRP confined material with a decrease in unconfined concrete strength. Hence, the capacity of concrete
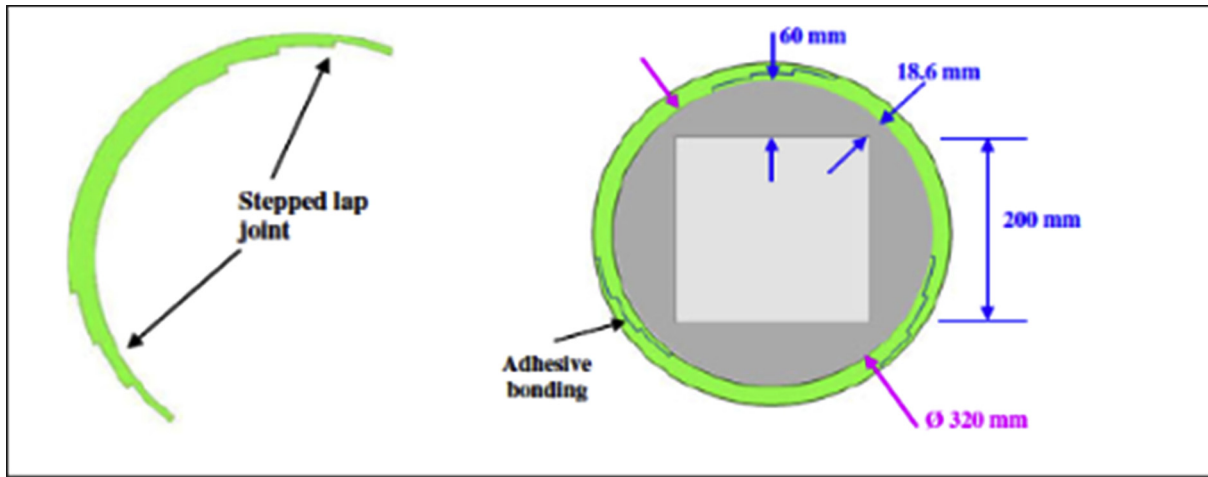
Fig. 2. Stepped lap joint of GFRP shell to modify the square concrete columns [9].
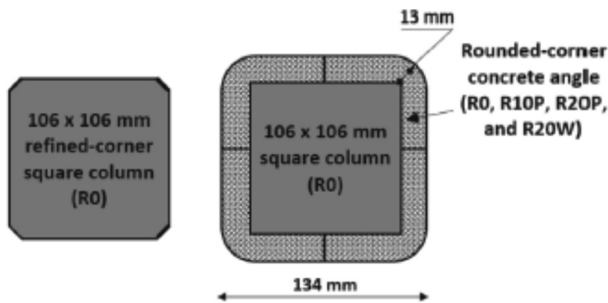
Fig. 3. Refined–corner and rounded-corner methods to modify the shape of the square columns [22].

with low compressive strength confined by FRP material shows higher improvement compared to high and ultra high strength concrete confined by the same amount of confinement. It is noted that the strain reduction factor does not significantly change due to various ways of preparing FRP confinement (FRP-wrapped and FRP-tube), while it changes because of variation in the concrete strength. This view is supported by the study of Lim and Ozbakkloglu [25] which reveals that the hoop rupture strain reduction factor decreases when either unconfined compressive strength of concrete (Fig. 4) or elastic modulus of FRP material increases.

The confinement of other types of concrete have been experimentally investigated by Yu et al. [26], Zhao et al. [27], Xie and Ozbakkaloglu [28], Zhou et al. [29], Lokuge and Karunasena [30], Ozbakkaloglu and Xie [18] and Wang et al. [31]. In these studies, circular concrete specimens were made of self–compacted concrete, recycled aggregate concrete, lightweight aggregate concrete, geopolymer concrete and seawater coral aggregate concrete. Generally, the results confirmed that FRP confinement improved the axial performance of confined specimens compared with unconfined specimens.

2.2.4. Influence of fibre orientation

In addition to the previous studies by Hong and Kim [4], Kim et al. [5] and, Vincent and Ozbakkaloglu [6] examined the impact of fibre orientation in FRP tube on the axial behavior of confined concrete specimens. They prepared different types of tubes using filament winding technique with carbon fibres oriented at various angles with respect to the axial direction. The study showed that the axial behavior of confined specimens is influenced by the fibre orientation and the effect is maximized when the fibres are aligned towards the hoop direction (Fig. 5). When there are more fibres in the hoop direction, they provide restraint to the lateral dilation of the concrete. This in fact is the confinement provided by the fibres which increases the compressive strength of the confined concrete and ultimately increase the axial capacity of the column.

2.2.5. Effect of other parameters

The effects of other factors such as manufacture methods of tubes,
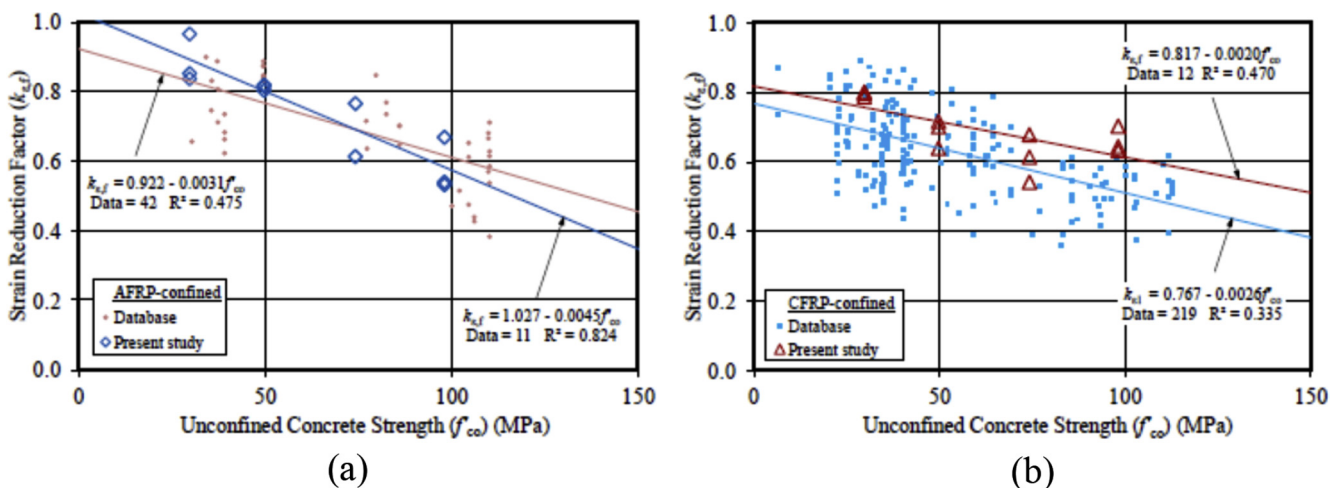
Fig. 4. Effect of unconfined compressive strength on the hoop strain reduction factor: (a) Aramid FRP confinement (b) Carbon FRP confinement [25].

18
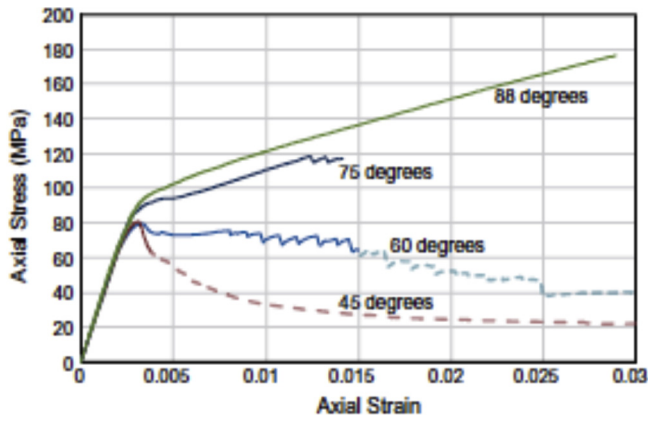
Fig. 5. Effects of fibre orientation on the performance of confined concrete specimens [6].

specimen size, amount and type of fibre on the behavior of FRP-concrete circular column specimens were studied by Ozbakkaloglu [32] and Ozbakkaloglu and Zhang [33]. The results showed that the compressive strength of FRP confined concrete was significantly affected by properties of FRP tubes while both manufacture methods and specimen size had less effect (Fig. 6).

2.3. Stress-strain models for FRP confined concrete columns

The axial stress-strain relationship of FRP confined concrete columns is needed in the structural analysis of the composite member. As the behavior of FRP confined concrete columns has been conducted by

researchers, many models to calculate confined compressive strength and strain of concrete have been suggested. Lam and Teng [34] classified these models into design oriented and analysis oriented models, and modified their previous models according to the collected data. The design oriented models are defined using simple closed-form equations to predict the confined compressive strength, the corresponding axial strain and the overall stress- strain relationship [7,34]. The use of design oriented models for design purposes is suitable compared with the analysis oriented models [35]. Analysis oriented models predict the stress-strain curves of FRP confined concrete by considering the interaction between the FRP confinement material and concrete core [36,37]. An incremental–iterative numerical procedure is followed to evaluate the axial stress and axial strain at a given confining pressure. This procedure makes the direct use of these models in design unsuitable. However, it is suitable for use in the finite element analysis [38]. Hong and Kim [4] summarized existing design oriented models and proposed a model that considers the winding angle of fibre orientation as a parameter and the model was modified later by Kim et al. [5]. Additional models were proposed by Teng et al. [38] and Teng et al. [35] for FRP confined concrete columns while Mohamed and Masmoudi [39] and Gao et al. [40] proposed models for FRP confined concrete columns that are reinforced with steel bar and steel wire mesh respectively.

Thorough assessment of the models for FRP confined circular concrete columns was done by Ozbakkaloglu et al. [36] who reviewed 88 stress–strain models (both design and analysis oriented models). The number of test results collected by authors was 2038 from 202 experimental studies published from 1991 to 2011. These 730 data sets from 92 experimental studies included circular sections confined with unidirectional fibres oriented in the hoop direction, height-diameter ratio less than 3 with unconfined concrete strength less than 55 MPa.
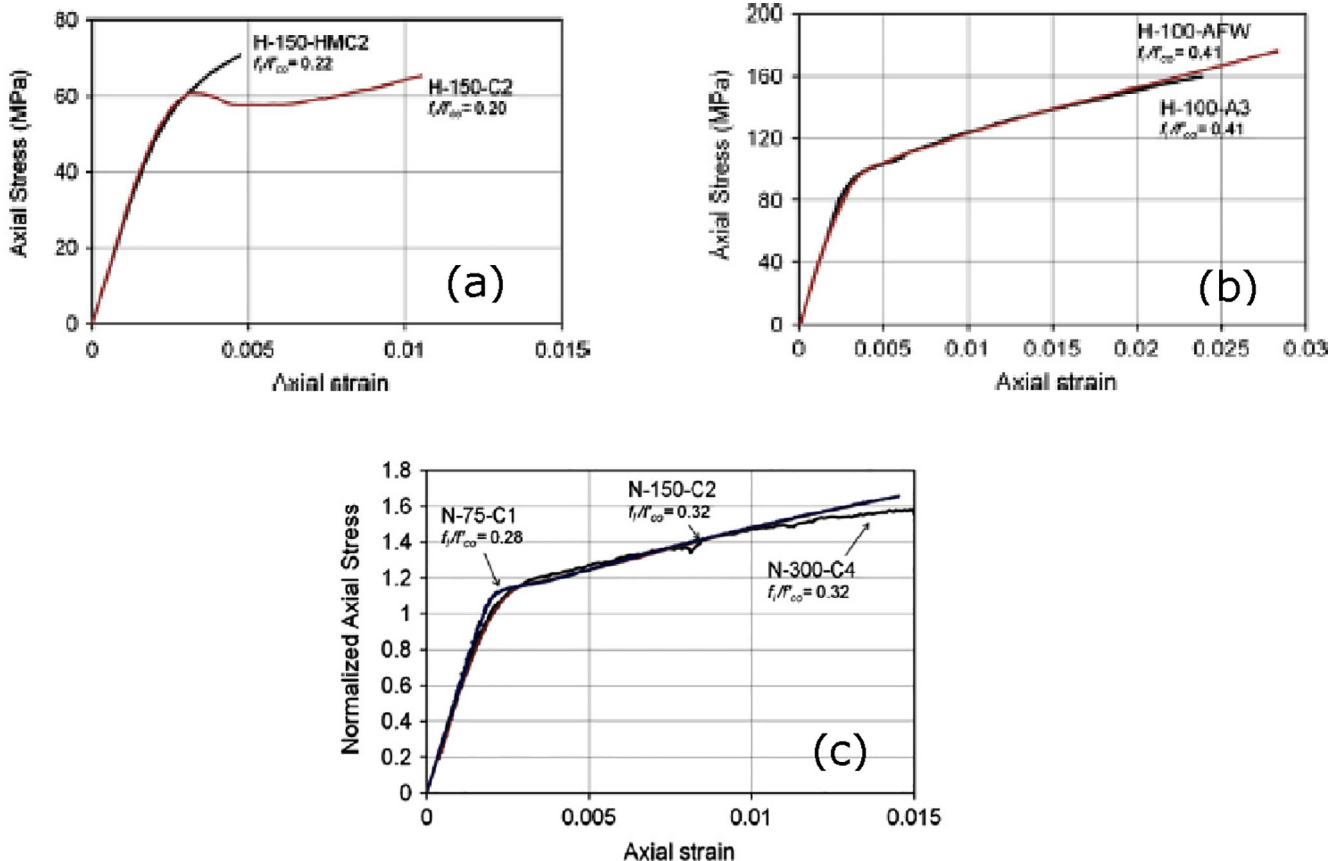
Fig. 6. Effects of different parameters on the compressive behavior of circular samples (a) FRP tubes with different modulus [32], (b) Manufacturing methods of tubes (lay-up and filament winding) [32] and (c) Diameter of specimens [33].

19

They stated that the accuracy of the model was improved when the value of the hoop rupture strain has been used instead of the ultimate tensile strain of fibres. Furthermore, the performance of design oriented model is better than that of the analysis oriented model because the former is calibrated with test database, while the latter is not.

2.4. Prestressing FRP confining material

It can be concluded from the available literature that the axial behavior of confined concrete is similar to that of unconfined concrete during initial stages of loading. This is because the activation of confinement is delayed until the lateral strain of concrete reaches a specific value. One way to overcome this delay is prestressing FRP material where hoop strain of confining materials is increased thus confinement by FRP will be better. This increment leads to enhance the level of lateral confining pressure and as a result, the axial behavior of FRP confined concrete specimens improves. Mortazavi et al. [3] and Yan et al. [19] had constituted initial prestress in the external FRP jacket or shell through inserting an expansive grout in the gap between original concrete specimens and external FRP Jacket. In order to minimise the axial expansion and allow the specimen expansion only in the hoop direction, steel plates and vertical weight had been used. Vincent and Ozbakkaloglu [41] could obtain this state for concrete filled FRP tube by adding an expansive agent to the concrete mix. They used prestressing rigs to restrain the axial extension of the concrete. The results showed that the prestressing of FRP material improves the axial behavior of FRP-confined concrete columns.

2.5. Summary of FRP confined concrete columns

Originally FRP use in the civil engineering applications aims to increase the strength and strain capacities of concrete columns and to retrofit existing columns that are subjected to damage due to either aggressive environment condition or load increments. The establishment of tensile stress in the FRP confining material is necessary to ensure a high degree of confinement. This explains why most researchers have aimed to include most fibres in the transverse direction of the column member for creating tensile stress in the FRP material which provides lateral confining pressure. Table 1 is the summary of the reviewed studies of FRP confined concrete columns.

3. All FRP column members

This section discusses the axial members that are made out of FRP only. FRP members that are fabricated by pultrusion method have the majority of fibres in the axial direction. This property makes pultruded FRP having higher capability to resist tensile stress. On the other hand, pultruded FRP tubes have been used as compression members too [42]. The instability condition due to either local or global buckling is created because of the low longitudinal modulus and the wall slenderness of FRP profiles [43,44] which prevents their maximum utilisation of the strength capacity. Below sections discuss the past research on all FRP column members with regards to the axial behavior, models for predicting load carrying capacity and the ways to overcome the issues in the axial compressive behavior.

3.1. Effect of slenderness on the axial behavior

Hassan and Mosallam [45] investigated the buckling behavior of 30 box section columns and 40 I-section columns with slenderness ratio (L/r) ranging from 20 to 120. They reported that the box and I–shape FRP columns failed due to global buckling when its slenderness ratio was equal to or greater than 60 and 50 respectively. Otherwise, they failed in either local buckling or a combination of local and global buckling. Based on the results of testing 24 full-scale columns having universal and box sections, Hashem and Yuan [46] have established a

distinguishing criterion for behaviors of short and long FRP composite columns. They stated that specimens with slenderness ratio (L/r) equal to or less than 50 fails by either local buckling of the flange plate or localised crushing of the composite material. In both situations, the composite material reached the inelastic range. The deciding factor about the type of failure is the length to thickness ratio of the flange and the web plates. On the other hand, a specimen with slenderness ratio (L/r) greater than 50 fails by global buckling. Moreover, they mentioned that using Euler's formula to predict critical buckling load provides very accurate results, and this accuracy becomes higher when the slenderness ratio of composite column increases. This is because the effect of the instability conditions due to global buckling will control ultimately the axial behavior of the slender FRP columns without interaction with local buckling or material failure. Therefore, the lateral movement occurs causing the entire profile to move out of its vertical plane while the shape of the FRP columns remains undeformed [47,48]. As a result, the accuracy of the Euler's buckling equation to predict the load carrying capacity of slender columns increases since the axial compressive behavior of pultruded FRP columns is controlled by the elastic Euler buckling mode.

Qian et al. [49] tested five circular GFRP tubes with an external diameter of 41.2 mm, thickness of 3.6 mm and length of 120 mm to determine the basic mechanical properties and four groups of GFRP tubes with various slenderness ratios ranging from 35 to 90 under axial compression to investigate the instability. They reported that there was a little difference in the values of elastic properties (5.5%), and the lateral displacement of long tubes increased rapidly when the value of axial load had reached buckling load. Also they stated that the failure mode of GFRP tube changed from fracture to buckle and failed in oversize lateral deformation when the slenderness ratio of tubes was increased.

Godat et al. [50] investigated the axial behavior of different FRP pultruded members to predict the failure mode. They tested angle and box sections (square and rectangular). The results show that if the global slenderness ratio is higher than local slenderness ratio, the global buckling failure dominates and vice versa while both types of failure may occur when the difference between slenderness ratios is not large enough. It further shows that the failure mode of box section is local plate buckling in all sides of the square section and in the wider side of the rectangular section.

Full–scale tests of the new type of pultruded GFRP square tube that has glass fibre plies at ±45°orientation were carried out by Guades et al. [51] in order to measure the compressive strength of the hollow tube, modulus of elasticity in the longitudinal direction and compared the results with coupon tests. The height of specimens was set to provide slenderness ratio (L/r) of about 2.6. The results showed that full-scale specimens exhibit linear elastic behavior up to the failure and the maximum variation between results of full scale tests and coupon tests is 8%.

3.2. Prediction models of axial load capacity

Developing a model to predict the axial strength of hollow FRP column member with buckling effects is more economical than conducting an extensive testing. Local and global buckling of pultruded FRP wide flange- I section (WF-I) was researched by Barbero and Tomblin [52]. Based on their experimental results, they proposed design equations which, in authors' opinion, do well to predict the critical loads of intermediate length of FRP–I section columns. Zureick and Scott [53] experimentally investigated 24 specimens made of E-glass and vinyl ester under concentric axial compressive load. They used two types of sections; pultruded wide flange sections and pultruded box sections. The slenderness ratio had a range from 36 to 103. As a result, they proposed design guidelines to consider effect of shear deformation in calculation the critical load of global buckling. Hassan and Mosallam [45] proposed a formula to predict the global buckling load for the box

Table 1

Summary for concrete columns with FRP confinement.

Reference	Cross section	Fibre type	Stacking sequence (respect to the axial direction of the tube)	f'_{co} (MPa)	$\frac{f'_{cc}}{f'_{co}}$	$\frac{\varepsilon_{cu}}{\varepsilon_{co}}$
Mirmiran et al. [10]	Circular	Glass	Unidirectional E-glass fibres ($\pm 75°$), (t = 3.68 mm)	22.4	–	–
Pessiki et al. [15]	Circular + Rectangular	Glass Carbon	1 – Multidirectional E-glass $(0°/ \pm 45°)^*$ 2 – Woven unidirectional E-glass $(0°)^*$ 3 – Unidirectional carbon sheet $(0°)^*$	26–32	1.12–2	1.4–8
Mortazavi et al. [3]	Circular	Carbon Glass	Pre-formed confining jackets	32	1–4	–
Hong and Kim [4]	Circular + Square	Carbon	Filament wound (t = 3 mm) $90°/90° – 90°/ \pm 60° – 90°/ \pm 45° – 90°/ \pm 30°$	17–19	1.2–5	11.2–23
Fam et al. [16]	Rectangular	Glass	Filament wound $(90°/(\pm 45°)_2/(0°)_2/90°/(0°)_2/(\pm 45°)_2/90°)$	52	–	–
Yan et al. [19]	Square, circular rectangular	Carbon, Glass	Unidirectional prefabricated shell	10–15	–	–
Mohamed and Masmoudi [39]	Circular	Carbon, Glass	Confine reinforced concrete column. $\pm 60_{3, 4°}$, ($\pm 65_{3°}$, $\pm 45°$, $\pm 65_{3°}$), $(60°, 90_{4°}, 60°)$, ($\pm 60°$, $90_{2°}$, $\pm 60°$, $90_{6°}$)	30,45	1.6–4.2	–
Fitzwilliam and Bisby [12]	Circular	Carbon	Unidirectional CFRP sheet towards hoop and longitudinal directions of RC columns	30.5	1.1–1.7	–
Kim et al. [5]	Circular	Carbon	CFRP sheet wrapping (t = 1.8 mm) $90°/90° – 90°/ \pm 75° – 90°/ \pm 60° – 90°/ \pm 45° – 90°/ \pm 30°$	17.5	2.2–4.17	4.5–12.3
Hadi et al. [20]	Square	Carbon	Horizontal wrapping with CFRP layers	32	–	–
Ozbakkaloglu and Zhang [33]	Circular, Square, Rectangular	Carbon, HM carbon, Aramid	Wrapping fibre sheet by wet-layup	55–100	–	–
Ozbakkaloglu [32]	Circular	Carbon HM- carbon Aramid	The majority of FRP tubes that their results were considered made with wet lay-up process. (fibre sheet in the hoop direction)	36–110	1.13–2.77	1.7–14.1
Vincent and Ozbakkaloglu [24]	Circular	Carbon	Unidirectional carbon sheet is used to confine specimens either by wrapped concrete cylinder or precast CFRP tube	35–65,100	1.01–1.68	1.6–7.16
Vincent and Ozbakkaloglu [6]	Circular	Aramid	1 – Filament winding tube with angles (45, 60, 75 and 88) degrees 2 – Wet lay-up process at 90° 3 – wrapped cylinder via wet lay-up process (90)	50–85	1.0–2.23	1.5–14.8
Lim and Ozbakkloglu [25]	Circular	Aramid Carbon	FRP single continuous sheets wrapped by using manual Lay–up method around polystyrene forms in the hoop direction	25–100	–	–
Yu et al. [26]	Circular	Glass Carbon	FRP Jackets (wet lay-up process)	30–105	1.1–2.09	2–7.89
Zhao et al. [27]	Circular	Glass	Wrapped in the hoop direction with unidirectional glass fibre sheet	34–45	1–1.8	3–6.3
Siddiqui et al. [14]	Circular	Carbon	Unidirectional CFRP sheet towards hoop and longitudinal directions of RC columns	35	–	–
Vincent and Ozbakkaloglu [41]	Circular	Aramid	Wrapping unidirectional aramid fibre sheet around Styrofoam templates in the hoop direction	100–110	1.2–2.11	5.4–7.97
Qasrawi et al. [8]	Circular	Glass	Continuous glass fibre wound ($\pm 55°$)	34	–	–
Beddiar et al. [9]	Square	Glass	Twill weave glass	38.2	1.31	1.76
Vincent and Ozbakkaloglu [11]	Circular	Aramid	Unidirectional aramid fibre sheet wrapped in the hoop direction	55–110	1–1.73	3–11
Gao et al. [40]	Circular	Glass	GFRP sheets	29.7	–	–
Zhou et al. [29]	Circular	Carbon	CFRP sheets	19–48	1.4–5.17	3.9–32
Lokuge and Karunasena [30]	Circular	Carbon Glass	Wrapping fibre sheet by wet-layup	19–45	1.1–2.7	1–1.8
Ozbakkaloglu and Xie [18]	Circular Square	Carbon S-glass Basalt	Wrapping fibre sheet by wet-layup	25	1.1–2.48	5.2–13.5
Xie and Ozbakkaloglu [28]	Circular Square	Carbon Basalt	Manual wet layup with unidirectional carbon and basalt fibre sheet	37–66	1.1–1.4	5.8–11.6
Zeng et al. [23]	Square	Carbon	Wrapping unidirectional CFRP sheet by wet-layup	24.3	0.9–2.91	1.58–8.33
Youssf et al. [22]	Square	Carbon	Wrapping unidirectional CFRP sheet by wet-layup	48.8–51.5	1–1.69	1–4.21
Bhowmik et al. [21]	Rectangular	Car-bon	Wrapping unidirectional CFRP sheet by wet-layup	24–27.2	–	–
Wang et al. [31]	circular	E-glass	Filament–wound process ($\pm 85°$)*	61–64	1.3–3.4	9.3–13.8
Lam and Teng [34]	Collected 76 results from others and present new model to anticipate the strength and strain capacities of FRP confined circular concrete specimens			–	–	–
Teng and Lam [7]	Review paper	–	–	–	–	–
Teng et al. [38]	Collected results from others and present new model to anticipate the strength and strain capacities of FRP confined circular concrete specimens			–	–	–
Teng et al. [35]	Make refinement to the previous Lam- Teng model			–	–	–
Jiang and Teng [13]	Circular	–	This paper present a theoretical model for FRP confined slender RC columns	–	–	–
Ozbakkaloglu et al. [36]	Review paper	–	–	–	–	–

Notes: f'_{co}, ε_{Co} = Unconfined compressive and strain of concrete values.

f'_{cc}, ε_{Cu} = Confined compressive and strain values.

  * Respect to the circumferential direction of the column.

21

and I–shaped pultruded FRP columns and the predictions were in good agreement with the experimental results.

A new design method to predict the load at which the pultruded FRP columns will fail due to either local or global buckling was proposed by Puente et al. [54] by testing pultruded FRP circular columns. The results of their model showed an acceptable degree of accuracy, as they were close or below the experimental values. Another model to calculate the axial strength of pultruded GFRP square column was proposed by Cardoso et al. [55]. Five different sizes of the square tubes with 14 specimens in each size were tested to cover a range of global and section slenderness ratios. When either the material stress reached to the ultimate strength or the value of lateral deflections at mid-height exceeded L/50, the test was stopped. The researchers found that the proposed equations perform well for short and intermediate columns, but not for long columns because the restriction of the lateral deflection at mid-height. Gangarao and Blandford [56] used another approach to predict axial strength of FRP columns by using the strain energy density model which used the area under the axial stress-strain curve of the column. The main objective of their work was to investigate the effects of local and global buckling on the strength of pultruded GFRP compression member. They tested 46 hollow box columns. The results of hollow box sections show that the difference between predicted and experimental values vary from 8% to 19%. The possibility of having shear failure in the pultruded GFRP profiles before compressive failure due to low shear-to-compressive strength ratio was also studied by Bai and Keller [57] for rectangular tubes with different lengths. Based on that, a model was proposed to predict ultimate load based on shear failure and second order deformation. A number of researchers [58–63] have been dealing with the calculation of local bucking load as a plate buckling problem. They did an analytical study of FRP plate element under various loading conditions and different states of restrained edges to assess the local buckling load of FRP section through evolving closed form equations. Different types of pultruded FRP shapes such as I-section, channels, angles, box sections and Z-sections were included in their studies.

3.3. Enhancing the axial behavior of all pultruded FRP profiles

Although pultruded FRP tubes have low self-weight and similar ultimate strength compared with steel, they have one-seventh of the modulus of steel. These features combined with thickness of the wall tube lead to buckling failure which prevents FRP pultruded member from reaching its ultimate strength. Thus, researchers have investigated on how to delay the buckling failure. Fam and Rizkalla [64] tested nine circular short columns cut from the ends of beams after testing to compare their behavior under different degree of concrete fill. According to the stacking sequence of glass fibre layers, different tubes were used to investigate the influence of laminate structure. The results of the pultruded tube with fibres only in the axial direction and filled with concrete reveal low ability to carry axial load compared with specimens of filament wound tubes that contain fibres in transverse direction. This is because the pultruded tube has low stiffness in the hoop direction to resist the lateral deformation of the concrete and to apply confining pressure.

Han et al. [65] studied the crushing performance of GFRP pultruded tube and the effect of wrapping with carbon or glass braid. Two values of braid thicknesses were used 0.3 mm and 1 mm. They stated that the crushing behavior had improved due to the restraint from braids to the crack propagation in the pultruded tube. In the same vein, Li et al. [42] confined hoop direction of the circular pultruded FRP tube with carbon fibre sheet. The numbers of carbon layers were limited between 2 and 8. The results revealed that the ultimate axial compressive stress increases when the number of CFRP sheets are increased for specimens of equal wall thickness.

Correia et al. [44] could increase the critical buckling load, the ultimate load and the axial stiffness of hybrid specimen by 14%, 13.5%,
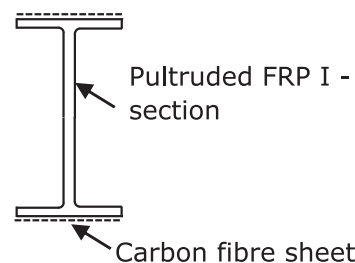
Fig. 7. Improving the behavior of pultruded I-section.

and 30% respectively than reference specimens of pultruded FRP I-section by adding carbon fibre sheet to the flanges as shown in Fig. 7.

The partial replacement of glass fibre with carbon fibre for pultruded FRP I-section to improve its axial performance was investigated by Nunes et al. [66]. Specimens were divided into four series in addition to the reference group. Each series includes short, intermediate and long columns. Specimens were prepared by using unidirectional and bidirectional carbon mats. The results showed the replacement method increases the axial stiffness of columns up to 17% and the load of global buckling rises in a range from 10% to 17%. In contrast, the load carrying capacity of the short and intermediate columns that fail by buckling was reduced by (1–13%) than reference columns due to delamination in the carbon mats. Further study needs to be conducted to enhance the axial behavior of all FRP columns. This enhancement can be obtained by overcoming the deficiency of the low axial stiffness and high wall slenderness ratio. Furthermore the stacking sequence of the fibre layers, their orientation, dimensions of the FRP profile together with the type of fibre type can be varied to investigate the effect of them on the axial behavior of all FRP columns.

3.4. Summary of all FRP column members

Pultruded FRP profiles have fibres oriented either totally or mostly towards axial direction compared to the other directions. This feature makes these sections behave better as column members. The main drawback that affects adversely in its axial behavior is low axial stiffness and length-thickness ratio of the wall plate (b/t). Both of these issues prevent FRP columns to reach their ultimate strengths. Studies in this area have focused on two objectives. The first one is increasing the accuracy of the predictive models and looking for the new methods to improve the load carrying capacity of FRP column profiles. The general frame of the calculated models is to determine the load values of local and global buckling and then, compare the results with ultimate compressive load of the section. The lower value among them is the safe load that should be considered in the design. The second objective is strengthening the low axial stiffness of FRP profiles. In order to do that, researchers either replace the fibre of low stiffness with fibre of high stiffness or confine the transverse direction of the FRP profile with FRP material to delay the delamination in the FRP column section. Summary of past studies on all FRP columns are shown in Table 2.

4. Hybrid FRP column members

The hybrid FRP column member is a combination of FRP profile with traditional structural materials such as steel and/or concrete. The purpose of this type of FRP column is to achieve improved performance due to composite action. The action of FRP material is generating a confining pressure on the concrete which it supports the steel profile against buckling. A variety of innovative, cost-effective and high-performance hybrid FRP column members have been studied by researchers. The following sections focus on these studies together with the numerical methods to evaluate the axial performances

Table 2
Summary on all FRP columns.

Reference	Cross section	FRP type	Stacking sequence (respect to the axial direction of the tube)	Enhancement methods	Critical load (kN)	Failure mode
Barbero and Raftoyiannis [43]	Box I-section	–	Pultruded	Analytical model	–	LB
Barbero and Tomblin [52]	I-section	–	Pultruded	–	79.2–174	LB + GB
Zureick and Scott [53]	I-section square	E-glass	Vinyl ester matrix reinforced with E-glass roving and nonwoven mats was used to made sections	–	33–494 54–334	GB
Fam and Rizkalla [64]	Circular	Glass	$1 - (+8°/-86°/(-86°/+8°)3/-86°$ $2 - (-88°/-88°/+4°/-88°/(-88°/+4°)2/-88°$ $3 - (0°)$ pultruded $4 - (-87°/+3°)4/-87°$ $5 - (+15°/-82°/(-82°/+15°)3/-82°$	Filled with concrete	350	Tube splits
Hashem and Yuan [46]	Universal square	E-glass	Specimens were made by using continuous filament at (0°), continuous mat and woven roving (0°/90°)	–	468–1361 185–663	LB, GB, CE
Puente et al. [54]	Circular	Glass	Pultruded	–	–	LB, GB
Qian et al. [49]	Circular	Glass	Short Pultruded tube. Long pultruded tube	–	71–92 10–60	LC GB
Bai and Keller [57]	Rectangular	Glass	Pultruded	–	25–148	Delamination (shear failure)
Han et al. [65]	Circular	Carbon Glass	Pultruded	Insert FRP tube into glass or carbon braid		–
Correia et al. [44]	I-sections	Glass	Pultruded (layers of unidirectional roving and strand mat)	Adding carbon sheet in the outer face of flanges	533–625	LB
Godat et al. [50]	angle Rectangular Square I- section	Glass	Pultruded	–	32.6 339 716 18.6–67	LB
Li et al. [42]	Circular	Glass	Pultrusion method (fibres lay in the axial direction)	Wrapping with CFRP sheet	Rupture CFRP sheet and splitting GFRP tube	
Gangarao and Blandford [56]	Square Wide flange	Glass	Pultruded	–	44.5 44.5	GB GB, LB, CM
Guades et al. [51]	Square	Glass	Pultruded	–	540–590	LB, CE
Cardoso et al. [55]	Square	Glass	Pultruded	–	13.2–957	GB, LB, CM, CE, LB + GB
Nunes et al. [66]	I-section	Glass	Pultruded	Partial replacing of GF mats with CF mats	133–690	LB, web-flange split, GB + LB, GB

Notes: GB = Global buckling, LB = Local buckling, CE = Crushing at end, CM = crushing at mid, GB + LB = buckling interaction, LC = longitudinal crack.
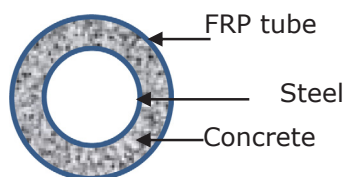
Fig. 8. Hybrid columns.

4.1. Columns with circular FRP and steel tubes

The first type of columns (Fig. 8) with a diameter of 152.5 mm and height of 305 mm consists of outer FRP tube, inner steel tube and the space between them filled by concrete were tested by Teng et al. [67]. The FRP tubes were fabricated by wrapping process of fibres oriented mainly in the hoop direction. They reported that the test results confirmed the positive influence of confinement on the concrete which it supports by the inner steel tube against buckling.

Fanggi and Ozbakkaloglu [68] examined the effect of inner steel tube diameter, concrete infill and loading pattern on the axial behavior of FRP-concrete-steel composite columns. They tested 32 specimens with concrete filled FRP tubes and two types of double-skin tubular columns (DSTCs). The inner steel tube in the first type was filled with concrete while it was kept unfilled in the second one. The dimensions of FRP tubes were 152.5 mm in diameter and 305 mm in height, and they were formed by layup process of S-glass fibre in the hoop direction. The unconfined concrete strength of the filler was ranging from 82.4 to 96.2 MPa. The results of filled specimens that were confined by both

FRP and steel tubes show a high level of improvement than others that were confined by FRP tube only due to the dual effects of FRP and steel confinements on the concrete. DSTCs specimens exhibit higher strength under cyclic loading as well. According to the study, the axial behavior was improved for filled compared to that of the hollow DSTCs especially when the diameter of inner steel tube increases (Fig. 9).

Ozbakkaloglu [69] investigated the effect of filling DSTCs with different concrete grades. Depending on the fill conditions of the inner steel tube, three series of specimens were set; hollow, filled with the same concrete that was used to fill annular section between tubes and filled with concrete of higher strength than that used to fill annular section. The research showed that specimens with dual grade concrete exhibit superior compressive behavior than those with single grade concrete.

Zhang et al. [70] tested FRP-concrete-steel double skin tubular columns (DSTCs) under seismic loading. In order to simulate seismic condition, columns were subjected to the axial compressive load and cyclic lateral loads. The dimensions of columns were 300 mm in diameter and 1350 mm in unsupported height. The point of applying lateral load lays at 175 mm from the upper end of the column. The space between FRP and steel tubes was filled with concrete at values of compressive strength ranging from 37 MPa to 117 MPa. The research concluded that the axial behavior of columns showed excellent ductility and seismic resistance even for those that were made out of high strength concrete. Also, they stated that filling the lower inner part of the steel tube with concrete resulted in better behavior.

Different types of concrete were used to cast hybrid FRP columns by Cao et al. [71], Zhou et al. [72] and Zhang et al. [73]. Cao et al. [71]

23
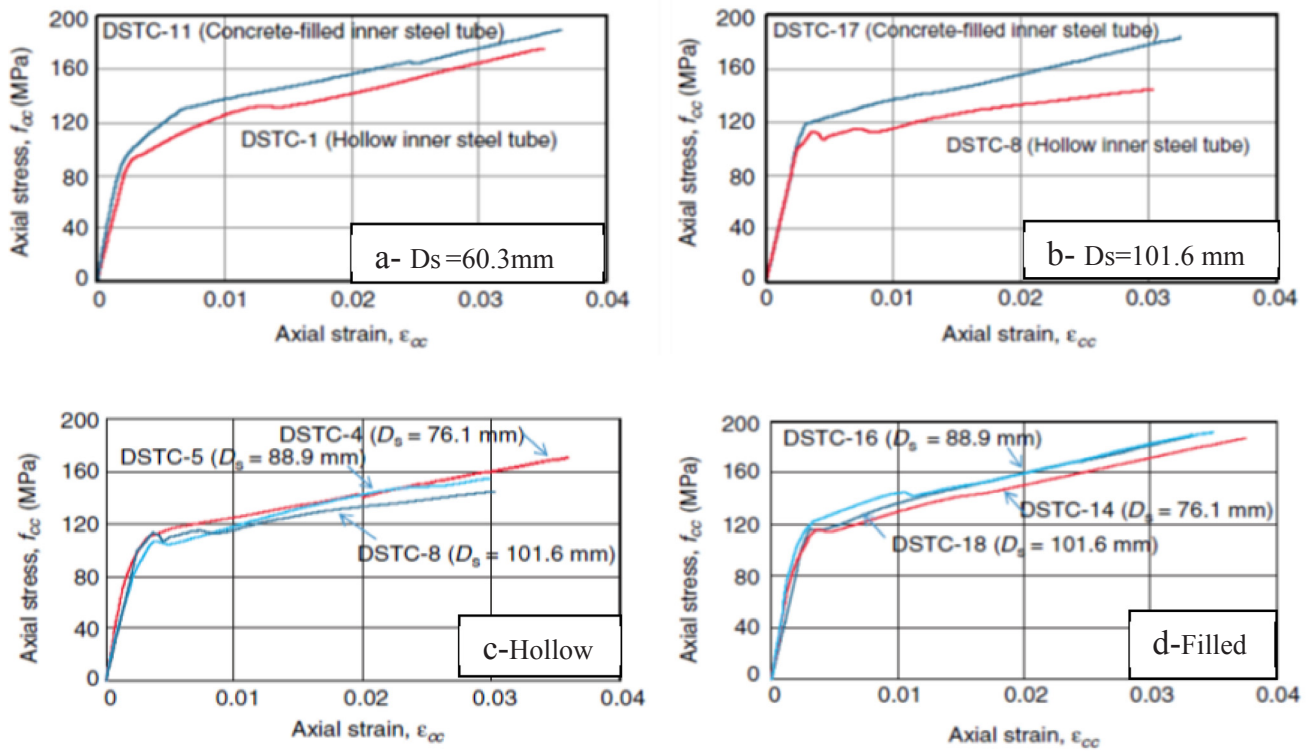
Fig. 9. Influence of the size and the filling of inner steel tube with concrete on the axial behavior of DSTCs [65].

prepared and tested three types of hybrid FRP columns; FRP-concrete steel double skin column, FRP confined solid concrete column and FRP confined concrete filled steel column. Self-consolidating concrete (SCC) and expansive self-consolidating concrete (ESCC) were used as the filler. They reported that creating prestress in the FRP tube influenced positively on the compressive behavior of all types of columns except those in the form of FRP–concrete steel double skin column. The reason for this behavior is due to the prestress in the FRP confined material related to the concrete expansion is not as high as that for other types of columns because the prestress in concrete close to the inner steel tube is much less than that close to FRP. Furthermore, the buckling of the hollow inner steel tube may influence adversely so that the effects of the prestress is not clearly visible in these columns. Use light weight concrete to fill the void between steel and FRP tubes to form the hybrid double skin columns was researched recently by Zhou et al. [72]. The results revealed that the light weight concrete was confined by FRP tubes effectively resulting in enhancements in the ductility and compressive strength. Zhang et al. [73] performed similar tests on double skin hybrid columns to examine the influence of using high strength concrete to fill the gap between FRP and steel tubes. The research concluded that the ductility of hybrid columns were not compromised even with high strength concrete filler.

4.2. Columns with circular FRP tube and different types of steel sections

A new form of a hybrid column was proposed by Xue and Gong [74]. Their columns consist of GFRP tube filled with concrete and reinforced with steel I- section. They investigated effects of concrete strength by using two types of both concrete (39.5 MPa, 51.6 MPa), and reinforcement ratio and three values of FRP wall thickness. Three types of GFRP tubes with same inner diameter and different wall thickness (4, 5, 6 mm) were fabricated using filament winding of fibres at an angle of 55° with the transverse direction and two different sizes of I-steel section. The reference specimen was a concrete filled GFRP tube. The research concluded that rupture of the GFRP tubes is the dominant failure
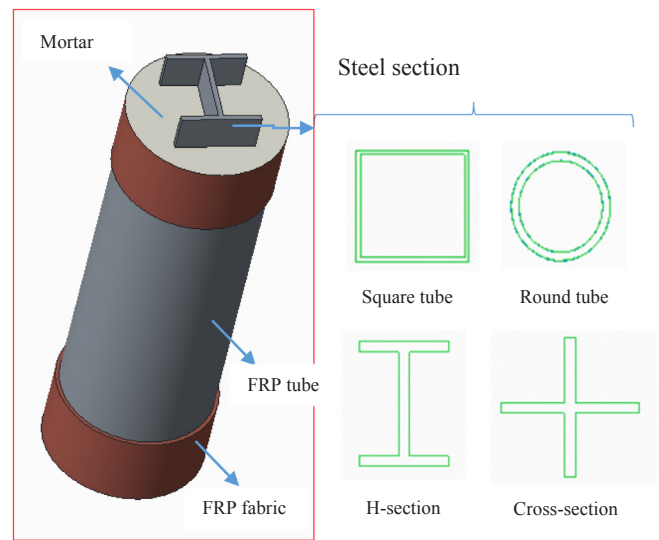
Fig. 10. Different steel sections in hybrid FRP-steel column.

mode, and the proposed hybrid column has higher strength and deformation (due to the steel I section reinforcement) than the concrete filled FRP tube.

The same type of hybrid FRP-steel column section was used by Zhang et al. [75] to strengthen the axial behavior of steel members (Fig. 10). They tested different cross sections of the steel core that were surrounded by pultruded FRP tube. The space between steel section and FRP tube was filled with mortar. The results reported in this study showed that both the bearing capacity and the capacity of axial deformation had been enhanced.

24

4.3. Other types of hybrid FRP columns

Hu et al. [76], Xie and Ozbakkaloglu [77] and Gao et al. [40] tested another type of hybrid FRP columns to examine the axial behavior of circular FRP tubes that were reinforced with either steel tube (no gap between FRP tube and steel tube), steel fibre or steel wire mesh and filled with concrete. FRP tubes were fabricated via wet lay-up procedure of unidirectional fibre sheet in the hoop direction. Hu et al. [76] tested three series of specimens with various diameters to thickness ratios of the steel tube and each series consisted of three confined specimens and one unconfined. The thickness of the FRP jacket was ranging from 0.17 to 0.68 mm. In this combination, steel tube is prevented to buckle inward and outward by the concrete and FRP jacket respectively. The research pointed out that the compressive behavior of concrete filled steel tube is improved because firstly, the buckling failure of steel tube is delayed by the FRP wrap, and secondly, additional confining pressure is created by FRP wrapping.

Xie and Ozbakkaloglu [77] used steel fibre to reinforce concrete filled FRP tubes. They studied the effect of fibre volume fraction, fibre aspect ratio and fibre shape on the axial behavior of specimens with dimensions 152.5 mm in diameter and 305 mm in height. The results indicate that the axial behavior is influenced significantly by the presence and the amount of steel fibre, whereas the fibre shape and its aspect ratio have less influence. Gao et al. [40] used wire mesh as a reinforcement to make hybrid FRP column. They reinforced their specimens that confined with FRP tubes by using a steel wire mesh and compared its results with unreinforced specimens. The thickness of GFRP tube and wire mesh volumetric ratio were chosen as research parameters. The test results show that the strength and ductility of reinforced specimens are improved.

4.4. Assessment of the axial behavior of the FRP hybrid columns

The confined concrete strength of FRP hybrid specimens (inner steel is empty) is calculated after subtracting the axial load resisted by the steel tube from the total load. Then, the concrete load at failure was divided by the cross sectional area of the concrete. The contribution of steel tube was assumed to be equal to the load carrying capacity of hollow steel tube. This procedure was followed by Teng et al. [67], Fanggi and Ozbakkaloglu [68] and Ozbakkaloglu [69]. A simple model of FRP hybrid columns was proposed by Yu et al. [78]. They modified the design oriented stress-strain model proposed by Teng et al. [35] to consider the influence of the hollow inner steel tube. This model was used to model the stress-strain curve of concrete in hybrid FRP columns subjected to cyclic axial compression and of high strength concrete in hybrid filament-wound FRP columns by Yu and Teng [79] and Zhang et al. [73] respectively. Another model was proposed by Yu and Teng [79] for the square FRP hybrid columns. The model of the FRP hybrid columns filled with light weight concrete was suggested by Zhou et al. [72]. In cases of filled inner steel tube, the concrete core will be confined by both FRP and steel tubes [76]. As a result, models of FRP confined concrete should be adjusted before using to shape stress-strain curves by considering the confinement effects of FRP and steel tubes. Gao et al. [40] investigated confinement effect of steel wire mesh and proposed model to predict the ultimate compressive behavior while a theoretical model had been proposed by Deng et al. [80] for FRP-steel concrete column.

4.5. Summary of hybrid FRP columns

The use of traditional construction material (steel and concrete) and the FRP tube to form hybrid FRP columns is similar to the first one because the orientation of fibres sets towards transverse direction of the column in order to create confining pressure. Furthermore, most studies were conducted on short column specimens. Although the main reason to innovate hybrid FRP columns is to provide the light weight property,

the hybrid FRP columns are ever evolving by the use of fillers, steel tubes or steel I sections. This process provides hybrid FRP–steel concrete column which can be researched in two ways. The first one is the axial behavior of hybrid column and the second one is the improvement in the axial behavior of steel section due to strengthening with concrete filled FRP tube. Table 3 gives a summary of research on FRP hybrid columns.

5. Gaps in knowledge

Factors that influence the degree of confinement are studied extensively in the past. Majority of the research used circular concrete specimens with height-to-diameter ratio equal to 2. These short columns will not fail due to local or global buckling. The combined effect of the slenderness ratio and effects of other factors that influence the degree of confinement are not investigated for columns at height-to-diameter ratio greater than 5 to specify how the axial strength and ductility of slender columns can be improved. Furthermore, it is important to study FRP confined lightweight concrete intensively because most previous studies examined the axial behavior of FRP confined normal concrete or high strength concrete columns. The confinement of the light weight concrete columns results in improvements in its ability to resist the axial load [29]. Consequently, the applicability to use FRP confined light weight concrete columns instead of unconfined normal concrete columns in construction industry will be increased. This will be an economical application because the dead load of the structural column members will drop.

A general study to describe the effect of potential variables in the behavior of pultruded FRP profiles having fibres in multiple directions is not done into greater depth in the past. Moreover, using a filler material with the pultruded FRP tubes to increase the stiffness of FRP tubes is not reported for short and slender columns.

The application and potential opportunities of FRP closed sections in civil and structural engineering will be improved due to further investigations into overcome the barriers that prevent them to be included in construction. Although extensive research have been done, significant and potential gaps in knowledge are still there. The combined effect of the slenderness ratio of the column and other factors such as strength of infill concrete, thickness and diameter of inner steel are not studied in depth. Particularly in the area of slenderness effects on the degree of confinement for concrete columns, the axial behavior of the hollow and filled pultruded FRP tubes that having fibre in multiple-directions and the different shapes of the hybrid FRP columns. Moreover, the use of lightweight concrete will provide an opportunity not to compromise much of the light weight feature of the FRP profiles. These areas will contribute to fill the gaps in knowledge which will improve the use of FRP tube in construction industry.

6. Conclusions

This paper reviewed three broad areas of FRP tubes in column applications in either new or existing construction; concrete columns confined by FRP, all FRP columns and hybrid FRP columns. Based on comprehensive review in this research area, the authors identify the following key findings.

- Research on FRP as a confinement has been well established over the last three decades which resulted in their enhanced structural applications.
- While research has been conducted on all FRP profiles, one of the major challenge is the adverse effect of buckling on overall axial performance. As a result there is a need to modify the cross sections in order to effectively utilize the capacity.

Research into the use of hybrid FRP columns is another area which will enhance the applications of these lightweight tubes. The following

25

Table 3
Summary of hybrid FRP columns.

Reference	Components of hybrid FRP columns	Cross section	FRP type	Stacking sequence[*]	Dimensions of steel tube (mm)		Gap between tubes (mm)	f_c' (MPa)
					d	t		
Teng et al. [67]	FRP tube, concrete, steel tube	Circular	Glass	Wrapping FRP sheet in the hoop direction	76.1	3.2	38.2	39
Fanggi and Ozbakkaloglu [68]	FRP tube, concrete, steel tube	Circular	S-Glass	Wet layup process of fibre sheet in the hoop direction	60–114	3.2, 6	–	82.4–96.2
Ozbakkaloglu [69]	FRP tube, concrete, steel tube	Circular Square	Aramid	(lay-up process) Unidirectional aramid fibre sheet	88.9, 114.3	3.2, 6	31.8, 19.1	49–113
Zhang et al. [70]	FRP tube, concrete, steel tube	Circular	Glass	Filament winding (± 80°)	219	6	40.5	37–114
Zhang et al. [75]	FRP tube, concrete, steel section	Circular	Glass	Pultruded GFRP tube	Cross, H, circle and square sections		–	36
Xue and Gong [74]	FRP tube, concrete, steel section	Circular	Glass	Filament winding (55°)[*]	I-section		–	39–51
Hu et al. [76]	FRP wraps, steel tube, concrete	Circular	Glass	Wet–layup with fibres in the hoop direction	202–204	1–2	0	35–42
Cao et al. [71]	FRP tube, concrete, steel tube	Circular	Carbon	(lay–up process) fibre sheet	150 114 89 60	3.5 4.5 4 4	–	26–32
Zhou et al. [72]	FRP tube, concrete, steel tube	Circular	Carbon	Alternate and orthogonal arrangement of unidirectional carbon fibre sheet	42 55 71	2 2 2	55.4 49.15 41.1	39.8
Zhang et al. [73]	FRP tube, concrete, steel tube	Circular	Glass	Filament winding (± 80°)	159 120 219	5 4.5 6	–	40–104
Xie and Ozbakkaloglu [77]	FRP tube, concrete, steel fibre	Circular	Aramid	(lay–up process) Unidirectional aramid fibre sheet	Hooked end, crimped steel fibre		–	116–125
Gao et al. [40]	FRP tube, concrete, steel wire mesh	Circular	Glass	(lay–up process) fibre sheet	reinforcement ratio of steel mesh (0.31, 0.6, 0.89)%		–	29.7

* Respect to the hoop direction of the column.

further investigations are recommended in order to address major challenges related to broader utilisation of FRP profiles in structural applications.

- Investigate the effect of the properties of filler material (light-weight, stiffness and creep) and properties of FRP (prestressed) on the behavior of FRP confined concrete columns under concentric and eccentric loads.
- Investigate the axial behavior of pultruded FRP profiles having fibres in the multiple directions under both concentric and eccentric loads for various cross section and support conditions.
- Comprehensive research work on FRP confined concrete column with larger length/least dimension ratio to study the combined effect of slenderness ratio and other factors.
- Examine the improvement in the strength and strain capacities of the non-circular concrete columns. This improvement can be created through confining the core of the concrete column with circular FRP tube that has fibres only in the hoop direction. This gives an opportunity to keep the original shape of the column and increase its capacity to resist loading.

Once these further studies are completed, there will be improved knowledge on the use of filled FRP tubes as column members which will enhance their applications in civil infrastructure.

Acknowledgment

Appendix A. Supplementary material

Supplementary data associated with this article can be found, in the online version, at https://doi.org/10.1016/j.compstruct.2018.07.109.

References

[1] Becque J, Patnaik AK, Rizkalla SH. Analytical models for concrete confined with FRP tubes. J Compos Constr 2003;7:31–8.
[2] Deskovic N, Triantafillou TC, Meier U. Innovative design of FRP combined with concrete: short-term behavior. J Struct Eng 1995;121:1069–78.
[3] Mortazavi AA, Pilakoutas K, Son KS. RC column strengthening by lateral pre-tensioning of FRP. Constr Build Mater 2003;17:491–7.
[4] Hong W-K, Kim H-C. Behavior of concrete columns confined by carbon composite tubes. Can J Civ Eng 2004;31:178–88.
[5] Kim H, Lee KH, Lee YH, Lee J. Axial behavior of concrete-filled carbon fiber-reinforced polymer composite columns. Struct Des Tall Spec Build 2012;21:178–93.
[6] Vincent T, Ozbakkaloglu T. Influence of fiber orientation and specimen end condition on axial compressive behavior of FRP-confined concrete. Constr Build Mater 2013;47:814–26.
[7] Teng J, Lam L. Behavior and modeling of fiber reinforced polymer-confined concrete. J Struct Eng 2004;130:1713–23.
[8] Qasrawi Y, Heffernan PJ, Fam A. Performance of concrete-filled FRP tubes under field close-in blast loading. J Compos Constr 2015;19:04014067.
[9] Beddiar A, Zitoune R, Collombet F, Grunevald YH, Abadlia MT, Bourahla N. Compressive behaviour of concrete elements confined with GFRP-prefabricated bonded shells. Eur J Environ Civ Eng 2014;19:65–80.
[10] Mirmiran A, Shahawy M, Beitleman T. Slenderness limit for hybrid FRP-concrete columns. J Compos Constr 2001;5:26–34.
[11] Vincent T, Ozbakkaloglu T. Influence of slenderness on stress-strain behavior of concrete-filled FRP tubes: experimental study. J Compos Constr 2015;19:04014029.
[12] Fitzwilliam J, Bisby LA. Slenderness effects on circular CFRP confined reinforced concrete columns. J Compos Constr 2010;14:280–8.
[13] Jiang T, Teng J. Behavior and design of slender FRP-confined circular RC columns. J Compos Constr 2012;17:443–53.
[14] Siddiqui NA, Alsayed SH, Al-Salloum YA, Iqbal RA, Abbas H. Experimental investigation of slender circular RC columns strengthened with FRP composites. Constr Build Mater 2014;69:323–34.
[15] Pessiki S, Harries KA, Kestner JT, Sause R, Ricles JM. Axial behavior of reinforced concrete columns confined with FRP jackets. J Compos Constr 2001;5:237–45.
[16] Fam A, Schnerch D, Rizkalla S. Rectangular filament-wound glass fiber reinforced polymer tubes filled with concrete under flexural and axial loading: experimental investigation. J Compos Constr 2005;9:25–33.
[17] Mirmiran A, Shahawy M, Samaan M, Echary HE, Mastrapa JC, Pico O. Effect of column parameters on FRP-confined concrete. J Compos Constr 1998;2:175–85.
[18] Ozbakkaloglu T, Xie T. Geopolymer concrete-filled FRP tubes: behavior of circular and square columns under axial compression. Compos B Eng 2016;96:215–30.
[19] Yan Z, Pantelides CP, Reaveley LD. Posttensioned FRP composite shells for concrete confinement. J Compos Constr 2007;11:81–90.

26

[20] Hadi MN, Pham TM, Lei X. New method of strengthening reinforced concrete square columns by circularizing and wrapping with fiber-reinforced polymer or steel straps. J Compos Constr 2012;17:229–38.

[21] Bhowmik T, Tan KH, Balendra T. Lateral load-displacement response of low strength CFRP-confined capsule-shaped columns. Eng Struct 2017;150:64–75.

[22] Youssf O, Hassanli R, Mills JE. Retrofitting square columns using FRP-confined crumb rubber concrete to improve confinement efficiency. Constr Build Mater 2017;153:146–56.

[23] Zeng JJ, Guo YC, Gao WY, Li JZ, Xie JH. Behavior of partially and fully FRP-confined circularized square columns under axial compression. Constr Build Mater 2017;152:319–32.

[24] Vincent T, Ozbakkaloglu T. Influence of concrete strength and confinement method on axial compressive behavior of FRP confined high- and ultra high-strength concrete. Compos B Eng 2013;50:413–28.

[25] Lim JC, Ozbakkloglu T. Factors influencing hoop rupture strains of FRP-confined concrete. Appl Mech Mater: Trans Tech Publ 2014:949–53.

[26] Yu T, Fang X, Teng J-G. FRP-confined self-compacting concrete under axial compression. J Mater Civ Eng 2013;26:04014082.

[27] Zhao J, Yu T, Teng J. Stress-strain behavior of FRP-confined recycled aggregate concrete. J Compos Constr 2014;19:04014054.

[28] Xie T, Ozbakkaloglu T. Behavior of recycled aggregate concrete-filled basalt and carbon FRP tubes. Constr Build Mater 2016;105:132–43.

[29] Zhou Y, Liu X, Xing F, Cui H, Sui L. Axial compressive behavior of FRP-confined lightweight aggregate concrete: an experimental study and stress-strain relation model. Constr Build Mater 2016;119:1–15.

[30] Lokuge W, Karunasena W. Ductility enhancement of geopolymer concrete columns using fibre-reinforced polymer confinement. J Compos Mater 2016;50:1887–96.

[31] Wang J, Feng P, Hao T, Yue Q. Axial compressive behavior of seawater coral aggregate concrete-filled FRP tubes. Constr Build Mater 2017;147:272–85.

[32] Ozbakkaloglu T. Compressive behavior of concrete-filled FRP tube columns: assessment of critical column parameters. Eng Struct 2013;51:188–99.

[33] Ozbakkaloglu T, Zhang W. Investigation of key column parameters on compressive behavior of concrete-filled FRP tubes. Appl Mech Mater 2012;256–259:779–83.

[34] Lam L, Teng JG. Design-oriented stress–strain model for FRP-confined concrete. Constr Build Mater 2003;17:471–89.

[35] Teng J, Jiang T, Lam L, Luo Y. Refinement of a design-oriented stress–strain model for FRP-confined concrete. J Compos Constr 2009;13:269–78.

[36] Ozbakkaloglu T, Lim JC, Vincent T. FRP-confined concrete in circular sections: review and assessment of stress–strain models. Eng Struct 2013;49:1068–88.

[37] Lim JC, Ozbakkaloglu T. Lateral strain-to-axial strain relationship of confined concrete. J Struct Eng 2014;141:04014141.

[38] Teng J, Huang Y, Lam L, Ye L. Theoretical model for fiber-reinforced polymer-confined concrete. J Compos Constr 2007;11:201–10.

[39] Mohamed HM, Masmoudi R. Axial load capacity of concrete-filled FRP tube columns: experimental versus theoretical predictions. J Compos Constr 2010;14:231–43.

[40] Gao C, Huang L, Yan L, Ma G, Xu L. Compressive behavior of CFFT with inner steel wire mesh. Compos Struct 2015;133:322–30.

[41] Vincent T, Ozbakkaloglu T. Compressive behavior of prestressed high-strength concrete-filled aramid FRP tube columns: experimental observations. J Compos Constr 2015;19:04015003.

[42] Li F, Zhao Q, Chen L, Shao G. Experimental and theoretical research on the compression performance of CFRP sheet confined GFRP short pipe. Sci World J 2014;2014:109692.

[43] Barbero EJ, Raftoyiannis IG. Local buckling of FRP beams and columns. J Mater Civ Eng 1993;5:339–55.

[44] Correia M, Nunes F, Correia J, Silvestre N. Buckling behavior and failure of hybrid fiber-reinforced polymer pultruded short columns. J Compos Constr 2012;17:463–75.

[45] Hassan NK, Mosallam AS. Buckling and ultimate failure of thin-walled pultruded composite columns. Polym Polym Compos 2004;12:469–81.

[46] Hashem ZA, Yuan RL. Short vs. long column behavior of pultruded glass-fiber reinforced polymer composites. Constr Build Mater 2001;15:369–78.

[47] Barbero EJ, Turk M. Experimental investigation of beam-column behavior of pultruded structural shapes. J Reinf Plast Compos 2000;19:249–65.

[48] Barbero EJ. Introduction to composite materials design. 3rd ed. Boca Raton, Fla: CRC Press; 2017.

[49] Qian P, Feng P, Ye L. Experimental study on GFRP pipes under axial compression. Front Archit Civ Eng China 2008;2:73–8.

[50] Godat A, Légeron F, Gagné V, Marmion B. Use of FRP pultruded members for electricity transmission towers. Compos Struct 2013;105:408–21.

[51] Guades E, Aravinthan T, Islam MM. Characterisation of the mechanical properties of pultruded fibre-reinforced polymer tube. Mater Des 2014;63:305–15.

[52] Barbero E, Tomblin J. A phenomenological design equation for FRP columns with interaction between local and global buckling. Thin-Walled Struct 1994;18:117–31.

[53] Zureick A, Scott D. Short-term behavior and design of fiber-reinforced polymeric slender members under axial compression. J Compos Constr 1997;1:140–9.

[54] Puente I, Insausti A, Azkune M. Buckling of GFRP columns: an empirical approach to design. J Compos Constr 2006;10:529–37.

[55] Cardoso DCT, Harries KA, Batista EdM. Compressive strength equation for GFRP square tube columns. Compos B Eng 2014;59:1–11.

[56] Gangarao HV, Blandford MM. Critical buckling strength prediction of pultruded glass fiber reinforced polymeric composite columns. J Compos Mater 2014;48:3685–702.

[57] Bai Y, Keller T. Shear failure of pultruded fiber-reinforced polymer composites under axial compression. J Compos Constr 2009;13:234–42.

[58] Qiao P, Davalos JF, Wang J. Local buckling of composite FRP shapes by discrete plate analysis. J Struct Eng 2001;127:245–55.

[59] Kollár LP. Buckling of unidirectionally loaded composite plates with one free and one rotationally restrained unloaded edge. J Struct Eng 2002;128:1202–11.

[60] Kollár LP. Local buckling of fiber reinforced plastic composite structural members with open and closed cross sections. J Struct Eng 2003;129:1503–13.

[61] Qiao P, Shan L. Explicit local buckling analysis and design of fiber–reinforced plastic composite structural shapes. Compos Struct 2005;70:468–83.

[62] Cardoso DC, Harries KA, Batista EdM. Closed-form equations for compressive local buckling of pultruded thin-walled sections. Thin-Walled Struct 2014;79:16–22.

[63] Ragheb WF. Development of closed-form equations for estimating the elastic local buckling capacity of pultruded FRP structural shapes. J Compos Constr 2017;21:04017015.

[64] Fam AZ, Rizkalla SH. Concrete-filled FRP tubes for flexural and axial compression members. Proceedings of ACMBS-3, Ottawa, Canada 2000:315–22.

[65] Han H, Taheri F, Pegg N. Crushing behaviors and energy absorption efficiency of hybrid pultruded and ± 45° braided tubes. Mech Adv Mater Struct 2011;18:287–300.

[66] Nunes F, Correia JR, Silvestre N. Structural behaviour of hybrid FRP pultruded columns. Part 1: Experimental study. Compos Struct 2016;139:291–303.

[67] Teng JG, Yu T, Wong YL, Dong SL. Hybrid FRP–concrete–steel tubular columns: concept and behavior. Constr Build Mater 2007;21:846–54.

[68] Fanggi BL, Ozbakkaloglu T. Behavior of hollow and concrete-filled FRP-HSC and FRP-HSC-steel composite columns subjected to concentric compression. Adv Struct Eng 2015;18:715–38.

[69] Ozbakkaloglu T. A novel FRP–dual-grade concrete–steel composite column system. Thin-Walled Struct 2015;96:295–306.

[70] Zhang B, Teng JG, Yu T. Experimental behavior of hybrid FRP–concrete–steel double-skin tubular columns under combined axial compression and cyclic lateral loading. Eng Struct 2015;99:214–31.

[71] Cao Q, Tao J, Wu Z, Ma ZJ. Behavior of FRP-steel confined concrete tubular columns made of expansive self-consolidating concrete under axial compression. J Compos Constr 2017;21.

[72] Zhou Y, Liu X, Xing F, Li D, Wang Y, Sui L. Behavior and modeling of FRP-concrete-steel double-skin tubular columns made of full lightweight aggregate concrete. Constr Build Mater 2017;139:52–63.

[73] Zhang B, Teng J, Yu T. Compressive behavior of double-skin tubular columns with high-strength concrete and a filament-wound FRP tube. J Compos Constr 2017;21:04017029.

[74] Xue B, Gong J. Study on steel reinforced concrete-filled GFRP tubular column under compression. Thin-Walled Struct 2016;106:1–8.

[75] Zhang Y, Feng P, Bai Y, Ye L. Morter-filled FRP tubes strengthening axially compresses steel members. 6th International conference on FRP composites in civil engineering. Rome, Italy; 2012. p. 1–6.

[76] Hu YM, Yu T, Teng JG. FRP-confined circular concrete-filled thin steel tubes under axial compression. J Compos Constr 2011;15:850–60.

[77] Xie T, Ozbakkaloglu T. Behavior of steel fiber-reinforced high-strength concrete-filled FRP tube columns under axial compression. Eng Struct 2015;90:158–71.

[78] Yu T, Teng J, Wong Y. Stress-strain behavior of concrete in hybrid FRP-concrete-steel double-skin tubular columns. J Struct Eng 2009;136:379–89.

[79] Yu T, Teng J. Behavior of hybrid FRP-concrete-steel double-skin tubular columns with a square outer tube and a circular inner tube subjected to axial compression. J Compos Constr 2012;17:271–9.

[80] Deng J, Zheng Y, Wang Y, Liu T, Li H. Study on axial compressive capacity of frp-confined concrete-filled steel tubes and its comparisons with other composite structural systems. Int J Polym Sci 2017;2017.

2.2 Summary

The review paper presents the usage areas of fibre reinforced polymer tubes in applications of civil infrastructure. It also shows the previous studies that are conducted for each type of use to specify gaps in knowledge that are needed for further research.

The key findings of the FRP confinement has been researched a lot during the last three decades and the buckling issues affect the axial behaviour of all FRP profile adversely. On the other hand, pultruded FRP profiles get high interest in the structural engineering as they have strength similar to steel strength and self-weight is much lower than that of steel. To utilise the potential strength of FRP tubes, it is necessary to prevent or delay buckling by increasing the axial stiffness of the FRP sections. One way to do that is using a filler material to support the wall against buckling and to increase the stiffness of FRP tube.

Therefore, this study concentrates on investigating the axial behaviour of pultruded FRP tubes in square and circular shapes using different types of fillers. Two types of normal concrete and lightweight perlite concrete were used as fillers. Moreover, the mechanical properties of the pultruded FRP tube is another factor that need to be examined for clarifying how the fibre orientation and their layup affect the tensile, compressive and shear strengths and modulus values. The properties of the filler materials are also investigated to figure out how they affect the stiffness, energy absorption capacity, load capacity and failure modes of the filled tubes.

Chapter 3 shows the details of material characterisation of pultruded FRP tubes and the fillers used in this study.

Chapter 3:

Characterisation of Materials

This chapter consists of two parts. Material characterisation of FRP tube and concrete are the first and second parts respectively. FRP material properties are presented as a research paper. The objective of the first part is to broaden the understanding of the correlation between the mechanical properties of pultruded fibre reinforced polymer tubes (PFRP) and their material constituents by investigating mechanical properties of several PFRP tubes. It presents the material characterisation tests for pultruded FRP tubes. Four types of material tests; burnout, tensile, compressive and shear tests were conducted for each type of pultruded square and circular FRP tubes. The results were discussed in terms of fibre orientation and fibre layup. Further details of the experimental individual results are shown in Appendix C.

The second part presents preliminary tests and the selected mixes of concrete infill. In the preliminary trials, four types of normal concrete and three types of perlite lightweight concrete were investigated. The concrete modulus and the compressive strength were computed and based on the results from the trial tests, two types of normal and two types of lightweight perlite concrete were selected to be used in the full scale testing of filled FRP tubes. The results of compressive strengths are used to understand the differences in failure modes and the stress-strain relationships for normal concrete and perlite concrete.

3.1 Paper 2:

Effects of fibre orientation and layup on the mechanical properties of the pultruded glass fibre reinforced polymer tubes

Ali Umran Al-saadi, Thiru Aravinthan and Weena Lokuge

University of Southern Queensland, School of Civil Engineering and Surveying, Centre for Future Materials (CFM), Australia.

Effects of fibre orientation and layup on the mechanical properties of the pultruded glass fibre reinforced polymer tubes

Ali Umran Al-saadi[1, 2], Thiru Aravinthan[1*] and Weena Lokuge[1]

[1] University of Southern Queensland, School of Civil Engineering and Surveying, Centre for Future Materials (CFM), Australia.

[2] University of Babylon, Iraq.

Email: AliUmranKadhum.Alsaadi@usq.edu.au, Thiru.Aravinthan@usq.edu.au, Weena.Lokuge@usq.edu.au

Abstract

Pultruded glass fibre reinforced polymer (PFRP) tubes are becoming popular in civil engineering applications due to their unique features. The focus of this paper is on column applications. It addresses the understanding of the correlation between the mechanical properties of PFRP and their material constituents. The burnout, tensile, compressive and shear tests were undertaken for square and circular PFRP tubes. The results show that increasing the percentage of axial fibre and decrease the angle of the non-axial fibre layer with respect to the axial direction lead to increase the tensile strength and modulus of FRP tubes. It further states that the better compressive properties can be obtained by increasing the axial and non-axial fibre content. The contribution of the oriented fibre layers to support the axial fibre against micro-buckling depends on their fibre content and orientation. Moreover, the shear properties are affected by the concentration of fibre in axial and diagonal tension field of shear forces. It is evident that the selection of appropriate FRP profiles with suitable fibre orientation is important for the targeted application for the best structural performance.

Keywords: Material characterisation; Coupon test; fibre content; fibre orientation; Pultruded FRP tube.

1. Introduction

The fibre reinforced polymer (FRP) material has been used in civil engineering applications as an alternative material to the traditional construction materials such as concrete and steel. The high strength to weight ratio, ability to resist corrosion and low maintenance cost are the attractive properties of FRP materials that have triggered researchers to work for dominating its safe adopting. Majority of fibres extend in axial direction is the main feature of pultruded GFRP profiles compared with other GFRP tubes. Using pultruded FRP profiles as an axial compression member or beams is increased in civil engineering applications due to their low-weight , high durability, low conductivity, ease of assembly and faster construction. Moreover, the cost of pultrusion manufacturing is low as it is continuous process to produce unlimited length profile with various cross-section shapes. Since they have low stiffness associated with thin wall thickness, buckling sensitivity in the serviceability limit state is an important issue in the design of pultruded structural members.

In order to address the above issues, experimental investigations on different shapes of pultruded FRP sections to study their axial behaviour and then propose a model to determine the load capacity was an approach followed by many researchers [1-6]. The other approach followed [7-11] was to assume the local buckling as a plate buckling problem and conducting an analytical study of FRP plate element by considering different kinds of loading and various states of restraint.

The experimental work in most of the previous studies consists of two parts. The first one focused on calculating the mechanical properties of FRP profiles which were used in the second part of the full-scale experimental tests. Generally, the first part did not receive enough attention from researchers other than determining the mechanical properties to be used in the proposed models to assess the load carrying capacity of pultruded FRP columns.

The improvement in the mechanical properties of hybrid composites were studied by Motoc et al. [12] . Different volume fraction ratio of glass fibre strand mat and uni-directional carbon fibre were used to prepare 5 –ply laminate composite specimens. Two values of uni-directional carbon fibre orientation were considered in preparing composite specimens 0˚ and 90˚. The results show that both the tensile and flexural properties are improved as the content of carbon fibre reinforced content increases.

For the same fibre content, the orientation of uni-directional carbon fibre causes a reduction in tensile modulus by around 50% when its angle increases from 0˚ to 90˚. Zhang et al. [13] studied effects of fibre orientation on the tensile strength and elastic modulus of the pultruded GFRP material. They conducted uniaxial tensile test for eighty coupons specimens with different fibre orientation from 0˚ to 90˚. The results show that when the angle of non-axial fibre layer decreases with respect to the axial direction the tensile properties improved.

Expanding the knowledge about the effect of fibre orientation and its layup on the FRP strength and modulus compliments the efforts in obtaining improvements in the axial behaviour of pultruded FRP tube columns.

This paper presents four types of tests conducted using square and circular pultruded GFRP tubes. These tubes are currently being used in civil infrastructure. They were selected mainly to investigate the effect of fibre orientation and its layup on the mechanical properties of the PFRP tubes.

2. Research significance

The mechanical properties of pultruded FRP tube depend mainly on the properties of its constituent material and on the structure of fibre layers. The aim of this study is to conduct material characterisation of pultruded FRP tubes and to understand how the properties are related to the fibre orientation and fibre layup. The finding of this study will provide an indication to improve the structural behaviour of pultruded FRP profiles by obtaining suitable fibre orientation and layup to create maximum properties. The significance of this work is to provide a comprehensive understanding of effects of fibre orientation in improving the mechanical properties of pultruded FRP profiles.

3. Experimental work

To conduct the experimental investigations, four types FRP tubes available in the market were selected consisting of two square and two circular tubes as shown in Table 1. Fig. 1 shows tubes that were planned to be used in the full scale testing. All

coupons were taken from the axial direction except those for the shear test of the square tubes which were taken from the transverse direction. All pultruded tubes are made of E-glass fibre and vinyl-ester resin except square tube S2 which is fabricated by using polyester resin. It should be noted that pultruded FRP tubes are selected as they are used in different application of civil engineering. Although S1 and S2 square tubes have a close dimension with different wall thickness, they have different fibre structure and made of various resin. Thus, the effect of fibre structure and resin properties on the mechanical properties can be studied.

Table 1. Details of the pultruded GFRP tubes

Tube notation	Shape	Dimensions (mm)	Fibre orientation(degrees)*
S1	Square	100 x 100, t = 5.2	0,+50,-50
S2	Square	102 x 102, t =6.4	0,+45,-45
C1	Circular	d=88.9, t=6.0	0,+56,-56
C2	Circular	d=88.9, t =6.0	0,+71,-71

*Fibre orientation with respect to the longitudinal axis
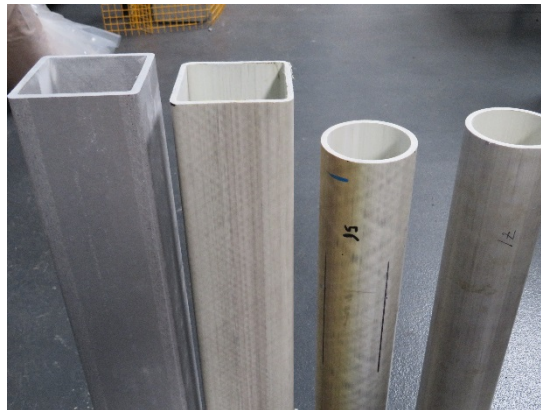
Fig.1 Pultruded FRP tubes.

3.1 Burnout test

The burnout test was conducted in accordance with ISO-1172 [14]. Three coupon specimens having dimensions of 20 mm in width and 30 mm in length for each tube were prepared (Fig. 2). The weight of the dry clean boat was taken to the nearest 0.1 mg. The coupon specimen was placed in the boat before reweighing the boat and coupon specimen. After that, the boat was placed in the furnace which was preheated to a temperature of 625˚C based on the standard to ensure calcination of matrix material and to keep non-combustible fibre content. Last of all, the boat was reweighed after calcination. The content of the fibre was obtained by determining the difference in weight of a specimen before and after the burning.

Fig. 2. Coupon specimens for burnout test.

3.2 Tensile test

The tensile test was performed on coupon specimens of the square and circular tubes according to ISO-527-4 [15] to ensure reaching failure load. Five coupon specimens were cut from each type of tube. Bi- axial clip-on extensometer was clipped to the coupon specimen to measure the axial and lateral strains for the determination of Poisson's ratio. Two coupons were instrumented with 5 mm uniaxial strain gauge (FLA-5-11-1L) to determine full stress-strain curves of tensile test. A 100 kN capacity MTS testing machine was used for the tensile testing with a loading rate of 2 mm/min. The data of the tensile test was recorded by using the data logger system. The dog-bone shape of the coupon specimens was considered for square tubes and prism shape for circular tubes. The concave side at the ends of the coupon prism of the circular tubes was filled with a mix of epoxy and calcium carbonate (30% by volume) for a length of 50 mm. The purpose of the end filling is to increase the contact area between

the coupon specimen and grips of the test machine in order to prevent the slipping and to avoid end crushing of the coupon. The details of the coupon specimens are shown in Fig. 3 (a), (b) and (c) while Fig. 3 (d) shows the test set-up. Before testing, the coupon specimen was accurately clamped onto jaws of the testing machine to prevent slipping at the grip length and to avoid misalignment between the ends of the coupon specimens. When the axial strain reached 3000 microstrains, the extensometer was removed from the specimen to avoid any damage to the test equipment. The test was continued up to failure to determine the strength and the failure mode.
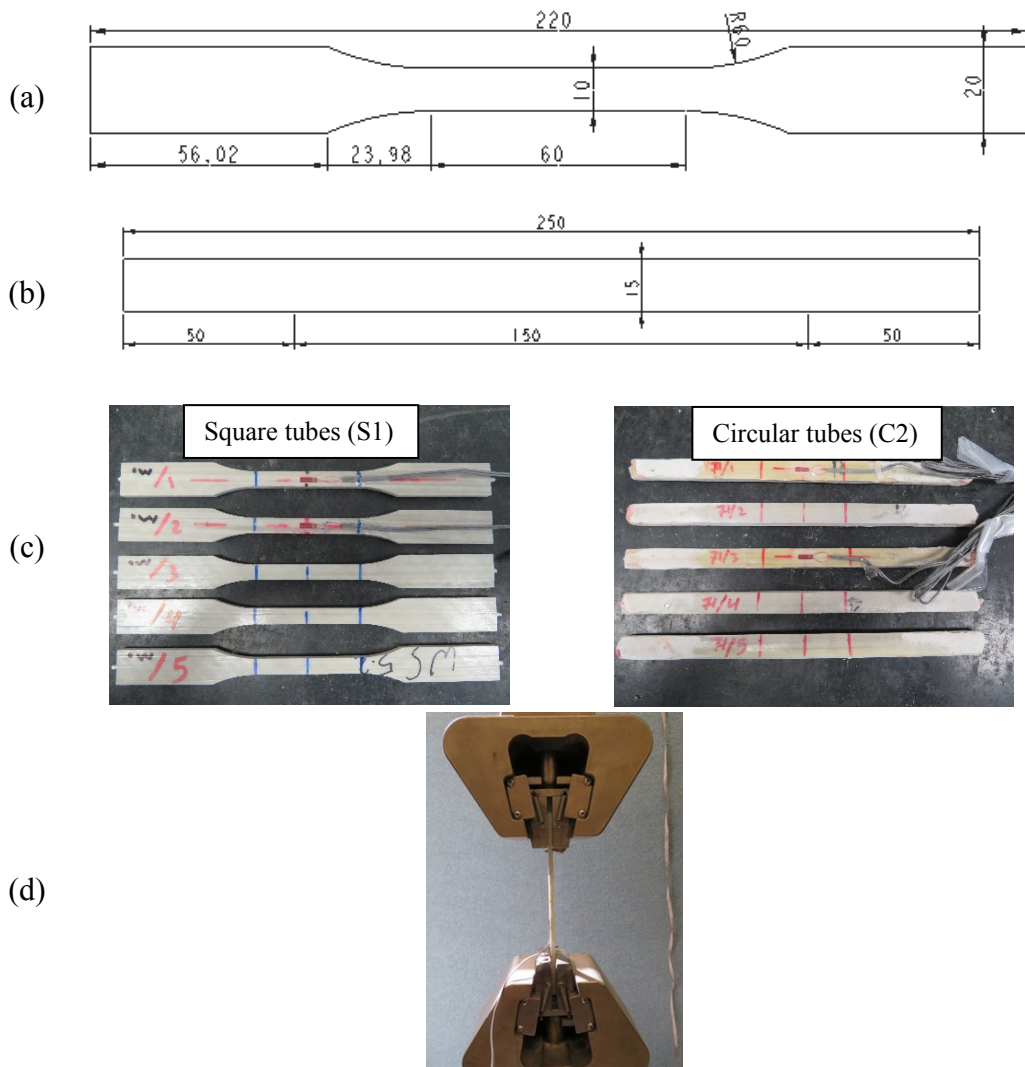
Fig.3. Details of tensile coupons (mm) (a) square tubes, (b) circular tubes, (c) coupon specimens of FRP tubes (d) tensile test set-up.

3.3 Compression test

The compression test of coupon specimens of different types of GFRP tubes was carried out according to the D695 [16] standard to ensure getting compression failure. The dimensions of prism coupons were estimated to keep the slenderness ratio (L/r) of the gauge length equal to 13 (Fig. 4). Coupon specimens of circular tubes were prepared in the same way as tension coupons to enhance the contact with machine grip. Two of the five coupon specimens were instrumented with 5 mm uniaxial strain gauge (FLA-5-11-1L) attached to the unsupported length. The coupons were carefully adjusted to being held by jaws of the testing machine correctly up to marks of the gauge length. The alignment of the coupon specimen was checked before testing to avoid the combined stress due to misalignment of the coupon specimens. The test was executed using MTS 810 testing machine with a loading rate of 1.3 mm/min. Compression test was continued until failure of the coupons. The data acquisition system 5000 was used to record the strain data. Fig. 4(e) shows compression test set up.
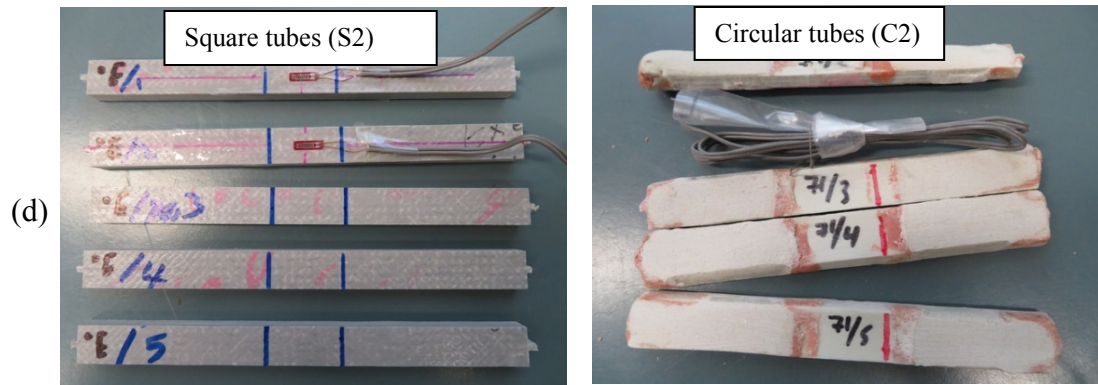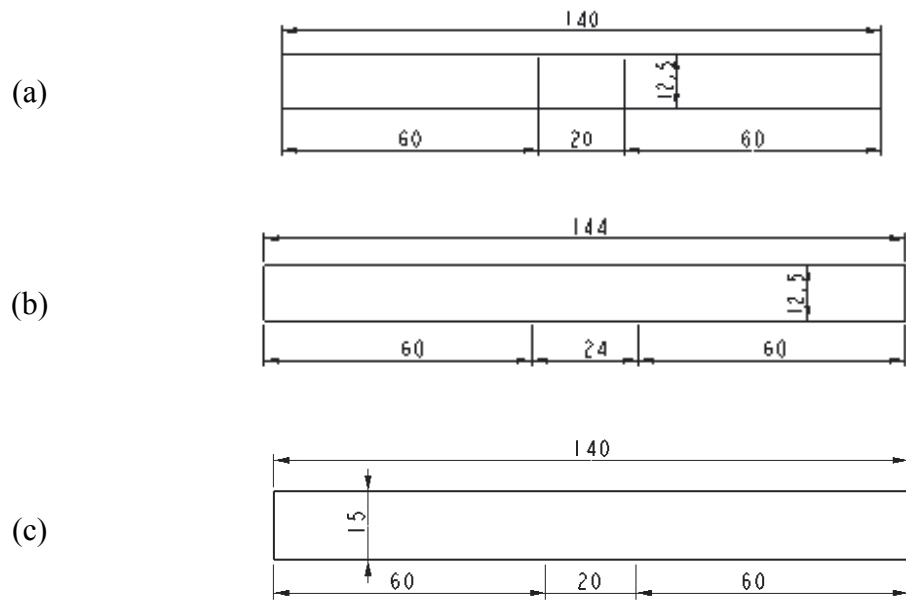
Fig. 4. Details of compression coupons (mm) (a) square tubes (S1), (b) square tubes (S2), (c) circular tubes, and (d) compression coupons of FRP tubes and (e) set-up of the compression test.

3.4 Shear test

The shear strength of the square tubes was carried out by using the V-notched test according to ASTM:D5379 [17]. This test was not conducted for circular tubes mainly due to the difficulty in preparing standard shear coupons from the transverse direction. The dimensions of the coupon specimen that was taken from the transverse direction of the square tubes are shown in Fig. 5 (a). A unique strain gauge (EC1-350-3HA-C-11-SD) was used to measure the shear strain at V-notch at ±45° angles. Fig. 5 (b) shows the samples that are ready to be tested. The shear coupon specimens were loaded on MTS testing machine using shear test fixture (Fig.5b) with a head speed of 1 mm/min. The data acquisition System 5000 was used to record the data from the load cell and the strain gauges.

(a)

(b)
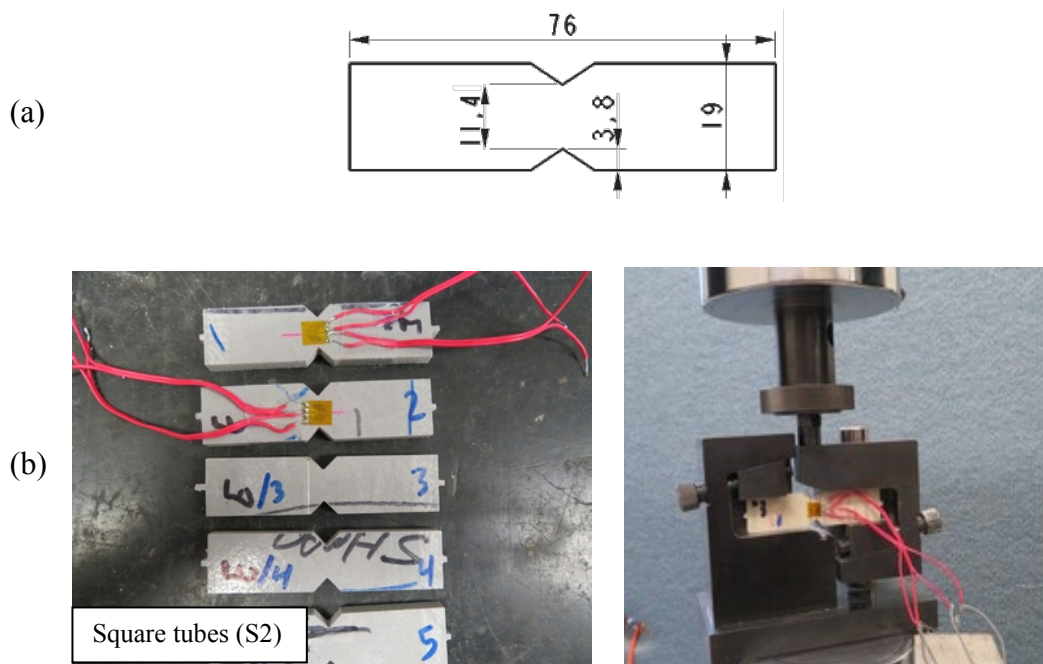
Fig. 5. Details of shear tests (a) Dimensions (mm) , (b) Coupons of squares tubes and test setup.

4. Results

4.1 Burnout test

The details of the burnout test can be shown in Table 2. The percentage of the fibre content of square tube S1 is higher than that of the square tube S2 by 7 % while circular tube C1 has fibre content larger than the circular tube C2 by 1.5 %.

Table 2. Results of burnout test for pultruded GFRP tubes.

		S1		S2		C1		C2	
	Unit	Average	SD	Average	SD	Average	SD	Average	SD
Fibre content	%	77.32	2.394	72.20	0.042	79.50	0.806	78.30	0.482
Density	g/cm^3	1.943	0.045	2.007	0.009	2.058	0.039	2.082	0.032
Fibre orientation	Degrees	0, +50, -50		mat, -45,0, +45		0, +56, -56		0, +71, -71	
Fibre content / layer	%	82.2, 8.9, 8.9		9.4, 9.5, 71.6, 9.5		74.4, 12.8, 12.8		56.0, 22.0, 22.0	

The stacking sequences of the fibre layers in the pultruded GFRP tubes were investigated after separating the layers of fibres. It is described below using 0˚ direction as the axial direction of the tube. The orientation of the fibre layers from the exterior to the interior of the wall is (0˚, 50˚, -50˚, 0˚, -50˚, 50˚, 0˚) and (mat,-45˚, 0˚, 45˚, mat) for the square tubes S1 and S2 respectively. The fibre orientation of C1 and C2 circular tubes are (0˚, 56˚, -56˚, 0˚, -56˚, 56˚, 0˚) and (0˚, 71˚, -71˚, 0˚, -71˚, 71˚, 0˚) respectively. Fig. 6 shows the stacking sequence of the pultruded tubes.
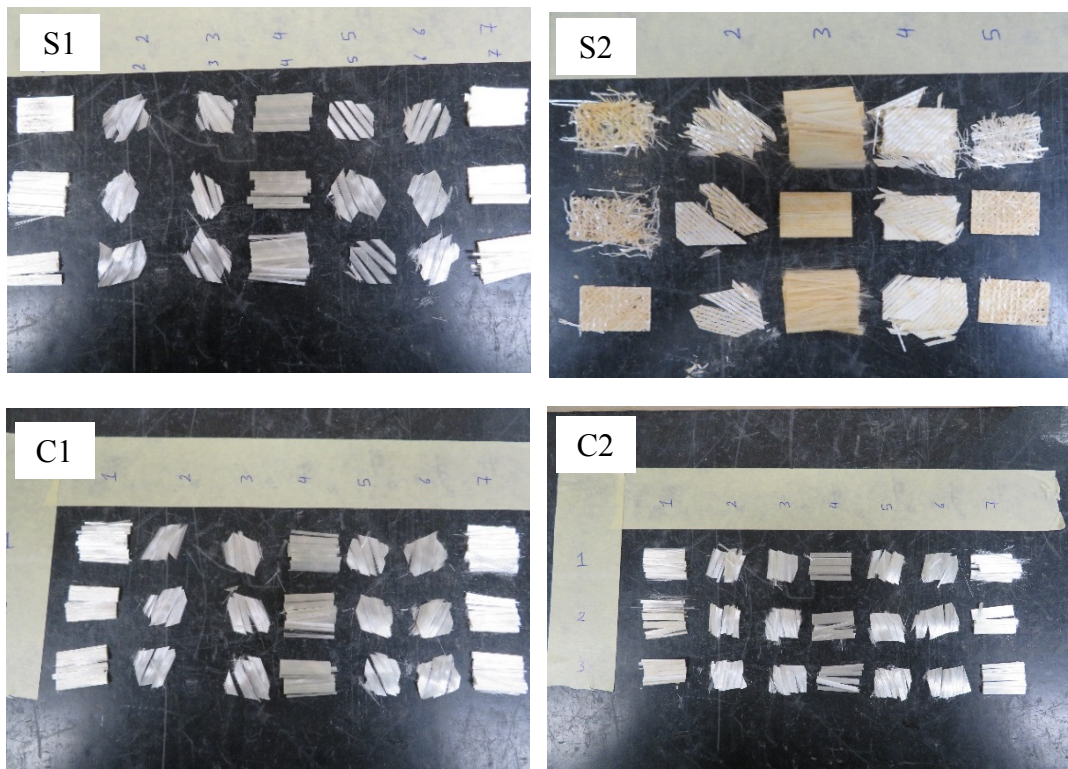
Fig. 6. Fibre layers of pultruded GFRP tubes.

4.2 Tension test

The load-displacement curves for all the tubes are shown in Fig. 7 to show the effects of fibre orientation and layup on the tensile properties of different FRP tubes. All coupons showed a linear behaviour up to the ultimate load capacity. The curves for square tubes S1 and S2 show a better similarity than those for circular tubes. This is due to the curvature in the coupons of the circular tubes which makes the possibility of coupon slipping. It indicates that the maximum tensile load of S1 ranges from (42.6 kN) to (45.6 kN) while the range of S2 square tubes is from (26.6 kN) to (32.2 kN). This is can be attributed to the difference in the fibre content in the axial direction. For the circular tubes, the range of C1 circular tubes is from (41.3 kN) to (48.3 kN) and it is from (34.0kN) to (42.8 kN) for the circular tubes C2. This difference in the range of tensile load is due to percentage of axial fibre and angle of the non-axial fibre layers which it governs their contribution to resist the tensile load. It also shows that the curves of C1 and C2 reveal the non-linearity due to tensile resistance of resin and non-axial fibres after failure in the axial fibres.
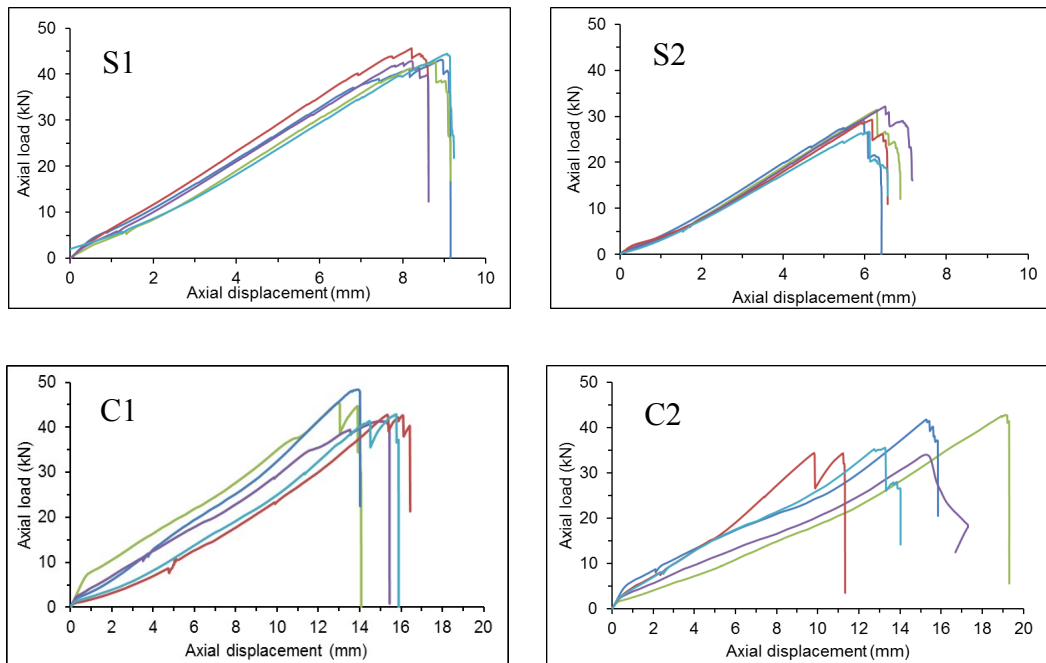
Fig. 7. Load-displacement curves of the tensile coupons.

The tensile stress for all the coupons was calculated by dividing the applied load by the cross-sectional area of coupons, while values of the tensile strain were measured using the uniaxial strain gauge at any time during the test up to failure. The tensile

elastic modulus was found by the slope of the linear part of the stress-strain curves of coupons using data of two points on the linear part. Poisson's ratio was computed by using the recorded data of the extensometer as a ratio of the transverse strain to the axial strain. The stress-strain curves of the coupon specimens that were instrumented with the strain gauges for all types of pultruded tubes under tensile loading are shown in Fig. 8.
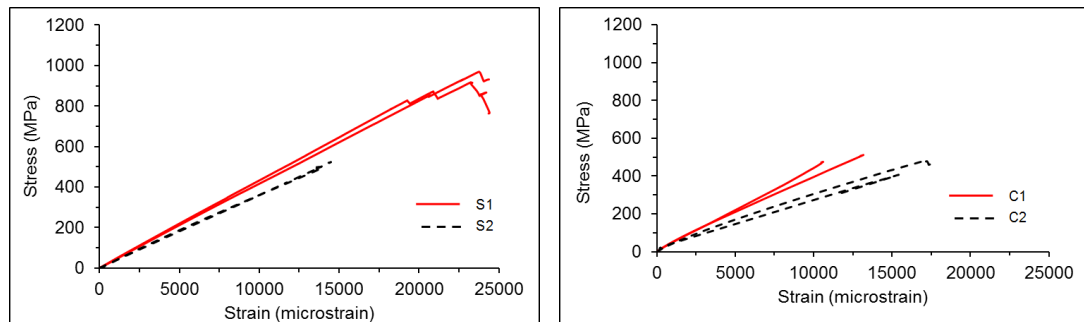
Fig. 8. The tensile stress-strain relationships of square and circular tubes.

Generally, the coupon specimens exhibit linear elastic behaviour in tension until the ultimate strength. The average tensile stress calculated in the axial direction of square tubes (S1) coupons is 952.8 MPa (Table 3) with approximate average strain value 23,500 microstrains. On the other hand, the average tensile stress calculated for coupon specimens of square tubes (S2) is 520.2 MPa with approximate average strain of 14,150 microstrains. The results of coupons of the circular tubes show that the average tensile strain of the circular tubes (C1) and circular tubes (C2) are 11,900 and 16,300 microstrains at average values of the tensile stress equal to 471.2 MPa and 419.9 MPa respectively. The results show that the average value of tensile modulus of pultruded FRP tube S1 and S2 are 42.60 GPa and 36.05 GPa respectively. The results show the impacts of fibre content and their orientation on the tensile properties of FRP tubes. The tensile modulus of circular tube C1 is higher than that of C2 by 51.0 %. Pultruded FRP tubes S1, S2, C1 and C2 show Poisson's ratio of 0.321, 0.229, 0347 and 0.232 respectively. It can be indicated that the percentage and orientation of non-axial fibre layers govern the value of Poisson's ratio.

Table 3. Tensile strength and modulus of pultruded GFRP tubes.

			S1		S2		C1		C2	
		Unit	Average	SD	Average	SD	Average	SD	Average	SD
Tension	Strength	MPa	952.8	25.51	520.3	35.08	471.2	31.70	419.9	48.53
	Modulus	GPa	42.60	0.849	36.05	0.636	40.40	3.536	26.75	2.051
	Poisson's ratio	-	0.321	0.023	0.229	0.035	0.347	0.025	0.232	0.010
	Peak strain	-	23,500	368.3	14,150	473.9	11,900	1813.9	16,300	1243.1

Tensile failure for all the coupon specimens occurred within the gauge length with no slip or failure in the grip length (Fig.9). The tensile failure was sudden with a loud noise in explosive manner. The failure modes of coupons show a correlation with the orientation of the fibre layers. The failure of coupons of the S2 square tube was a longitudinal splitting of layers through coupon thickness while coupons of other tubes (S1, C1 and C2) failed in the shape of layers separation as shown in Fig. 9.
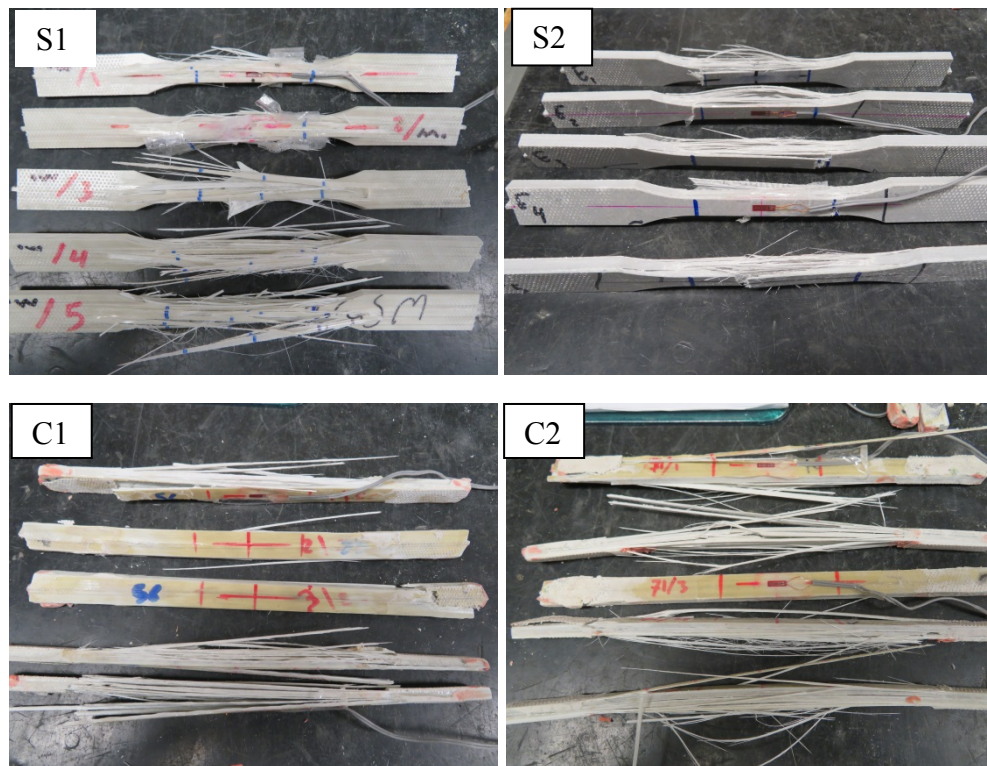
Fig. 9. Failure modes of tensile coupon specimens.

4.3 Compression test

The load-deformation behaviour for all the tests are shown in Fig. 10. The subsequent failure of plies can be noticed in the fluctuation in the load-displacement curves. Due to the curvature, the compression coupons of the circular tubes showed slipping which is similar to that observed in specimens of the tension coupons. The range of compressive load for square tube S1 is from (32.0 kN) to (33.4 kN) which is lower than the range of S2 (35.1kN- 43.0 kN) This is because the square tubes S2 has thicker wall. The contribution of oriented fibre layer to support the axial fibres against micro-buckling can be seen in results of circular tubes C1 and C2. The range of compressive load of C2 (31.5 kN- 43.5 kN) is higher than that of C1 (29.4 kN- 36.1 kN) as their percentage and angle of oriented fibres are larger than those of C1. Thus, the contribution of resisting will be higher.
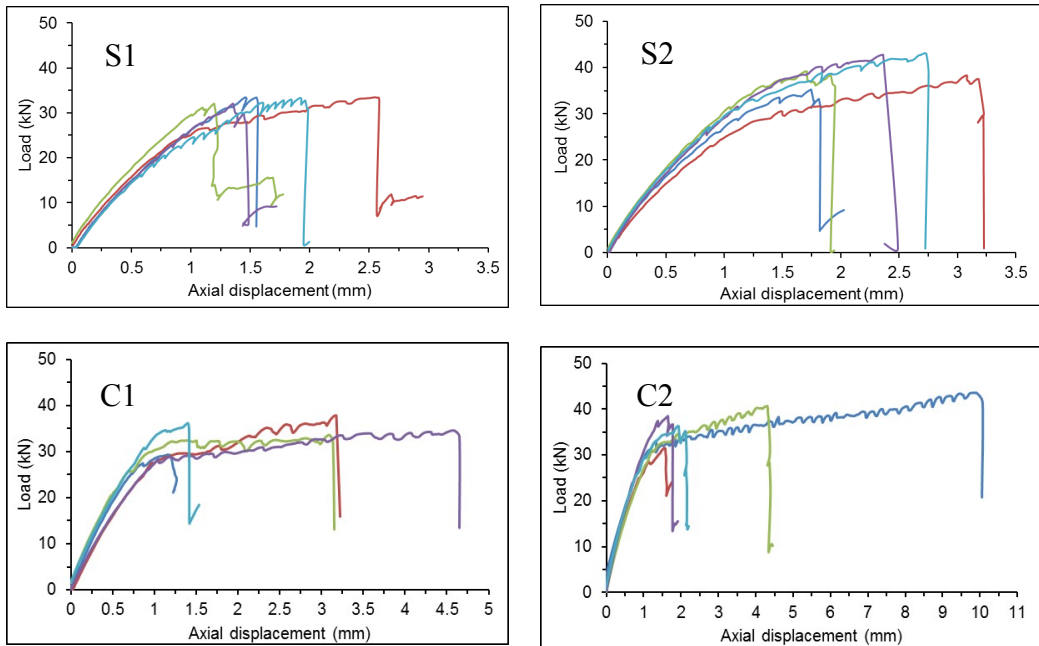
Fig. 10. Load-displacement curves of the compressive coupons.

The compressive strength of the coupon specimens was calculated by dividing the ultimate load by the cross-sectional area of the coupon. The data from the uniaxial strain gauges attached to the specimens were used to determine the peak compressive strain. The stress-strain curves of the compressive tests of the coupon specimens that were instrumented with the strain gauges for all types of pultruded tubes are shown in Fig. 11. The compressive elastic modulus was calculated as per D695 [16] standard

using the linear part of the stress-strain curve. The average compression stress of the square tubes (S1) coupons was 525.7 MPa (Table 4) with strain value of 12,150 microstrains as the strain gauge of the second specimen failed to measure the data. The coupon specimens of square tubes (S2) could reach to 506.2 MPa with approximate average strain at 11,460 microstrains. The results of coupons of the circular tubes show that the approximate average compressive strain of the circular tubes C1 and C2 are 7,300 and 13,500 microstrains while the average compressive stress are 365.5 MPa and 407.6 MPa respectively. The axial compressive modulus of coupons of the FRP tubes S1, S2, C1 and C2 are 49.50 GPa, 43.65 GPa, 49.35 GPa and 33.90 GPa respectively.   The strain values of coupons of circular tubes C1 and C2 show that increase fibre content and orientation from the axial direction leads to increase the compressive stress and strain.
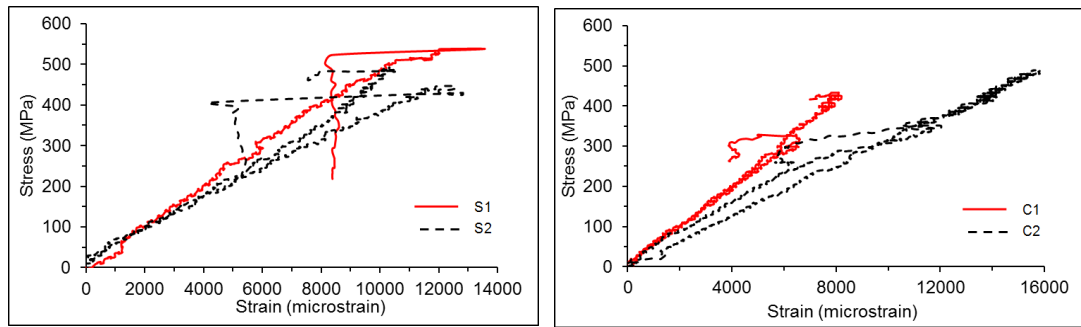
Fig.11. Compressive stress-strain relationships for square and circular tubes.

Table 4. Compression strength and modulus of pultruded GFRP tubes.

			S1		S2		C1		C2	
		Unit	Average	SD	Average	SD	Average	SD	Average	SD
Compression	Strength	MPa	525.7	8.643	506.2	44.03	365.6	42.22	407.7	52.68
	Modulus	GPa	49.50	-	43.65	3.040	49.35	4.596	33.90	2.121
	Peak strain	-	12,150	-	11,460	743.1	7,300	1155.5	13,500	3100.6

Compression failure for all of the coupon specimens was observed in the gauge length region with no failure in the grip length (Fig.12). The compression failure was gradually combined with low noise until the final failure with a loud noise. The separation of layers at failure can be noticed clearly in coupons of S2 compared with coupons of S1 and circular tubes C1 and C2 as shown in Fig. 12.
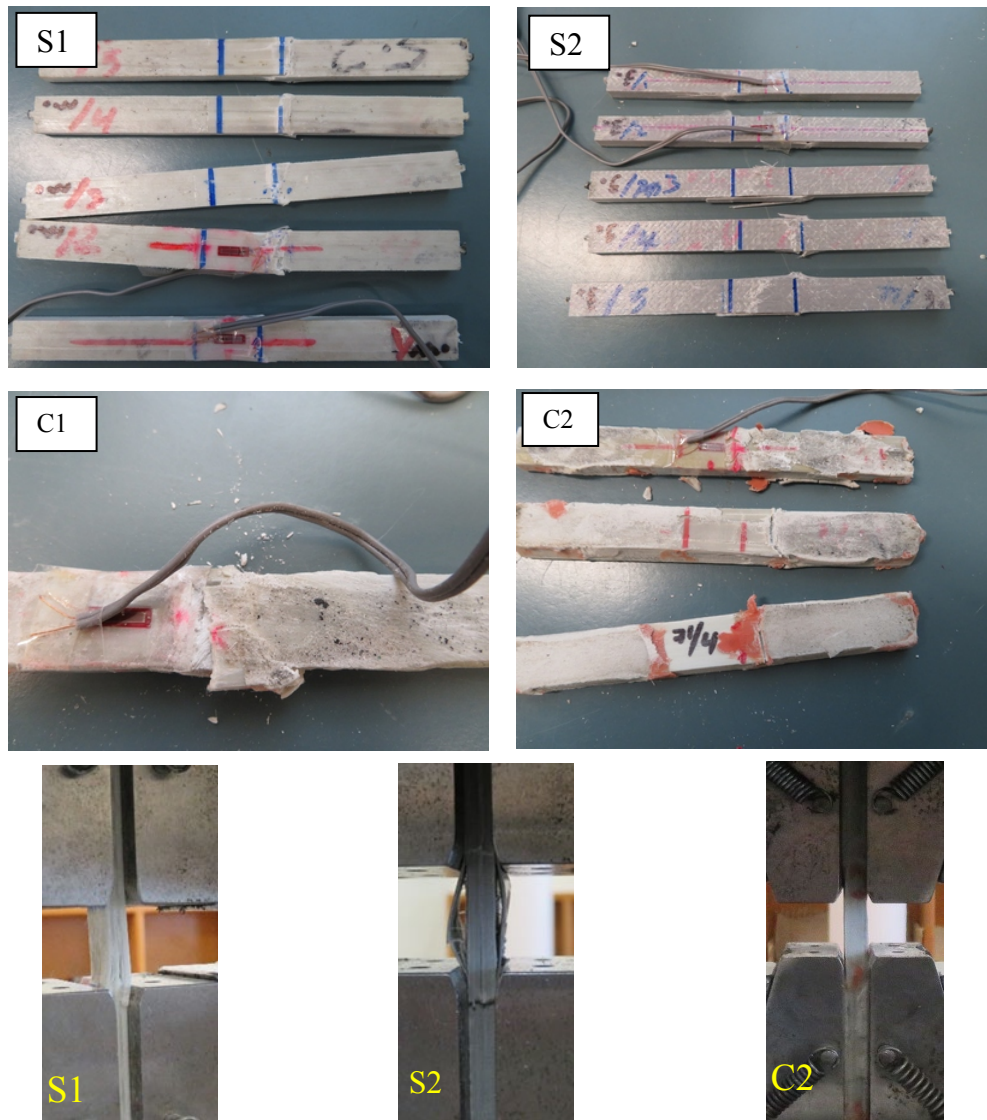
Fig. 12. Failure modes of the compression coupons.

4.4 Shear test

The shear strength and shear modulus of the transverse coupon specimens were calculated based on the ASTM:D5379 [17] standards. The shear stress is determined by dividing the applied load by the cross-section area of shear coupon at centre (between notches) while the shear modulus is calculated as the slope of the linear part of the shear stress-strain graph. Fig.13 shows the shear stress-strain curves of the square tubes while Table 5 shows the results of shear test for pultruded square tubes. It should be noted that the strain gauge of second specimen of S1 square tube did not work. Generally, the linear behaviour of the shear coupon of S1 square tube continued

up to 5,000 microstrains where a reduction in the stiffness was observed until failure. However, the linear behaviour of the shear coupon of S2 square tube was noticed only up to a shear strain ranged from 200-400 microstrains. The results of shear test shows that the shear strength of coupons of pultruded FRP tubes S1 is higher than that of S2. However, the shear modulus of S2 is larger than that of S1.
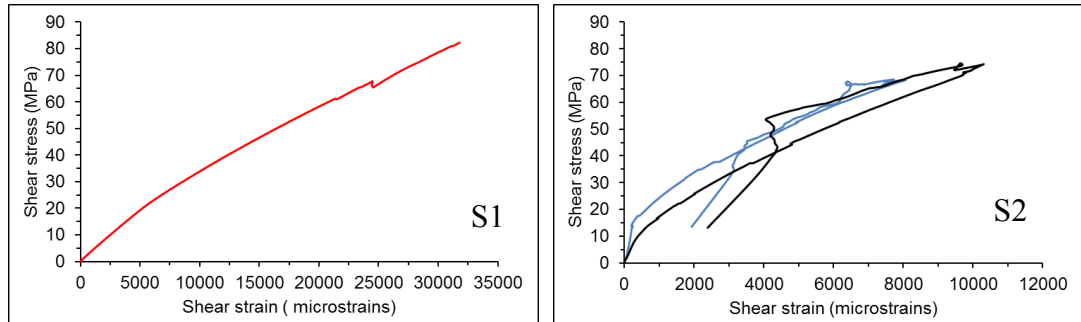
Fig.13. Shear stress-strain curves for coupons of the square tubes.

Table 5. Shear strength and modulus of pultruded square GFRP tubes.

			S1		S2	
		Unit	Average	SD	Average	SD
Shear	Strength	MPa	101.0	5.632	70.25	4.455
	Modulus	GPa	3.757	-	6.690	0.407

Fig .14 shows the failure of the shear coupon specimens of square tubes S1 and S2. The vertical cracking of the shear failure occurred at the notch region and at the side region.
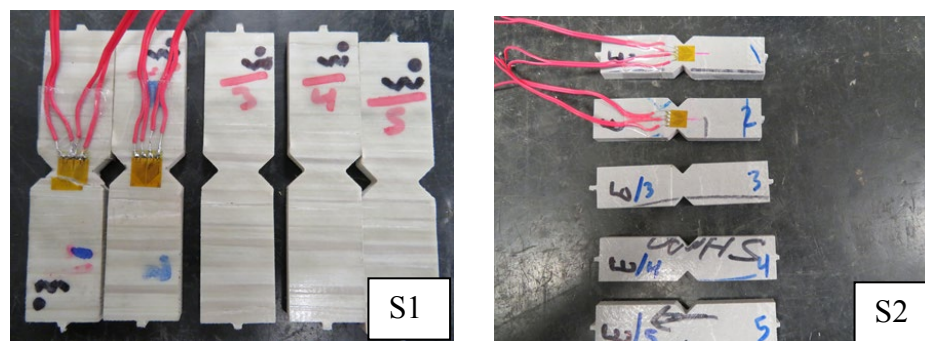
Fig. 14. Failure modes of the shear coupons.

5. Discussion

Table 3 shows the average results of tension test for the four types of pultruded GFRP tubes. The results show that the fibre orientation and fibre layup affect the tensile properties of pultruded FRP tubes. The tensile stress and tensile modulus of S1 square tube coupons are higher than those of S2 square tube as shown in Fig. 8. This can be attributed mainly to the fibre layup where the percentage of the fibre content of the axial layers (0˚) of S1 square tube is higher than that of the S2 square tube by 10.4 %. Although the major resistance to the tensile load generates by fibres, the other reason could be due to the difference in properties of the resin which binds the fibre layers. S1 tubes are made of vinyl ester resin while S2 are made of polyester resin. It is reported that the tensile strength of the vinyl ester resin on average is higher than that of the polyester resin[18] .

The stress-strain curves of circular tubes C1 and C2 are matching in the initial part and show a significant difference afterwards (Fig.8). This is because the contribution of the non-axial fibre layer of C1 to resist the tensile load after failure of the axial fibres is higher than that of C2 as the angle is smaller with respect to the axial direction. Although both types of the circular tubes have approximately the same total fibre content, the variation in the mechanical properties is due to the fibre orientation and fibre layup. C1 circular tube has fibre layers oriented closer to the axial direction compared with the C2 circular tube. As a result, the contribution of the fibres to resist tensile stress of C1 is higher, and the resistance to the lateral deformation (strain) will be lower than C2 tubes. Thus, the Poisson's ratio of the circular tube (C1) is 49.5 % more than the Poisson's ratio of the circular tube (C2). The fibre layup is the second reason where the percentage of the fibre content in the axial direction of the C1 is larger than that of C2 while the percentage of fibre in the non-axial fibre layers is lower than that of the C2 (Table 2).

The results of the compression tests (Table. 4) show that the fibre layup and fibre orientation have a significant influence on the results of the square tubes. The high compressive stress and compressive modulus were observed (525.7 MPa, 49.5GPa) for coupons of the square tube S1 compared with the values of the square tube S2

(506.2 MPa, 43.6GPa). This is because firstly the percentage of the axial fibre in the S1 is greater than that of S2. Secondly, the angle of the non-axial fibre layer of S1 with respect to the axial direction is greater than the angle of S2. Thus, the support against micro-buckling will be higher. The orientation of the fibre layers is the main parameter to illustrate the results of compression test of circular tubes because C1 and C2 have approximately the same cross-sectional area and same fibre content. The resistance of the compressive load and support the axial fibre layers against micro-buckling are actions of the non-axial fibre layers. The circular tube C1 has a higher compressive modulus (49.3 GPa) compared with circular tube C2 (33.9 GPa) because fibres are oriented at 56° with the axial direction compared to 71° of the circular tube C2 and the percentage of fibre in the axial direction is higher than that of C2 . Thus, the non-axial fibre layers provide further resistance to the applied compressive load. On the other hand, the compressive stress of the circular tube C2 (407.6 MPa) is higher than that of circular tube C1 (365.5 MPa). This is because the contribution of the non-axial fibre layers in supporting the axial layers of fibres against micro-buckling of the circular tube C2 and percentage of non-axial fibres are higher than those of the circular tube (C1). Therefore, coupons of the circular tube (C2) can resist a high level of loading with high axial compressive strain .

Table 5 shows that the average shear strength of the transverse coupon specimens of the square tube S1 was 101.0 MPa, with approximate 31,800 microstrains ultimate shear strain while the average shear stress of the square tube S2 was 70.2 MPa with a shear strain of around 8,700 microstrains. However, the shear modulus of square tube S2 is larger than that of square tube S1. This is because firstly, the percentage of the axial fibres that are parallel to the loading axis of coupon specimens of S1 is larger than the axial fibre of S2. Secondly, the percentage of non-axial fibre layers on the diagonal tension field of the shear forces in S2 is higher than that of S1. Finally, the shear strength of the Vinylester resin of square tube S1 (53 MPa) is higher than that of the Polyester resin of the square tube S2 (45 MPa) [18] .

It should be noted that the structural and mechanical properties of the pultruded square tube S1 had been investigated previously by Guades et al. [19]. Although, tubes of previous and current studies are from the same supplier, the GFRP tube used in this study are not similar to the one used in the previous study [19] as the number and orientation of fibre layers of the tubes they used are nine (9) and 45 degrees

respectively while they are seven (7) and 50 degrees in case of the S1 pultruded FRP tube used in this study.

As the thickness of fibre layers is proportional to its fibre content, the calculations of the separated fibre layers of the tube in this study shows that the thickness of the mid-fibre layer is higher than the thickness of the mid layer of the previously reported tube [19] by three times. As a result, the value of the wall thickness is unchanged. The results of the burnout test shows that the current tube has fibre content larger than the previous tube by 1.3 %. It appears that the non-axial fibre layers of the current tube is oriented at an angle larger than that of the previous tube. Therefore, the mechanical properties of the current FRP tube are not as those of the previous study. Table 6 shows the tensile and compressive strength and modulus of the square tube S1 of the previous[19] and current studies in the axial direction .

Table 6. Comparison of mechanical properties of the square tube S1 [19].

	Strength (MPa)		Modulus (GPa)	
	Previous	Current	Previous	Current
Tensile	618	952.8	39.2	42.6
Compressive	459	525.7	51.1	49.5

The tensile strength and modulus in the axial direction of the tube used in this study are higher than the values reported in the previous study [19] . This can be attributed mainly to the percentage of the fibre content. On the other hand, the compressive modulus is higher and the strength is lower for the tube in the previous study than those for the tube in the current study. This can be attributed to the fibre content and to the contribution of the non-axial fibre layer in resisting the axial compressive load and in supporting the axial fibre layer against micro-buckling.

6. Conclusions

This study reports the results of the coupon tests of square and circular pultruded FRP tubes. The mechanical properties of different FRP tubes are discussed in terms of the fibre orientation and their layup. Based on the results obtained from the experimental material tests, the following conclusions can be drawn:

- The results of tension material test of square tubes verify that the high tensile strength and modulus can be obtained by increasing the percentage of fibres in the axial direction. On the other hand, the results of the circular tubes reveal that the tensile strength and modulus are increased as the angle of the fibre layers with respect to the axial direction is decreased and fibre percentage in the axial direction increases.

- Both the fibre layup and fibre orientation have influenced the compression strength and modulus. In case of square tubes, the higher values are obtained for the square tubes S1 as they have high percentage of axial fibre and the angle of the non-axial fibre layers in the S1 is greater than that of S2. However, in case of the circular tubes, the compressive strength decreases while the modulus increases as the percentage of fibres and angle of the non-axial fibre layer with respect to the axial direction decrease. This is because the contribution of the non-axial fibre layer to support the axial fibre layers against micro-buckling is reduced.

- The shear strength of resin and availability of the fibre layers in the diagonal tension field of shear forces govern the shear strength and modulus of pultruded FRP tubes.

The structural performance of pultruded FRP profiles in various applications of the civil engineering can be improved based on their material constituents. The stacking sequence of the fibre layers and their fibre content have positive impact to produce better mechanical properties in pultruded FRP profiles.

Acknowledgement

References

[1] Barbero E, Tomblin J. A phenomenological design equation for FRP columns with interaction between local and global buckling. Thin Walled Struct. 1994;18:117-31.

[2] Zureick A, Scott D. Short-term behavior and design of fiber-reinforced polymeric slender members under axial compression. J Compos Constr. 1997;1:140-9.

[3] Puente I, Insausti A, Azkune M. Buckling of GFRP columns: An empirical approach to design. J Compos Constr. 2006;10:529-37.

[4] Bai Y, Keller T. Shear failure of pultruded fiber-reinforced polymer composites under axial compression. J Compos Constr. 2009;13:234-42.

[5] Gangarao HV, Blandford MM. Critical buckling strength prediction of pultruded glass fiber reinforced polymeric composite columns. J Compos Mater. 2014;48:3685-702.

[6] Hassan NK, Mosallam AS. Buckling and ultimate failure of thin-walled pultruded composite columns. Polymers and Polymer Composites. 2004;12:469-81.

[7] Kollár LP. Buckling of unidirectionally loaded composite plates with one free and one rotationally restrained unloaded edge. J Struct Eng-ASCE. 2002;128:1202-11.

[8] Kollár LP. Local buckling of fiber reinforced plastic composite structural members with open and closed cross sections. J Struct Eng-ASCE. 2003;129:1503-13.

[9] Qiao P, Shan L. Explicit local buckling analysis and design of fiber–reinforced plastic composite structural shapes. Compos Struct. 2005;70:468-83.

[10] Cardoso DC, Harries KA, Batista EdM. Closed-form equations for compressive local buckling of pultruded thin-walled sections. Thin Walled Struct. 2014;79:16-22.

[11] Ragheb WF. Development of closed-form equations for estimating the elastic local buckling capacity of pultruded FRP structural shapes. J Compos Constr. 2017;21:04017015.

[12] Motoc DL, Bou SF, Gimeno RB. Effects of fibre orientation and content on the mechanical, dynamic mechanical and thermal expansion properties of multi-layered glass/carbon fibre-reinforced polymer composites. J Compos Mater. 2015;49:1211-21.

[13] Zhang S, Caprani C, Heidarpour A. Influence of fibre orientation on pultruded GFRP material properties. Compos Struct. 2018;204:368-77.

[14] ISO-1172. Textile-glass-reinforced plastics-Prepregs,moulding compounds and laminates-Determination of the textile-glass and mineral-filler content-Calcination methods. Geneve,Switzerland.1996.

[15] ISO-527-4. Plastics-Determination of tensile properties. Part4: Test conditions for isotropic and orthotropic fibre -reinforced plastic composites,European Committee for Standardization, Brussels, Belgium1997.

[16] D695 A. Standard Test Method for Compressive Properties of Rigid Plastics. United States2010.

[17] ASTM:D5379. Standard test method for shear properties of composite materials by the V-Notched Beam method United States2012.

[18] Daniel IM, Ishai O. Engineering mechanics of composite materials. 2nd ed. ed. New York: Oxford University Press; 2006.

[19] Guades E, Aravinthan T, Islam MM. Characterisation of the mechanical properties of pultruded fibre-reinforced polymer tube. Materials & Design. 2014;63:305-15.

3.2 Characterisation of filler material

Using filler materials with varied modulus for pultruded FRP tubes is the aim of the full scale testing reported in Chapter 4. Using concrete as filler material instead of use other material such as timber or foam is easy as it can arrange its desired properties and ensure complete filling. It can be used to fill different cross-section shape tubes. Therefore, mechanical properties of different types of concrete were investigated in this chapter. These types include normal concrete and lightweight concrete to cover a range of variation in concrete modulus up to 30 GPa. Firstly, a pilot study was conducted to determine the modulus and compressive strength for various concrete types. Then, the suitable types that meet the targeted range of modulus values were selected in preparing filled FRP columns.

3.2.1 Pilot study of fillers

As the stiffness of the infill concrete is the main research parameter, different types of concrete were prepared to cover a range of concrete stiffness from 5 GPa to around 30 GPa. Four types of normal concrete and three types of perlite concrete were used in the pilot study to investigate the compressive strength and modulus.

For normal concrete, different types of premix concrete were used in the range of compressive strength from 12 MPa to 55 MPa. The premix concrete bags contain the mixed ingredients of the concrete (cement, fine aggregate and coarse aggregate). The quantity of mixing water is specified on the bags to get the intended concrete strength. Table 3.1 shows the details of preliminary mixes of normal concrete. The labelling of concrete mixes has been carried out as: "P" is used to identify preliminary mixes, "N" represents normal concrete and the number afterwards indicates number of mix. Both P-N1 and P-N2 were prepared using the same concrete bag, but with different quantity of water. The content of the premix concrete bags was poured in the laboratory mixer before adding and mixing with water gradually. The mixing process continued for 4-5 minutes before casting concrete cylinders. The top end of all cylinders was made smooth by using sheets of plastic and glass (Figure 3.1 (a)).

Table 3.1 Preliminary normal concrete mixes

Preliminary mixes	Quantity of water (kg/bag)
P-N1	2.00
P-N2	2.65
P-N3	2.50
P-N4	1.90

The preliminary mixes (P-P1, P-P2,P-P3) of perlite concrete were prepared using three percentages of perlite aggregate; 60%, 40% and 20% as a replacement ratio of the fine aggregate. This type of concrete was prepared by replacing the fine aggregate with the given percentage of perlite aggregate. Thus, the properties of perlite concrete rely on the replacement ratio (Karakoç & Demirboga 2010; Lanzón & García-Ruiz 2008; Sengul et al. 2011; Topçu & Işıkdağ 2008; Türkmen & Kantarcı 2007). Table 3.2 shows the ingredients of the preliminary mixes of perlite concrete. The mixes of the perlite concrete were adopted from a series of tests that were done by Sengul et al. (2011). The mixing of the perlite concrete was done in the same way as normal concrete noting that the perlite aggregate was added after the other ingredients of concrete are mixed to avoid crushing of the perlite aggregate (Jedidi et al. 2015). Before mixing, perlite aggregate should be kept in water for 30 minutes to 1 hour so that the perlite can absorb water without affecting the effective water-cement ratio. The mixing procedure includes adding the cement and sand firstly in the drum mixer with a little amount of water. The ingredients were mixed for 1 minute. Then, the wet perlite aggregates were added with the remaining water and admixtures (Figure 3.1 (b)).

Table 3.2 Mix design for perlite concrete in preliminary tests

Preliminary perlite concrete	% of perlite aggregate	Cement kg/m^3	Perlite 2-4 mm (kg/m^3)	Sand kg/m^3	Water/ cement ratio	Super plasticiser Litres/m^3	Air entraining admixture (kg/m^3)
P-P1	60	301	47	581	0.55	0.0	0.9
P-P2	40	326	33	937	0.55	1.5	1.0
P-P3	20	337	17	1288	0.55	2.6	1.0

(a)

(b)
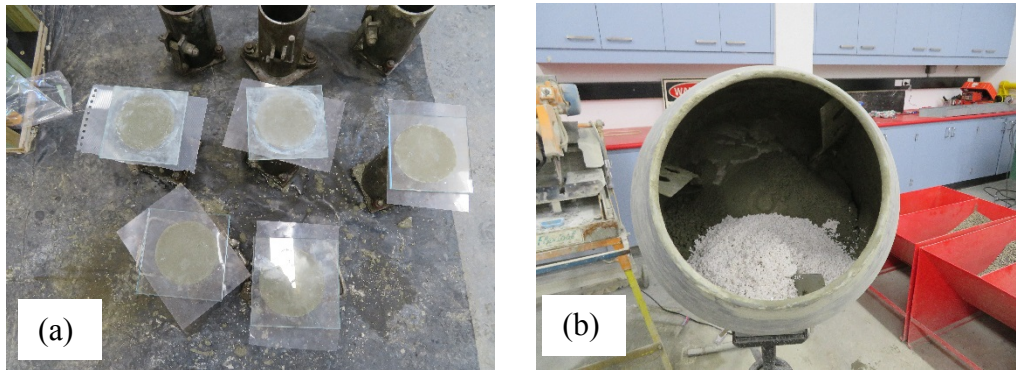
Figure 3.1 Concrete specimens (a) cylinder preparation and (b) mixing of perlite concrete

100 mm diameter and 200 mm height four samples were prepared for each type of the concrete in order to be tested them for compressive strength. All concrete cylinders were kept in curing room 78.8% humidity and temperature of 26±2˚C for 28 days before testing. The compressive test of concrete cylinders was done according to the AS1012.9 (2014) and the value of the concrete modulus was computed based on the AS1012.17 (1997) standard using the compressometer for measuring axial strain (Figure 3.2). The measured axial deformation values were used to calculate the modulus of concrete.

Figure 3.2 Measurement of longitudinal deformation

The modulus, compressive strength, and the unit weight for each type of the concrete were calculated as the average of the individual results of the cylindrical specimens.

The summary results of all mixes are shown in Table 3.3 while Appendix B gives all the experimental results for the pilot study. The results show that the modulus of concrete is increased as the compressive strength increases either those of normal concrete or perlite concrete. Moreover, the modulus results of P-N2 and P-P3 show the influence of unit weight since they have approximately same values of compressive strength.

Table 3.3 Results of all preliminary mixes

Preliminary mixes	Concrete modulus (GPa)		Compressive strength (MPa)		Unit weight (kg/m^3)	
	Average	SD	Average	SD	Average	SD
P-N1	29.80	1.98	26.1	1.10	2171	9.52
P-N2	19.45	0.07	11.3	1.40	2144	4.79
P-N3	24.30	0.00	23.4	0.73	2210	17.4
P-N4	32.45	0.07	52.9	2.52	2255	11.2
P-P1	4.50	0.07	2.4	1.71	1222	8.05
P-P2	9.90	1.13	6.0	0.75	1477	14.7
P-P3	12.95	0.28	11.8	0.17	1665	19.5

3.2.2 Selected mixes for fillers

Preliminary normal concrete mixes P-N2 and P-N4 were selected from the results of pilot study to meet the high modulus value of around 30GPa and moderate modulus value in range of 15-20 GPa. They are named in the next chapters as N1 and N2 respectively. The low target values of concrete stiffness were obtained by using lightweight perlite concrete. Mixes of P-P1 and P-P3 perlite concrete were selected to be used in the research. This is because P-P1 gives the lowest modulus for concrete and P-P3 gives close value to concrete modulus and strength of P-N2. Mixes of perlite concrete from preliminary tests, P-P1 and P-P3 are named in the next chapters as P1 and P2 respectively. According to the properties of both concrete ingredients and the perlite aggregate, the ingredients were altered. Table 3.4 shows the mix proportion of the perlite concrete.

Table 3.4 Mix design for perlite concrete for main experiments

Perlite concrete	Cement (kg/m3)	Perlite (kg/m3)	Sand (kg/m3)	Water (kg/m3)	Superplasticiser (kg/m3)	Air-entraining (kg/m3)	W/C ratio
P1	301	47.0	581.0	166	0.0	0.9	0.55
P2	380	19.1	1453.0	209	2.8	1.1	0.55

The selected mixes from the preliminary tests were used to prepare the samples for the main material characterisation of the filler. In this main testing, three cylinders were tested without strain gauges while two were tested with strain gauges. The selected mixes were used as the filler for the full scale testing of FRP tubes and hence the cylinders and the filled FRP tubes were prepared at the same time. All the cylinders and filled full-scale FRP-concrete columns were kept in the curing room for 14 days and 7 days in the laboratory condition before testing.   The surface of the concrete cylinder was prepared by filling the voids with Araldite epoxy adhesive before strain gauges (PL-90-11-1L) were attached. Two strain gauges in the longitudinal direction and two in the transverse direction were used to measure the axial and the hoop strains (Figure 3.3 (c)). The compressive test of the concrete cylinders was done according to the AS1012.9 (2014) by using SANS machine with a capacity of 2000 kN (Figure 3.3). All cylinders were tested using displacement controlled process with a rate of 0.5mm/min. Applied load and the axial deflection were collected from the computer system of the SANS machine while the recorded data of the strain gauges and the load cell have been collected from the computer system of the system 5000 data logger.

| (a) | (b) | (c) |
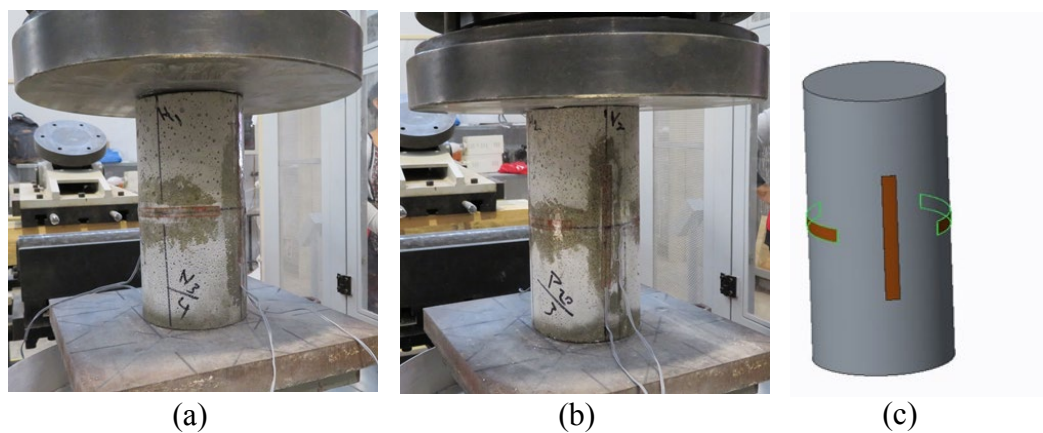
Figure 3.3 Testing (a) normal concrete, (b) perlite concrete and (c) distribution of strain gauges

Figure 3.4 shows the stress-strain curves for normal and perlite concrete using both the calculated strain data based on the total deflection of concrete cylinder (dashed line) and strain data of the strain gauges (continuous line). It should be noted that the strain gauge data was not available after the peak load due to the failure of concrete. Moreover, debonding issues of strain gauges and cracks propagating through strain gauges are the main factors that affected strain gauge readings after the peak.

The slope of the elastic region of the stress-strain curve up to 45% of the compressive strength was calculated for specimens that were instrumented with strain gauges to find the concrete modulus. Poisson's ratio was calculated using the strain data of the transverse and longitudinal strain gauges. Table 3.5 shows the average properties of all types of concrete.

Table 3.5 Mechanical properties of infill concrete

Concrete type	P1		P2		N1		N2	
	Average	SD	Average	SD	Average	SD	Average	SD
E_c (GPa)	4.9	0.20	6.7	1.4	17.0	0.70	30.4	1.70
Unit weight(kg/m³)	1271	26.2	1760	17.3	2117	15.4	2169	14.7
f'_c(MPa)	4.5	0.30	10.4	1.0	11.2	0.50	33.0	3.00
Poisson's ratio	0.17	0.10	0.18	0.10	0.23	0.03	0.21	0.04

* Appendix C presents the individual results of all the samples.

The modulus of perlite concrete P1 is lower than that of the perlite concrete P2 as can be seen in Figure 3.4 (a) and (b). In addition, the modulus of the normal concrete N2 is higher than the modulus of the N1 (Figure 3.4 (c) and (d)).

Differences in the descending branches of the stress strain curves can be seen in Figure 3.4. Although normal concrete shows a sudden drop after the peak indicating a more brittle behaviour than the perlite concrete. Comparison of perlite concrete indicates that P1 is less brittle behaviour than P2 although P1 is having lower stiffness and compressive strength than P2.

Figure 3.4 also shows that the lateral dilation of the four types of concrete is not the same and there is a clear difference between perlite and normal concrete. Generally,

the transverse strain values of the perlite concrete are lower than those of the normal concrete. The maximum transverse strain value of perlite concrete P2 is lower than that of the normal concrete N1 although the compressive strength of both concrete types is approximately the same (Figure 3.4 (b) and (c)). On the other hand, the reduction in transvers strain can be noticed for P1 compared with P2. This can be due to the increased amount of perlite aggregates in P1. The low transverse strain at peak load of the perlite concrete might lead to reduced FRP confinement on the axial behaviour of the filled FRP tube since the confinement of FRP materials depends on the lateral dilation of concrete. Transverse strains are larger in normal concrete compared with perlite concrete.

Normal concrete N1 and N2 shows Poisson's ratio of 0.23 and 0.21 respectively (Table 3.5) which matches with the generally accepted value of 0.2. However, perlite concrete P1 and P2 shows a lower Poisson's ratio of 0.18 and 0.17 respectively indicating a smaller lateral dilation compared with normal concrete.
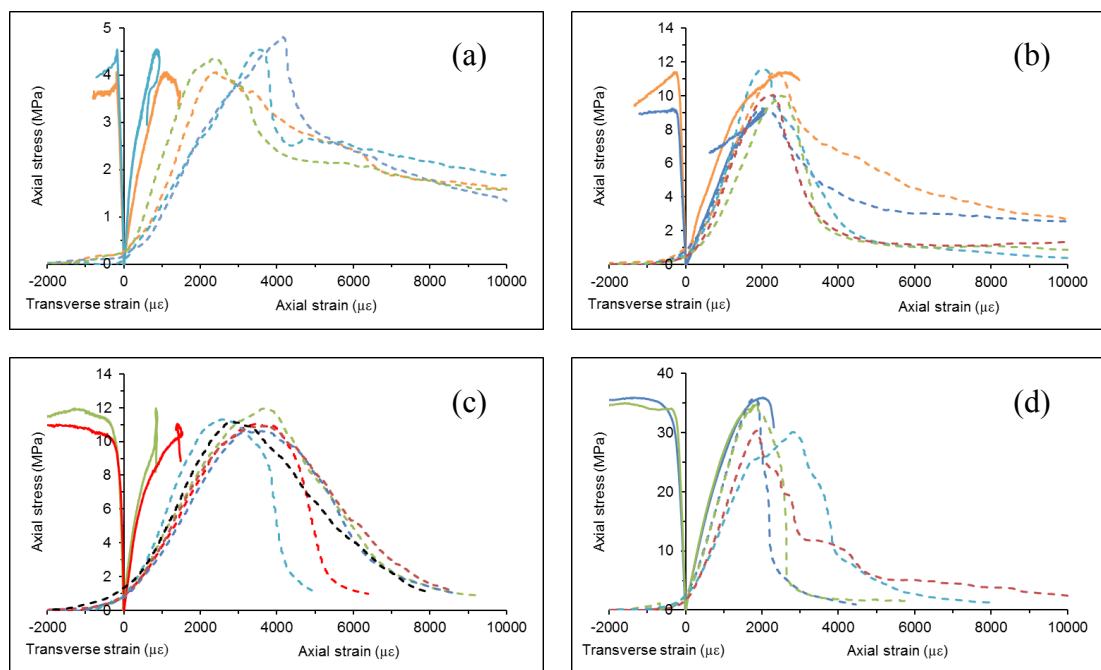
Figure 3.4 Stress-strain curves for (a) perlite concrete P1, and (b) perlite concrete P2, (c) normal concrete N1 and (d) normal concrete N2

Figure 3.5 shows the failure of concrete cylinder for normal and perlite concrete. It can be concluded the axial deformation of perlite concrete is larger than that of normal concrete. the stress-strain curves of perlite concrete reflects that since the ability to resist the load after the peak reduces slowly at strain value higher than that of normal concrete.
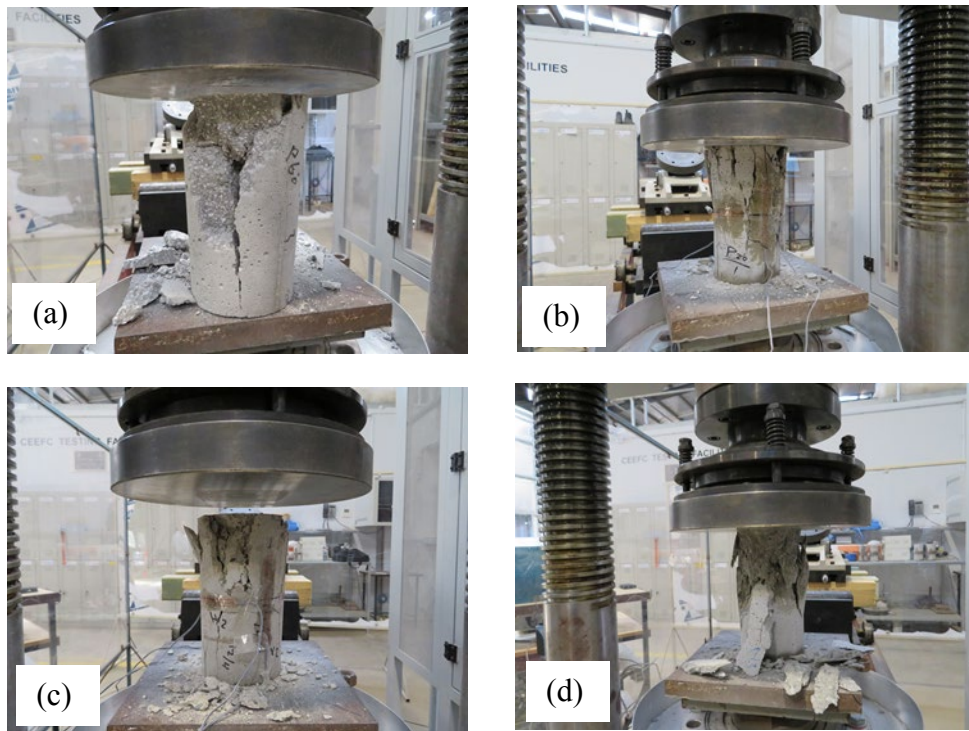
Figure 3.5 Failure of (a) perlite concrete P1, (b) perlite concrete P2, (c) normal concrete N1 and (d) normal concrete N2

3.2.3 Conclusions

Four types of normal concrete and three types of perlite concrete were investigated in the preliminary study of the second part of this chapter. Having investigated the compressive strength and modulus of elasticity, two types of normal concrete and two types of perlite concrete were investigated further as the material characterisation of the filler for FRP tubes. Perlite concrete show a higher deformation properties due to low modulus compared to normal concrete. Moreover, the lateral strain of perlite concrete at peak load is lower than the corresponding lateral strain of normal concrete. These features give an indication that the FRP confinement of perlite concrete is less

effective than that of normal concrete and the ability of perlite concrete to sustain the load after the peak value is higher than that of normal concrete. The selected perlite mixes represent a lightweight mix with lower compressive strength, stiffness and lateral dilation compared to the selected normal concrete mixes. Furthermore, one type of perlite concrete mix (P2) is selected to have close compressive strength to that of normal concrete N1.

3.3 Summary

This chapter presents the material characterisation of pultruded FRP tubes and the filler material. Four types of material tests (burnout, tensile, compressive and shear tests) were conducted for each type of pultruded square and circular FRP tubes. Axial stress, axial strain and lateral strain behaviour was investigated for the two types of filler; perlite and normal concrete.

In the first part of this chapter, the strength and modulus levels of tensile, compressive and shear properties were investigated in relation to fibre concentration, fibre orientation and their layup. Both the fibre concentration and orientation have a significant effect on the mechanical properties of FRP tubes. The tensile strength and modulus can be improved by increasing the percentage of axial fibres. On the other hand, compression modulus and strength depends on the fibre orientation and fibre layup. Finally, the shear strength and modulus of FRP tube depend on the shear strength of resin and the availability of fibres in the diagonal tension field of shear forces.

The important outcome from the material characterisation of pultruded FRP tubes is that the structural performance of the PFRP profiles could be improved by adopting a proper design for the FRP layer, fibre concentration and orientation.

In the second part of this chapter, compressive strength, modulus and Poisson's ratio together with the stress strain relationships of different filler materials were investigated. Based on the preliminary tests, two types of perlite concrete and two types of normal concrete were selected for further analysis and to be used as the filler

for the FRP tubes in the full scale testing of filled FRP tubes. The results show that the lateral deformation of the lightweight perlite concrete is lower than that of normal concrete indicating a less confinement effectiveness in the former than the latter if it is to be used as the filler for FRP tubes. Although perlite concrete shows a lower modulus and compressive strength than the normal concrete, it shows less brittle behaviour after the peak load compared to normal concrete.

The selected types of concrete were used in filling pultruded FRP tubes to investigate the effect of the properties of filler material, fibre orientation, cross-section shape and wall thickness on the axial behaviour of pultruded FRP tubes. It is carried out using a detailed experimental investigation on hollow and filled square and circular PFRP tubes in Chapter 4.

References

AS1012.9 2014, Methods of testing concrete, Methods 9:Compressive strength tests-Concrete,mortar and grout specimens., Sydney, Australia.

AS1012.17 1997, Methods of testing concrete, Determination of the static chord modulus of elasticity and Poisson's ratio of concrete specimens, Australia.

Jedidi, M, Benjeddou, O & Soussi, C 2015, 'Effect of Expanded Perlite Aggregate Dosage on Properties of Lightweight Concrete', Jordan Journal of Civil Engineering, vol. 9, no. 3, pp. 278-91.

Karakoç, MB & Demirboga, R 2010, 'HSC with expanded perlite aggregate at wet and dry curing conditions', Journal of materials in civil engineering, vol. 22, no. 12, pp. 1252-9.

Lanzón, M & García-Ruiz, P 2008, 'Lightweight cement mortars: Advantages and inconveniences of expanded perlite and its influence on fresh and hardened state and durability', Construction and Building Materials, vol. 22, no. 8, pp. 1798-806.

Sengul, O, Azizi, S, Karaosmanoglu, F & Tasdemir, MA 2011, 'Effect of expanded perlite on the mechanical properties and thermal conductivity of lightweight concrete', Energy and Buildings, vol. 43, no. 2, pp. 671-6.

Topçu, İB & Işıkdağ, B 2008, 'Effect of expanded perlite aggregate on the properties of lightweight concrete', Journal of materials processing technology, vol. 204, no. 1, pp. 34-8.

Türkmen, İ & Kantarcı, A 2007, 'Effects of expanded perlite aggregate and different curing conditions on the physical and mechanical properties of self-compacting concrete', Building and Environment, vol. 42, no. 6, pp. 2378-83.

Chapter 4:

Experimental Investigation on the Compressive Behaviour of Filled Pultruded Glass Fibre Reinforced Polymer Tubes

Having completed the material characterisation for FRP tube and the filler in Chapter 3, this chapter focusses on the experimental investigation of axial behaviour of hollow and filled FRP tubes. Short compressive tests was conducted for hollow tubes with length-to-lateral dimension ratio (L/D) of 2 in the first stage to compare the axial behaviour of pultruded FRP tubes. Length to lateral dimension ratio of five was maintained for all the hollow and filled columns in the second stage. Two types of square tubes (100 mm with 5.2 mm wall thickness and 102 mm with 6.4 mm wall thickness) and two types of circular tubes (88.9 mm diameter with 6.0 mm wall thickness) with varying thickness, fibre orientation and percentage of fibres in axial direction were considered in the experimental programme using two samples for each case. This was necessary to check any diversity in experimental results. Two types of normal concrete (fc'=11.2 MPa and 33.0 MPa) and two types of the lightweight perlite concrete (fc'=4.5 MPa and 10.4 MPa) were used to prepare the filled columns. Test variables include the stiffness and compressive strength of filler material and the shape. Fibre orientation and percentage of fibres in axial/non axial direction of the FRP tube. The effect of these parameters on the axial behaviour of pultruded FRP tubes is shown in Paper 3. The results are discussed in terms of load-defection behaviour, stiffness, energy absorption capacity, failure mode and load capacity for hollow and filled FRP tubes.

4.1 Short compressive tests of pultruded FRP tubes

4.1.1 Experimental work

Full-scale compressive tests were carried out on the selected four types of tubes. The specimens were prepared as short-columns with a length-to-lateral dimension ratio of 2 to eliminate the stress concentration at the ends and to ensure the uniform stresses in the mid region of the FRP columns. The specimen length for square tube S1 and S2 are 200 mm and 204 mm respectively while the specimen length of circular tubes is 178 mm. The compressive test for full-scale specimens was carried out in the 2000 kN capacity SANS testing machine. A total of 2 replicates for each type of pultruded FRP tube were tested in which one of them was tested with strain gauges. Two strain gauges of 20 mm length were attached on FRP tube positioned along its mid-height to measure the axial and transverse strains (Figure 4.1 (a)). The axial deformation was measured by Linear Variable Differential Transducers (LVDT) that was installed between the loading and supporting plates of the testing machine (Figure 4.1 (b)). The values of load and axial deformation were recorded by the computer connected to the testing machine. Another computer was connected to the load cell of 2000 kN with System 5000 data logger to record the data of strain gauges and the load. All columns were loaded using a displacement controlled process with a rate of 0.5 mm /min.
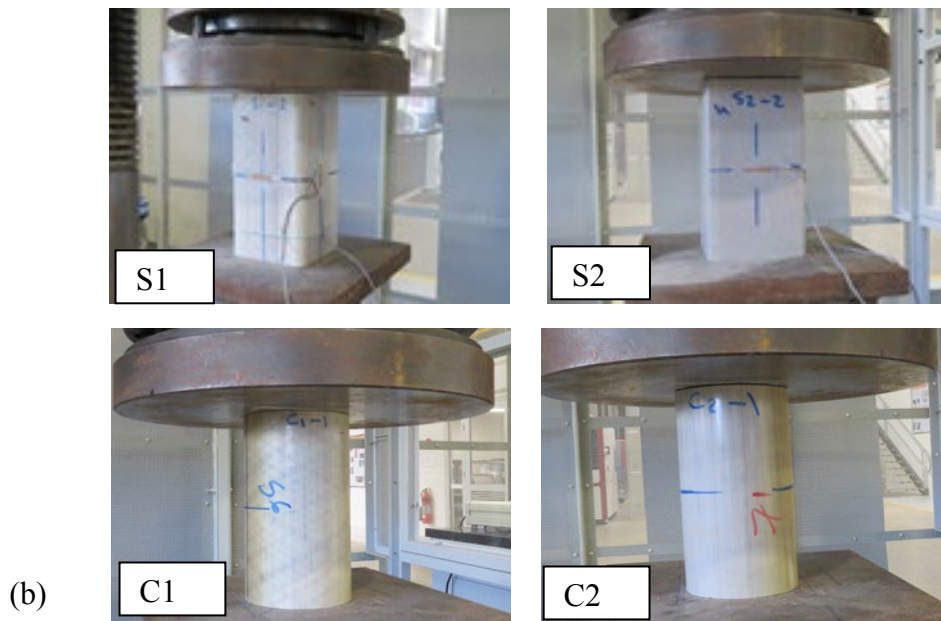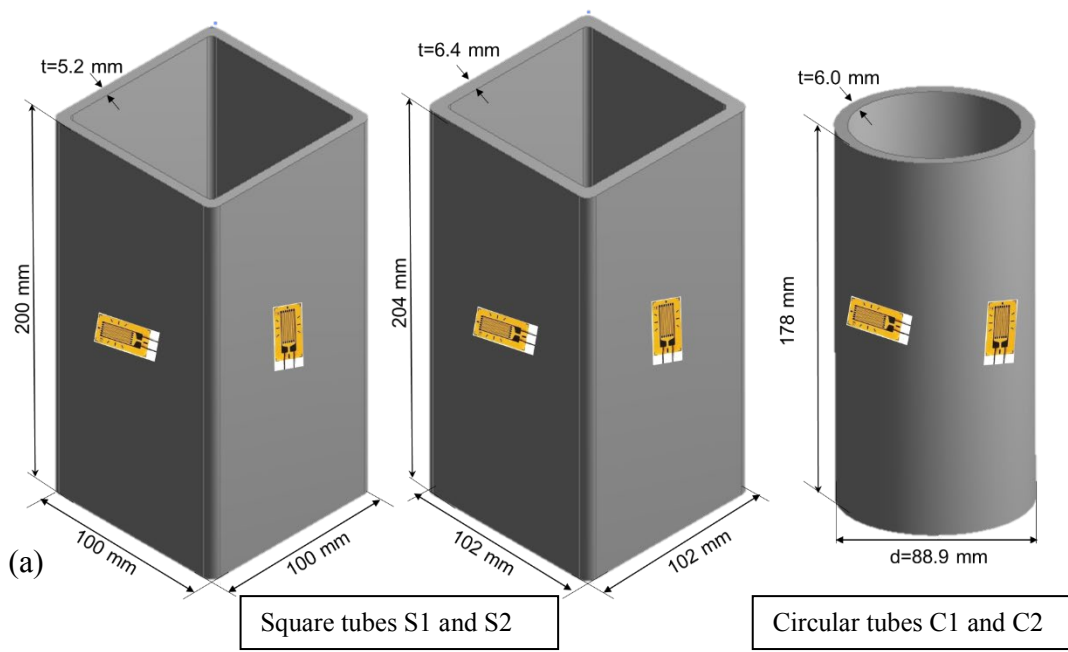
Figure 4.1 FRP column specimens (a) specimen dimensions and distribution of strain gauges and (b) test set up

4.1.2 Results

Table 4.1 shows the peak load and calculated compressive strength for all types of pultruded FRP tubes. The average load capacity and strength of pultruded square tube S1 are 633.3 kN and 325.1 MPa respectively. On the other hand, the load capacity of square tube S2 is higher than that of S1 by 43.7% to reach 910.2 kN. The compressive strength of S2 is also greater than that of S1 by 14.3 %. This is because the plate slenderness ratio of S2 square tube is lower than that of S1. The results of circular tubes show that the load capacity and compressive strength of C1 are slightly larger than those of C2. This is because the percentage of axial fibre and the contribution of non-axial fibre layers of C1 to resist the axial load is higher than those of C2.

Table 4.1 Peak load and compressive strength for pultruded GFRP tubes

GFRP tubes	Specimen No.	Peak load (kN)	Area (mm^2)	Compressive strength (MPa)
S1	1	643.3	1939.0	331.8
	2	623.3	1957.0	318.5
Average		633.3		325.1
S2	1	1001.8	2434.0	411.6
	2	818.5	2466.0	331.9
Average		910.2		371.8
C1	1	434.4	1580.0	274.9
	2	552.3	1599.0	345.4
Average		493.4		310.2
C2	1	434.4	1577.0	275.5
	2	530.6	1573.0	337.3
Average		482.5		306.4

The axial load –deflection curves for all the pultruded FRP tubes tested are shown in Figure 4.2. The relationship between axial load and deflection is linear up to the peak load and has sudden decrease afterwards for all the tubes. The curves of S1 columns show a small reduction by about 12-15 % of the peak load due to buckling initiation before it drops rapidly to lower value. On the other hand, the capacity of S2 columns drops directly to less than 10 % of peak value without showing this reduction. The curves of circular tubes show a linear behaviour up to the peak load. The only

exception is that C1 reflects a gradual reduction in capacity after reaching the peak load.
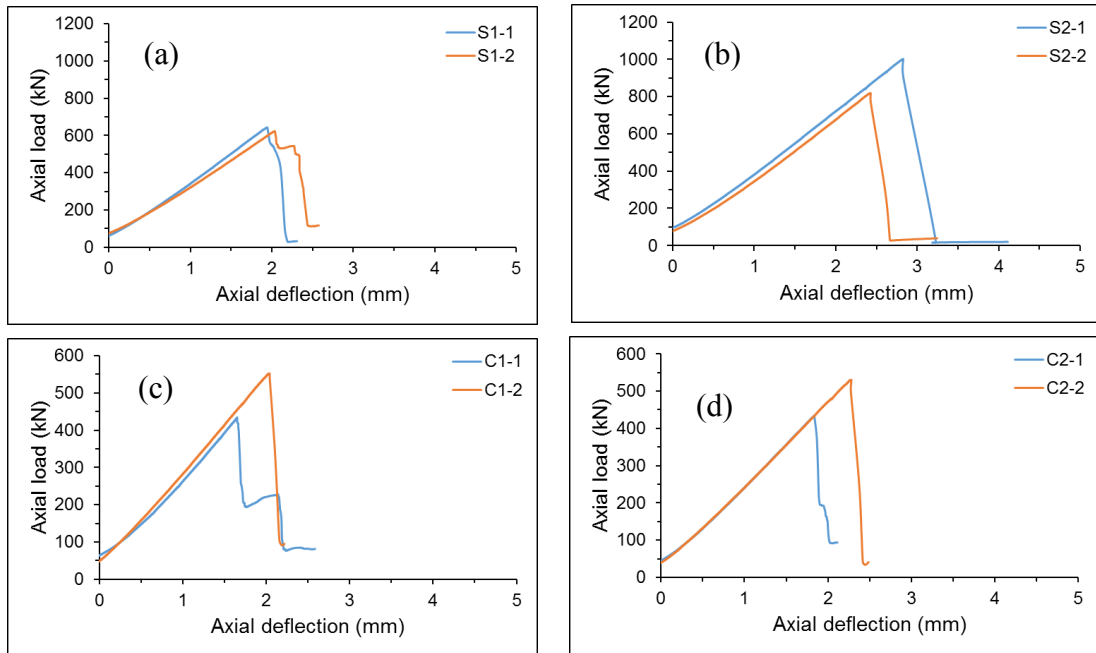
Figure 4.2 Load deflection curves for pultruded FRP tubes of ratio 2 (a) square tube S1, (b) square tube S2, (c) circular tube C1 and (d) circular tube C2

Figure 4.3 shows the axial load, axial strain and transverse strain curves for square and circular Pultruded FRP tubes. It can be seen that the maximum axial strain is around 8500 microstrains for S1 and it is around 4000 microstrains for S2. The axial strain at peak load of circular tube C1 and C2 are around 2600 and 8400 microstrains respectively. Figure 4.3 shows that the axial strain value of S1 at failure is higher than that of S2 mainly due to the continuity of the fibres at the corners of S1. It also indicates that the axial and transverse strains of S2 square tube are decreased due to splitting failure at corners (Figure 4.4 (b)). On the other hand, the load –strain curves of circular tubes drops directly after crushing failure at ends. It also indicates that the axial strain of C2 is higher than that of C1 because the transverse stiffness is higher as the angle of oriented fibre layer and its percentage of C2 is greater than that of C1.
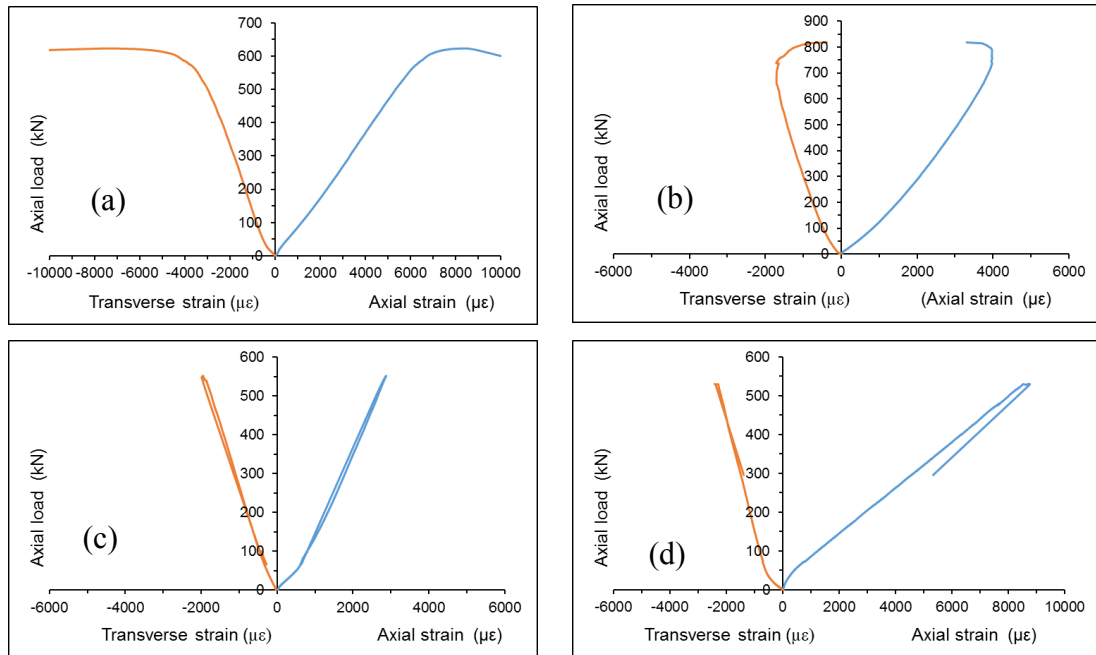
Figure 4.3 Load-strain curves of pultruded FRP tubes (a) S1, (b) S2, (c) C1 and (d) C2 columns

Local buckling is the failure mode of square tube S1. The sides of the column are buckled inside or outside as shown in Figure 4.4. It can also notice that one specimen subjected to end crushing after buckling. On the other hand, the failure mode of S2 square tubes was splitting at corners followed by buckling either inside or outside because the non axial fibre layers of S2 are discontinuous at corners. The failure mode of circular tubes is different to that of the square tubes. The failure started with crushing at one end combined with loud noise. Then, the crushed end is separated into strips around the perimeter before a crack is growing in steps pattern through the thickness towards the other end. This is because the circular short column fails due to crushing rather than buckling as the diameter to thickness ratio is low.
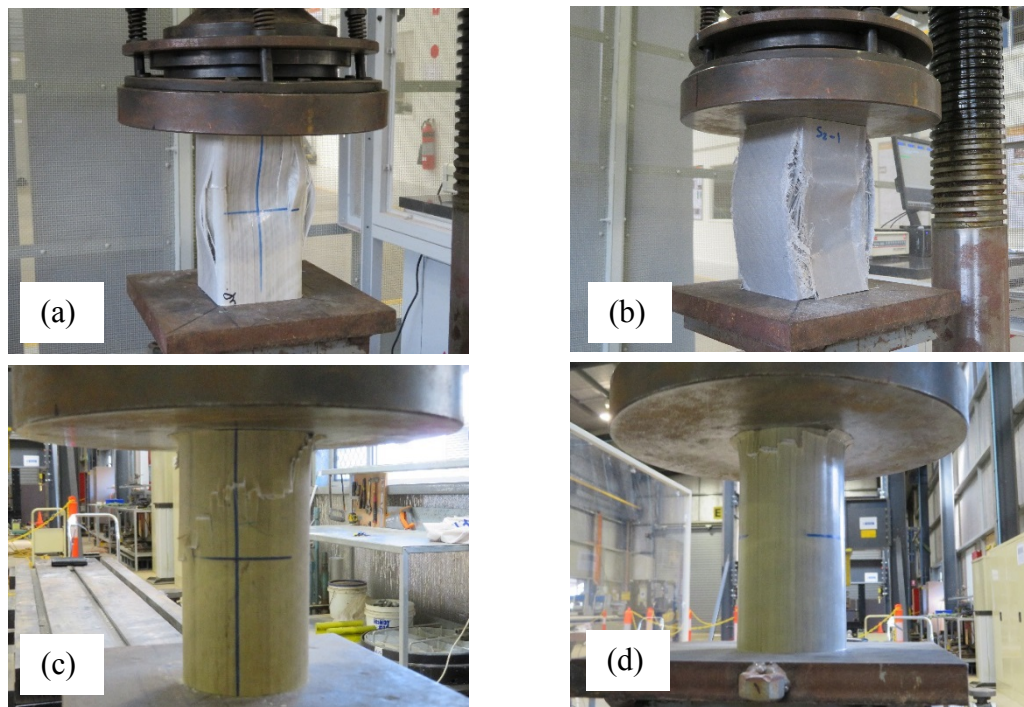
Figure 4.4 Failure modes of pultruded FRP tubes (a) S1, (b) S2 c, (c) C1 and (d) C2 columns

4.1.3 Comparison of full-scale tube behaviours with coupon tests

The full scale tests of pultruded FRP tubes reveal that the axial compressive behaviour of FRP tubes is linear till the peak load (Figure 4.2). This behaviour is similar to the compressive behaviour of coupon tests. The compressive strength of FRP tubes is lower than the compressive strength of coupon tests. This is because the compressive strength of short pultruded PFRP tubes is governed by plate slenderness ratio (width/thickness), fibre orientation and layup, continuity of fibre layers, thickness, shape of pultruded FRP tubes and diameter to thickness ratio. All these factor effects on FRP tubes to fail due to buckling, splitting at corner and crushing at ends rather than due to compression material failure. Although S1 square tubes have more fibres in the axial direction than S2 square tubes, S1 has higher plate slenderness ratio, which causes failure due to local buckling before reaching the potential compressive strength. On the other hand, due to the lack in continuity of the non axial fibres in S2, splitting occurred firstly in the corners followed by buckling of the sides. Table 4.1 shows that the load capacity of S2 square tubes is higher than that of S1, although the compressive

strength of S1 coupon test is larger than the strength of S2. This is because the cross-sectional area of S2 is larger than that of S1.

The post peak behaviour of full-scale S1 square columns displays a gradual reduction as opposed to the sharp drop for S2 square tubes (Figure 4.2). This can be attributed to the fact that S1 tubes have continuous non-axial fibre layers at corner while S2 square tubes do not. The failure mode of S2 square tube verifies that since it fails due to splitting at corner followed by buckling.

The results of circular tubes show that the load capacity of C1 columns is larger than that of C2 columns (Table 4.1). This is because the percentage of axial fibre layer of C1 circular tubes is larger than that for C2 by 32.8 % . Moreover, the angle of the non axial fibre layers of C1 (56 degrees) is smaller than that of C2 (71 degrees) with respect to the axial direction. The load –deflection curves of FRP circular tubes does not show a gradual reduction in strength after the peak load , although both types of circular tubes consisted of non axial fibre layers. This is because the dominated failure mode of hollow short circular tube with low diameter to thickness ratio was due to crushing at ends of column.

4.2 Paper 3

Experimental investigation on the compressive behaviour of filled pultruded glass fibre reinforced polymer tubes

Ali Umran Al-saadi, Thiru Aravinthan and Weena Lokuge

University of Southern Queensland, School of Civil Engineering and Surveying, Centre for Future Materials (CFM), Australia.

Experimental investigation on the compressive behaviour of filled pultruded glass fibre reinforced polymer tubes

Ali Umran Al-saadi[1,2] , Thiru Aravinthan[1*] and Weena Lokuge[1]

[1] University of Southern Queensland, School of Civil Engineering and Surveying, Centre for Future Materials (CFM), Australia.

[2] University of Babylon, Babil, Iraq.

Email: AliUmranKadhum.Alsaadi@usq.edu.au, Thiru.Aravinthan@usq.edu.au, Weena.Lokuge@usq.edu.au

Abstract

The excellent features of pultruded fibre reinforced polymer (PFRP) tubes such as lightweight, corrosion resistance and high strength to weight ratio make this product competitive to traditional steel profiles. However buckling is the main drawback of the use of these tubes in column applications.

This study investigated the use of a concrete filler to compensate the low axial stiffness and to support the walls of pultruded GFRP tube against buckling. Using four types of fillers having concrete modulus up to 30 GPa, it can be concluded that the stiffness, load carrying capacity and energy absorption capacity of filled tubes increase as the modulus of concrete improves. Circular columns show better performance than square columns in terms of these evaluation criteria. Post peak behaviour of the columns and energy absorption capacity were governed by the amount of fibres in the transverse direction and properties of the filler materials. Columns filled with perlite show high capacity of energy absorption compared with columns filled with normal concrete. The failure of the circular columns was due to end crushing while the failure of square columns was mainly due to the corner splitting. The outcomes of this experimental investigation will enhance the use of GFRP profiles in civil infrastructure.

Keywords: Filler materials; failure mode; fibre orientation; lightweight perlite concrete; Pultruded FRP tube.

---

* Corresponding author, tel. (+61) 7 4631 1385
Email addresses: Thiru.Aravinthan@usq.edu.au (Thiru Aravinthan),
        AliUmranKadhum.Alsaadi@usq.edu.au (Ali Umran Al-saadi).

1. Introduction

The use of fibre reinforced polymer (FRP) materials in civil engineering applications has gained increased popularity due to their advantages over traditional construction materials such as high stiffness to weight ratio, lightweight and corrosion resistance. Pultruded fibre reinforced polymer (PFRP) profiles are being used as compression members in the construction industry although they have high axial tensile strength as the majority of fibres in the pultruded FRP profiles extends axially [1]. Due to the low axial stiffness and high wall slenderness, pultruded FRP profiles are unable to utilize their full potential effectively [2, 3].

Pultruded FRP wide flange -I columns was studied by Barbero and Tomblin [4] and proposed design equations to predict the critical loads of intermediate lengths of the FRP–I sections. Zureick and Scott [5] tested two types of sections; pultruded wide flange and pultruded box, which were made of E-glass and vinyl ester and offered design guidelines for slender FRP columns. Hashem and Yuan [6] studied the axial behaviour of the pultruded universal and box cross-sectional configurations to establish a distinguishing criterion between short and long pultruded FRP column behaviour. They reported that columns fail by either plate local buckling or localised crushing of the composite material when its slenderness ratio (L/r) is equal to or less than 50. The length to thickness ratio of the plate governs the failure mode. On the other hand, columns buckle globally when their slenderness ratio is greater than 50. Qian et al. [7] tested five circular GFRP tubes with various slenderness ratios ranging from 35 to 90 under axial compression to investigate their instability. They noticed that the global buckling was the dominant failure mode with the increased slenderness ratio. Godat et al. [8] stated that the possible failure mode of the FRP pultruded angle and box sections (square and rectangular) was global buckling when the global slenderness ratio was higher than the local slenderness (plate width to thickness) ratio, and it was local buckling when the global slenderness ratio was lower than the local slenderness ratio.

More studies were conducted for different PFRP column profiles to propose models to find the load carrying capacity by considering both local and global buckling and the shear failure effects [9-12]. These studies set the base for safe use of pultruded FRP columns in the construction industry. Based on the previous studies, enhancing

the axial stiffness of the FRP profiles and delaying the buckling failure are the appropriate solutions to overcome the issues associated with the compressive behaviour of the pultruded FRP profiles.

The use of concrete to fill FRP tubes was done by Fam and Rizkalla [13] to investigate the effects of the fibre orientation on the FRP confinement effectiveness. The column specimens were cut from the ends of filled tubes after being tested as beams. The height of stub specimens was set twice the diameter of the tube. One kind of FRP tubes was prepared in a way that all fibres extended in the axial direction. They compared the results of filled filament wound tubes with results of the filled uni-axial FRP tubes. Han et al. [14] and Li et al. [1] followed a different approach to improve the axial compressive behaviour of the pultruded FRP tubes. They used FRP material (glass or carbon sheets) to confine circular pultruded FRP tubes laterally. The third approach is compensating the low axial modulus of the FRP layer by adding or replacing it with a high modulus fibre layer. By joining carbon fibre sheet to flanges of the pultruded FRP I –section, the critical buckling load, the ultimate load and the axial stiffness of the modified specimen was increased by 14%, 13.5%, and 30% respectively than reference specimens in the study by Correia, Nunes, Correia and Silvestre [2]. The partial replacement of the glass fibre by the carbon fibre for pultruded FRP I –section to improve its axial performance was investigated by Nunes et al. [15]. The results show the replacement method increases the axial stiffness of long columns up to 17% and the load at global buckling increases by 10% to 17%.

The other use of FRP materials in civil engineering is enhancing the axial strength and axial strain of concrete columns by providing lateral pressure around the column perimeter [16]. This type of FRP tubes should have an adequate stiffness in the transverse direction [17-19]. The impact of different parameters (slenderness ratio of column, column cross-section, properties of filler, fibre orientation, fabrication method of the FRP tube, fibre type) on the performance improvement of FRP columns was studied extensively during the last two decades [20-34]. The results showed that the degree of confinement was significantly affected by the slenderness ratio of the concrete column, concrete type and its properties, fibre type and fibre orientation while the FRP fabrication method has less effect. Moreover, the confining pressure of the non-circular cross-sections columns is not uniform around the perimeter of the column due to bending in the flat sides.

Energy absorption capacity is another characteristic of FRP tubes. It shows how much the structure can sustain the work done by the external forces before showing a significant drop in load carrying capacity. The energy absorption capacity can be determined from the area of the load-deflection curves of columns. It is considered as an index to the behaviour of the concrete structures under earthquake motion or impact load due to incidents or terrorists attacks [35, 36] . It also an index to the behaviour of the composite materials that are used in different industries such as automotive and aerospace as a crashworthy components [14, 37, 38].

Having conducted a comprehensive literature review, it is obvious that the effect of the modulus of the filler on the stiffness improvement, load carrying capacity and energy absorption enhancements of the pultruded FRP columns is not well understood [39]. This paper reports an experimental study to address this research gap by examining the influences of the filler modulus, cross-section of tubes with multi-directional fibre layers on the axial behaviour of filled pultruded FRP columns. The effect on stiffness, axial load, mode of failures and energy absorption capacity are discussed in this paper.

2. Research significance

Although pultruded FRP tubes have high strength and stiffness to weight ratios, their use as a structural column member is limited since the design process of PFRP column is governed by the serviceability limit state due to its low stiffness. It is important to increase the stiffness of these profiles. Therefore, this study makes a major contribution to knowledge on axial behaviour of the pultruded FRP columns by demonstrating the effect of filler properties on the stiffness, axial shortening, peak load capacity, post-peak behaviour, failure modes and energy absorption capacity of the pultruded FRP columns. The findings of this study will provide baseline information to use pultruded FRP tubes in applications of civil infrastructure effectively.

3. Experimental work

3.1 Test matrix

A total of twenty square and twelve circular pultruded GFRP tubes were prepared and tested. There were two types of square and round tubes. The dimensions of the square tube types S1 and S2 are 100 mm with 5.2 mm thickness and 102 mm with 6.4 mm thickness respectively. The stacking sequence of fibre layers is not identical. There were ten samples of each type of square tubes. In addition to the hollow reference tube, there were four filled groups; two filled with two types of normal concrete and two filled with two types of perlite concrete and the tests were duplicated.

Both types of the circular pultruded GFRP tubes, C1 and C2 have the same dimensions (88.9 mm diameter and 6 mm wall thickness) although they have a different structure of fibres in the tube wall. Six samples were tested from each type of circular tubes; one hollow, one filled with the normal concrete and one filled with the perlite concrete and the tests were duplicated. Concrete types with a high modulus of elasticity were used to prepare filled circular tube columns. The length of all GFRP tubes was set to be five times the least lateral dimension to avoid issues of global buckling. Fig.1 shows square and circular GFRP tubes.

Fig. 1. Pultruded GFRP tubes.

Column specimens have been labelled in Tables 1. "S1" and "S2" refer to 100 mm and 102 mm square tubes with height of 500 mm and 510 mm respectively. "H" and

F" identify the condition of hollow or filled FRP tubes while "N" and "P" indicate normal and perlite concrete. The same naming system was used for the circular columns where "C1" and "C2" has the same diameter of 88.9 mm while the secondary fibre orientation is 56˚ and 71˚ respectively, with respect to the axial direction of the tubes. The height of both types of circular columns was set of 445 mm. The height of column specimens was set to provide the short column behaviour since the slenderness ratio (L/r) of square columns S1 and S2 are 13.0 and 13.1 respectively and it is 15.1 for circular columns.

Table 1. Test matrix.

	Concrete type	Concrete strength (f'_c) (MPa)	Concrete modulus (E_c) (GPa)	Specimen
Hollow	-	-	-	S1-H, S2-H, C1-H, C2-H
Filled	Normal	11.1	17.0	S1-FN1, S2-FN1
		32.0	30.4	S1-FN2, S2-FN2, C1-FN2, C2-FN2
	Perlite	4.50	4.90	S1-FP1, S2-FP1
		10.4	6.70	S1-FP2, S2-FP2, C1-FP2, C2-FP2

3.2 Materials

3.2.1 Pultruded GFRP tubes

Two profiles of pultruded GFRP tubes were selected in this study; square and circular tubes. They are representatives of the full-scale profiles that have been used in different applications of civil infrastructure. The square tubes were collected from two providers to study the effect of fibre orientation. S1 series has fibre layers oriented in directions other than the axial direction, while S2 series has fibres oriented mostly in the axial direction. The circular tubes (C1 and C2) have the same diameter, but they have different fibre orientation as explained before.

The tests of material characterization of all FRP tubes were conducted to obtain the mechanical properties. The fibre content of all pultruded GFRP tubes was calculated using the burnout test according to ISO-1172 [40] standard. The stacking sequence of the fibre layers was observed. Tensile and compressive tests of coupon specimens were executed as per ISO-527-4 [41] and D695 [42] standards respectively. All

79

coupon specimens were cut from the axial direction of the tubes. The structural properties for all tubes are reported in Table 2 and the mechanical properties of the pultruded GFRP square tubes are given in Table 3.

Table 2. Physical properties of the pultruded GFRP tubes.

		S1		S2		C1		C2	
	Unit	Average	SD	Average	SD	Average	SD	Average	SD
Shape		Square		Square		Circular		Circular	
Dimensions	mm	100x100, t=5.2		102x102, t=6.4		d=88.9, t=6.0		d=88.9, t=6.0	
Fibre content	%	77.3	2.393	72.2	0.042	79.5	0.806	78.3	0.482
Density	g/cm^3	1.943	0.045	2.007	0.009	2.058	0.039	2.082	0.032
Fibre orientation	Degrees	0,50, -50		0, +45, -45		0, +56, -56		0, +71, -71	

Table 3. Mechanical properties of pultruded GFRP tubes.

GFRP tube	Ultimate tensile strength (MPa)	Ultimate compressive strength (MPa)	Shear strength (MPa)	Tensile modulus of elasticity (GPa)	Compressive modulus of elasticity
S1	953	525	101.0	42.6	49.5
S2	520	506	70.2	36.0	43.7
C1	471	366	-	40.4	49.4
C2	420	408	-	26.8	33.9

Note: Properties given for the longitudinal direction.

3.2.2 Filler material

As the stiffness of the filler is one of the main research parameters in this study, different types of fillers were trialled to cover a range of modulus from 5 GPa to around 30 GPa. In addition to the normal concrete, perlite based lightweight filler was also selected. Two types of normal concrete (N1 and N2) with compressive strength 11 MPa and 33 MPa respectively were selected from results of a pilot study using different types of premix concrete bags to meet the high and moderate levels of concrete modulus. The low target values of filler stiffness were obtained by using lightweight perlite concrete. Mix of P1 gives the lowest modulus for filler and P2 gives the close value to concrete strength of N1. This type of concrete was prepared by replacing the fine aggregate with the perlite aggregate. Thus, the properties of perlite concrete rely on the replacement ratio of fine aggregate [43-47]. The mixing of the perlite concrete was similar to that used for normal concrete with the exception that

perlite aggregate was added last to avoid potential crushing [48]. The target compressive strength of the perlite concrete mixes P1, P2 was 4.5 MPa and 10.4 MPa respectively. Table 4 shows the mix proportions of the perlite concrete.

Table 4. Mix proportions of the perlite concrete mixes.

Types of Perlite concrete	Cement (kg/m³)	Perlite (kg/m³)	Sand (kg/m³)	Water (kg/m³)	Concrete admixtures		W/C ratio
					Superplasticiser (kg/m³)	Air-entraining (kg/m³)	
P1	301	47.0	581.0	166	0.0	0.9	0.55
P2	380	19.1	1453	209	2.8	1.1	0.55

The compression testing of each type of filler (100 mm diameter and 200 mm high cylinders) was carried out according to AS1012.9 [49]. The measured data on the axial stress, axial and transverse strain were used for calculating the modulus of filler. Table 5 shows the calculated properties for all the fillers. Fig. 2 presents the stress-strain curves of two concrete cylinders for each type of concrete that were instrumented with strain gauges.

Table 5. Properties of filler material.

Filler type	P1		P2		N1		N2	
	Average	SD	Average	SD	Average	SD	Average	SD
E_c (GPa)	4.9	0.20	6.7	1.4	17.0	0.70	30.4	1.70
Unit weight(kg/m³)	1271	26.2	1760	17.3	2117	15.4	2169	14.7
f'_c (MPa)	4.5	0.30	10.4	1.0	11.2	0.50	33.0	3.00
Poisson's ratio	0.17	0.10	0.18	0.10	0.23	0.03	0.21	0.04

Fig. 2. Stress-strain relationships for (a) perlite concrete and (b) normal concrete.

3.3 Preparation of column specimens

Timber formwork had been made to hold FRP tubes longitudinally during casting as shown in Fig. 3. Steel ring was used to fix FRP columns in the formwork during the compaction process of the concrete.

Fig. 3. Formwork of column specimens.

The filled pultruded GFRP columns and five concrete cylinders (100 mm diameter and 200 mm high) were cast separately for each type of filler. A sheet of glass was used to ensure a levelled top surface of the columns. Filled pultruded GFRP-concrete columns and concrete cylinders were kept in the curing room with 78.8% humidity and temperature of 26±2˚C until one week before testing. The surface of the concrete cylinders was prepared by filling the voids with Araldite epoxy adhesive before strain gauges (type PL-90-11-1L) were attached in the axial and hoop directions.

3.4 Test setup and instrumentation

The 2000 kN capacity SANS testing machine was used for testing FRP columns and concrete cylinders. The FRP tubes were placed vertically at the centre of the testing machine to provide uniform distribution of applied load. A Linear Variable Differential Transducers (LVDTs) that was mounted between the loading and supporting plates were used to measure the axial deformation of the columns. The computer of the testing machine recorded the load and axial deformation. A load cell 2000 kN with System 5000 data logger connected to another computer was also used to record the data of strain gauges and the load. Two strain gauges were attached at

mid height of column specimen to measure the axial and lateral strains. All columns were tested using a displacement controlled process with a rate of 0.5 mm/min.

4. Results of the hollow and filled columns

The calculated and experimental results of the pultruded GFRP columns in terms of stiffness and failure load are presented in Tables 6 and 7 respectively.

Table 6. Stiffness of pultruded GFRP columns (x10^3 N/mm).

GFRP tubes	Specimen No.	Hollow	Filled			
			P1	P2	N1	N2
S1	1	150.3	174.3	194.1	252.5	294.1
	2	150.9	154.8	188.6	198.8	241.5
	Average	150.6	164.6	191.3	225.6	267.8
S2	1	163.0	175.2	179.9	185.4	300.3
	2	159.3	161.2	170.9	222.6	318.6
	Average	161.1	168.2	175.4	204.0	309.4
C1	1	132.4	-	109.7	-	197.4
	2	129.5	-	167.0	-	186.3
	Average	131.0	-	138.3	-	191.8
C2	1	112.5	-	156.8	-	215.6
	2	116.1	-	129.4	-	166.4
	Average	114.3	-	143.1	-	191.0

Table 7. Peak loads for pultruded GFRP columns (kN).

GFRP tubes	Specimen No.	Hollow	Filled			
			P1	P2	N1	N2
S1	1	464.0	445.0	539.7	662.0	686.6
	2	470.0	433.0	539.2	628.5	643.0
	Average	467.0	439.0	539.4	645.3	664.8
S2	1	751.0	488.0	555.9	627.2	702.0
	2	740.0	484.0	549.3	631.9	672.0
	Average	745.5	486.0	552.6	629.5	687.0
C1	1	410.9	-	460.9	-	738.0
	2	537.5	-	490.9	-	721.0
	Average	474.2	-	475.9	-	729.5
C2	1	506.0	-	609.2	-	1039.2
	2	415.6	-	584.6	-	972.0
	Average	460.8	-	596.9	-	1005.6

The energy absorption capacity can be determined from the area of the load-deflection curves of columns. In this study, the energy absorption capacity was calculated using the trapezoidal rule. The area under curve of filled columns was assumed up to axial shortening of 2% of height of FRP column or to a drop point of load. This is because the post–peak behaviour of filled columns shows ability to continue carrying load. The post –peak behaviour depends on the properties of filler and pultruded FRP tubes. Table 8 shows the calculated values of energy absorption capacity for all columns.

Table 8. Energy absorption capacity for pultruded FRP tubes (J).

GFRP tubes	Specimen No.	Hollow	Filled			
			P1	P2	N1	N2
S1	1	713.7	4284.2	3532.2	3630.9	5024.3
	2	721.4	4311.7	3559.4	3321.3	5266.9
	Average	717.5	4297.9	3545.8	3476.1	5145.6
S2	1	1712.3	2883.8	3226.7	1495.9	1500.1
	2	1701.7	3349.5	2341.2	1284.2	1532.2
	Average	1707.0	3116.6	2784.0	1390.0	1516.2
C1	1	704.9	-	5562.6	-	4020.0
	2	1127.6	-	4339.2	-	4830.4
	Average	916.3	-	4950.9	-	4425.2
C2	1	1180.8	-	14647.4	-	10224.2
	2	769.2	-	12842.6	-	9208.7
	Average	975.0	-	13745.0	-	9716.5

4.1 Behaviour of square columns

Table 6 shows that the stiffness of hollow S1 columns is 150.6 x 10^3 N/mm while it is 161.1 x 10^3 N/mm for hollow S2. The stiffness of S1 columns is lower than stiffness of hollow S2 column by 6.5%. This can be attributed to difference in wall thickness and fibre orientation and layup. The average load carrying capacity of the hollow square tubes S1 and S2 are 467.0 kN and 745.5 kN respectively. It can be seen in Fig. 4(a) that both S1 columns showed linear relationship between axial load and deflection till the peak load and the load carrying capacity is reduced approximately by 14% of the peak load after buckling initiation, continued to carry that load and decreased rapidly to less than 10% of the peak load eventually. On the other hand, after reaching the peak load, S2 had a sudden loss of capacity. The failure of square tube S1 is due

to local buckling where the sides of the column continued to buckle either inward or outward. On the other hand, a snapping sound could be heard, when the applied load of square tube S2 reached 500 kN, due to the initiation of failure in the fibre layers. The failure started with the corner splitting at the mid-height of the S2 columns followed by the split propagation towards both ends (Fig. 5(a)).

Pultruded FRP tubes S1 filled with perlite concrete P1 showed an enhancement in the stiffness by 9.3% to reach 164.6×10^3 N/mm compared with the hollow tubes although the load capacity of the filled columns was 439.0 kN (94% of hollow tubes). This reduction in the load capacity is caused by concrete failure due to crushing at the upper end of the FRP tube. Similarly, the load capacity of the pultruded square tube S2 filled with perlite concrete P1 reached 486.0 kN, which is 65% of the capacity of the hollow columns (Fig. 4(b)). However, the stiffness of S2 filled with P1 reached 168.2×10^3 N/mm, which is 4.4% higher than the stiffness of hollow column. Perlite concrete, P1 changed the post-peak behaviour of the load-deformation curves as well as the failure modes for both S1 and S2 columns. The filled pultruded GFRP tubes S1 continued to resist the load for further axial shortening even after reaching the peak load (Fig. 4(b)). The load carrying capacity of the filled S1 tubes reached approximately 34% of the average peak load for further 10 mm of axial deformation. Conversely, the square columns S2 filled with P1 could continue in resisting the applied load for additional 3-5 mm of axial deflection before losing the column strength significantly. The failure mode of columns S1 changed from local buckling in case of the hollow columns to crushing at one end followed by splitting of fibre layers at corner and around the perimeter of the tube for filled columns (Fig. 5(b)). Correspondingly, the failure of filled columns S2 initiated at the top end of the column when the load had reached 450 kN. The mode of failure was corner splitting followed by the crack propagation towards the lower end. At the end of the test, the full splitting had occurred along the length of columns (Fig. 5(b)).

Filling columns with perlite concrete P2 exhibits a different axial behaviour. The higher the modulus of infill concrete is, the higher the stiffness and capacity of FRP-concrete composite columns. Filling with P2 results in increasing the stiffness of S1 columns to reach 191.3×10^3 N/mm (Table 6). Stiffness is improved by 27% compared with that of hollow columns. On the other hand, the stiffness of S2 columns is increased by 8.8% due to filling with P2. The average value of stiffness for pultruded

columns S2 filled with P2 was 175.4 x 10^3 N/ mm (Table 8). Table 7 shows that the average value of the peak load for pultruded columns S1 filled with P2 was 539.4 kN which represents 15.5% higher than the load capacity of the respective hollow columns. It further shows that the load carrying capacity of square columns S2 that were filled with perlite concrete P2 reached 13.7% higher load capacity of columns filled with perlite concrete P1 to reach 552.6 kN. The slow reduction in the ability of square columns S1 to resist the applied load after hitting the peak point is gradual. Fig. 4(c) shows that the load carrying capacity of columns filled with P2 decreased to approximately 46% of the peak load at an axial deflection of twice that at the peak load. As the separation of the fibre layers started for S1 columns, the load capacity of the columns reduced to around 150 kN at axial deflection greater than that of the failure initiation by 14 times. On the other hand, S2 columns showed a sharp reduction in the load after the peak load. The failure of the square tube S1 started from one end combined with loud noise followed by a longer splitting at corners compared to those along the sides of the tube while the mode of failure of square columns S2 was similar to that of pultruded columns filled with perlite concrete P1 (Fig. 5(c)).

 Filling with normal concrete N1 contributes more towards the stiffness and load carrying capacity of square columns S1 reaching an average of 225.6 x 10^3 N/mm and 645.3 kN respectively. The degree of improvement compared with values of the hollow tubes is 49.8% for stiffness and 38% for load capacity. The stiffness of square tube S2 is also developed by 26.6% to be 204.0 x 10^3 N/mm due to filling with N1. Furthermore, filling with normal concrete N1 increases the load capacity of pultruded square tube S2 up to 629.5 kN which represents an improvement by 14% compared with those filled with perlite concrete P2. After the peak load, the load capacity of columns S1 decreased suddenly to about 38% of the ultimate load before it increased again for the next 10 mm axial deformation (Fig. 4(d)). The response of columns S2 was completely different. The enhancement in stiffness in S2 is lower than that of S1 and the strength of the columns dropped sharply after the peak load. Modes of failure for pultruded GFRP square tube S1 and S2 filled with normal concrete N1 is similar to those filled with perlite concrete. The failure of both S1 columns started due to lower end perimeter extension followed by a longitudinal crack at corner combined with falling of the concrete debris, while for S2, the failure initiated due to splitting at

corners of one end of the square columns followed by split propagation towards the other end (Fig. 5(d)).

The maximum level of stiffness enhancement for square columns was obtained for those filled with N2 filler. The stiffness of S1 and S2 columns increased up to 267.8 x 10^3 N/mm and 309.4 x10^3 N/mm respectively (Table 6). The stiffness values of S1 and S2 increased by 77.8 % and 92.0% respectively compared with stiffness of hollow columns. The high degree of improvement in the column capacity could be achieved by using normal concrete N2 filler with compressive strength of 33 MPa. The average peak load of columns S1 was 664.8 kN, which represents 42.3% greater than the capacity of the hollow columns while S2 reached 687 kN (8% lower than the respective hollow column). Fig.4(e) shows that the capacity of the square columns S1 dropped gradually up to 10-12 mm of axial deflection and continued to carry about (20-35) % of the peak load. On the other hand, the axial behaviour of pultruded columns S2 filled with normal concrete N2 after the peak load is similar to those filled with normal concrete N1. It can be seen in Fig. 4(e) that columns S2 are unable to resist the applied load in the post-peak region. The failure modes of the square columns S1and S2 filled with normal concrete N2 are similar to those filled with normal concrete N1. Crushing at one end combined with longitudinal splitting at the corner was the failure mode of pultruded columns S1 and splitting close to one end with crack propagation was the failure mode of pultruded square columns S2 (Fig. 5(e)).

The results show that the energy absorption of filled square columns S1 with N2 is improved to reach by around 7.2 times the energy of hollow columns (Table 8). Furthermore, results of S1 filled with P2 displays an increase in the energy absorption compared with those filled with N1 although the compressive strength of filler is approximately the same. This can be attributed to the compressive behaviour of the filler material where the lateral dilation of perlite concrete is lower than the dilation of normal concrete.

The results of square tube S2 are differed a lot compared with results of S1. There is not a significant improvement in the values of the energy absorption for filled columns compared with hollow columns except those filled with P1 and P2 by 82.6% and 63.1% respectively to reach 3116.6 J and 2784.0 J respectively as shown in Table 8. This is because the fibre arrangement and discontinuity at corners prevent columns to

exhibit high deformation before failure. However, the energy of hollow square columns S2 is 1707.0 J, which is greater than that of the S1 by 2.3 times. This can be attributed to the effects of the wall thickness. The energy absorption of square columns S2 filled with P2 and N1 reflects an increment trend as those of S1 but in lower rate.
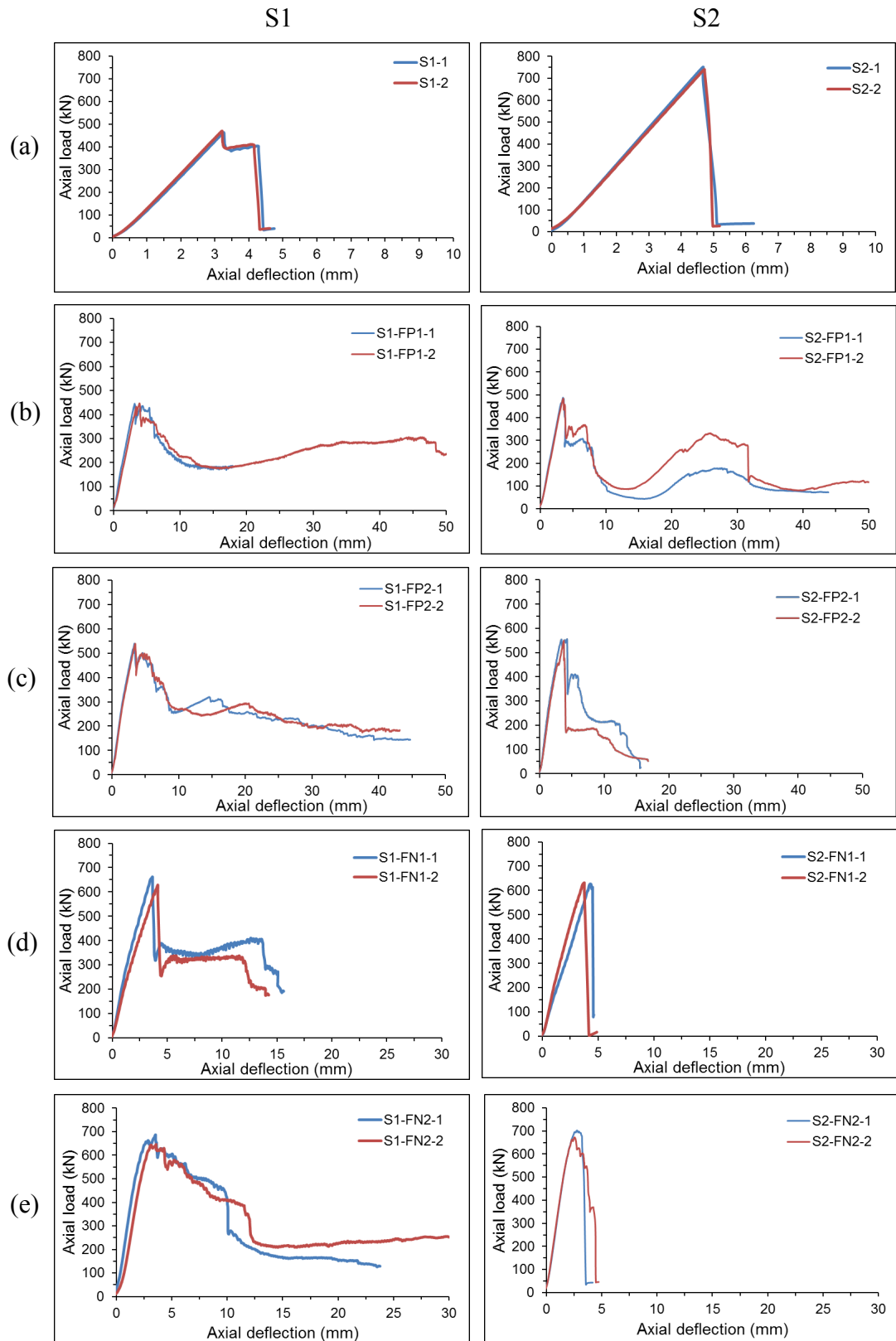
S1   S2

Fig. 4. Load-deflection curves for pultruded S1 and S2 square tubes: (a) hollow and filled with (b) perlite concrete P1, (c) perlite concrete P2, (d) normal concrete N1 and (e) normal concrete N2.
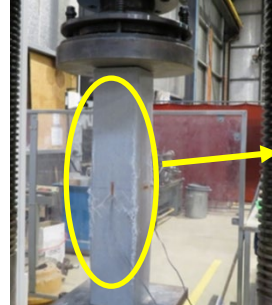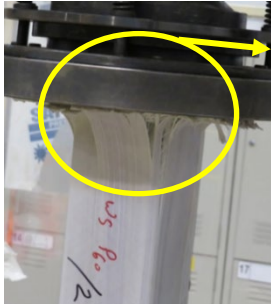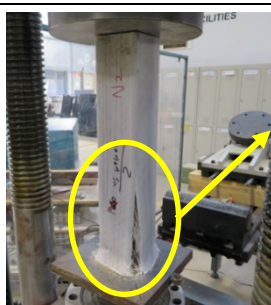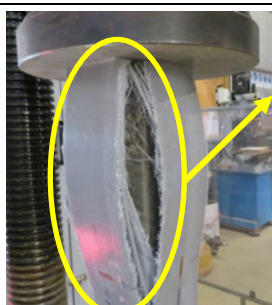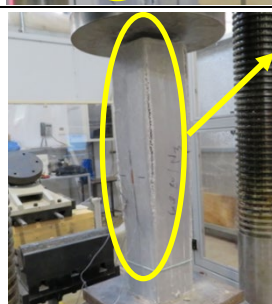
	S1	S2
(a)	Local buckling	Corner splitting + local buckling
(b)	Crushing at one end + splitting	Crushing at one end + corner splitting
(c)	Crushing at one end + corner splitting	Crushing at one end+ full corner splitting
(d)	Crushing at one end + corner splitting	Crushing at one end + full corner splitting
(e)	Crushing at one end + corner splitting	Crushing at one end + long corner splitting

Fig. 5. Failure modes of the pultruded square tubes S1 and S2: (a) hollow and filled with (b) perlite concrete P1, (c) perlite concrete P2, (d) normal concrete N1 and (e) normal concrete N2.

4.2 Behaviour of the circular columns

The fibre orientation and lay out of C1 and C2 circular columns are the main factors that affect the stiffness level of hollow columns since the cross-sectional area of columns is same. The stiffness of C1 columns was 131.0 x10^3N/mm while it was 114.3 x10^3N/mm for C2 columns (Table 6). This is because the angle of non-axial fibre layer of C1 is closer to the axial direction compared with angle of C2 columns. Therefore, the contribution in boosting the axial modulus increases. As shown in Fig. 6(a), the hollow pultruded circular columns C1 and C2 show a linear relationship between the axial load and deflection until the peak load. The average load capacity of C1 and C2 is 474.2 kN and 460.8 kN respectively (Table7). The strength of the pultruded GFRP hollow columns C1 and C2 reduced rapidly after the peak load (Fig. 6(a)). The failure mode of both types of the hollow column is crushing at one end of the column combined with loud noise and the crushed end separated the column into strips around the perimeter (Fig. 7(a)).

Filling with P2 did not bring a significant improvement to the stiffness of C1 and C2 circular columns. The stiffness of C1 improves by 5.6% to be 138.3 x10^3N/mm while it improves by 9.3% to reach 143.1 x10^3N/mm for C2 (Table 6). Even though the average result of the circular tubes C1 filled with perlite concrete P2 (Table 7) shows low improvement in the load carrying capacity (475.9 kN) compared with the hollow columns (474.2 kN); they exhibited a completely different behaviour in the post peak region. The high improvement in the load capacity of the circular tube is exhibited for circular columns C2 filled with perlite concrete P2. It is increased by 29.5% (596.9 kN) compared with the hollow column. Fig. 6 (b) shows that circular columns C1 could resist 75% of the peak load for approximately twice the axial deformation at failure before a sudden drop to reach around 175 kN followed by a series of the successive slow reductions in the capacity of columns. The capacity of column C2 increases up to 474 kN before a small capacity loss due to extension at the upper end followed by a second drop at 486 kN due to extension of the lower end. Splitting in the pultruded tube started at 530 kN load causing another drop before a sharp declination at 609 kN due to the growth of the upper FRP splitting. The filled columns of C1 failed due to longitudinal splitting created at the crushed end and growing towards the other end while the failure of the filled pultruded circular columns C2

happened due to crushing at both ends of columns and growing as the longitudinal splitting (Fig. 7(b)).

The significant development in columns' stiffness was achieved by using filler N2. The stiffness is increased by 46.5% to be 191.8 x10³N/mm for C1 and by 45.9% for C2 to reach 191.0 x10³N/mm compared with stiffness of hollow columns. Better axial performance can be seen in results of pultruded circular columns C1 and C2 that were filled with the normal concrete N2 (Fig. 6(c)). C1 and C2 columns can carry load up to 729.5 kN and 1005.6 kN respectively on average that represents an improvement in the load capacity by 54% and 118% respectively compared with the capacity of the hollow columns. The axial behaviour of the circular columns C1 was almost identical to C2 especially in the post-peak region (Fig. 6(c)). After hitting the peak value, the capacity of C1 columns dropped firstly to around 675 kN before decreasing sharply to 23%-38% of the peak load for C1. Then, it continued to carry this load until the crack splitting of the pultruded tube grew. The axial behaviour of columns C2 is similar to that of C1 except that C2 continue in resisting up to the peak load where the load capacity of columns dropped sharply. The failure of columns C1 began at one end with a loud noise followed by spreading the splitting towards the other end. Due to the lateral pressure of the concrete, a zigzag crack was noticed in one specimen (Fig. 7(c)). Columns of C2 filled with normal concrete N2 failed due to crushing at both ends of the column with longitudinal splitting around the perimeter.

Although both types of circular columns show a clear of increasing trend for filled columns compared with hollow columns, the great energy absorption performance is observed for circular columns C2. Those filled with N2 and P2 can absorbs energy up to 9.9 and 14 times the energy of hollow columns respectively (Table 8). Moreover, the capacity of hollow columns C2 is higher than that is of hollow columns C1. The results prove that the ability of columns to show large work due to external load before failure is affected by the fibre orientation.
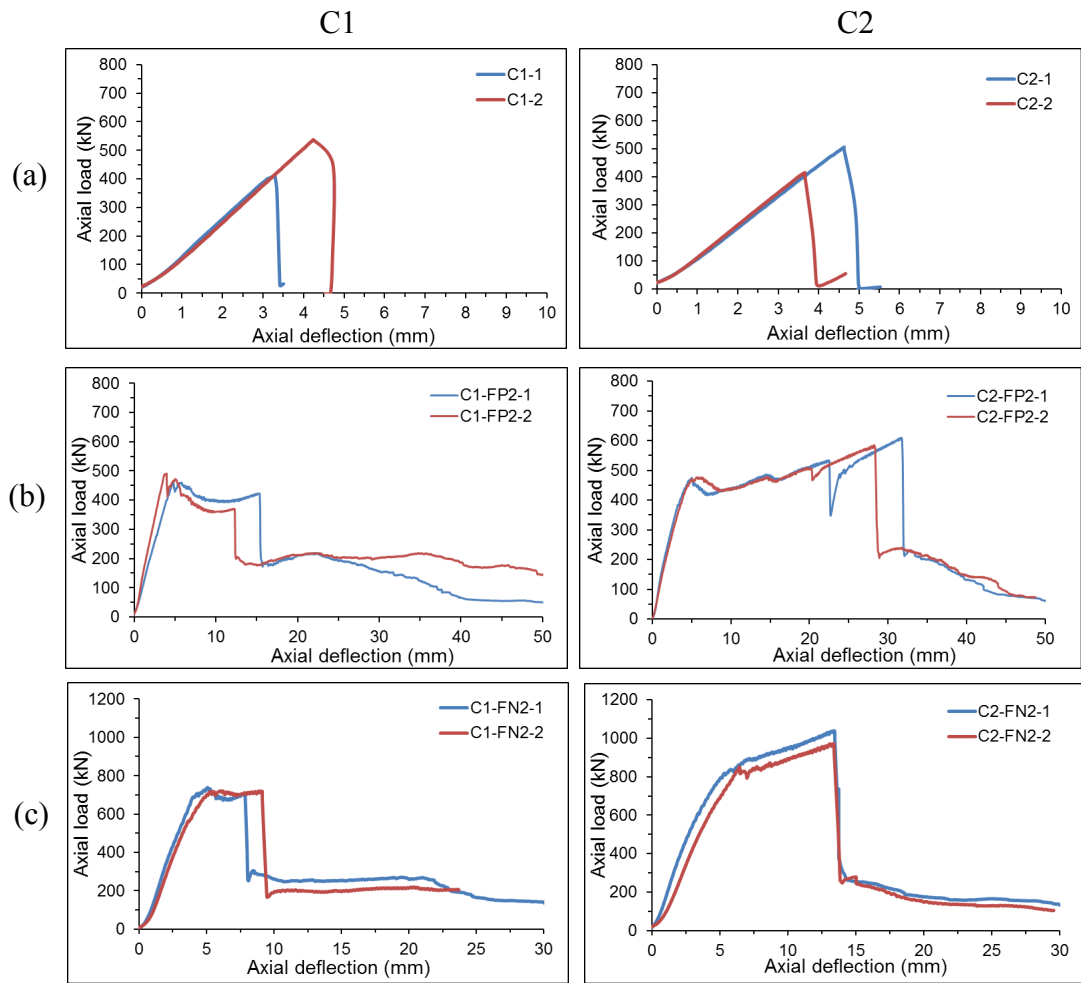
Fig. 6. Load-deflection curves of pultruded circular tubes C1 and C2 (a) hollow and filled with (b) perlite concrete P2 and (c) normal concrete N2.
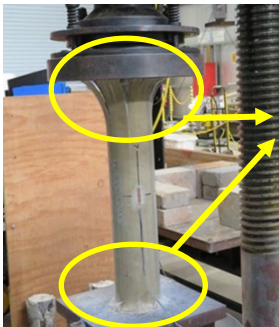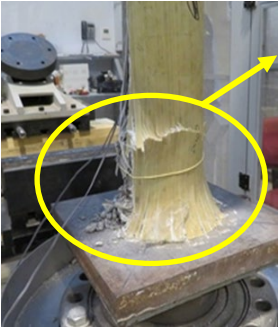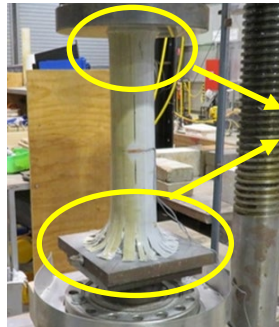
	C1		C2	
(a)		Crushing at one end + perimeter separated		Crushing at one end + perimeter separated
(b)		Crushing at one end +long splitting		Crushing at ends +perimeter splitting
(c)		Crushing at one end + splitting		Crushing at ends +perimeter splitting

Fig. 7. Failure modes of the pultruded circular tubes C1 and C2 (a) hollow and filled with (b) perlite concrete P2 and (c) normal concrete N2.

5. Discussion

5.1 Effect of filler and its properties

The contribution of the filler in strengthening the axial behaviour of pultruded GFRP square tubes S1 and S2 is shown in Fig. 8(a) and Fig. 8 (b) respectively which gives only one curve for the duplicated samples for better clarity of the load- deflection curves. Fig. 8 (a) shows that for a specific value of the applied load, the axial deflection of the square columns S1 decreases as the modulus of the concrete increases. As the wall structure of the square tube S1 contains layers of fibre in directions other than the axial direction (Table 4), restraint in the hoop direction against the lateral dilation of concrete is generated. As a result of the combined effects of the filler and FRP lateral

94

restraint, the load carrying capacity of columns is improved with increasing modulus of elasticity of concrete (Fig. 8(a)). The filled pultruded GFRP square tubes S2 performed in a different way than filled S1 columns. Although the load carrying capacity of the filled columns increases as the stiffness of infill concrete increases, it did not exceed the capacity of the hollow tubes. However, for the same axial load, the axial deflection of the filled columns decreases when the modulus of elasticity of the infill concrete increases (Fig. 8(b)). This behaviour can be attributed to the stacking sequences of fibre layers in the walls of the pultruded square tubes S2. They did not have sufficient layers of fibres oriented in the hoop direction to generate the required restraint. The lateral dilation of the concrete creates tensile stress in the transverse (hoop) direction of the pultruded tube S2 which is higher than its circumstantial tensile resistance, resulting in failure due to splitting at the corners.

The properties of filler were the primary factor that governs the post-peak behaviour where columns show a gradual decrease in the capacity instead of the rapid reduction in the capacity for hollow columns. The low lateral dilation of perlite concrete leads to reduce the effects of FRP confinement on the concrete strength and strain compared with normal concrete. The ability to sustain the load after reaching the peak load appeared clearly in the behaviour of columns of S1 and S2 that were filled with perlite concrete compared with those of S2 filled with normal concrete. This is because the lateral dilation of the perlite concrete is smaller than that of normal concrete. Fig. 2 shows that although the values of the compressive strength of normal concrete N1 and perlite concrete P2 are approximately the same, the value of the lateral strain of normal concrete N1 at peak load is higher than the value of the lateral strain of the perlite concrete P2. FRP confinement provided by S1 and S2 to perlite filler material is lower because of the lower Poisson's ratio resulting in a lower peak load than the columns with normal concrete filler. The fluctuated behaviour in the post-peak region can be attributed to the change in the lateral restraint action of FRP due to bonding and loosening between the FRP tube and infill concrete. On the other hand, the post-peak behaviour of the square columns S2 filled with normal concrete was slightly modified compared with the post-peak behaviour of the hollow columns where the load capacity of columns declined dramatically after getting the peak point.

Due to filling, the failure mode of pultruded GFRP tubes S1 is changed. The influence of the filler can be described as a combination of resistance provided by the walls of

the tube against buckling and creating tensile stress in the GFRP tube due to lateral dilation of concrete. The results show that the transverse tensile stress of the GFRP tube controls the mode of failure of filled columns as they failed by splitting at corners after crushing at the end of the column. Pultruded FRP columns of S1 filled with P1 did not generate a longitudinal splitting at corner because the lateral dilation of filler was low and the transverse modulus of tube is high. Even though the failure modes of filled columns of pultruded square columns S2 did not differ a lot more than that of S1, the filled columns of the square tube S2 shows a rapid propagation of the longitudinal splitting of the FRP tube. The sides of the tube almost separated along the length of filled column S2. This can be attributed to discontinuity of fibres at corner, thus the splitting occurred directly after crushing at end of column even the dilation of filler is low.

The capacity of energy absorption of square pultruded FRP columns is influenced by the properties of filler material and FRP tube. Generally, the capacity increases as the modulus of normal or perlite fillers increases. The range of improvement for columns S1 is higher than that of column S2. This is due to differences in fibre orientation, layup and fibre continuity at the corners in S1 and S2. Furthermore, properties of perlite filler cause an improvement in energy absorption capacity of columns compared with those filled with same compressive strength of normal concrete. This can be attributed to low dilation rate of perlite filler. It should be noted that the capacity of energy of columns filled with perlite filler P1 is higher than those are filled with perlite filler P2. This is because the dilation of perlite filler P1 is lower than that of perlite filler P2.
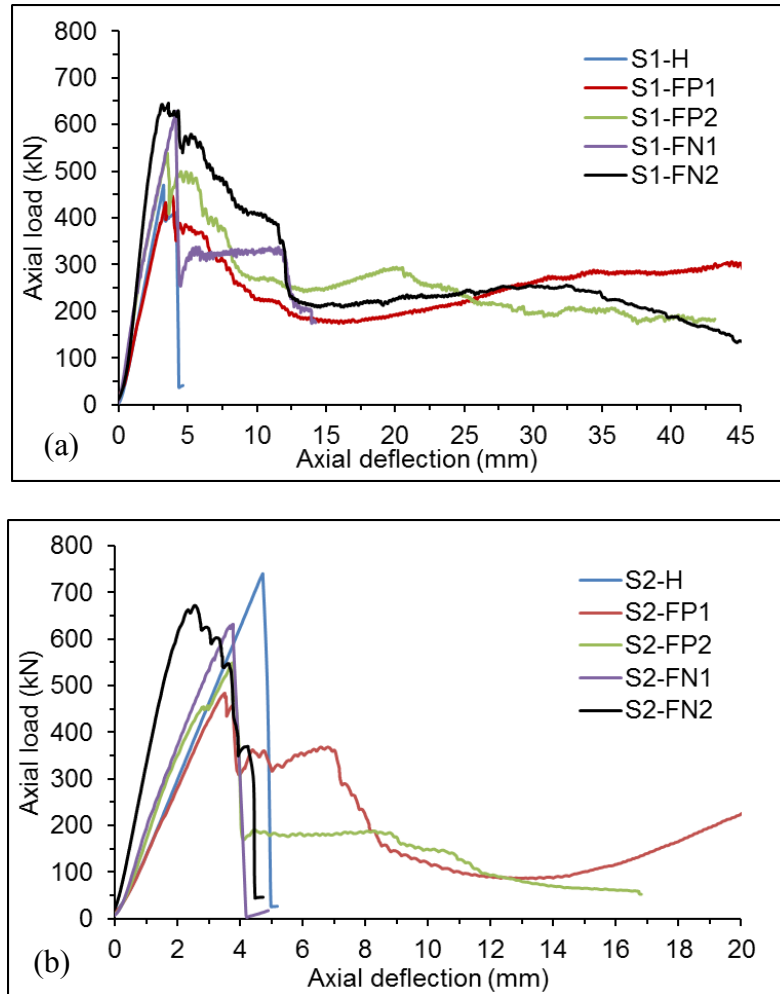
Fig. 8. Load-deflection curves of the hollow and filled columns (a) square S1 and (b) square S2.

The confinement effect of FRP is more prominent in circular tubes than in square tubes. The load capacity of the pultruded circular tubes C1 and C2 increases as the stiffness of the infill concrete increases. Nevertheless, the axial deflection of the filled columns decreases with the increasing concrete stiffness for the same level of loading. Due to the combined effects of concrete modulus and the confinement effectiveness of the pultruded circular tubes, the load capacity of the circular column C1 that was filled with either the perlite concrete P2 or the normal concrete N2 increases to reach 460.9 kN and 738 kN respectively. The circular column (C1-FP2-2) that was filled with perlite concrete did not reveal an increment in the load capacity due to the premature failure while C1-FN2-2 could hold an enhancement by 34% of the capacity of the hollow one (Fig. 9(a)). The load capacity of the pultruded columns filled with perlite concrete is increased by 20%-40% of that of the hollow columns and by 105%-

97

134% in case of using normal concrete N2 to fill the pultruded tubes C2 as can be seen in Fig. 9(b). It should be noted that the ability to sustain the load after reaching the peak load is better for columns C1 and C2 filled with perlite concrete compared with those filled with normal concrete.

C1 and C2 Columns that were filled with perlite concrete (P2) or with normal concrete (N2) show a capacity drop after the peak and sustain load for some time until it shows a sudden capacity reduction in the end (Fig.9). However, the post-peak behaviour of FRP circular columns C2 is not as that of the circular columns C1. The capacity of the pultruded columns C2 filled with concrete reduces at a rate higher than that of the circular columns C1 filled with the same type of concrete (Fig. 9(b)). This is because the contribution of the fibre in the hoop direction in carrying the load is not high enough to create a gradual load reduction.

Filled circular columns could obtain high level of energy absorption compared with hollow columns. The increment of C1 and C2 filled with P2 was larger than that of hollow by 446.2% and 1309.7 % respectively. On the other hand, the capacity of energy absorption of C1 and C2 filled with N2 were 4425.2 J and 9716.5 J (Table 8). The degree of increment of filled C2 is larger than that of filled C1.The reason is due to difference in fibre structure. Columns filled with perlite filler shows high ability to absorb energy compared with those filled with normal concrete.
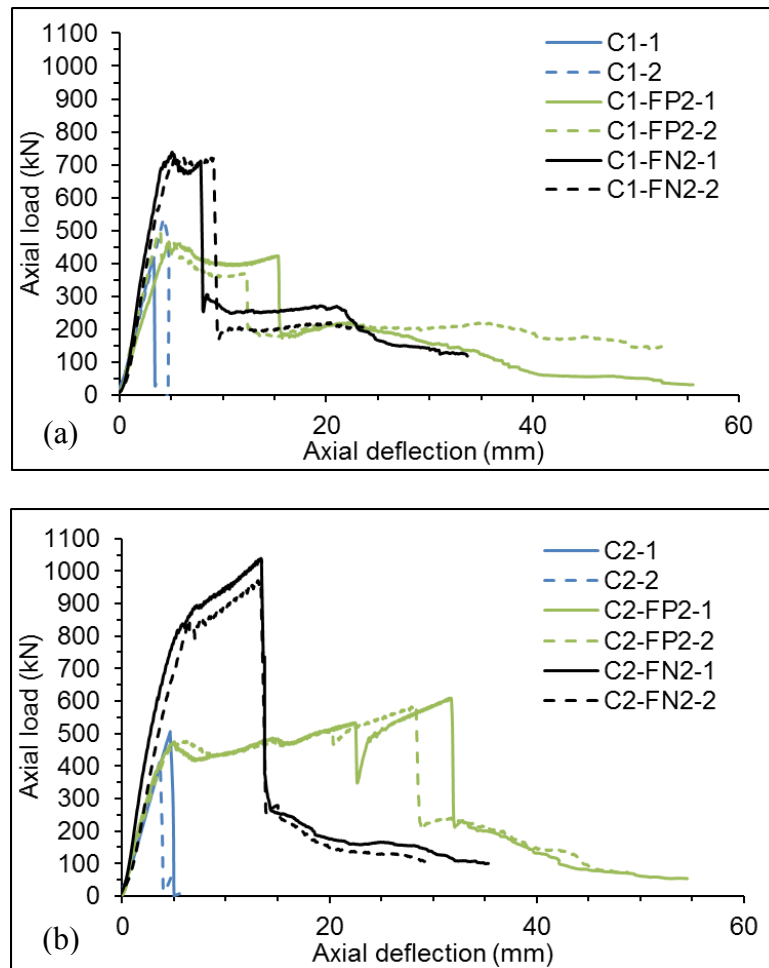
Fig. 9. Load-deflection curves of the hollow and filled circular columns (a) circular C1 and (b) circular C2.

Fig. 10 shows a comparison of the axial load-axial strain and axial load-hoop strain curves of the hollow and filled columns for different types of pultruded tubes. Experimental load-strains curves were terminated at the point where the columns reached the peak load value unless the strain gauges were damaged due to the column deformations. It can be seen that at the same load level both the axial and hoop strains were decreased as the stiffness of the infill concrete increased. Fig. 10 further reveals that the load capacity of all the filled columns was improved compared with pultruded GFRP hollow tubes except those of the S2 square tubes. Moreover, the load-strain curves obtained for the pultruded GFRP tube filled with the perlite concrete were similar to those were obtained for the pultruded GFRP tube filled with the normal concrete.
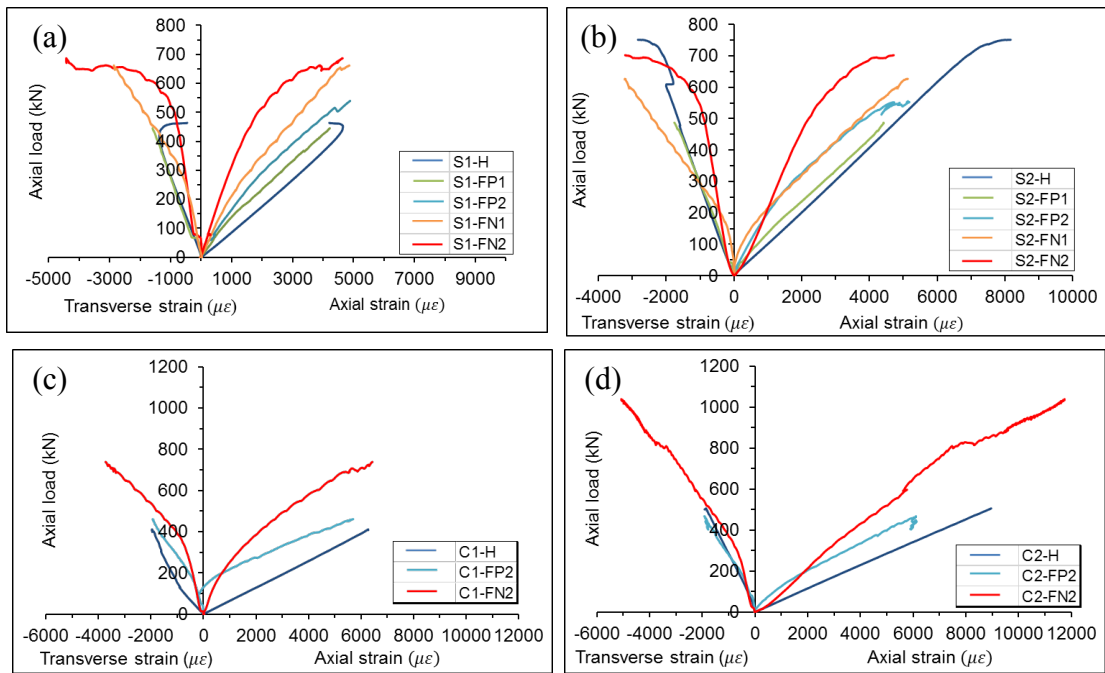
Fig. 10. Influence of the infill concrete properties on the load-strain curves of FRP tubes (a) Square S1, (b) Square S2, (c) Circular C1 and (d) Circular C2.

5.2 Effect of fibre orientation

The axial compressive behaviour of pultruded FRP tubes is affected by the availability of fibre layers in the axial and transverse directions. The direct comparison of specimens is the approach to establish effects of the fibre orientation on the axial behaviour of hollow, filled with perlite concrete P2 and filled with the normal concrete N2. Fig.11 shows the normalised sectional stress-axial deflection curves of square and circular columns.

The effects of the fibre orientation on the axial behaviour of the square and circular FRP tubes S1, S2, C1 and C2 can be classified into three areas; resisting axial load, support against micro-buckling and improvement in the confinement effectiveness. Fig.11 shows a comparison of the axial behaviour of the hollow and filled square and circular FRP columns. The contribution of the fibres in resisting the axial load is increased as the angle between the fibres and axial direction of the FRP tube is smaller. Figs. 11 (a) and 11 (b) show that the normalised sectional stress of the hollow square tubes S2 and the circular tubes C1 are higher than that of the square tubes S1 and the circular tubes C2 respectively. This is because the majority of the fibre layers of square tubes S2 are oriented in the axial direction, and for the circular tubes; this is because

100

the fibre layers of the circular tubes C1 are closer to the axial direction compared with the fibre layers of the circular tubes C2.

The second area of the contributions of the fibre in the hoop direction is supporting the longitudinal fibre layers against micro-buckling. Although the normalised sectional stress-axial deflection relationship of the hollow square tubes S1 and S2 is similar up to the peak load, the post-peak behaviour is different. The strength of the square tubes S1 has not dropped immediately after reaching the peak sectional stress due to the resistance of the fibres in the hoop direction to the buckling stress; instead, the strength reduction is gradual. On the other hand, the stress of the square tube S2 is not sustained after the peak load due to lack of continuous fibres in the hoop direction. For circular tubes, the involvements of the oriented fibre layers in supporting the axial load of tubes C2 is higher than that of tubes C1 since the angle that the fibres make with the axial direction is larger than that of C1 circular tubes (Table 3). As a result, the axial strain of hollow tubes C2 at peak load is higher than that of the circular tubes C1 (Figs. 10 (c) and 10 (d)).

Fig. 11 shows the effects of the fibre orientation on the axial behaviour of the filled columns. The post-peak behaviour of both types of square tubes S1 and S2 filled with the normal concrete N2 has verified the effects of the oriented fibre layers where the filled square tube S1 exhibited a considerable gradual reduction in the strength while square tubes S2 showed slightly shorter reduction branch. The energy absorption capacity of all types of filled columns S1 is larger than that of filled S2 columns. This is because the transverse resistance of S1 is better as fibres are extended close to the hoop direction. The sectional stress of the circular columns that are filled with either the perlite concrete P2 or the normal concrete N2 is improved when the angle of the oriented fibre increases to be close to the hoop direction. The results of the filled circular tube C2 verify that the ability of the pultruded FRP tubes to reveal high sectional stress has been affected positively when there are more fibres in the hoop direction. This positive effect of fibre orientation is also reflected on the energy absorption capacity. The filled columns of C2 shows higher ability compared than those filled with same filler type of column C1 because the angle of the oriented fibre of C2 is larger than that of C1.
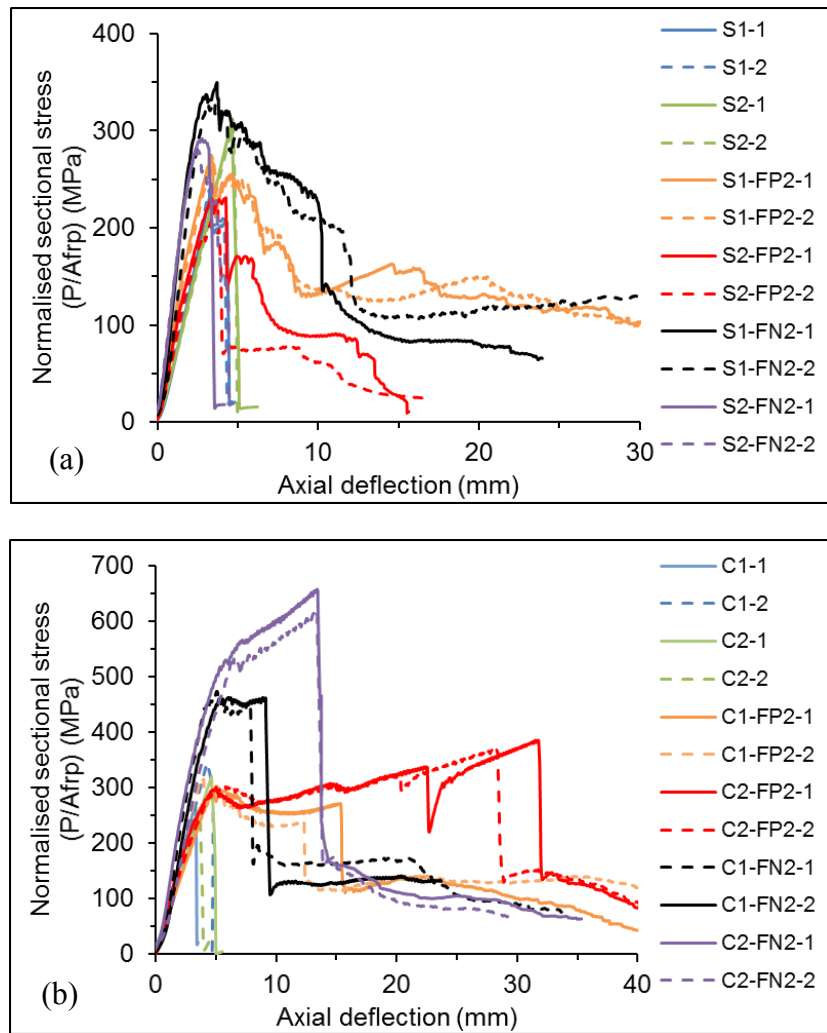
Fig. 11. Normalised sectional stress-deflection curves of the hollow and filled columns

(a) square tubes (S1 and S2) and (b) circular tubes (C1 and C2).

5.3 Effect of the cross section

The confining pressure provided by FRP tube is more effective in circular cross-sections than in square sections. In case of the square cross-section, the larger confining pressure is generated at corners than on the sides because of the flexural behaviour at sides of the square section. This difference in the effectiveness of the FRP confinement affects the failure modes, the degree of enhancement of the load carrying capacity and the post-peak axial behaviour. The filled columns of the square tube failed by the crushing at one end of the column after concrete failure. Then, the longitudinal corner splitting was propagated from the crushed end to the other end. Cracks propagated rapidly in S2 square tubes due to the restriction of the availability

102

of the fibre layers in the hoop direction (Fig. 5). The failure mode of the circular columns was crushing at one or both ends of the column followed by separation the perimeter into strips before growing towards the other end (Fig.7). This can be attributed to the non-uniform confining pressure of square columns and uniform pressure of the circular columns.

The second effect is the amount of improvement in the load capacity of columns. The uniform confining pressure of the circular columns and effects of the oriented fibre layers provide high enhancement in the load capacity of the circular columns compared with the enhancement of the square columns.

The post-peak axial behaviour is the third effect observed from the results of the experimental work. Load-axial deflection curves of the pultruded square columns S2 that were filled with normal concrete N1 and N2 did not declare gradual reduction of the columns' resistance after the peak load (Fig.4). On the other hand, both types of the circular columns C1 and C2 show that the resistance of the filled columns with normal concrete is not suddenly dropped after achieving the peak load (Fig. 6). The energy absorption capacity of filled square S2 and circular columns C1 and C2 demonstrates influence of cross-section. Energy absorption of circular columns is larger than that of square columns as shown in Table 8. This is because the lateral resistance of FRP circular columns is uniform. Although the cross-sectional area of S1 is larger than that of C2, the energy absorption of C2 filled with N2 is higher, but it is lower for C1. This is because the angle of oriented fibre of C2 is closest to the transverse direction compared with C1. Further, the capacity of hollow circular columns shows the positive effect of fibre orientation.

5.4 Effect of the wall thickness

The effects of the wall thickness on the load capacity of hollow columns can be recognized from results of the hollow square tube columns. The results of the material tests of the square tube S1 (fibre content, longitudinal compressive strength and the longitudinal compressive modulus) are higher than those of the square tube S2. On the other hand, the experimental results showed that the normalised sectional stress of the square column S2 is higher than that of square S1 (Fig. 11(a)). This result can be attributed to the effects of the instability conditions due to the local buckling. Although the slenderness ratios (L/r) of the square tubes S1 and S2 are approximately similar

(13.0 and 13.1 respectively) and lower than the limit of global buckling of 50 [6], the plate slenderness (width/thickness) ratios are different. The plate slenderness ratio of square tubes S1 is 18.2 while it is 14.9 for square tubes S2. Therefore, the load carrying capacity of square tube S1 is controlled by the possibility of local buckling which limits its strength to reach a higher level. The compressive strength failure was apparent in the case of hollow circular columns. The failure modes of the global and local buckling never occurred due to low global slenderness (15.1) and diameter to thickness ratios (14.8). According to the Chinese Code, the upper limit of diameter to thickness ratio is 80 to avoid the adverse effects of local buckling [50]. When the stress reached the compressive strength of the material, the fibres at bottom buckled before delamination of fibre layers, end extension and virtual crushing at the end of the column.

6. Conclusions

This research presented the results of axial compressive tests on square and circular pultruded GFRP tubes filled with different types of concrete. Hollow and filled column specimens were prepared and tested to investigate the effects of the modulus of filler material, shape and the fibre orientation of the FRP tubes. Based on the test results, the following conclusions are drawn:

- The improvement in the stiffness of the square and circular pultruded GFRP tube columns depends on the modulus of infill concrete. When the modulus of filler increases up to 30 GPa, stiffness values of square tubes S1 and S2 are improved by 77.8% and 92.0 % respectively compared with stiffness of respective hollow columns while stiffness of circular tube C1 and C2 is increased by 46.5% and 45.9% respectively.

- The axial behaviour of hollow pultruded square FRP tubes was governed by the plate slenderness ratio (width/thickness) and the global slenderness ratio (L/r). While L/r is similar for S1 and S2, S1 was predominantly governed by the plate slenderness ratio. Moreover, the failure of S2 initiated at the corners were aggravated by the lack of continuous fibres in the transverse direction. The ratio of diameter-to-thickness ratio of circular tubes makes crushing at end as the dominated failure mode.

- Significant improvement in the peak load was observed for the filled circular columns compared to that of the hollow circular columns. When majority of the fibres are in the axial direction, hollow square columns reached higher peak load than the filled columns. The post-peak behaviour of hollow columns is a rapid drop after the peak load compared to the gradual decrease due to filling with concrete.

- The load carrying capacity of the filled pultruded GFRP tube columns is increased with the increasing modulus of the concrete filler. Moreover, the ability of the square and circular columns to sustain the load after the peak load is influenced by the properties of the infill concrete and FRP tube. Tubes filled with perlite concrete showed sustained load carrying capacity post peak load. This behaviour is attributed to the material characteristics of the perlite based filler.

- The energy absorption capacity of filled square and circular columns increases due to filling with concrete when the transverse modulus of pultruded FRP tube is capable of resisting the dilation of filler. Columns filled with perlite concrete shows improvement in the capacity of energy absorption, although the perlite concrete strength is lower or equal to the strength of normal concrete. Increasing the angle of oriented fibre layers with respect to the axial direction of filled columns provide an improvement in the energy absorption.

- Continuous fibres oriented towards the transverse direction in circular columns (C1 and C2) and square column, S1 provide substantial transverse resistance, which is apparent in terms of the peak load, post peak behaviour, the failure mode and capacity of energy absorption.

This research mainly focussed on the behaviour of short filled GFRP square and circular columns. It is necessary to extend this work to investigate the behaviour of slender columns as well so the effect of global buckling could be better understood when such tubes are used as column members in civil infrastructure.

Acknowledgement

References

[1] F. Li, Q. Zhao, L. Chen, G. Shao, Experimental and theoretical research on the compression performance of CFRP sheet confined GFRP short pipe, Ci. World. J. 2014 (2014) 109692.

[2] M. Correia, F. Nunes, J. Correia, N. Silvestre, Buckling behavior and failure of hybrid fiber-reinforced polymer pultruded short columns, J. Compos. Constr. 17(4) (2012) 463-475.

[3] E.J. Barbero, I.G. Raftoyiannis, Local buckling of FRP beams and columns, J. Mater. Civ. Eng 5(3) (1993) 339-355.

[4] E. Barbero, J. Tomblin, A phenomenological design equation for FRP columns with interaction between local and global buckling, Thin-Walled Structures 18(2) (1994) 117-131.

[5] A. Zureick, D. Scott, Short-term behavior and design of fiber-reinforced polymeric slender members under axial compression, Journal of Composites for Construction 1(4) (1997) 140-149.

[6] Z.A. Hashem, R.L. Yuan, Short vs. long column behavior of pultruded glass-fiber reinforced polymer composites, Constr. Build. Mater. 15(8) (2001) 369-378.

[7] P. Qian, P. Feng, L. Ye, Experimental study on GFRP pipes under axial compression, Frontiers of Architecture and Civil Engineering in China 2(1) (2008) 73-78.

[8] A. Godat, F. Légeron, V. Gagné, B. Marmion, Use of FRP pultruded members for electricity transmission towers, Compos. Struct. 105 (2013) 408-421.

[9] I. Puente, A. Insausti, M. Azkune, Buckling of GFRP columns: An empirical approach to design, J. Compos. Constr. 10(6) (2006) 529-537.

[10] Y. Bai, T. Keller, Shear failure of pultruded fiber-reinforced polymer composites under axial compression, J. Compos. Constr. 13(3) (2009) 234-242.

[11] D.C. Cardoso, K.A. Harries, E.d.M. Batista, Closed-form equations for compressive local buckling of pultruded thin-walled sections, Thin Walled Struct. 79 (2014) 16-22.

[12] H.V. Gangarao, M.M. Blandford, Critical buckling strength prediction of pultruded glass fiber reinforced polymeric composite columns, J. Compos. Mater. 48(29) (2014) 3685-3702.

[13] A.Z. Fam, S.H. Rizkalla, Concrete-filled FRP tubes for flexural and axial compression members, Proceedings of ACMBS-3, Ottawa, Canada (2000) 315-322.

[14] H. Han, F. Taheri, N. Pegg, Crushing behaviors and energy absorption efficiency of hybrid pultruded and ±45° braided tubes, Mech. Compos. Mater. Struct. 18(4) (2011) 287-300.

[15] F. Nunes, J.R. Correia, N. Silvestre, Structural behaviour of hybrid FRP pultruded columns. Part 1: Experimental study, Compos. Struct. 139 (2016) 291-303.

[16] J. Teng, L. Lam, Behavior and modeling of fiber reinforced polymer-confined concrete, J. Struct. Eng-ASCE. 130(11) (2004) 1713-1723.

[17] W.-K. Hong, H.-C. Kim, Behavior of concrete columns confined by carbon composite tubes, Can. J. Civil. Eng. 31(2) (2004) 178-188.

[18] H. Kim, K.H. Lee, Y.H. Lee, J. Lee, Axial behavior of concrete-filled carbon fiber-reinforced polymer composite columns, Struct. Des. Tall SPEC. 21(3) (2012) 178-193.

[19] T. Vincent, T. Ozbakkaloglu, Influence of fiber orientation and specimen end condition on axial compressive behavior of FRP-confined concrete, Constr. Build. Mater. 47 (2013) 814-826.

[20] A. Mirmiran, M. Shahawy, T. Beitleman, Slenderness limit for hybrid FRP-concrete columns, J. Compos. Constr. 5(1) (2001) 26-34.

[21] T. Vincent, T. Ozbakkaloglu, Influence of slenderness on stress-strain behavior of concrete-filled FRP tubes: experimental study, J. Compos. Constr. 19(1) (2015) 04014029.

[22] S. Pessiki, K.A. Harries, J.T. Kestner, R. Sause, J.M. Ricles, Axial behavior of reinforced concrete columns confined with FRP jackets, J. Compos. Constr. 5(4) (2001) 237-245.

[23] A. Fam, D. Schnerch, S. Rizkalla, Rectangular filament-wound glass fiber reinforced polymer tubes filled with concrete under flexural and axial loading: experimental investigation, J. Compos. Constr. 9(1) (2005) 25-33.

[24] Z. Yan, C.P. Pantelides, L.D. Reaveley, Posttensioned FRP composite shells for concrete confinement, J. Compos. Constr. 11(1) (2007) 81-90.

[25] A. Beddiar, R. Zitoune, F. Collombet, Y.H. Grunevald, M.T. Abadlia, N. Bourahla, Compressive behaviour of concrete elements confined with GFRP-prefabricated bonded shells, Eur. J. Environ. Civ. En. 19(1) (2014) 65-80.

[26] T. Vincent, T. Ozbakkaloglu, Influence of concrete strength and confinement method on axial compressive behavior of FRP confined high- and ultra high-strength concrete, Compos. Part B 50 (2013) 413-428.

[27] J.C. Lim, T. Ozbakkloglu, Factors influencing hoop rupture strains of FRP-confined concrete, A.M.M., Trans Tech Publ, 2014, pp. 949-953.

[28] T. Yu, X. Fang, J.-G. Teng, FRP-confined self-compacting concrete under axial compression, J. Mater. Civ. Eng 26(11) (2013) 04014082.

[29] J. Zhao, T. Yu, J. Teng, Stress-strain behavior of FRP-confined recycled aggregate concrete, J. Compos. Constr. 19(3) (2014) 04014054.

[30] Y. Zhou, X. Liu, F. Xing, H. Cui, L. Sui, Axial compressive behavior of FRP-confined lightweight aggregate concrete: An experimental study and stress-strain relation model, Constr. Build. Mater. 119 (2016) 1-15.

[31] T. Ozbakkaloglu, Compressive behavior of concrete-filled FRP tube columns: Assessment of critical column parameters, Eng. Struct. 51 (2013) 188-199.

[32] T. Ozbakkaloglu, W. Zhang, Investigation of key column parameters on compressive behavior of concrete-filled FRP tubes, A.M.M. 256-259 (2012) 779-783.

[33] A.A. Mortazavi, K. Pilakoutas, K.S. Son, RC column strengthening by lateral pre-tensioning of FRP, Constr. Build. Mater. 17(6) (2003) 491-497.

[34] T. Vincent, T. Ozbakkaloglu, Compressive behavior of prestressed high-strength concrete-filled aramid FRP tube columns: experimental observations, J. Compos. Constr. 19(6) (2015) 04015003.

[35] M.S. Abdulraheem, Experimental investigation of fire effects on ductility and stiffness of reinforced reactive powder concrete columns under axial compression, Journal of Building Engineering 20 (2018) 750-761.

[36] S.A. Sheikh, S.S. Khoury, Confined concrete columns with stubs, ACI Structural Journal 90 (1993) 414-414.

[37] Y. Wang, J. Feng, J. Wu, D. Hu, Effects of fiber orientation and wall thickness on energy absorption characteristics of carbon-reinforced composite tubes under different loading conditions, Compos. Struct. 153 (2016) 356-368.

[38] L. Wang, W. Liu, Y. Fang, L. Wan, R. Huo, Axial crush behavior and energy absorption capability of foam-filled GFRP tubes manufactured through vacuum assisted resin infusion process, Thin Walled Struct. 98 (2016) 263-273.

[39] A.U. Al-saadi, T. Aravinthan, W. Lokuge, Structural applications of Fibre Reinforced Polymer (FRP) composite tubes: a review of columns members, Compos. Struct. 204 (2018) 513-524.

[40] ISO-1172, Textile-glass-reinforced plastics-Prepregs,moulding compounds and laminates-Determination of the textile-glass and mineral-filler content-Calcination methods, Geneve,Switzerland., 1996.

[41] ISO-527-4, Plastics-Determination of tensile properties, Part4: Test conditions for isotropic and orthotropic fibre -reinforced plastic composites,European Committee for Standardization, Brussels, Belgium., 1997.

[42] A. D695, Standard Test Method for Compressive Properties of Rigid Plastics, United States, 2010.

[43] İ. Türkmen, A. Kantarcı, Effects of expanded perlite aggregate and different curing conditions on the physical and mechanical properties of self-compacting concrete, Build. Environ. 42(6) (2007) 2378-2383.

[44] M. Lanzón, P. García-Ruiz, Lightweight cement mortars: Advantages and inconveniences of expanded perlite and its influence on fresh and hardened state and durability, Constr. Build. Mater. 22(8) (2008) 1798-1806.

[45] İ.B. Topçu, B. Işıkdağ, Effect of expanded perlite aggregate on the properties of lightweight concrete, J. Mater. Process. Technol. 204(1) (2008) 34-38.

[46] M.B. Karakoç, R. Demirboga, HSC with expanded perlite aggregate at wet and dry curing conditions, J. Mater. Civ. Eng 22(12) (2010) 1252-1259.

[47] O. Sengul, S. Azizi, F. Karaosmanoglu, M.A. Tasdemir, Effect of expanded perlite on the mechanical properties and thermal conductivity of lightweight concrete, Energ. Building. 43(2) (2011) 671-676.

[48] M. Jedidi, O. Benjeddou, C. Soussi, Effect of Expanded Perlite Aggregate Dosage on Properties of Lightweight Concrete, J.J.C.E. 9(3) (2015) 278-291.

[49] AS1012.9, Methods of testing concrete, Methods 9:Compressive strength tests-Concrete,mortar and grout specimens., Sydney, Australia, 2014.

[50] T. Yu, J.G. Teng, Design of Concrete-Filled FRP Tubular Columns: Provisions in the Chinese Technical Code for Infrastructure Application of FRP Composites, J. Compos. Constr. 15(3) (2011) 451-461.

4.3 Summary

This chapter shows the experimental work of hollow and filled pultruded FRP tube column to investigate their axial behaviour and improvements due to filling in stiffness, axial load capacity and energy absorption capacity. The results of short hollow tubes show that the behaviour is linear up to the peak load and the failure mode of square tubes is changed from buckling bulge to local buckling when the length-to-lateral dimension ratio (L/D) ratio increases from 1 to 5. On the other hand, the failure mode of hollow circular tubes remains due to end crushing. It should be noted that results of hollow circular tubes C1 and C2 are showing a bit higher variation in axial loads as only 2 samples were selected for each case in the experimental investigations.

The results of columns of L/D ratio of 5 show that the stiffness of the square columns is improved when they are filled with concrete. Furthermore, the axial behaviour of the hollow square columns is governed by the plate slenderness (width-to-thickness) ratio. Increasing the concrete filler material modulus results in improving load carrying capacity of square columns S1 compared with load capacity of hollow S1. The filled columns S2 show a decreasing trend because most fibres are positioned in the axial direction and the discontinuity of the non-axial fibre layers at corners adversely affects the ability of filled columns to resist further loads. The post peak behaviour is modified to gradually decrease, instead of a rapid drop in strength of the hollow columns. The degree of enhancement of the energy absorption capacity of square columns is affected by the properties of filler, wall thickness and fibre orientation for pultruded FRP tube.

The stiffness of hollow circular columns at same cross-sectional area is affected by the angle of non-axial fibre layer. On the other hand, the improvement in the stiffness of filled columns depends mainly on the modulus of filler. The ability of circular column to resist loading is increased when properties of filler are improved and angle of the non-axial fibres increase with respect to the axial direction. Moreover, the properties of the infill concrete and confinement effectiveness due to the fibre orientation and their layup influence the ability of columns to continue sustaining the load after the peak load. Finally, the energy absorption capacity of FRP columns could be improved by selecting proper filler material and fibre orientation for pultruded FRP tubes.

Conducting an experimental study of other parameters that can influence the axial behaviour of columns is not a cost or time-effective approach. A better approach is using finite element analysis to simulate the axial behaviour of pultruded FRP tubes. The details of the finite element model of pultruded FRP tubes, infill concrete material, results of the numerical study and verification of the accuracy level of numerical simulations against the results of experiments is the focus of Chapter 5.

Chapter 5:

Finite Element Analyses of Filled Glass Fibre Reinforced Polymer (GFRP) Pultruded Tubes under Axial Loading

After finishing the experimental work of hollow and filled pultruded FRP tubes in chapter 4, this chapter presents the finite element simulation of the axial behaviour of pultruded FRP tubes either those in hollow or filled conditions using finite element analysis. The finite element simulation was conducted for square and circular FRP tubes in hollow condition and those filled with different types of filler. Both lamina and plate methods were followed in defining the material properties of the FRP tubes. In lamina method, the mechanical properties of the FRP lamina, stacking sequence of the laminate, thickness and orientation of each lamina are the necessary data to define inside the software program STRAND7. On the other hand, the orthotropic properties were used to define the pultruded FRP tubes in plate method to check the accuracy of simulation with limited manufacturer's data using the results of simple tests to define the properties of FRP tubes. The stress- strain curve for confined concrete was used to simulate concrete behaviour. The details of the boundary conditions, loading and solver setup were described properly. Both the geometric and material nonlinearities were considered. Two failure criteria followed based on the defining method of pultruded FRP tubes. The Tsai-Wu theory and uni-axial maximum strength were followed for the lamina and plate methods where appropriate. The results of the simulation study were compared with those obtained experimentally. The load – deflection behaviour, load carrying capacity and modes of failure were discussed in paper 4.

Further, finite element simulation was conducted for the pultruded FRP hollow tubes with different length-to-lateral dimension ratio to investigate the effect of slenderness ratio on their failure mode.

5.1 Paper 4

Finite element analyses of filled glass fibre reinforced polymer (GFRP) pultruded tubes under axial loading

Ali Umran Al-saadi, Thiru Aravinthan and Weena Lokuge

University of Southern Queensland, School of Civil Engineering and Surveying, Centre for Future Materials (CFM), Australia.

Finite element analyses of filled glass fibre reinforced polymer (GFRP) pultruded tubes under axial loading

Ali Umran Al-saadi[1,2], Thiru Aravinthan[1*] and Weena Lokuge[1]

[1] University of Southern Queensland, School of Civil Engineering and Surveying, Centre for Future Materials (CFM), Australia.

[2] University of Babylon, Babil, Iraq.

Email: AliUmranKadhum.Alsaadi@usq.edu.au, Thiru.Aravinthan@usq.edu.au, Weena.Lokuge@usq.edu.au

Abstract

Investigation on the load carrying capacity of pultruded fibre reinforced polymer (PFRP) tubes using finite element analysis is a challenging task. This is because the accuracy of simulation depends mainly on modelling the PFRP tube in case of hollow and infill concrete material in case of filled columns. The lamina and plate methods inside the finite element software program STRAND 7 are used in this study to model PFRP tubes while an available stress-strain curve for confined concrete was adopted to simulate concrete behaviour. Both the material and geometric nonlinearities were considered in the numerical analysis. The load-deflection curves, load carrying capacity and failure modes are validated with experimental results. It can be concluded that depending on the availability of the material properties either the lamina method or the plate method can be used to model filled FRP tubes. The outcomes of this study will enhance the use of pultruded FRP profiles in applications of the civil engineering since the numerical results provide a good correlation to the actual behaviour.

Keywords: Confined concrete; Finite element analysis; Laminate; Pultruded FRP tube; Tsai-Wu failure criterion.

1. Introduction

During the last decades, the use of Fibre Reinforced Polymer (FRP) profiles as structural members has become increasingly popular. The extent of using the pultruded FRP profiles in the construction industry depends on the ways the issues associated with them can be solved while utilising their excellent features such as high strength and stiffness to weight ratios, corrosion resistance and durability. Previous research shows that the weakness on deformability and buckling of pultruded FRP profiles due to their low modulus and high plate slenderness can be addressed using different methods to reach their potential strength [1-3].

The pultruded FRP sections have comprehensively been researched through experimental investigation while little attention was paid for numerical investigations of concrete filled pultruded FRP tubes. The research areas of the previous studies are the influence of instability conditions due to buckling on the load carrying capacity of pultruded FRP columns and proposed numerical models to assess their load carrying capacity [4-9]. The core of the other research area is to make an improvement in the capacity of pultruded FRP columns by compensating the low axial stiffness by adding a layer of high stiffness fibre or replacing the low stiffness fibre layer with one of high stiffness fibre layer [2, 10, 11].

Filling with concrete was another way to boost the axial stiffness of the pultruded FRP tube and to delay or prevent the failure due to buckling [12]. The axial behaviour of concrete filled circular FRP tubes (CFFT) with length-to diameter ratio of 2 was studied by Fam and Rizkalla [13]. The FRP tubes are filled either totally or partially with central hole. The FRP tubes were designed to provide strength and stiffness in axial and transverse directions rather than all fibres oriented only in the transverse direction to investigate the effects of the fibre orientation on the FRP confinement effectiveness. The results show that the pultruded tube (all fibres extend in axial direction) fails to confine the concrete due to the lack of stiffness in transverse direction. It also shows that the confinement effects is increased as the angle of fibre increases towards the transverse direction. The effects of eccentricity of the applies load and the influences of the FRP laminate structures on the behaviour of concrete filled circular FRP tubes was investigated by Fam et al. [14]. The results show that the

flexural strength is improved as the ratio of fibres increases in axial direction and the axial compressive strength of CFFT thin tubes showing enhancement when the ratio of fibres in the transverse direction increases. Although the experimental results show that the load carrying capacity of pultruded FRP columns is enhanced due to a concrete filler, predicting the amount of increment is crucial in broadening the use of this innovative structural column members in civil infrastructure. One way to make this prediction is using Finite Element Analysis (FEA).

FRP material in the finite element analysis can be modelled using two methods; lamina and plate methods. In lamina method, the properties of the FRP lamina should be determined before establishing the stacking sequences of the FRP laminate and the thickness of each lamina [15-18]. The mechanical properties of the FRP lamina can be obtained by using micromechanical equations to get an acceptable estimation to the elastic properties of the FRP lamina [15]. This method contains mathematical equations to calculate the properties of the FRP lamina and it provides an ability to study the effects of different parameters related to the material properties. This approach is capable of reforming the stacking sequence of the laminate layers, changing its thickness and defining the laminate properties in the axial and transverse directions. The second method is the plate method by considering the FRP material as a linear elastic orthotropic material [19-21]. Nine mechanical properties such as elastic modulus, shear modulus and Poisson's ratio for three mutually perpendicular directions are needed as input parameters. Depending on the structure of the FRP laminate, some values can be assumed [22, 23]. The advantage of this method is its easiness to follow by carrying out the necessary material tests to obtain the orthotropic material properties. On the other hand, the ability to study the effect of different parameters such as fibre orientation, fibre type and fibre content on the axial behaviour is limited as mechanical properties of the overall FRP material need to be determined experimentally for each case.

The FRP confinement delays the development of the damage within the concrete element indicating an extended region in which the elastic parameters are considered [24]. Due to the internal damage of the concrete, a gradual degradation in the elastic modulus of concrete occurs. This degradation is small in a pre-peak load before it turns to be more substantial in the region of the post-peak load. Many models are adopted to define concrete properties inside the finite element. The plasticity models in the

117

ABAQUS software program are used to simulate the compressive behaviour of concrete confined with FRP material. Concrete Damage Plasticity (CDP) type was followed in these models and were modified by researchers to include plasticity parameters of concrete [17, 18, 20, 21, 23, 25, 26]. The parameters of the other plasticity model Drucker-Prager (D-P) have also been reshaped based on the experimental results [24, 27-31]. The stress-strain curve of the confined concrete was used to define the concrete properties in the finite element simulation for concrete filled steel tubes in the past [29, 30, 32]. The axial stress-axial strain relationship of concrete confined with FRP can be used within the STRAND7 software program to exhibit concrete behaviour in tension and compression [33].

As the mechanism of the FRP confinement depends on the concrete dilation, it varies with the lateral expansion of concrete. Consequently, the complete stress-strain curve of confined concrete can be described by using an analysis oriented model [34]. The process of determining the stress-strain curve of the FRP confined concrete includes incremental approach. The calculation of the confining pressure and axial strain for a specified lateral strain is the first step in this procedure. Then, the confined concrete strength and confined axial strain corresponding to the value of the confining pressure are determined. Finally, the axial stress corresponding to the calculated axial strain is computed using the axial stress-axial strain relationship of the concrete.

This paper initially provides a description of the two approaches used in the simulation of the behaviour of FRP tubes. Lamina method being the first approach defines FRP properties in the finite element and the second approach considers FRP as a linear elastic orthotropic material. Finally, the load-deflection curves, the calculated load carrying capacity using finite element simulation and modes of failure are compared with experimental results.

2. Research significance

Using finite element analysis to predict the load carrying capacity of pultruded hollow or concrete filled FRP tubes contributes in broadening the safe use of pultruded FRP sections in civil engineering applications. Although some research has been carried out on pultruded FRP profiles and concrete filled FRP or steel tubes, there is a limited studies to simulate the axial behaviour of hollow and concrete filled pultruded FRP tubes. The significance of this study is to identifying the axial behaviour of different

shapes of pultruded FRP tubes with length –to-lateral dimension of 5 by modelling the FRP tubes in two different ways; lamina and plate method. The differences in fibre orientation and wall thickness as well as modulus of filler are considered. The findings of this study will be helpful in the decision making process of selecting hollow or filled FRP pultruded profiles based on the capacity and failure mechanisms.

3. Finite element simulation

In order to perform an accurate finite element analysis for filled pultruded GFRP tubes, the two main components of these columns should be appropriately modelled. These components are the pultruded GFRP tubes and the confined concrete. The general-purpose finite element program (STRAND 7) was used to implement the numerical analysis.

3.1 Modelling of pultruded GFRP tubes

Four types of pultruded FRP tubes were examined in this study, two square and two circular tubes. The dimensions of the square tubes, S1 and S2 are 100 mm x 100 mm with 5.2 mm thickness and 102 mm x 102 mm with 6.4 mm thickness respectively. The diameter (88.9 mm) and the wall thickness (6 mm) of both C1 and C2 circular FRP tubes are similar although their fibre orientations are not identical. The length of all the tubes was selected to provide length-to-lateral dimension ratio of 5. The pultruded FRP tubes selected in this study are mostly formed with axial and angle-ply stacking sequence. The fibre layers of the square tube S1 are oriented at angles of [0/+50/-50] while layers of the square tube S2 are [mat/-45/0/+45]. The only difference in the stacking sequence of the circular FRP tubes C1 and C2 is the angle of the non-axial fibre layers. The sequence of fibre layers of the circular tube C1 is [0/+56/-56], and it is [0/+71/-71] for the circular tube C2.

Two approaches were used to model the FRP tube elements in the analyses; (a) lamina method where the plate is defined using the unidirectional lamina and relevant thickness and (b) plate method using orthotropic properties.

3.1.1 Lamina method

The unidirectional FRP lamina (ply) is the building unit of FRP laminate, which is made out of a number of unidirectional FRP plies stacked together in multi-directions. Use of micromechanical equations to calculate the mechanical properties of FRP lamina could deliver sensible evaluation of mechanical properties of FRP ply [15]. The mechanical properties of the lamina are elastic modulus in the fibre direction (E_1), the elastic modulus in the transverse direction (E_2), Poisson's ratio (v_{12}), in-plane shear modulus (G_{12}) and out-of-plane shear modulus (G_{13} and G_{23}).

The fibre layers and thickness can be estimated through conducting burnout test for FRP tubes to determine the fibre content . The stacking sequences of FRP laminate can be identified by separating layers one after the other. The weight of each layer is also measured. Finally, the calculated thickness value of FRP layer can be computed by multiplying the total laminate thickness with the ratio of the individual layer weight to total weight of the fibre content. Table 1 shows the FRP lamina and their thicknesses in each orientation for all the tubes. The fibre volume fraction was assumed to be uniform for all plies.

The standard mechanical properties of fibre and matrix that are considered in the calculation of the mechanical properties of the unidirectional lamina are listed in Table 2 [35] . It should be noted that the pultruded square (S1) and circular (C1 and C2) FRP tubes were made of E-glass fibre and Vinyl-Ester resin while the pultruded square tube S2 was made of E-glass fibre and Polyester resin.

Table 1. Lamina orientation and thickness of FRP tubes.

FRP tubes	Stacking sequence	Lamina thickness (mm)
S1	[0/+50/-50/0/-50/+50/0]	[4.274, 0.463, 0.463]
S2	[mat/-45/0/+45/mat]	[0.6,5.2,0.6]
C1	[0/+56/-56/0/-56/+56/0]	[4.466, 0.767, 0.767]
C2	[0/+71/-71/0/-71/+71/0]	[3.355, 1.324, 1.321]

Table 2. Properties of fibre and matrix

E-glass fibre				Vinyl- Ester resin			Polyester resin		
E_{1f} (MPa)	E_{2f} (MPa)	G_{12f} (MPa)	v_f	E_m (MPa)	G_m (MPa)	v_m	E_m (MPa)	G_m (MPa)	v_m
73000	73000	30000	0.23	3500	1300	0.35	3350	1350	0.35

The elastic modulus in the fibre direction (E_1) and the in-plane Poisson's ratio (v_{12}) of the FRP lamina were calculated based on the rule of mixtures formula, while, the transverse elastic modulus (E_2) and the in-plane shear modulus(G_{12}) were obtained using a semi empirical approaches of Halpin-Tsai [35] as shown in equations (1) and (2). Finally, the value of the out-of-plane shear modulus (G_{23}) was calculated using equations (3) and (4) while the value of (G_{13}) is assumed to be equal to (G_{12}) [3].

$$E_2 = E_m \frac{(1+V_f)E_{2f}+V_m E_m}{V_m E_{2f}+(1+V_f)E_m} \tag{1}$$

$$G_{12} = G_m \frac{(1+V_f)G_{12f}+V_m G_m}{V_m G_{12f}+(1+V_f)G_m} \tag{2}$$

$$G_{23} = G_m \frac{V_f+\eta(1-V_f)}{\eta(1-V_f)+(V_f G_m/G_{12f})} \tag{3}$$

$$\eta = \frac{3-4v_m+(G_m/G_{12f})}{4(1-v_m)} \tag{4}$$

E_m and E_{2f} are the matrix moduli and transverse fibre modulus. V_f and V_m are the volume fraction of fibres and matrix respectively. G_m and G_{12f} are the shear modulus of the matrix and fibre respectively and v_m is the Poisson's ratio of the matrix.

The input data required by the finite element program STRAND 7 to evaluate the properties of the FRP laminate are the calculated mechanical properties of the lamina, orientation related to the local axis of the plate element and the thickness of fibre layers. Based on the mechanical properties of plies and their stacking sequence, STRAND7 computed effective elastic modulus, shear modulus, Poisson's ratios and stiffness matrices of the laminate.

The mechanical properties of the uni-directional FRP lamina were calculated using the procedure presented above for all pultruded FRP tubes. The providers' data of the fibre content for square tubes were used in the calculation (S1=77.4 %, S2=70%) while the fibre content of the circular tubes is assumed as that of the square tubes S1. The modulus in the fibre direction (E$_1$), modulus in the transverse direction (E$_2$), Poisson's ratio (v_{12}), in-plane shear modulus (G$_{12}$) and out-plane shear modulus (G$_{23}$) obtained are shown in Table 3. It should be noted that the average values of resin are used in the calculations and the mat layers of S2 are not represented in the stacking sequences of its laminate.

Table 3. Mechanical properties and strength limits of FRP lamina

FRP tube	Calculated mechanical properties					Strength limits				
	E_1 (GPa)	E_2 (GPa)	v_{12}	G_{12} (GPa)	G_{23} (GPa)	Longitudinal strength (MPa)		Transverse strength (MPa)		Shear strength (MPa)
						σ_t	σ_c	σ_t	σ_c	
S1,C1,C2	45.7	12.1	0.28	4.6	4.0	799.0[1]	558.3[1]	43	187	64
S2	41.3	9.9	0.28	4.0	3.6	684.0[1]	581.6[1]	22.5[2]	105[2]	52.6[2]

[1]Tensile and compressive strengths of Vinyl ester are 75 MPa and 127 MPa respectively while they are 65 MPa and 170 MPa (in average) respectively for Polyester [35].

[2] The average values are considered in the analysis.

3.1.2 Plate method

The second approach used to simulate FRP materials in the finite element analysis is to consider it as a linear elastic orthotropic material. As the fibre layers are oriented in multi-directions, varied modulus of elasticity in three main directions should be defined. The effective properties calculated using the lamina method such as elastic modulus in the axial (E$_1$) and transverse (E$_2$) directions, shear modulus and Poisson's ratio are utilised to define the orthotropic material properties. The modulus of elasticity through the thickness of plate FRP element (E$_3$) is the modulus of resin as no fibre layers extend in the local z-axis. The Poisson's ratio (v_{12}) was the calculated value of FRP laminate based on the lamina method while values of v_{13} and v_{23} were assumed as 0.3 and 0.45 respectively. The main shear modulus (G_{12}) was the effective value of

the FRP laminate calculated from lamina method, and the shear moduli G_{13} and G_{23} were calculated from equation (5). Orthotropic properties used in this plate method are shown in Table 4.

$$G_{xy} = \frac{E_x E_y}{E_x + E_y + (2\,v_{xy}E_x)} \tag{5}$$

Table 4. Orthotropic material properties of the pultruded FRP tubes.

FRP tube	(E$_1$) GPa	(E$_2$) GPa	(E$_3$) GPa[1]	v_{12}	(G$_{12}$) GPa	(G$_{23}$) GPa	(G$_{31}$) GPa
S1	40.0	13.9	3.50	0.337	6.037	3.001	2.496
S2	35.8	10.6	3.35	0.325	4.994	2.843	2.228
C1	37.1	15.8	3.50	0.320	6.435	2.968	2.585
C2	30.8	23.9	3.50	0.194	5.915	2.878	2.836

[1] The modulus of Vinyl ester resin is (3000-4000) MPa while it is (3200-3500) MPa for the Polyesters [35].

3.2 Modelling of the filler material

The concrete material has different behaviour in compression and tension; thus both the positive and negative quadrants should be defined in the finite element program to describe the non-linear stress-strain compressive curve and the linear stress-strain tensile curve. Four types of concrete (perlite concrete, P1 and P2 and normal concrete, N1 and N2) used in the experimental work were considered in this study. The mechanical properties for all these concrete types are listed in Table 5.

Table 5. Properties of the infill.

Concrete type	P1	P2	N1	N2
Compressive strength (MPa)	4.5	10.4	11.2	33
Unit weight(kg/m^3)	1271	1760	2117	2169
Poisson's ratio (v_c)	0.169	0.183	0.230	0.216

3.2.1 Compressive behaviour

In order to define the compressive behaviour of concrete filled steel or FRP tube in the finite element analysis, the constitutive model of the confined concrete is used [17, 18, 30]. The primary data of the unconfined concrete and suitable model of the confined concrete are essential to simulate the axial behaviour of the different types of concrete filled pultruded GFRP tubes. Both the compressive strength (f'_{co}) and the corresponding axial strain (ε_{co}), the modulus of elasticity (E_c) and the Poisson's ratio (v_c) of concrete are fundamental data of the unconfined concrete. It should be noted that the values of concrete modulus are calculated using equation (6) for normal concrete and equation (7) for the lightweight concrete [36, 37] .

$$E_c = 4400\sqrt{f'_{co}} \tag{6}$$

$$E_c = 4400\sqrt{f'_{co}} \left(\frac{\rho_{lc}}{2400}\right)^{1.4} \tag{7}$$

E_c and f'_{co} are in MPa and ρ_{lc} is the unit weight (kg/m^3) of lightweight perlite concrete (P1 or P2).

Axial strain (ε_{co}) corresponding to the unconfined compressive stress (f'_{co}) is calculated using equations (8) and (9).

$$\varepsilon_{co} = \frac{f_{co}^{0.225\,k_d}}{1000} \left[\frac{152}{Di}\right]^{0.1} \left[\frac{2Di}{H}\right]^{0.13} \tag{8}$$

$$k_d = \left(\frac{2400}{\rho_{lc}}\right)^{0.45} \tag{9}$$

Di and H are the diameter and height of the concrete cylinders in *mm*.

On the other hand, confined concrete model includes the relationship of the axial strain, lateral strain and the corresponding compressive strength of the concrete.

The following equation is used to calculate the axial strain of the confined concrete under various confining pressure [34].

$$\frac{\varepsilon_c}{\varepsilon_{co}} = 0.85 \left\{\left[1 + 0.75\left(\frac{-\varepsilon_l}{\varepsilon_{co}}\right)\right]^{0.7} - exp\left[-7\left(\frac{-\varepsilon_l}{\varepsilon_{co}}\right)\right]\right\} * \left(1 + 8\frac{\sigma_l}{f'_{co}}\right) \tag{10}$$

Where ε_c and ε_l are the axial and lateral strains of the concrete filled FRP tube respectively. σ_l denotes the lateral confining pressure provided by the FRP composite tube.

$$\sigma_l = \frac{2\, E_{frp}\, t_{frp}\varepsilon_l}{D} \qquad (11)$$

E_{frp} and t_{frp} are the transverse stiffness and the thickness of the FRP tube. D is either the diameter of the circular section or sectional dimension of the square profile which is defined by equation (12) where b and h are the width and depth of the section [17, 38]. Confining pressure exerted by the FRP tube is assumed to be varying from zero at zero axial strain and the value obtained by equation 11 at the strain corresponding to peak compressive strength of confined concrete.

$$D = \sqrt{(h^2 + b^2)} \qquad (12)$$

As observed in the previous experiments, the effectiveness of FRP confinement depends on the geometry of the cross-section [39-42]. Thus, a shape factor (k_s) is introduced to take into account the ineffective confinement area of the square section by calculating the ratio of the effective confined area to the total cross-sectional area [27]. The shape factor of the square cross-section tube can be expressed as follows [43].

$$k_s = 1 - \frac{2\,[(b/r)-2]^2}{3(b/r)^2} \qquad (13)$$

Where b is the side dimension of the square cross-section, and r is the corner radius. The confined lateral pressure of the GFRP square tube is calculated by multiplying equation (11) and equation (13) while equation (11) is considered for the circular tube. The direct use of this equation gives an overestimation for the circular columns as they have fibres in multi-directions. Reduction factor was used in this situation to take into account the less contribution from the fibres that are not directed towards the hoop direction as opposed to the fibre layers mainly in the hoop direction [34].

Peak confined concrete strength (f'_{cc}) is defined in Equation 14.

$$f'_{cc} = \left(1 + 3.5\frac{\sigma_l}{f'_{co}}\right)f'_{co} \tag{14}$$

Following equation is used to calculate the axial strain (ε^*_{cc}) corresponding to peak concrete strength, f'_{cc} [34].

$$\varepsilon^*_{cc} = \left(1 + 17.5\ \frac{\sigma_l}{f'_{co}}\right)\varepsilon_{co} \tag{15}$$

The confined compressive strength and corresponding axial strain of the perlite concrete were calculated using equations (14) and (15) with a modification to take into account its lightweight characteristic. The modification was the second part in brackets had been multiplied by ($\frac{\rho_{lc}}{2400}$).

The analysis oriented stress-strain model for the confined concrete is generated using equations (8-15) together with a stress-strain model of Popovics [44]. The hoop rupture strain of the pultruded FRP tube is specified using the tensile strength and the elastic modulus in the transverse direction as a first step in the modelling process using the provider's data (Table 6).

Table 6. Tensile and compressive strength of FRP tubes

FRP tube	Tensile strength (MPa) (Transverse)	Compressive strength (MPa)[*] (Longitudinal)
S1	55.0	525.7
S2	48.3	506.2
C1	58.3	365.6
C2	69.9	407.7

[*] It is obtained from the coupon material tests.

By gradual increasing the lateral strain (ε_l), the corresponding values of the axial strain (ε_c) and the confining pressure (σ_l) are obtained from equation (10) and equation (11) respectively in the second step. Then, the confining compressive strength and corresponding axial strain are calculated from equations (14) and (15). Finally, the shape of the stress-strain of the confined concrete based on equation (16) is generated.

$$\frac{\sigma_c}{f'_{cc}} = \frac{r(\varepsilon_c/\varepsilon^*_{cc})}{r - 1 + (\varepsilon_c/\varepsilon^*_{cc})^r} \tag{16}$$

$$r = \frac{E_c}{E_c - (f'_{cc}/\varepsilon^*_{cc})} \tag{17}$$

3.2.2 Tensile behaviour

Although the concrete contribution in tension is ignored in the analysis and design of concrete structural members, the tensile property of the concrete was assumed linearly up to the ultimate strength, which is equal to $0.1f'_{co}$. To avoid convergence difficulties and getting numerical stability, the cracking stress is sustained rather than the sudden drop post cracking. The complete stress strain curve of confined concrete is shown in Fig. 1.
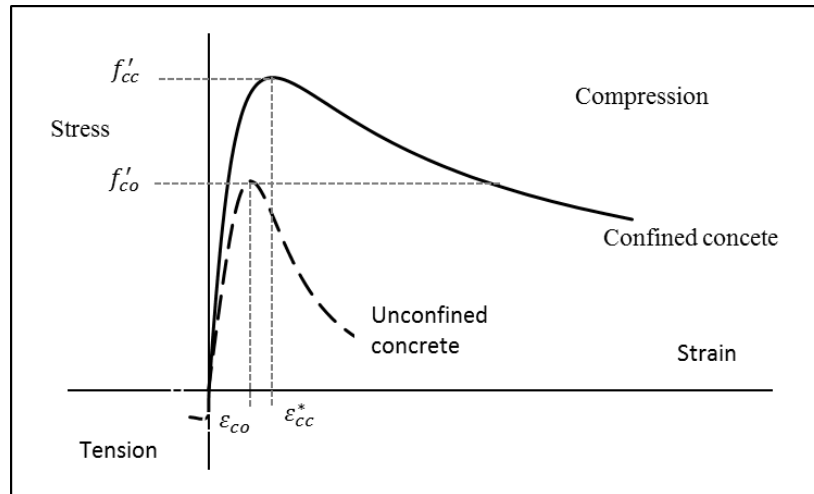
Fig. 1. Stress-strain curve of the confined concrete.

3.3 Element types and meshing

The pultruded GFRP tube is modelled as a four-node plate/shell element while the concrete is modelled as an 8-node brick element (Fig. 2). To avoid any discontinuity in the distribution of the stresses and strains in the concrete and GFRP tube and to determine the optimum mesh size that gives an accurate solution in a reasonable computational time, the mesh is refined. The number of plate elements and brick elements for a thinner square column is 1250 and 3450 respectively, and for the thicker square column is 1734 and 5151 respectively. The mesh of the circular columns

consists of 540 plate elements and 2430 brick elements. The bond between pultruded GFRP tube and infill concrete was assumed to be perfect [21, 23]. This condition was simulated by sharing the same nodes at the contact surfaces of pultruded FRP plate/shell element and the concrete solid element [19].

3.4 Boundary conditions and loading

All degrees of freedom of nodes at the bottom end of the column were restrained, as well as, nodes at the top end of the column except translational movement in the Z-axis. This is because the contact between the ends of the columns and loading plates leads to create restraint against meridional rotations [32, 45, 46]. For imposing boundary conditions, two references nodes have been created, one at the top and one at the bottom. All nodes at the top surface of the column were linked with the top reference node through links. In the same way, nodes at the bottom surface of the column were linked with the bottom reference node. Due to symmetric geometry, only one-quarter of the column was modelled. The boundary condition of the symmetry plane (Z-Y) was restrained for the displacement in the x-direction and rotations about both z-axis and y-axis. The displacement in the y-axis and rotations about both z-axis and x-axis are prevented at the Z-X plane of symmetry as shown in Figure 2. Modelling was conducted for the hollow and filled columns.

The loading was applied as a vertical displacement load in the negative direction of Z-axis through the top reference node of the column. The total displacement is applied in separate steps in order to observe the degradation in the stiffness due to either geometric deformation or non-linear behaviour of the concrete material.
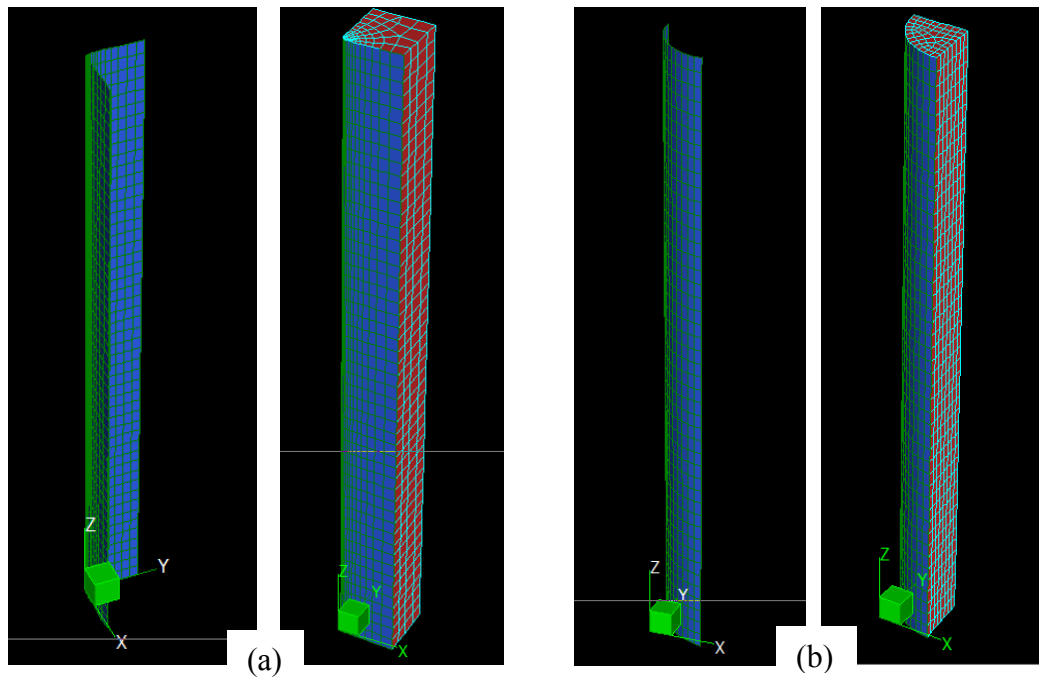
Fig.2 FE model for the quarter of the filled (a) square and (b) circular columns.

3.5 Solver setup and yield criteria of concrete and FRP tubes

Nonlinear static solver is used in the finite element analysis of the column. Both the material and geometric nonlinearity have been considered. The stiffness of the elements is updated according to the stress level and element deformation at every iteration. The termination criterion of the iteration is based on the displacement norm tolerance and residual norm tolerance, which are equal to the 0.0001 and 0.001 respectively. Automatic sub-stepping procedures inside the program provide an ability to obtain the converged solution when either the solution diverges within a specified number of iterations or the load increment is too large. The displacement control (arc length), load scaling and displacement scaling are types of sub-stepping inside the Strand7. Arc length method is adopted in this study as it can handle the solution to proceed especially for buckling and post-buckling analysis [47].

The yield criterion of the nonlinear elastic material (concrete) in this study is the maximum stress because it covers the tension and compression behaviour of concrete [33]. The failure of the FRP composite material can be assigned based on different levels such as ply level, laminate level, constituent level and element level [15]. In the first approach, the strength of the PFRP laminate depends on the strength of its building unit FRP lamina. Thus, for design purposes, the loading that causes the first

ply failure is fundamental to keep the applied load low. Many failure criteria were proposed to predict the initiation of the first ply failure (FPF) [3]. The performance of the Tsai-Wu failure criterion compared with the other failure theories is reported to be better [48]. Therefore, Tsai-Wu failure criterion was used to predict the peak load capacity of the pultruded GFRP tube. The expression for Failure Index (FI) of the Tsai-Wu theory is:

$$\frac{\sigma_t^2}{\sigma_{tt}\,\sigma_{tc}} + \frac{\sigma_a^2}{\sigma_{at}\,\sigma_{ac}} + \frac{\tau_{ta}^2}{\tau_{tap}^2} + \left(\frac{1}{\sigma_{tt}} - \frac{1}{\sigma_{tc}}\right)\sigma_t + \left(\frac{1}{\sigma_{at}} - \frac{1}{\sigma_{ac}}\right)\sigma_a - \frac{\sigma_a\sigma_t}{\sqrt{\sigma_{tt}\sigma_{tc}\sigma_{at}\sigma_{ac}}} = \text{FI} \quad (18)$$

σ_t and σ_a are the transverse tensile stress and axial compressive stress of the FRP lamina respectively. τ_{ta} and τ_{tap} are the shear stress of FRP lamina and allowable shear stress respectively. σ_{tt} and σ_{tc} are the allowable transverse tensile and compressive strength of the FRP lamina respectively, σ_{at} and σ_{ac} are the allowable axial tensile and compressive strength of the FRP lamina respectively.

When the failure index (FI) of equation (18) is greater than 1, the first ply failure happens. In Strand7, the reserve factor was calculated to refer the condition of each ply, where it is considered unsafe if the reserve factor is less than 1.

The limits of the longitudinal tensile and compressive strength were calculated using the results of the coupon test [49]. Based on the volume fraction of fibre and resin, the strength of the FRP lamina is calculated as a summation of fibre and resin strength. The average value of glass-vinyl ester tubes is considered. However, the strength values of the FRP lamina of pultruded GFRP tubes in the transverse direction and shear strength are assumed [50, 51] . Strength limits of the FRP lamina for all types of FRP tubes shown in Table 3 are used in the analysis.

In the second approach using orthotropic properties, the failure is defined when either the transverse tensile stress of the plate element is larger than the transverse tensile strength or the axial compressive stress of the plate element is larger than the axial compressive strength (Table 6).

130

4. Results and discussion

The accuracy of the finite element simulation has been checked with the experimental results of the hollow and filled columns. Three criteria have been considered in discussing the results of the finite element simulation; load-deflection behaviour, peak load capacity and failure mode.

4.1 Load - deflection behaviour

Numerical load-deflection behaviour of the concrete filled pultruded FRP columns is affected by the constitutive model of the confined concrete. The confined concrete model is described before and modified based on the results of the concrete specimens that are confined with FRP tubes. The structure of FRP confined material in the considered specimens consists of fibre layers mainly in the transverse (hoop) direction [34]. On the other hand, the structure of the fibre layers of the pultruded FRP tubes in this study contains layers of fibres in axial and non-axial directions. Thus, the confinement effectiveness of the pultruded FRP tube differs due to variation in fibre structure and orientation.

To assess the accuracy level of the calculated mechanical properties of FRP tubes based on the lamina method using standard properties of the constituent materials, the axial modulus of the hollow full-scale test was used. The average axial modulus calculated using the full-scale tests were 40.3 GPa, 35.0 GPa, 36.9 GPa and 32.3 GPa for S1, S2, C1 and C2 respectively. These values are approximately similar to those calculated by the lamina method (values of E_1 in Table 4).

Fig. 3 and Fig. 4 show a comparison between the load-deflection curves from the finite element simulation and the experimental results for hollow and filled square and circular pultruded FRP columns respectively. Based on the approaches used to define the failure criterion of FRP plate element, the load capacity of columns were marked. The curves of the finite element simulation using the lamina method (FEA-L) shows good agreement with experimental curves compared with curves of the plate method (FEA-OL) (Figs. 3 and 4). However, the empirical equations used for calculating the mechanical properties of the FRP lamina and the constitutive model for confined concrete are the reasons for the minor differences between the experimental curves and those of the finite element analyses. The simulation curves in the post-peak region

cannot be obtained because of a program limitation; the stiffness of the FRP plate element does not update after reaching the failure limit of the Tsai-Wu failure criterion. Thus, the load step that the first ply failure occurs is the last reliable step as the FRP stiffness reduction due to material failure is not considered in the calculation of the next load step. The right representation of FRP plate elements in the finite element analysis should include a reduction in the stiffness after hitting the failure limit, redistributing the force carried by the failed element and recalculating the stiffness of the FRP plate element by taking into account the failed element before considering the new load step.

The simulation curves show a reduction in the stiffness for hollow square columns. This is because of the buckling issues. Although the experimental curves shows that the square tube S1 did not release its strength after reaching the buckling load, the simulation curve does not present this case due to the limitation in the program to simulate the stiffness reduction in the FRP plate elements due to buckling. In case of hollow circular columns, the stiffness reduction did not happen as FRP columns failed due to crushing at the end.

Numerical curves of the filled columns can be described by using three regions. In the first region, concrete behaves as a linear elastic material. The second region is a stagger stage. In this region, the compressive strength in the concrete brick elements reaches the confined concrete strength and, as a result, curves show a bit of reduction in the load. This comes together with lateral expansion in the pultruded FRP tubes due to dilation of the failed concrete element. Also in this stage, the curve shows a reduction in stiffness. In the third region, the failure of the concrete has progressed and moved away from the ends of the column. The stresses in the FRP material further increases and the failure limit is marked in the curve (Load-L). The length of the third region depends on the concrete properties and confinement effectiveness of the pultruded FRP tubes.

The curves of the plate method (FEA-OL) are not significantly different compared to those of lamina method as the same modulus values were used for FRP material in the finite element model. The only difference is the value of the load capacity (load-OL). This is due to the failure criteria where the results of the material coupon tests were used in the plate method. Firstly these standard material tests are designed to measure

the potential strength of FRP material with limitations on the dimensions of the coupon specimens in order to avoid the effects of the instability conditions. On the contrary, the actual axial behaviour of full-scale column specimen is influenced by the instability conditions. Secondly, the stress distribution in the FRP coupon test is not like that in the full-scale specimen since the continuity of the non-axial fibre layers in the coupon specimens was ignored. The failure criterion is the other reason. The uniaxial maximum stress criterion and the results of the axial compressive stress and transverse tensile stress are considered to assess the load capacity while failure in the FRP material is generated due to multi-axial stress state.
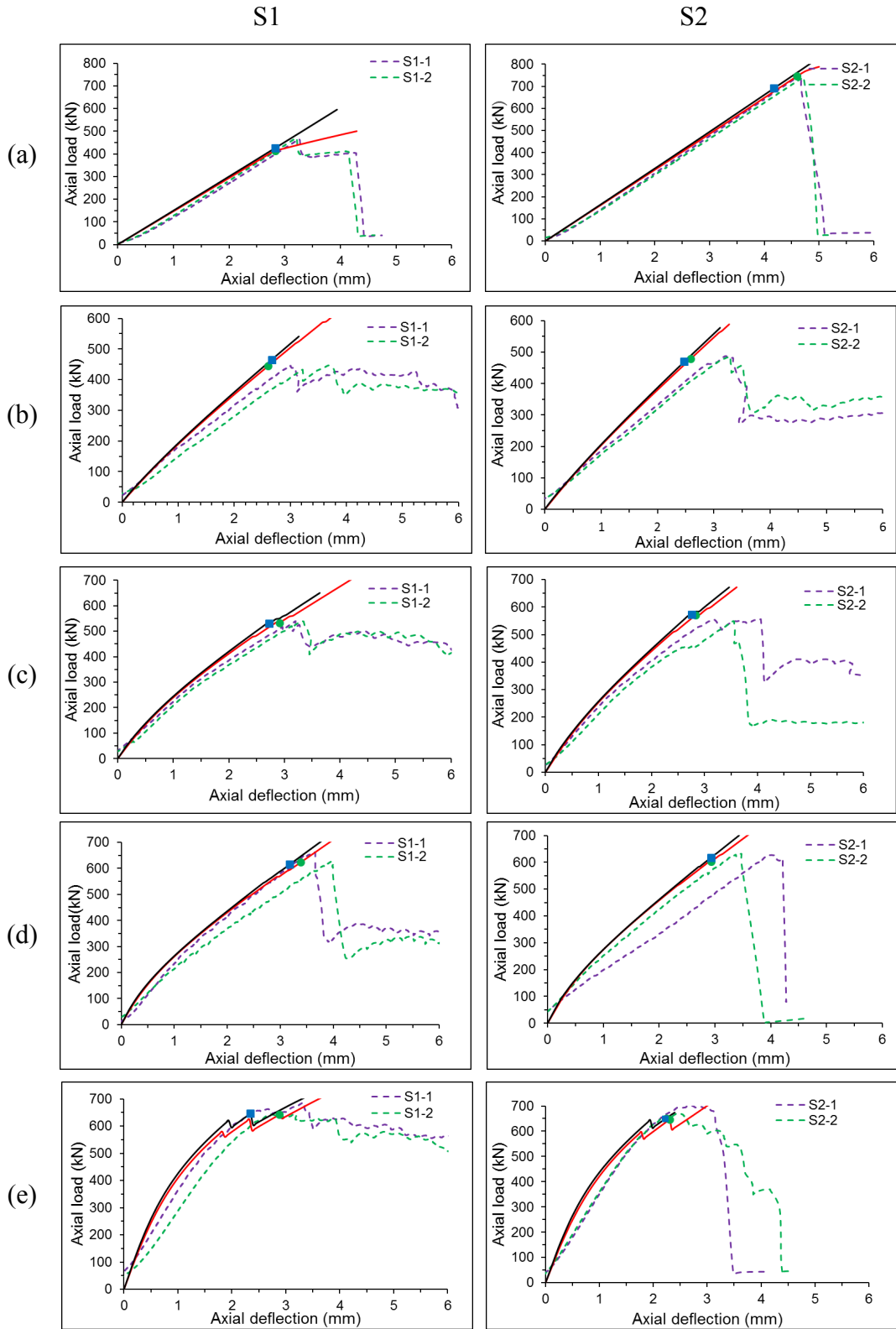
S1   S2

⎯⎯ (FEA-L) and ⎯●⎯ (Load-L) are numerical curve and load capacity based on the lamina method.

⎯⎯ (FEA-OL) and ⎯■⎯ (Load-OL) are numerical curve and load capacity based on the plate method.

Fig. 3 Comparison of load- deflection curves from FEA and experiments for square tubes S1 and S2 (a) hollow and filled with (b) perlite concrete P1, (c) perlite concrete P2, (d) normal concrete N1 and (e) normal concrete N2.

C1   C2

(a)

(b)

(c)

── (FEA-L) and ──●── (Load-L) are numerical curve and load capacity based on the lamina method.

━━(FEA-OL) and ━■━ (Load-OL) are numerical curve and load capacity based on the plate method.
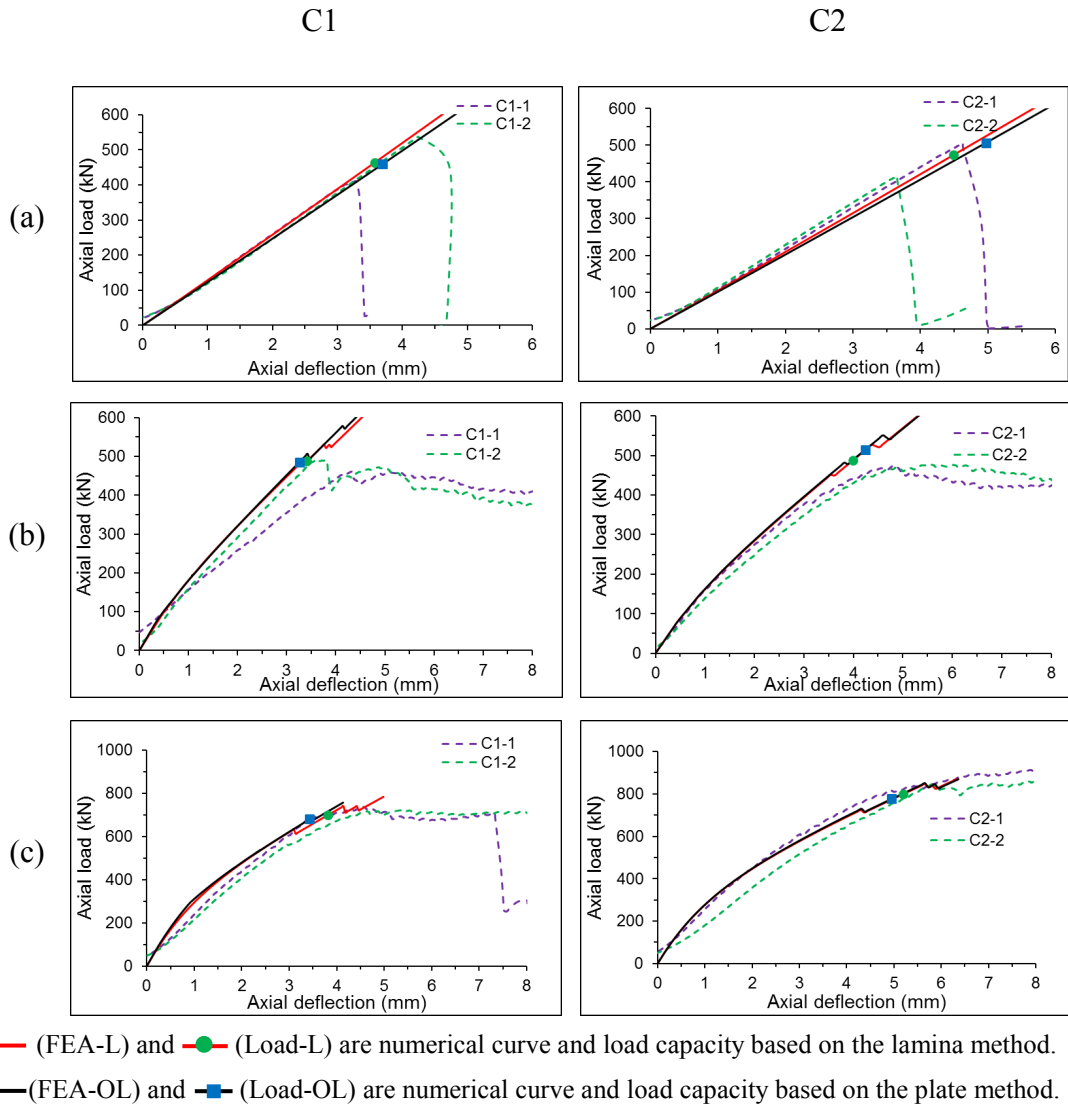
Fig. 4 Comparison of load- deflection curves from FEA and experiments for circular tubes C1 and C2 (a) hollow and filled with (b) perlite concrete P2, and (c) normal concrete N2.

4.2 Peak load

The percentage of error was calculated by taken only the average values from the experimental work and the peak load using FEM as shown in Table 7. This is because the average results covers the variation in the pultruded FRP tube columns due to production issues. The experimental curves of the filled square tubes show that the load increases until the peak. The post peak behaviour depends on the properties of the concrete infill and confinement effectiveness of the FRP tube. The circular

columns behave linearly up to the first peak load where the capacity of column decreases before getting another increase. This behaviour leads to further exaggeration in the capacity of column especially when the tube shape, structure of fibre layer and their orientation produce high confinement such as the circular column C2. The behaviour after the first reduction point could not be represented properly in the FE study due to limitations in the program to simulate the failure in the FRP material. Thus, the consideration of the first reduction point of full-scale circular tube tests as reference value for comparison with values of the numerical simulation is reasonable. The first reduction point of the experimental circular columns C2 filled with N2 occurred at axial deformation of around 6 mm while the points of maximum load capacity based on the failure criteria for the FEA-L and FEA-OL were marked at axial deformation of 5.2 mm and 4.94 mm respectively.

The results based on the lamina method show a better agreement with the experimental peak load as the maximum error is around 11.4 % for hollow columns, 5.14 % for columns filled with perlite concrete and 5.8 % for those filled with normal concrete. On the other hand, the error between the results based on the plate method and the experimental results is around 9.9% in case of hollow columns, 10.8 % for columns filled with perlite concrete and it is around 6.0% for columns filled with normal concrete. Generally, the percentages of maximum difference of plate method are larger than values of lamina method for filled columns. This is because the strength limits based on the material coupon tests are not the perfect representation of exact stress distribution in a full-scale column test. The results show that finite element simulation can be used to predict the capacity of the filled pultruded FRP columns. It should be noted that the variation between the experimental peak load values and finite element results is being a bit higher when the actual results of individual experimental columns are considered that needs further investigation.

Table 7. Summary of experimental results and FE results

FRP tubes		Load (kN)			Error percentage (%) between $P_{(Exp.)}$ and $P_{(FEA-L)}$	Error percentage (%) between $P_{(Exp.)}$ and $P_{(FEA-OL)}$
		$P_{(Exp.)}$	$P_{(FEA-L)}$	$P_{(FEA-OL)}$		
S1	Hollow	467.0	413.8	426.0	11.4	8.77
	FP1	439.0	445.1	465.3	1.38	5.99
	FP2	539.4	532.9	529.8	1.20	1.77
	FN1	645.2	623.0	615.7	3.44	4.57
	FN2	664.8	641.7	645.7	3.47	2.86
S2	Hollow	745.5	745.6	690.5	0.01	7.37
	FP1	486.0	479.3	469.5	1.37	3.39
	FP2	552.6	570.6	571.8	3.25	3.47
	FN1	629.5	602.2	617.5	4.33	1.89
	FN2	687.0	646.9	649.3	5.83	5.48
C1	Hollow	474.2	464.2	459.7	2.10	3.05
	FP2	475.9	487.7	485.2	2.47	1.96
	FN2	721.5	699.9	680.2	2.98	5.72
C2	Hollow	460.8	473.0	506.7	2.64	9.96
	FP2	464.5	488.4	515.0	5.14	10.87
	FN2	826.0	799.7	776.5	3.18	5.99

4.3 Failure modes

The failure modes of the experimental columns had been described in detail in the chapter 4 . The failure modes of both hollow and filled columns of the square tubes are due to local buckling and crushing at one end of the column followed by lengthwise splitting at the corner respectively. The circular columns fail due to crushing at one or both ends followed by splitting crack around the perimeter. As the lamina method provides more details of FRP plies compared with the plate method, the failure modes shown in Fig. 5 are related to the lamina method. The failure of the hollow columns in the numerical analysis reveal the same failure mode as that for the experimental columns (Fig.5(a)). As the failure modes of each type of pultruded FRP tubes do not differ significantly due to properties of the filler concrete, only one failure shape of each tube was presented in Fig. 5(b). It shows that failure of square tube S1 happened at the corner of the column end or close to it in axial plies giving an indication of the crushing at the end of FRP column. The failure modes based on the uni-axial maximum strength was due to maximum compressive stress except for columns filled

with P1 was due to maximum tensile stress in the transverse direction. On the other hand, the non-axial plies of square tube S2 failed initially at the corner of the column end because their strength is not enough to bear the high tensile stress in FRP due to concrete dilation. This explains the rapid progress of splitting at corner of the experimental columns. The failure modes of S2 based on plate method are also due to the maximum transverse tensile stress.   The failure of the circular columns that occurred along the perimeter of the circular tube (Fig.5 (b) agreed well with failure mode of the experimental columns. The first ply failure of hollow and filled circular columns happened in the axial FRP ply. This failure coincided well with the failure modes based on the uni-axial maximum strength of the circular columns where they are due to compressive stress at column end. The results of failure modes show that both approaches could model the failure modes properly. The finite element simulation has depicted the observed failure modes of the experimental columns accurately.
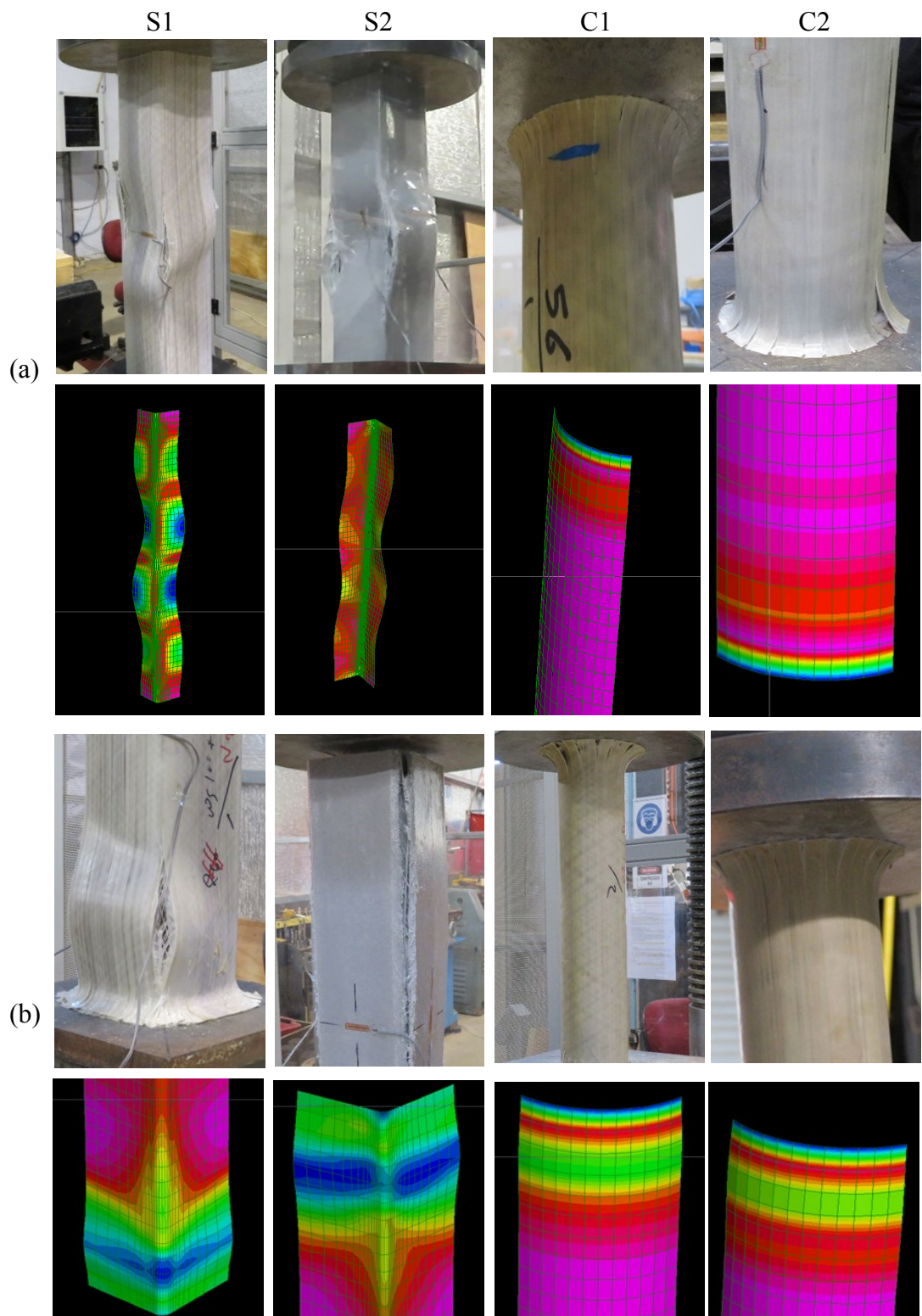
Fig.5. Failure modes of pultruded GFRP columns based on the experimental and the finite element simulation for (a) hollow columns and (b) filled columns.

5. Conclusions

In this paper, finite element analysis was carried out to simulate the axial behaviour of the hollow and filled pultruded GFRP tubes. Both lamina and plate methods were followed in defining the material properties of the tubes. The stress- strain curve of confined concrete is used to define the properties of the infill concrete. The results of the simulation study were compared with those obtained experimentally. The following key conclusions can be drawn from this study:

- As the accuracy of the load-deflection curves depends on the properties of FRP and constitutive behaviour of confined concrete, the best performance was obtained using the lamina method in defining the FRP material in the finite element analysis since their load-deflection curves are generally in good agreement with the experimental curves.

- The failure modes and peak loads of columns can be simulated properly using both lamina and plate methods. The peak loads of filled pultruded FRP columns based on the lamina method showed better agreement with the experimental results. When detailed material properties are available for the fibre lay up in FRP tube, lamina method can be used. However the plate method can still be used with limited manufacturer's data to model the filled FRP tubes.

- The analysis oriented model proposed previously to model the confined normal concrete overestimates the stress-strain curve of the lightweight perlite concrete. However, the density of lightweight to normal concrete ratio can be used as a reduction factor to the confined concrete model for improved accuracy.

- Due to program limitation in representing the degradation of the FRP stiffness after failure, the post-peak response is not available. However, the predicted values of the peak load based on the failure criteria provide a safe approach to assess the capacity of filled FRP columns for civil engineering applications.

Circular tubes with normal concrete filler are proven to give better overall performance compared to that of square tubes due to effective confinement. Further investigations are recommended to study and identify key parameters that would influence the design of these structures.

Acknowledgement

References

[1] Barbero EJ, Raftoyiannis IG. Local buckling of FRP beams and columns. J Mater Civ Eng. 1993;5:339-55.

[2] Correia M, Nunes F, Correia J, Silvestre N. Buckling behavior and failure of hybrid fiber-reinforced polymer pultruded short columns. J Compos Constr. 2012;17:463-75.

[3] Barbero EJ. Introduction to composite materials design. Third ed. Boca Raton, Fla: CRC Press; 2017.

[4] Hashem ZA, Yuan RL. Short vs. long column behavior of pultruded glass-fiber reinforced polymer composites. Constr Build Mater. 2001;15:369-78.

[5] Qian P, Feng P, Ye L. Experimental study on GFRP pipes under axial compression. Frontiers of Architecture and Civil Engineering in China. 2008;2:73-8.

[6] Godat A, Légeron F, Gagné V, Marmion B. Use of FRP pultruded members for electricity transmission towers. Compos Struct. 2013;105:408-21.

[7] Zureick A, Scott D. Short-term behavior and design of fiber-reinforced polymeric slender members under axial compression. J Compos Constr. 1997;1:140-9.

[8] Puente I, Insausti A, Azkune M. Buckling of GFRP columns: An empirical approach to design. J Compos Constr. 2006;10:529-37.

[9] Cardoso DC, Harries KA, Batista EdM. Compressive strength equation for GFRP square tube columns. Compos Part B. 2014;59:1-11.

[10] Li F, Zhao Q, Chen L, Shao G. Experimental and theoretical research on the compression performance of CFRP sheet confined GFRP short pipe. Ci World J. 2014;2014:109692.

[11] Nunes F, Correia JR, Silvestre N. Structural behaviour of hybrid FRP pultruded columns. Part 1: Experimental study. Compos Struct. 2016;139:291-303.

[12] Al-saadi AU, Aravinthan T, Lokuge W. Structural applications of Fibre Reinforced Polymer (FRP) composite tubes: a review of columns members. Compos Struct. 2018;204:513-24.

[13] Fam A, Rizkalla SH. Behavior of axially loaded concrete-filled circular FRP tubes. ACI Structural Journal. 2001;98:280-9.

[14] Fam A, Flisak B, Rizkalla S. Experimental and analytical modeling of concrete-filled FRP tubes subjected to combined bending and axial loads. ACI Struct J. 2003;100:499-509.

[15] Carrion JE, Hjelmstad KD, LaFave JM. Finite element study of composite cuff connections for pultruded box sections. Compos Struct. 2005;70:153-69.

[16] Guades E, Aravinthan T, Islam MM. Characterisation of the mechanical properties of pultruded fibre-reinforced polymer tube. Materials & Design. 2014;63:305-15.

[17] Hany NF, Hantouche EG, Harajli MH. Finite element modeling of FRP-confined concrete using modified concrete damaged plasticity. Eng Struct. 2016;125:1-14.

[18] Lin G, Teng JG. Three-Dimensional finite-element analysis of FRP-Confined circular concrete columns under eccentric loading. J Compos Constr. 2017;21.

[19] Youssf O, ElGawady MA, Mills JE, Ma X. Finite element modelling and dilation of FRP-confined concrete columns. Eng Struct. 2014;79:70-85.

[20] Abdelkarim OI, Elgawady MA. Analytical and Finite-Element Modeling of FRP-Concrete-Steel Double-Skin Tubular Columns. Journal of Bridge Engineering. 2015;20.

[21] Lima MM, Doh JH, Hadi MN, Miller D. The effects of CFRP orientation on the strengthening of reinforced concrete structures. Struct Des Tall SPEC. 2016;25:759-84.

[22] Jiang J-F, Wu Y-F. Identification of material parameters for Drucker–Prager plasticity model for FRP confined circular concrete columns. International Journal of Solids and Structures. 2012;49:445-56.

[23] Teng J, Xiao Q, Yu T, Lam L. Three-dimensional finite element analysis of reinforced concrete columns with FRP and/or steel confinement. Eng Struct. 2015;97:15-28.

[24] Rousakis TC, Karabinis AI, Kiousis PD, Tepfers R. Analytical modelling of plastic behaviour of uniformly FRP confined concrete members. Compos Part B. 2008;39:1104-13.

[25] Talaeitaba SB, Halabian M, Ebrahim Torki M. Nonlinear behavior of FRP-reinforced concrete-filled double-skin tubular columns using finite element analysis. Thin Walled Struct. 2015;95:389-407.

[26] Yu T, Teng J, Wong Y, Dong S. Finite element modeling of confined concrete-II: Plastic-damage model. Eng Struct. 2010;32:680-91.

[27] Pan Y, Guo R, Li H, Tang H, Huang J. Analysis-oriented stress–strain model for FRP-confined concrete with preload. Compos Struct. 2017;166:57-67.

[28] Hu H-T, Huang C-S, Wu M-H, Wu Y-M. Nonlinear Analysis of Axially Loaded Concrete-Filled Tube Columns with Confinement Effect. J Struct Eng-ASCE. 2003;129:1322-9.

[29] Haghinejada A, Nematzadeh M. Three-Dimensional Finite Element Analysis of Compressive Behavior of Circular Steel Tube-Confined Concrete Stub Columns by New Confinement Relationships. Latin American Journal of Solids and Structures. 2016;13:916-44.

[30] Ellobody E, Young B, Lam D. Behaviour of normal and high strength concrete-filled compact steel tube circular stub columns. Journal of Constructional Steel Research. 2006;62:706-15.

[31] Koksal H, Doran B, Turgay T. A practical approach for modeling FRP wrapped concrete columns. Constr Build Mater. 2009;23:1429-37.

[32] Zhu L, Ma L, Bai Y, Li S, Song Q, Wei Y et al. Large diameter concrete-filled high strength steel tubular stub columns under compression. Thin Walled Struct. 2016;108:12-9.

[33] Strand7 Pty Ltd. ST7-1.57.10.3 Nonlinear elastic material. Sydney, NSW: Strand7 Pty Ltd. p. Webnotes.

[34] Teng J, Huang Y, Lam L, Ye L. Theoretical model for fiber-reinforced polymer-confined concrete. J Compos Constr. 2007;11:201-10.

[35] Daniel IMI, O. . Engineering mechanics of composite materials. 2nd ed. Oxford University Press, New York.2006.

[36] Lim JC, Ozbakkaloglu T. Unified stress-strain model for FRP and actively confined normal-strength and high-strength concrete. J Compos Constr. 2014;19:04014072.

[37] Lim JC, Ozbakkaloglu T. Stress–strain model for normal-and light-weight concretes under uniaxial and triaxial compression. Constr Build Mater. 2014;71:492-509.

[38] Rocca S, Galati N, Nanni A. Review of design guidelines for FRP confinement of reinforced concrete columns of noncircular cross sections. J Compos Constr. 2008;12:80-92.

[39] Pessiki S, Harries KA, Kestner JT, Sause R, Ricles JM. Axial behavior of reinforced concrete columns confined with FRP jackets. J Compos Constr. 2001;5:237-45.

[40] Hong W-K, Kim H-C. Behavior of concrete columns confined by carbon composite tubes. Can J Civil Eng. 2004;31:178-88.

[41] Fam A, Schnerch D, Rizkalla S. Rectangular filament-wound glass fiber reinforced polymer tubes filled with concrete under flexural and axial loading: experimental investigation. J Compos Constr. 2005;9:25-33.

[42] Mirmiran A, Shahawy M, Samaan M, Echary HE, Mastrapa JC, Pico O. Effect of column parameters on FRP-confined concrete. J Compos Constr. 1998;2:175-85.

[43] Pantelides CP, Yan Z, Reaveley LD. Shape modification of rectangular columns confined with FRP composites. 2004.

[44] Popovics S. A numerical approach to the complete stress-strain curve of concrete. Cement and concrete research. 1973;3:583-99.

[45] Teng J, Hu Y. Behaviour of FRP-jacketed circular steel tubes and cylindrical shells under axial compression. Constr Build Mater. 2007;21:827-38.

[46] Park J-W, Yeom H-J, Yoo J-H. Axial loading tests and FEM analysis of slender square hollow section (SHS) stub columns strengthened with carbon fiber reinforced polymers. International Journal of Steel Structures. 2013;13:731-43.

[47] Nonlinear solver. NewsSt7. Sydney-Australia: Strand7Pty Ltd; 2008. p. 3-10.

[48] Wang W, Sheikh MN, Hadi MNS, Gao D, Chen G. Behaviour of concrete-encased concrete-filled FRP tube (CCFT) columns under axial compression. Eng Struct. 2017;147:256-68.

[49] Al-saadi AU, Aravinthan T, Lokuge W. Effects of fibre orientation and layup on the mechanical properties of the pultruded glass fibre reinforced polymer tubes. Eng Struct. 2019;Under review.

[50] Kollár LP, Springer GS. Mechanics of Composite Structures. New York, UNITED STATES: Cambridge University Press; 2003.

[51] Module7: Strength and Failure Theories 2014. p. Learning notes,Indian Institute of Technology, Kharagpur.

5.2 Effect of slenderness ratio on failure mechanism

The finite element simulation was extended to study the effect of slenderness ratio on the failure mode of pultruded FRP tubes. The failure modes was compared with the experimental results of additional column tests with different length-to-lateral dimension ratios (L/D). Finite elements software STRAND 7 was used in the simulation process. Lamina approach that explained in this Chapter was used to define the FRP laminate properties in the finite element.

In order to investigate the effect of slenderness ratio on failure mechanism of square and circular pultruded FRP tubes, the numerical analysis was extended for L/D ratio equal to 1 and 5. The results show that the failure mode of square tubes changed to buckling bulge when this ratio was reduced to 1 (Figure 5.1 (a)). It can be seen that the maximum compressive stresses occur in the axial ply in the corners near end supports. This results correspond well with the experimental and numerical results previously conducted by Guades et al. (2014). It should be noted that when the L/D ratio was two, the failure mode in S1 and S2 tubes was due to adjacent faces showing inside and outside local buckling. On the other hand, when L/D ratio was increased to 5, S1 and S2 square columns showed local buckling failure with multiple waves on the same face as shown in Figure 5.1 (b).

For the circular tubes C1 and C2, the simulation was extended to L/D ratio of 5, as the failure observed for the L/D ratio of 2 was compressive failure of tubes. The failure modes remained the same for circular tubes when L/D ratio was increased to 5 as shown in Figure 5.1(c). This could be attributed to the lower diameter to thickness ratio of circular tubes. These effects should be considered carefully in designing FRP tubes for axial compression loading.
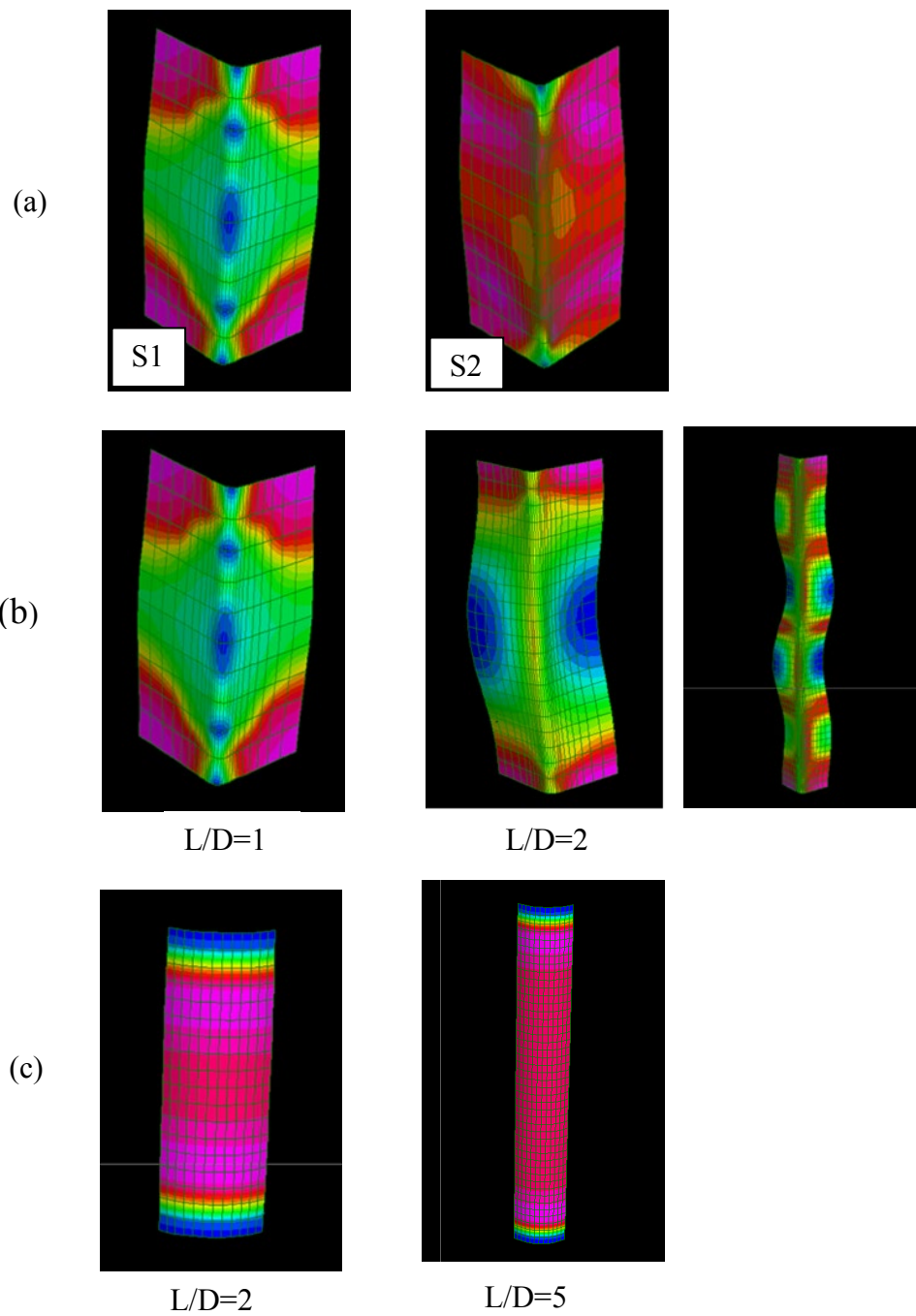
Figure 5.1 Numerical failure modes for (a) S1 and S2 square tubes of L/D=1, (b) square tubes S1 with different L/D ratios and (c) circular tube C1 with various L/D ratios

5.3 Summary

This Chapter presents the finite element analysis, which was carried out to simulate the axial behaviour of hollow and filled pultruded GFRP tubes.

The results show that the load-deflection curves of the lamina method have coincided well with the experimental curves. The study reveals that the load carrying capacity of filled columns, based on the lamina method, agreed well with the experimental results. Results further states that the both the lamina and plate of FRP tubes defining methods inside the finite element simulate failure modes of columns suitably. It can be stated that, depending on the availability of the material properties, either the lamina method or the plate method can be used to model filled FRP tubes since both methods provide load-deflection curves and load capacity values that are not differ a lot compared with experimental results. The other key finding is that the simulation was unable to model the post–peak behaviour of columns, as there is a limitation in the software to represent the reduction in stiffness of FRP tubes after failure. However, it provides a helpful approach to estimate the load carrying capacity of hollow and filled pultruded FRP columns without risk for civil engineering applications.

The results of finite element analysis for pultruded FRP hollow tubes with different L/D ratios show that the failure of square tubes is changed from buckling bulge to local buckling as the slenderness ratio increases from 1 to 5. On the other hand, the failure mode of circular tube does not change when the slenderness ratio increases. It indicates that further study is needed to understand the behaviour of columns with large L/D ratios.

The finite element model delivers applicability to further explore effect of different parameters related to dimensions of the pultruded FRP tube, structural properties of the fibre layers and strength of the concrete infill. These parameters using the finite element model of the lamina method were investigated in Chapter 6.

Chapter 6:

Parametric Study on Compressive Behaviour of Pultruded FRP Tubes

6.1 Introduction

Having completed the finite element simulation in chapter 5, this chapter presents the parametric study to the axial behaviour of the hollow and filled pultruded FRP tubes. The structural behaviour of pultruded FRP tubes has been studied for decades since the demand for its use in civil engineering applications increases due to their excellent features such as high strength and stiffness to weight ratios, corrosion resistance and durability (Correia et al. 2012). Pultruded FRP profiles having majority of the fibres in the axial direction have been used as a column members (Li et al. 2014). However the instability conditions associated with buckling prevent pultruded FRP sections to utilise their potential strength (Qiao et al. 2001). A number of researchers addressed this issue by conducting experimental work for different shapes of pultruded FRP profiles (Barbero & Raftoyiannis 1993; Hashem & Yuan 2001). The slenderness ratio of pultruded FRP profiles was studied to investigate how their axial behaviour changes and to propose models for assessing the load carrying capacity of columns (Barbero & Tomblin 1994; Barbero & Turk 2000; Cardoso et al. 2014; Godat et al. 2013; Hassan & Mosallam 2004; Puente et al. 2006; Qian et al. 2008; Zureick & Scott 1997).

Adding carbon fibre sheets or replacing the fibre layers with low stiffness by fibre layers with higher stiffness were followed to overcome the above issue in the axial behaviour of pultruded FRP profiles (Correia et al. 2012; Nunes et al. 2016). In chapter 4, the stiffness and load capacity of pultruded square and circular tubes are improved by using different types of fillers. The degree of improvement depends on the properties of the filler, the shape of the FRP tube, confinement due to fibre orientation and wall thickness. An extensive investigation is vital to study the changes in the axial behaviour of pultruded FRP tubes due to variations in these effective parameters. This can be achieved by using finite element analysis to simulate the axial performance of

pultruded FRP tubes with varying parameters. Such a comprehensive parametric study will cost extensive computational efforts. Therefore, it is important to select several cases to represent this entire parametric study.

One effective tool used in the past to consider the important cases and to figure out the effect of each parameter with a reduced number of cases is Taguchi approach (Ozbay et al. 2009). This method has been used in different engineering applications (Chitawadagi et al. 2010; Türkmen et al. 2008) since it is a beneficial methodology to determine the best combination of the important parameters. The cases of the parametric study were selected based on the Taguchi approach with an L9 orthogonal array. It was utilised to identify the most influential parameters for the axial behaviour of FRP tubes. Moreover, additional cases were designed to highlight the influence of the most influential parameter identified through Taguchi method.

This study focussed mainly on the hollow and filled pultruded square and circular tubes with L/D ratio of 5. The finally agreed finite element model from Chapter 5, which compared well with the experimental results, was used in this parametric study. Lamina method inside the finite element program was used to define the properties of the FRP tube.

6.2 Research significance

The stiffness and load capacity are governing the design of pultruded FRP tubes. They are affected by the wall thickness, fibre orientation and layup. In case of filled FRP tube columns, the properties of filler material is another factor. This study aims to investigate effects of variation in these parameters on the stiffness, load capacity and failure modes of pultruded FRP tubes. Both the square and circular columns were considered. Additional cases for square and circular tubes were also considered to study the influence of change in one parameter with keeping others constant. The findings of this study will provide an indication to improve the axial behaviour of pultruded FRP tube columns through strengthening the knowledge of the interaction effects of factors. The significance of this work is to provide design recommendations for improving the axial behaviour of pultruded FRP tube columns either in hollow or in filled conditions.

6.3 Research parameters

The aim of this study is to determine the best combination of various parameters related to concrete and FRP tube in order to maximize the overall performance of pultruded FRP tubes. Taguchi method was used to design the cases that needed to be studied further. The response data was analysed using software program, Minitab-18. Parametric study was conducted on square and circular tubes using compressive strength of the filler, wall thickness, percentage of fibres in the axial and non-axial directions and fibre orientation of the FRP tube as the research parameters.

6.3.1 Parameters using Taguchi method

The results of experimental work shows that the stiffness, load capacity and failure modes are affected by the wall thickness, fibre orientation and layup of FRP tube and properties of filler material. Therefore, it is important to investigate the effect of these parameters on the overall axial performance of hollow and filled FRP tubes. Three parameters were considered for the hollow FRP tube; wall thickness (5.2, 6.4 and 7.8 mm for the square tubes and 6.0, 7.4 and 8.6 mm for the circular tubes), fibre orientation with respect to the axial direction of FRP tubes ([0,45,-45], [0,60,-60] and [0,75,-75]), percentage of fibre distribution in the axial and non-axial directions ([80,10,10], [70,15,15] and [60,20,20]). The study of the filled columns was performed by considering the compressive strength of filler material (20, 32 and 50 MPa) as another parameter (Table 6.1). Studies of hollow and filled columns were carried out depending on L9 array obtained using the Taguchi method.

Table 6.1 Parameters and levels used in Taguchi method

Parameters		Level 1	Level 2	Level 3
Wall thickness	Square	5.2	6.4	7.8
(mm)	Circle	6.0	7.4	8.6
Fibre orientation (degrees)		0/45/-45	0/60/-60	0/75/-75
Percentage of fibre		80/10/10	70/15/15	60/20/20
Concrete strength (MPa)		20	32	50

The details of the cases selected based on the Taguchi method are shown in Table 6.2 and Table 6.3.

Table 6.2 L9 arrays adopted for square columns

Series	Wall thickness (mm)	Fibre orientation (degrees)	Percentage of fibre (%)	Concrete strength (MPa)
S1	5.2	0/45/-45	80/10/10	20
S2	5.2	0/60/-60	70/15/15	32
S3	5.2	0/75/-75	60/20/20	50
S4	6.4	0/45/-45	70/15/15	50
S5	6.4	0/60/-60	60/20/20	20
S6	6.4	0/ 75/-75	80/10/10	32
S7	7.8	0/ 45/-45	60/20/20	32
S8	7.8	0/60/-60	80/10/10	50
S9	7.8	0/ 75/-75	70/15/15	20

Table 6.3 L9 arrays adopted for circular columns

Series	Wall thickness (mm)	Fibre orientation (degrees)	Percentage of fibre (%)	Concrete strength (MPa)
C1	6	0/45/-45	80/10/10	20
C2	6	0/60/-60	70/15/15	32
C3	6	0/75/-75	60/20/20	50
C4	7.4	0/45/-45	70/15/15	50
C5	7.4	0/60/-60	60/20/20	20
C6	7.4	0/ 75/-75	80/10/10	32
C7	8.6	0/ 45/-45	60/20/20	32
C8	8.6	0/60/-60	80/10/10	50
C9	8.6	0/ 75/-75	70/15/15	20

6.4 Results and dissuctions- Parameters of Taguchi method

The design process of pultruded FRP tube as axial members should meet the requirements of serviceability limit state and the ultimate limit state. This is because the axial shortening of pultruded FRP tube is high due to its low stiffness and they fail due to buckling before reaching its potential compression capacity. Therefore, stiffness and load capacity responses of FRP tubes are selected to assess effects of different parameters. The stiffness and load capacity of columns acquired from the numerical analysis for the selected L9 array were used to calculate an index of response for each trial series; signal to noise ratio (SNR). The SNR is calculated using the log function(Ferdous et al. 2017). There are three models used in Taguchi method based on the objectives of the problem. They are smaller is better, larger is better and nominal is best (Ozbay et al. 2009). The option that was used in this study is the larger the better as the goal of the current study is to maximise the response. The mean SNR of each level for each parameter was calculated as an average of SNR of its trial series. Subsequently, the difference between maximum and minimum values of SNR of each parameter gives an indication of the influence of that parameter on load carrying capacity/ stiffness of columns. The highest difference means that the specific parameter has the greatest influence. Finally, analysis of variance (ANOVA) was used to determine percentages of contribution of each parameter.

6.4.1 Square tubes

For the selected cases shown in Table 6.2 based on the Taguchi method, the load-deflection curves from FEM simulations are shown in Figure 6. 1. The hollow column S8 (7.8 mm thickness, 60 degrees fibre orientation and 80% of axial fibres) has the highest stiffness while the hollow column, S3 (5.2 mm thickness, 75 degrees fibre orientation and axial fibre of 60%) has the lowest (Figure 6.1 (a)). This is because the hollow S8 has a larger cross-sectional area and it has 80% of the fibres in the axial direction while S3 has only 60% of fibres in the axial direction. Furthermore, the mode of failure changes from local buckling (with a reduction in the stiffness of column) to compression failure when the wall thickness of the FRP square tube increases (5.2 mm to 7.8 mm). Curves of S1, S2 and S3 show that increasing the percentage of axial fibres and reducing fibre orientation for the same wall thickness results in an increase in the stiffness (as shown in Table 6.3) and yield almost the same load capacity while reducing the axial deflection. This can be attributed to increase the stiffness of FRP tube.

The load-deflections curves of filled square pultruded FRP columns are shown in Figure 6.1 (b). The highest stiffness of filled square columns can be seen in S8 where it is filled with 50 MPa concrete and it has 80% of the fibres in axial direction with 7.8 mm wall thickness. S1 and S5 columns filled with 20 MPa concrete have low stiffness among filled columns (Table 6.3). The load-deflection curves of S1 and S3 show the effect of filler on increasing the stiffness and load capacity. On the other hand, curves of S3 and S4 filled columns show the influence of wall thickness and percentage of axial fibre. Although S4 column has lower percentage of non-axial fibre in orientation closer to the axial direction compared with S3 column, it shows higher stiffness and load capacity.
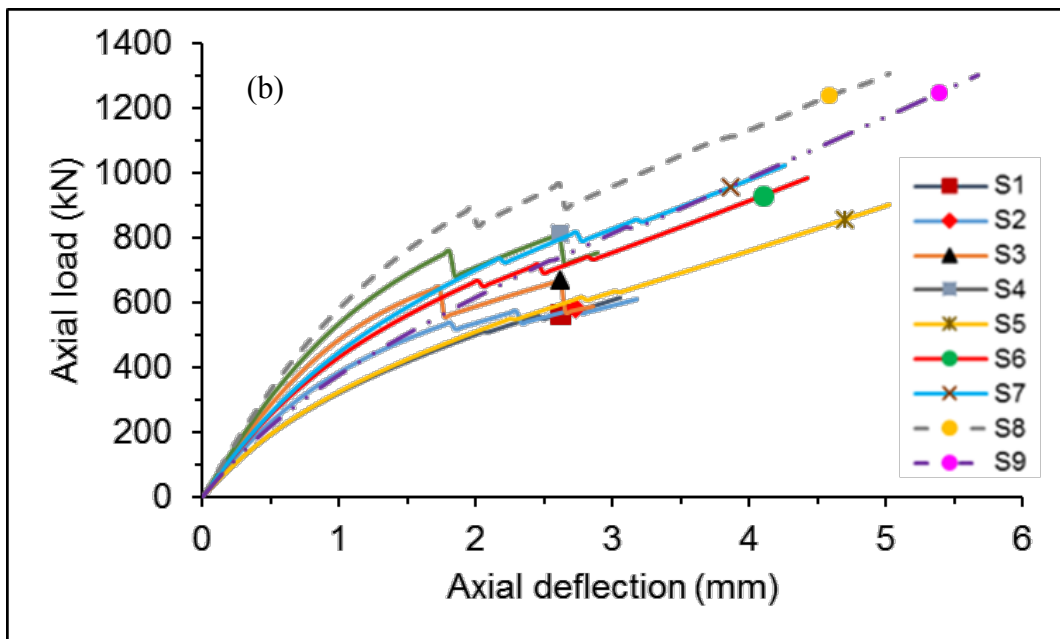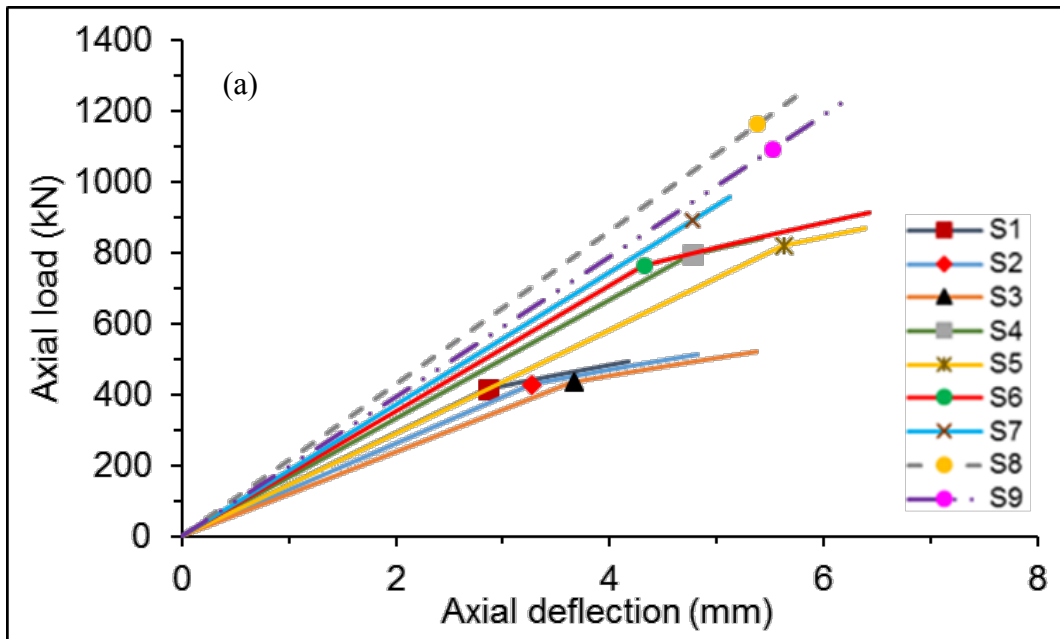
Figure 6.1 Load-deflections curves for square FRP tubes (a) hollow and (b) filled

Table 6.4 shows the calculated stiffness, load capacity and failure modes of hollow and filled square FRP tubes. The highest load capacity of hollow square columns was reported for S8 with wall thickness of 7.8 mm, fibre orientation [0/60/-60] and percentage of fibre distribution of [80/10/10]. On the other hand, S1 shows lowest load capacity of hollow square columns. The thickness, fibre orientation and percentage of fibre distribution of this trial column were 5.2 mm, [0/45/-45] and [80/10/10] respectively. The main differences between hollow S8 and S1 are the wall thickness and fibre orientation.

The calculated maximum load capacity of filled square tube is 1248.7 kN for S9. The FRP thickness of this tube is 7.8 mm with 30% non-axial fibres at 75 degrees with respect to the axial direction and filled with 20 MPa concrete strength. The minimum load capacity of 566.3 kN was calculated for S1 with thickness equal to 5.2 mm, angle of oriented fibre of 45 degrees, percentage of non-axial fibre of 20% and concrete filling material with 20 MPa. FRP wall thickness and fibre orientation are the main differences between the maximum and minimum load capacities of columns. Both the thickness and fibre orientation contribute to improved load capacity of column because of the increased cross-sectional area and confinement effectiveness of FRP tube.

Table 6.4 Stiffness, load capacity and failure modes of hollow and filled square tubes

Series	Hollow tubes			Filled tubes		
	Stiffness $(x10^3 N/mm)$	Load (kN)	Failure mode*	Stiffness $(x10^3 N/mm)$	Load (kN)	Failure mode*
S1	146.1	415.8	B	402.7	566.3	C
S2	130.7	426.7	B	487.7	583.0	C
S3	118.7	434.0	B	596.3	667.8	C
S4	166.9	793.4	B	638.3	812.5	C
S5	146.2	821.1	B	354.1	855.3	C
S6	177.0	764.7	B	498.8	931.6	C
S7	186.8	890.9	C	517.7	955.8	C
S8	215.9	1161.6	C	654.2	1237.4	C
S9	197.8	1093.1	C	377.1	1248.7	C

*B: Buckling failure, C: Compression failure in axial plies.

Table 6.5 shows the SNR of hollow square columns with respect to wall thickness, fibre orientation and percentage of fibres in the axial direction. Stiffness and axial load are used as evaluation parameters. The wall thickness of hollow FRP square tube is the most influential parameter when the stiffness and axial load capacity are considered. The percentage of axial fibres is the second influential parameter for stiffness of hollow columns, but it is the third parameter for load capacity. The fibre orientation is third influential parameter for stiffness, while it is the second influential parameter on the load capacity.

Table 6.5 Mean SNR for parameters at each level for hollow square tubes

Response	Levels	Wall thickness (mm)	Fibre orientation (degrees)	Percentage of fibre
Stiffness	1	102.4	104.4	105.0
	2	104.2	104.1	104.2
	3	106.0	104.1	103.4
	Max.	106.0	104.4	105.0
	Min.	102.4	104.1	103.4
	ΔSNR	3.6	0.3	1.6
	Rank	1	3	2
Load capacity	1	52.58	56.46	57.12
	2	57.98	57.40	57.12
	3	60.36	57.06	56.68
	Max.	60.36	57.40	57.12
	Min.	52.58	56.46	56.68
	ΔSNR	7.78	0.94	0.44
	Rank	1	2	3

It can be seen in Figure 6.2 that SNR is increased as the wall thickness of tube increases (5.2, 6.4 to 7.8 mm). This means that the stiffness and load capacity of hollow columns increases with increasing wall thickness. The reason for this can be attributed to the increased cross-sectional area of column and decreased plate slenderness ratio. Thus, the mode of failure for thin and thick tubes moved from local buckling to compression failure respectively. The sensitivity of the stiffness decreases slightly when the angle of fibre layers increases from 45 to 60 degrees while it remains constant until angle of 75 degrees. The ability to carry load is enhanced as the angle of fibre layer is increased from 45 degree to 60 degree with respect to the axial direction. A reduction in trend of SNR can be noticed when the angle of fibre layer is increased more than 60 degree.

The trend of third parameter, percentage of fibre distribution in axial and non-axial directions shows that the stiffness of hollow square columns increases as the percentage of axial fibre increases. At the same time, the hollow square columns could carry more load as percentage of axial fibre layers increases up to 70 % while it remains constant until percentage of 80 %.
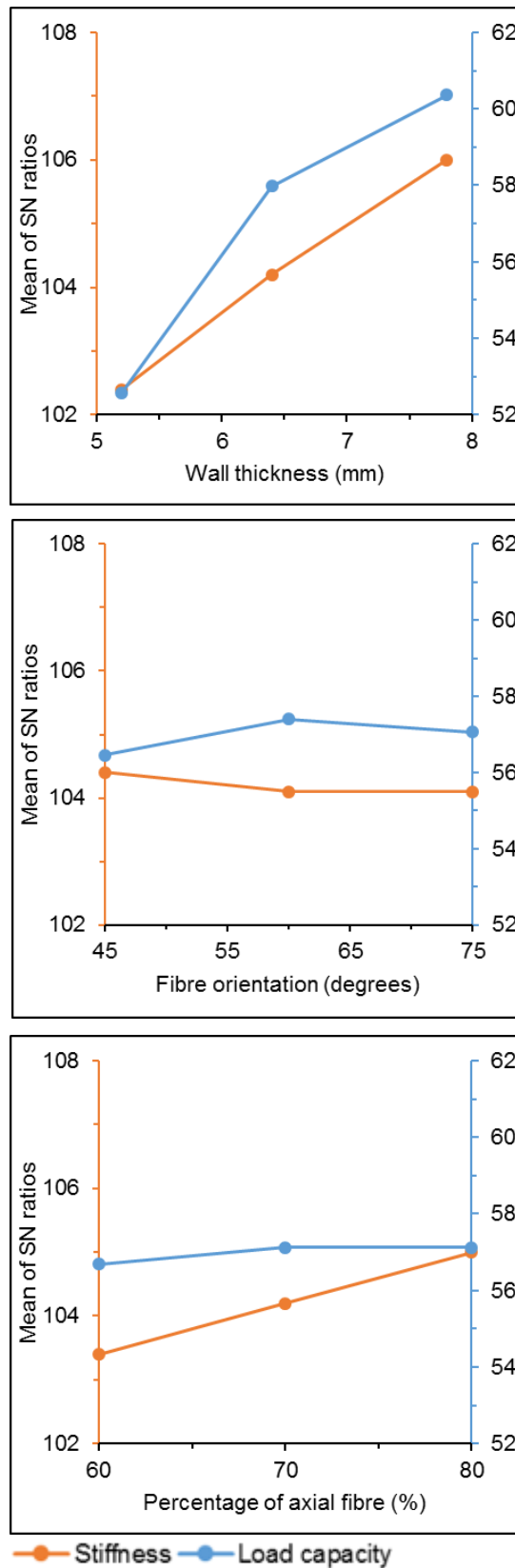
Figure 6.2 Effect of key parameters on the stiffness and load capacity of hollow square tubes

The percentage of contribution of each parameter can be computed using the analysis of variance (ANOVA). Table 6.6 shows that the highest percentage of contribution comes from wall thickness (84.36 %) for stiffness and it is 93.43 % for load capacity. This means that the wall thickness of hollow FRP square tube is the most influential parameter when the stiffness and the axial load capacity are considered. The percentage of axial fibres contributes by 15.26 % on improving the stiffness of hollow columns, but it is 1.18% for development of load capacity. The fibre orientation has lower contribution towards increasing the stiffness with 0.12%, while it is 2.58 % for the load capacity.

Table 6.6 Percentage of contribution of key parameters for hollow square tubes

Response	Wall thickness (mm)	Fibre orientation (degrees)	Percentage of fibre	% of Error
Stiffness	84.36	0.12	15.26	0.26
Load capacity	93.43	2.58	1.18	2.80

The strength of concrete makes the largest influence on the stiffness of filled square columns while the percentage of axial fibre, fibre orientation and wall thickness are ordered as second ,third and fourth respectively (Table 6.7). For filled columns, FRP wall thickness is the most influential parameter on the load capacity of square columns. The influence of fibre orientation, compressive strength of concrete and percentage of fibre in axial and non-axial direction are ordered as second, third and fourth respectively for columns in square shapes.

Table 6.7 Mean SNR for parameters at each level for filled square tubes

Response	Levels	Wall thickness (mm)	Fibre orientation (degrees)	Percentage of fibre	Concrete strength (MPa)
Stiffness	1	113.8	114.1	114.1	111.5
	2	113.7	113.7	113.8	114.0
	3	114.0	113.7	113.6	116.0
	Max.	114.0	114.1	114.1	116.0
	Min.	113.7	113.7	113.6	111.5
	ΔSNR	0.3	0.4	0.5	4.5
	Rank	4	3	2	1
Load capacity	1	55.62	57.62	58.77	58.54
	2	58.74	58.60	58.48	58.10
	3	61.13	59.27	58.25	58.85
	Max.	61.13	59.27	58.77	58.85
	Min.	55.62	57.62	58.25	58.10
	ΔSNR	5.51	1.65	0.52	0.75
	Rank	1	2	4	3

Figure 6.3 shows the SNR of all parameters for filled square columns. Increasing wall thickness from 6.4 mm to 7.8 mm for square columns leads to a slightly improved stiffness. The effect of wall thickness on the load capacity is significantly positive.

The effects of fibre orientation on the stiffness and load capacity of filled square columns are researched using three angles for fibre layers of 45, 60 and 75 degrees. The SNR response based on the numerical results obtained shows that the sensitivity of stiffness decreases and the load capacity increases when the angle increases from 45 to 75 degrees.

The percentage of axial fibres also influences on the stiffness and load capacity of FRP columns filled with concrete. The SNR values indicate that the stiffness and load capacity can be improved if axial fibre percentage is changed from 60% to 80%.

The trend of the fourth parameter, compressive strength of concrete shows that the stiffness of filled columns goes up with increasing concrete strength. On the other hand, the trend of load capacity shows an increase when the strength of filler is higher than 32 MPa.
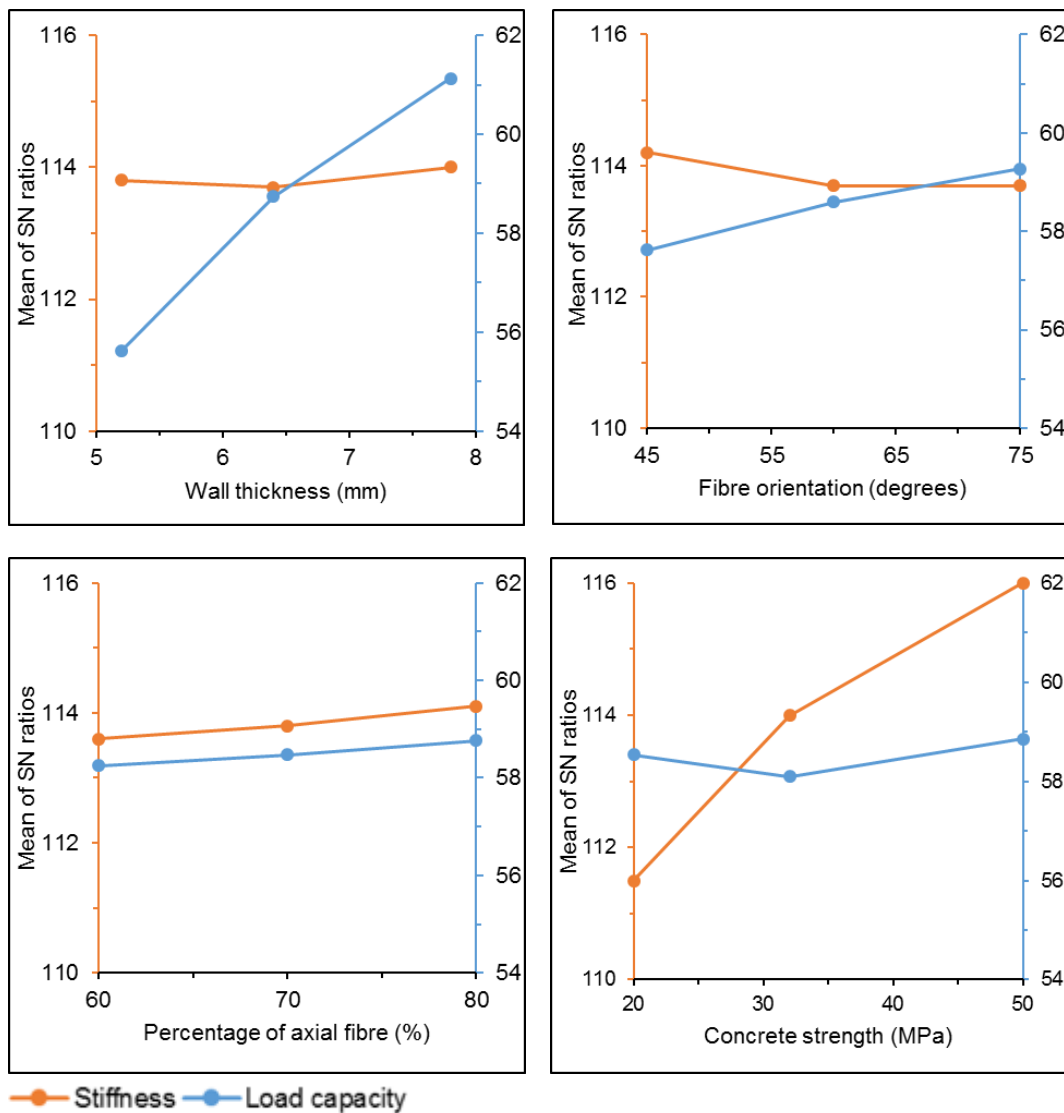
Figure 6.3 Effect of key parameters on the stiffness and load capacity of filled square tubes

The percentage of contribution of the FRP wall thickness, fibre orientation, percentage of axial fibre and compressive strength of concrete for filled square columns are 0.82 %, 1.36%,1.32%,96.51% respectively for stiffness and they are 86.57%, 8.95%, 2.22% and 2.26 % respectively for load capacity (Table 6.8). Figure 6.3 indicates that the optimum level of load capacity for the FRP square column can be obtained by using a combination of 7.8 mm wall thickness with 20 % of fibre oriented at angle 75 degrees and using 50 MPa concrete filler.

Table 6.8 Percentage of contribution of key parameters for filled square tubes

Response	Wall thickness	Fibre orientation (degrees)	Percentage of fibre	Concrete strength (MPa)	% of Error
Stiffness	0.82	1.36	1.32	96.51	0
Load capacity	86.57	8.95	2.22	2.26	0

6.4.2 Circular tubes

The load-deflection curves for cases of circular columns based on the Taguchi method (Table 6.3) are shown in Figure 6.4. The highest and lowest stiffness of hollow circular columns are C8 and C3 respectively as shown in Figure 6.4 (a). Increased cross-sectional area and percentage of axial fibre lead to improved stiffness of the column. It should be noted that the compression material failure was the predominant failure mode. The positive effect of increasing of both percentage of non-axial fibre layer and their orientation on the stiffness and load capacity can be seen clearly in load-deflection curves of C1, C2 and C3 hollow columns (Figure 6.4 (a)).

On the other hand, circular column C1is filled with 20 MPa concrete strength exhibits the lowest column stiffness. Column C8 filled with 50 MPa concrete represents the highest column stiffness among circular filled columns (Figure 6.4 (b)). The structure of C8 consists of 20% of fibres that are making 60^0 with the axial direction and with 8.6 mm wall thickness. The stiffness and load capacity of filled C6 are larger than those of C5 are due to increased percentage of axial fibres and filling with higher concrete strength.
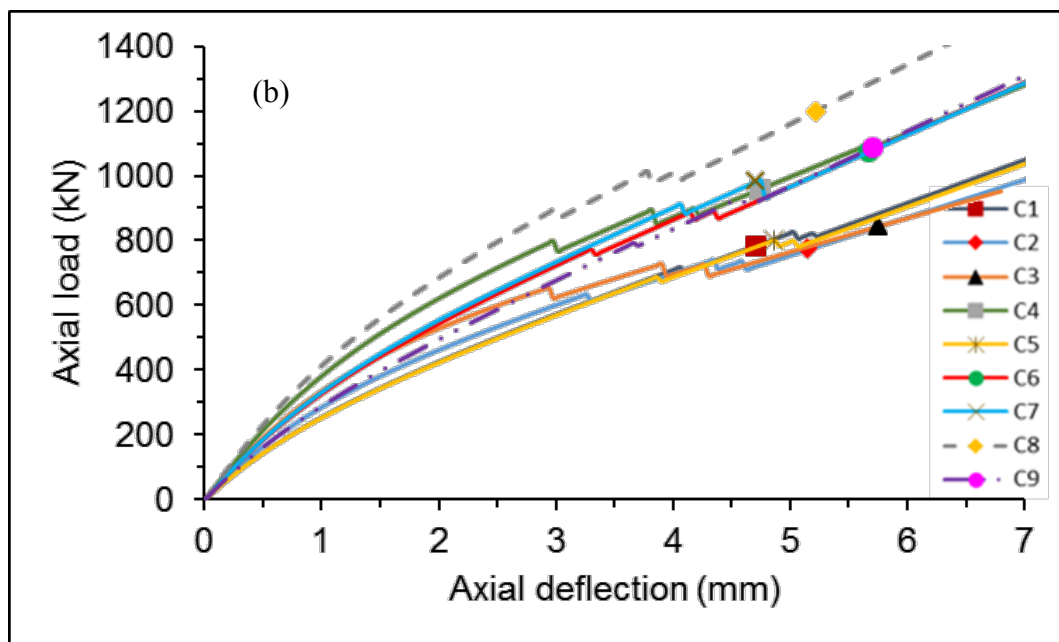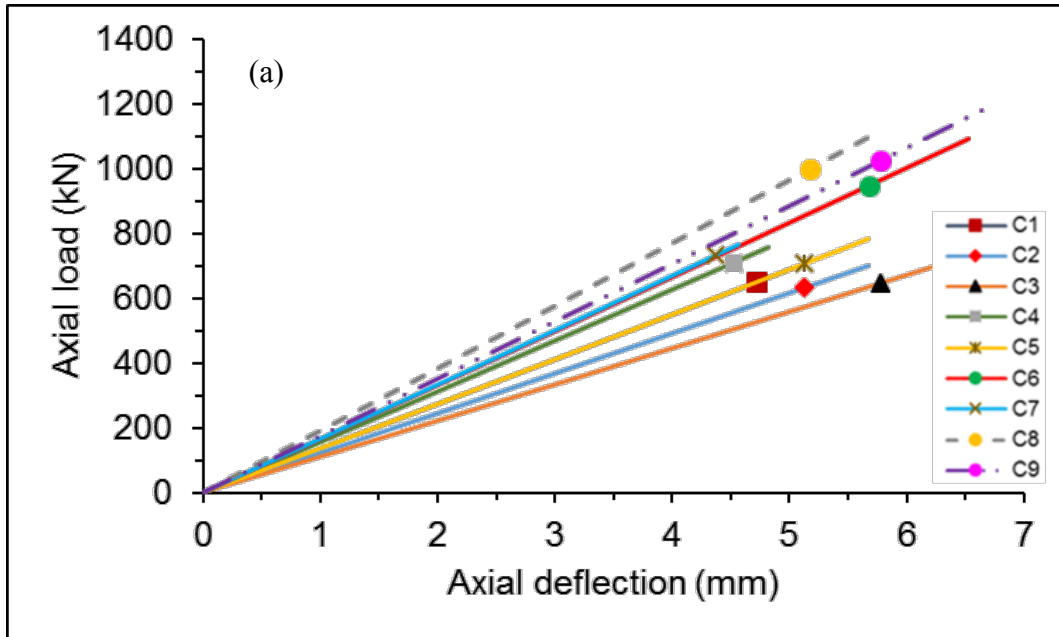
Figure 6.4 Load-deflections curves for circular FRP tubes (a) hollow and (b) filled

For circular hollow columns, C9 showed the highest load capacity of 1025.1 kN while C2 showed the lowest load of 631.4 kN (Table 6.7). The thickness, fibre orientation and percentage of fibre are 8.6 mm, [0/75/-75] and [70/15/15] for the C9 and they are 6.0 mm, [0/60/-60] and [70/15/15] for the C2 respectively (Table 6.9).

The column C8 is the strengthening circular column filled with concrete (1195.2 kN) while the C2 is the weakening column (772.0 kN) as shown in the Table 6.9. In addition to use different concrete strength in filling, they have different structure related to the wall thickness and percentage of axial fibre. The C8 has wall thickness of 8.6 mm and 20% of fibre oriented at 60 degrees, but the C2 has 6.0 mm wall thick and 30 % of fibre oriented at 60 degrees. Their results indicate that although the C2 has non-axial fibre larger than that of C8, the influence of FRP wall thickness on the axial behaviour of pultruded FRP tubes is significantly. Also, the enhancement in the concrete due to FRP confinement is increased as the strength of the concrete decreases (Vincent & Ozbakkaloglu 2013).

Table 6.9 Stiffness, load capacity and failure modes of circular tubes

Series	Hollow tubes			Filled tubes		
	Stiffness $(x10^3 N/mm)$	Load (kN)	Failure mode*	Stiffness $(x10^3 N/mm)$	Load (kN)	Failure mode*
C1	137.2	649.7	C	254.6	783.3	C
C2	122.9	631.4	C	308.8	772.8	C
C3	111.9	648.1	C	376.2	842.8	C
C4	156.5	709.4	C	413.0	958.6	C
C5	137.4	705.6	C	256.4	801.8	C
C6	166.7	947.4	C	328.5	1074.0	C
C7	166.8	731.4	C	343.3	980.5	C
C8	193.0	1000.6	C	433.5	1195.2	C
C9	177.3	1025.1	C	280.0	1089.2	C

* C: Compression failure in axial plies.

Table 6.10 shows values of mean SNR, delta and rank of parameters. It indicates that the larger impact on the stiffness and load capacity of FRP circular columns is done by the wall thickness. The percentage of fibre distribution and fibre orientation ranked as the second and third impacts respectively on the stiffness of hollow circular tube

columns. On the other hand, the impact of fibre orientation on the load capacity is higher than that of fibre percentage.

Table 6.10 Mean SNR for parameters at each level for hollow circular tubes

Response	Levels	Wall thickness (mm)	Fibre orientation (degrees)	Percentage of fibre
Stiffness	1	101.8	103.7	104.3
	2	103.7	103.4	103.6
	3	105.0	103.5	102.7
	Max.	105.0	103.7	104.3
	Min.	101.8	103.4	102.7
	ΔSNR	3.2	0.4	1.6
	Rank	1	3	2
Load capacity	1	56.16	56.85	58.60
	2	57.84	57.66	57.75
	3	59.17	58.66	56.83
	Max.	59.17	58.66	58.60
	Min.	56.16	56.85	56.83
	ΔSNR	3.01	1.81	1.77
	Rank	1	2	3

Figure 6.5 shows that impacts of wall thickness on the stiffness and load capacity of hollow circular columns. It is in increasing trend since the mean of SNR increases when the wall thickness of circular tube increases from 6.0 mm, 7.4 mm to 8.6 mm. The effect of fibre orientation on the stiffness is decreasing the sensitively of stiffness as the angle of oriented fibre increase from the axial direction. However, the load capacity of hollow circular tubes is significantly influenced by fibre orientation where its ability to carry load is improved as the angle of fibre layer increased from 45 degrees to 75 degrees with respect to the axial direction. Therefore, the contribution to support the axial fibre layer improves. The percentage of fibre distribution in axial and non-axial directions shows that the stiffness and strength of hollow circular tubes gets enhancement as fibres laid in axial direction.
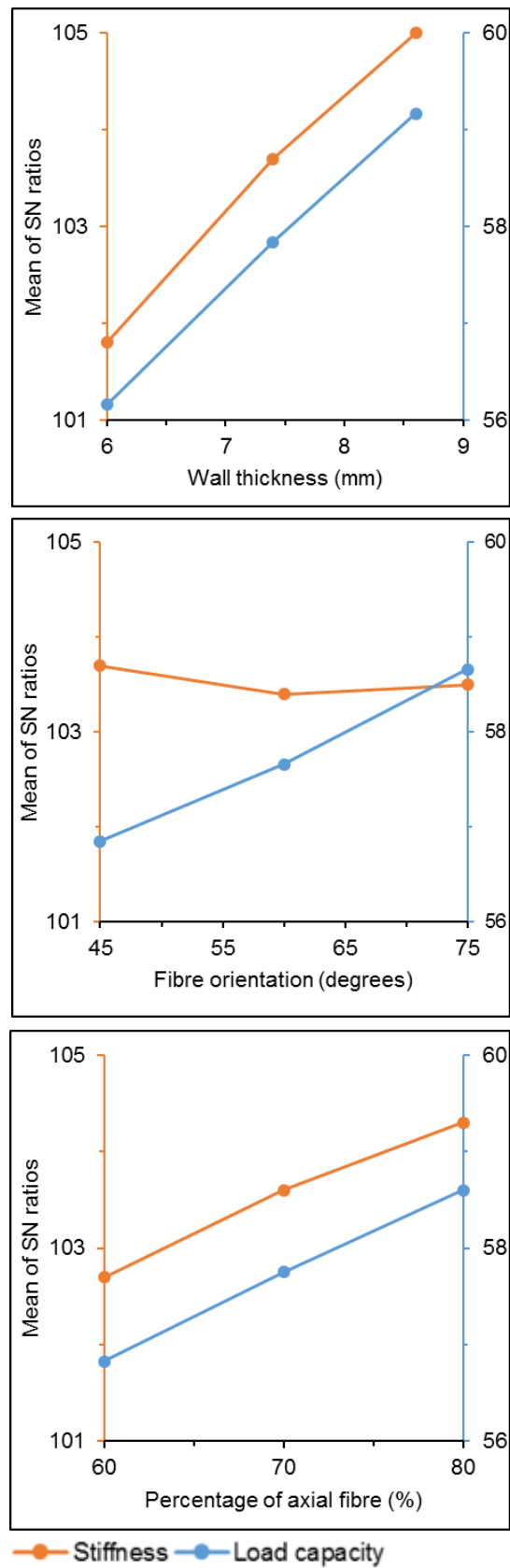
Figure 6.5 Effect of key parameters on the stiffness and load capacity of hollow circular tubes

Table 6.11 shows the contribution of each parameter on the enhancement of the stiffness and load capacity of hollow circular column. It can be seen that the contribution of wall thickness for both stiffness and load capacity is the largest compared with contribution of other parameters. Furthermore, the contribution of fibre orientation and percentage of axial fibre of circular tubes are higher than those of square tube.

Table 6.11 Percentage of contribution of key parameters for hollow circular tubes

Response	Wall thickness (mm)	Fibre orientation (degrees)	Percentage of fibre	% of Error
Stiffness	80.42	0.15	19.16	0.27
Load capacity	55.50	22.77	21.31	0.42

The stiffness of filled columns is depends mainly on the compressive strength of the concrete filler material (Table 6.12). Also, it can conclude that the FRP wall thickness has the bigger influence on the load capacity of filled circular columns. The wall thickness is the second parameter that effect positively on the stiffness of the column, while both the percentage of axial fibre and fibre orientation have low influence. The percentage of axial fibre comes in second order of parameters that are enhanced the load capacity of FRP circular columns followed by the compressive strength of the filler material then the fibre orientation.

Table 6.12 Mean SNR for parameters at each level for filled circular tubes

Response	Levels	Wall thickness (mm)	Fibre orientation (degrees)	Percentage of fibre	Concrete strength (MPa)
Stiffness	1	109.8	110.4	110.4	108.4
	2	110.3	110.2	110.4	110.3
	3	110.8	110.3	110.1	112.2
	Max.	110.8	110.4	110.4	112.2
	Min.	109.8	110.2	110.1	108.4
	ΔSNR	1.0	0.2	0.3	3.8
	Rank	2	4	3	1
Load capacity	1	58.05	59.11	60.02	58.90
	2	59.44	59.13	59.38	59.40
	3	60.71	59.96	58.81	59.90
	Max.	60.71	59.96	60.02	59.90
	Min.	58.05	59.11	58.81	58.90
	ΔSNR	2.66	0.85	1.21	1.00
	Rank	1	4	2	3

Increase wall thickness from 6.0 mm to 8.6 mm for circular columns results in increase the response of SNR, which it means that the influence of increase wall thickness is benefit on both the stiffness and load carrying capacity of filled columns (Figure 6.6). The sensitivity of stiffness of filled circular columns drops slowly from 45 to 60 degrees before it turns up ward beyond. This can be attributed to the enhancement of concrete infill due to FRP confinement. The effect of fibre orientation on the load capacity of filled circular columns is increase slightly from 45 to 60 degrees but it increases greatly beyond until 75 degrees. This is because the contribution of the oriented fibres in enhancing confinement effects increases as the angle of fibre grows away from the axial direction. The rate of change in sensitivity of stiffness of filled circular columns due to percentage of axial fibre is minimal. On the other hand, the percentage of axial fibre has affected positively the magnitude of the axial load capacity of circular FRP columns filled with concrete. Although effects of concrete compressive strength causes a moderate increase in the load capacity in range from 20 MPa - 50 MPa, it is main factor of increasing the stiffness of column.
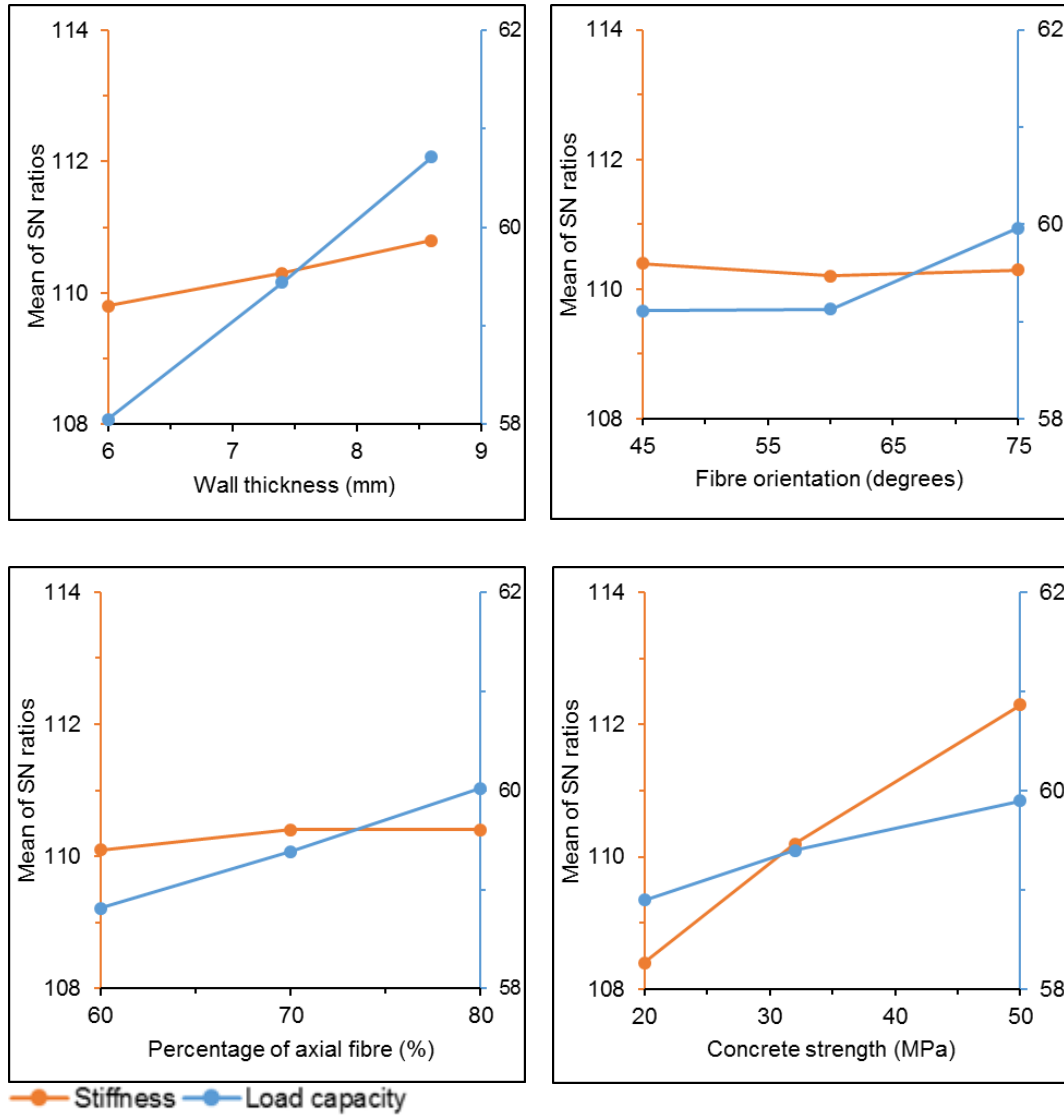
Figure 6.6 Effect of key parameters on the stiffness and load capacity of filled circular tubes

The percentage of contribution of compressive strength on the improving the stiffness of filled columns is 92.08 % (Table 6.13). Also, it can conclude that the FRP wall thickness has the bigger influence on the load capacity of filled circular columns with a percentage of contribution of 66.38 %. The fibre orientation and percentage of axial fibre have low contributions on the stiffness of filled columns. However, they can contribute in improving the load capacity of filled circular columns by 8.18 % and 16.23 % respectively.

Table 6.12 indicates also that the optimum level of load capacity for the FRP circular column can be achieved by combination 8.6 mm wall thickness with keeping 20 % of fibre extends in non-axial direction at angle 75 degrees and using concrete strength of 50 MPa for filling.

Table 6.13 Percentage of contribution of key parameters for filled circular tubes

Response	Wall thickness (mm)	Fibre orientation (degrees)	Percentage of fibre	Concrete strength (MPa)	% of Error
Stiffness	6.74	0.34	0.83	92.08	0
Load capacity	66.38	8.18	16.23	9.20	0

6.5 Additional parameters

Based on the results of the parameters selected from Taguchi method, further cases were selected to study the effect of wall thickness on the failure modes of hollow tubes and the influence of concrete strength and fibre orientation on the load capacity and stiffness of FRP tubes.

The results of hollow tubes show that the failure mode of square tube is changed from local buckling to compression failure when the wall thickness increased up to 7.8 mm. On the other hand, the dominant failure mode of hollow circular tubes is compressive failure. Thus, the square tubes are considered to further analyse on how the wall thickness can be changed to prevent local buckling.

Both the square and circular tubes were considered to investigate the improvement in the load capacity and stiffness of pultruded FRP tubes due to filling with different types of concrete.

Finally, the effects of fibre orientation on the stiffness and load capacity of filled columns are studied for the circular columns.

6.5.1 Square tubes

Two series are selected as additional cases for square FRP tubes (S-a and S-b). S-a series is used to investigate the influence of the wall thickness on the failure mode of the hollow square columns (Table 6.14). Moreover, the influence of the compressive strength of concrete infill on load capacity of filled square columns was also studied by considering S-b series as shown in Table 6.14.

Table 6.14 Effect of wall thickness and concrete strength on square tubes

Series	Wall thickness (mm)	Fibre orientation (degrees)	Percentage of fibre (%)	Concrete strength (MPa)
S-a1	5.200			
S-a2	6.400			
S-a3	6.750	0/45/-45	80/10/10	-
S-a4	7.100			
S-a5	7.800			
S-b1				Hollow
S-b2				20
S-b3	5.200	0/45/-45	80/10/10	32
S-b4				50
S-b5				65

6.5.2 Circular tubes

Similar to square tubes, two series are selected for circular columns to investigate the effect of concrete strength and fibre orientation on the overall performance. The impact of concrete strength on the column capacity was investigated by using four (4) concrete strengths 20, 32, 50, 65 MPa as shown in Table 6.15 for C-a series. The effect of the fibre orientation of the circular FRP tubes was another research parameter selected for further study (series C-b). In this series, four different angles were used in analysing the circular columns filled with 32 MPa concrete. The same wall thickness and percentage of axial fibres were assumed for all the cases (Table 6.15).

Table 6.15 Effect of concrete strength on filled circular tubes

Series	Wall thickness (mm)	Fibre orientation (degrees)	Percentage of fibre (%)	Concrete strength (MPa)
C-a1				Hollow
C-a2				20
C-a3	6	0/60/-60	70/15/15	32
C-a4				50
C-a5				65
C-b1		0/45/-45		
C-b2		0/60/-60		
C-b2	6	0/75/-75	70/15/15	32
C-b3		0/85/-85		

6.6 Results of additional parameters

6.6.1 Square tubes

The purpose of carrying out finite element analyses for the additional cases of hollow square tubes is to determine the effect of wall thickness on the mode of failure. Table 6.16 shows the stiffness and load capacity of the columns considered in S-a series. The assumed values of the fibre orientation and percentage of fibres in axial direction are kept the same for all the cases (45 degrees and [80/10/10] respectively). Figure 6. 7 (a) shows that the load deformation curves for columns that are indicate that the stiffness of columns is increased as the wall of FRP tube becomes thicker. The trend of change the stiffness is improving when the compressive strength of concrete increases (Figure 6.7 (b). Figure 6.7 (c) shows that columns fail due to buckling up to around 6.75 mm wall thickness while the compression failure becomes the dominant failure mode for thicker tubes. This means the potential strength of pultruded FRP tubes could be utilised when the wall thickness increases.

Table 6.16 Stiffness, load capacity and failure modes of S-a series

Series	Wall thickness (mm)	Stiffness $(\times 10^3 \text{N/mm})$	Load capacity (kN)	Failure mode*
S-a1	5.200	145.4	415.9	B
S-a2	6.400	179.8	769.4	B
S-a3	6.750	192.7	856.8	B/C
S-a4	7.100	199.6	866.0	C
S-a5	7.800	220.8	974.0	C

*B: Buckling failure, C: Compression failure in axial plies.
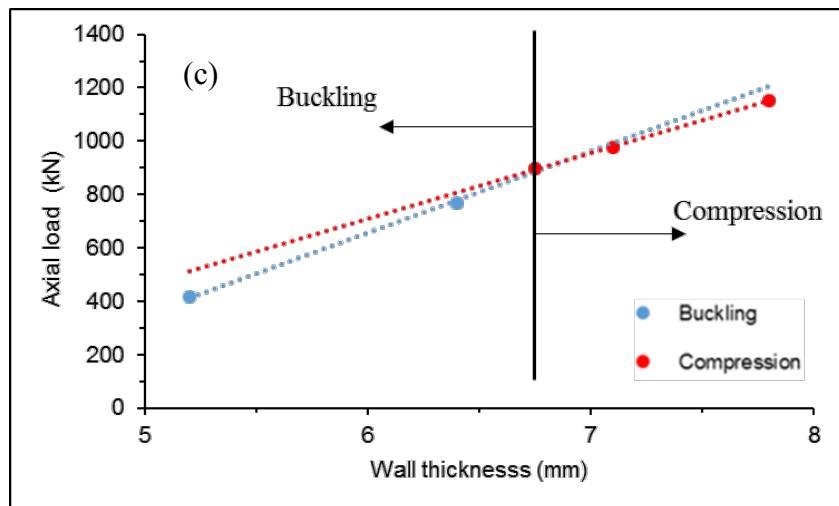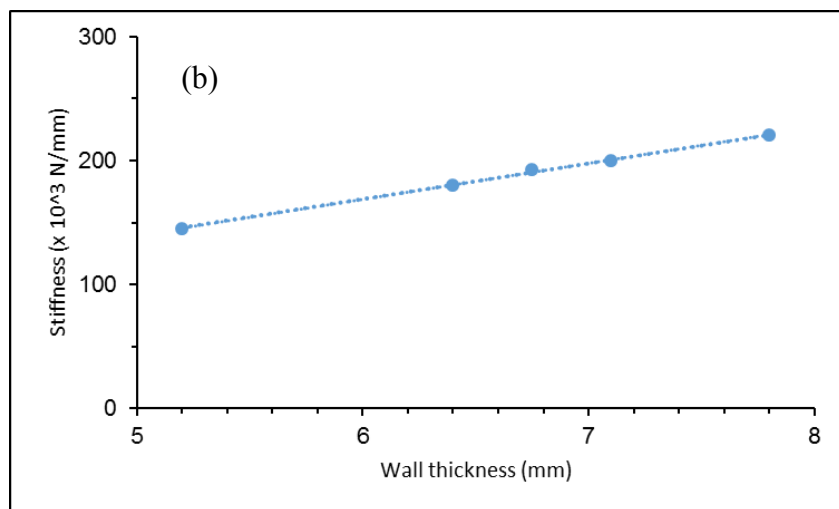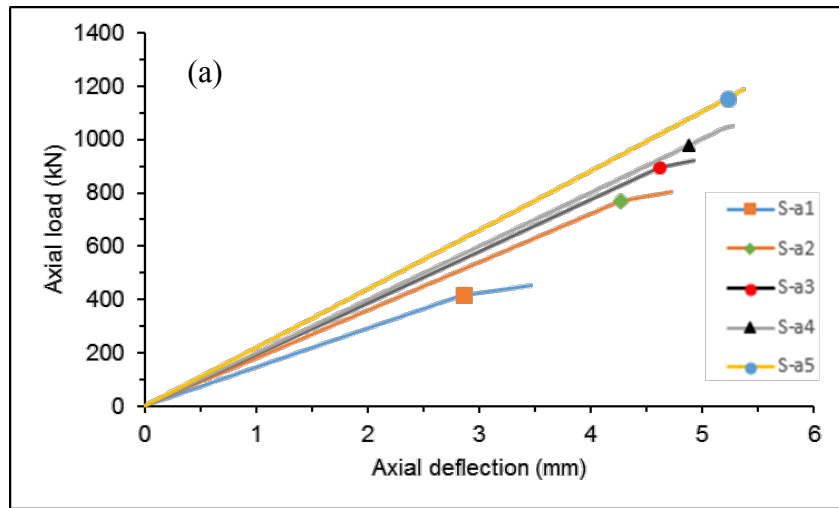
Figure 6.7 Effect of wall thickness on (a) load-deflection curves, (b) stiffness
of square tubes and (c) mode of failure

Investigating the trend of change in the stiffness and load capacity of filled tube is the aim of the remaining additional cases of the square tubes. Different values of compressive strength of concrete are used while keeping the angle and percentage of non-axial fibre layers of the pultruded FRP tube at 45 degrees and 20% respectively. Stiffness and load capacity values of the column based on the FE simulation are presented in Table 6.17. The compression material failure of FRP tube is the common mode of filled columns Figure 6. 8(a) shows the load deformation curves and it can be seen that the stiffness of the column is increased as the properties of the concrete infill improves. Figure 6.8 (b) shows that the trend of stiffness is increasing as the properties of filler improve. Figure 6.8 (c) shows that the general trend of load capacity is improving when the compressive strength of concrete is increased.

Table 6.17 Stiffness, load capacity and failure modes of S-b series

Series	Concrete strength (MPa)	Stiffness ($\times 10^3$N/mm)	Load capacity (kN)	Failure mode*
S-b1	Hollow	145.4	415.9	B
S-b2	20	270.4	566.3	C
S-b3	32	316.2	616.6	C
S-b4	50	391.4	728.4	C
S-b5	65	446.5	822.6	C

* B; Buckling failure, C: Compression failure in axial plies
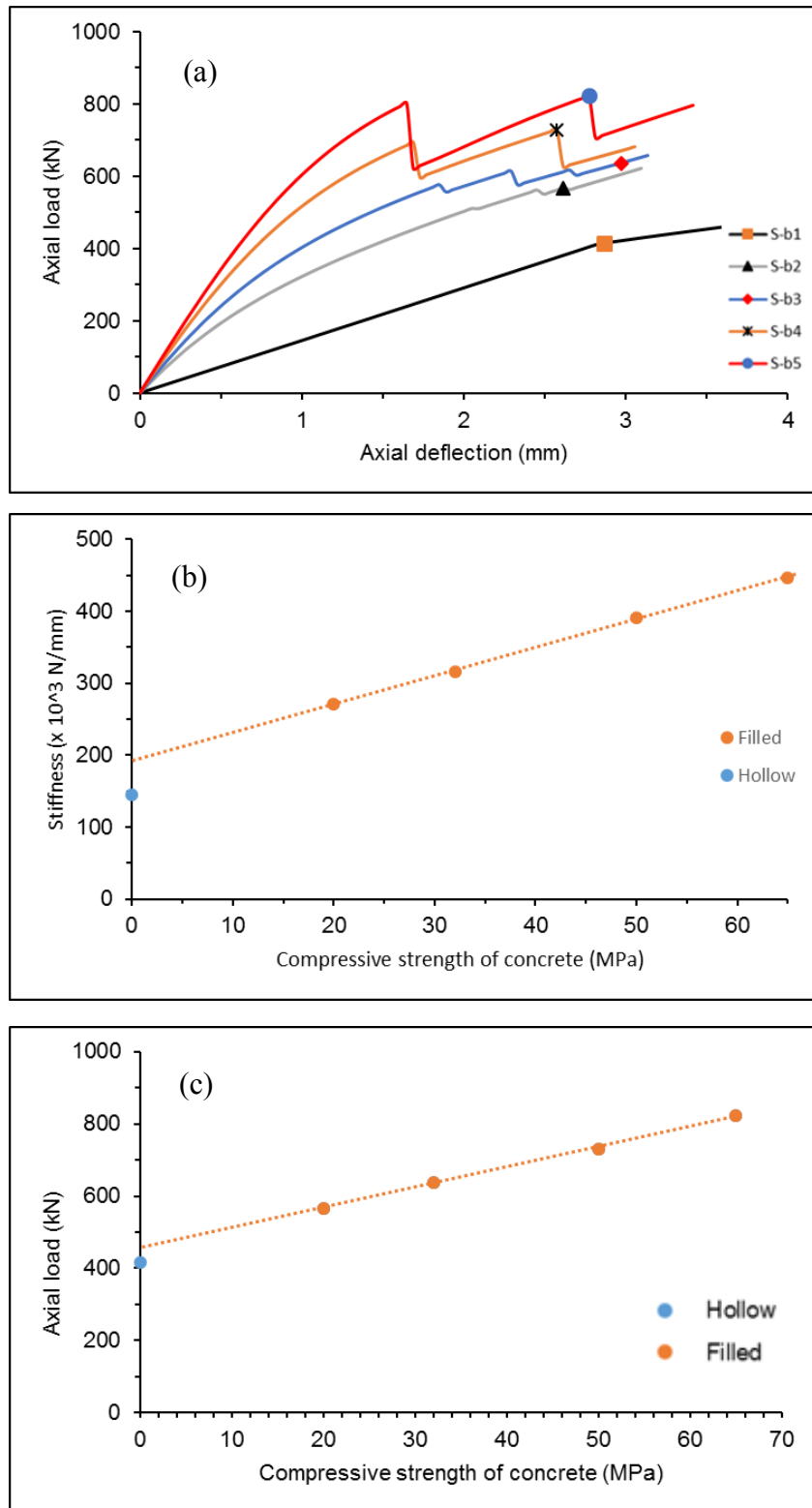
Figure 6.8 Square tubes filled with different types of concrete (a) load-deflection curves, (b) trend of stiffness and (c) trend of load capacity

6.6.2 Circular tubes

Table 6.18 shows the stiffness and load capacity values of additional cases to study the effect of filler properties on the axial behaviour of FRP circular columns. All columns were failed due to compression failure. The strengthening in the stiffness of the pultruded FRP tubes due to filling with high strength concrete can be seen in Figure 6. 9 (a). Increasing is the dominated trend of change in the stiffness of FRP columns due to filling with different types of concrete (Figure 6.9 (b)). Although the general trend of the load capacity for the pultruded FRP tubes can be described as an increase trend, the degree of improvement is decreased as the strength of concrete infill increases (Figure 6.9 (c)).

Table 6.18 Stiffness, load capacity and failure modes of C-a series

Series	Concrete strength (MPa)	Stiffness ($\times 10^3$N/mm)	Load capacity (kN)	Failure mode*
C-a1	Hollow	122.9	631.4	C
C-a2	20	255.6	701.3	C
C-a3	32	308.8	772.8	C
C-a4	50	391.4	829.7	C
C-a5	65	446.5	874.1	C

* C: Compression failure in axial plies.
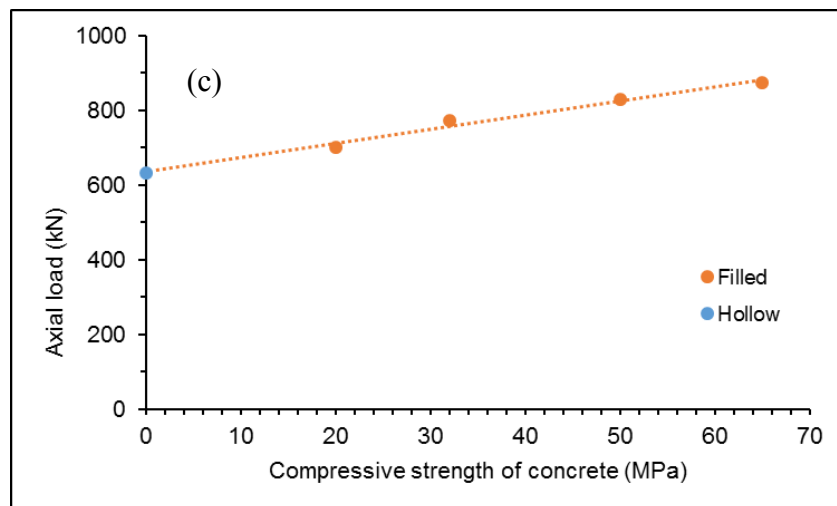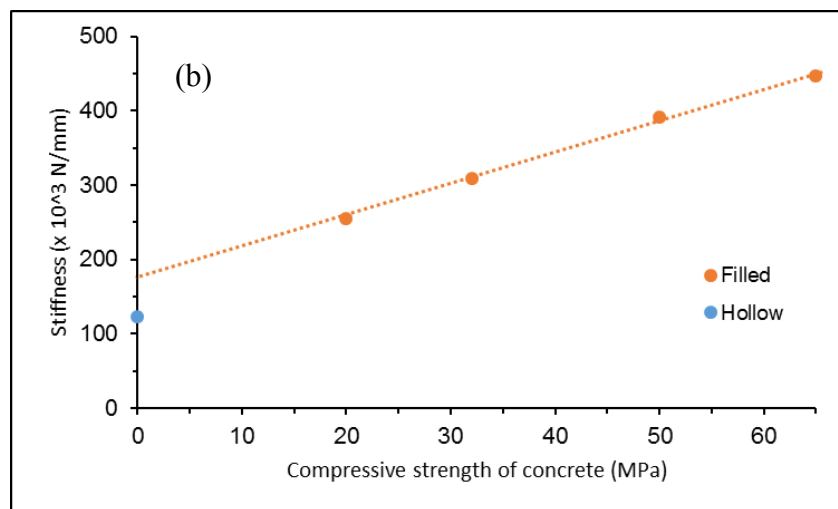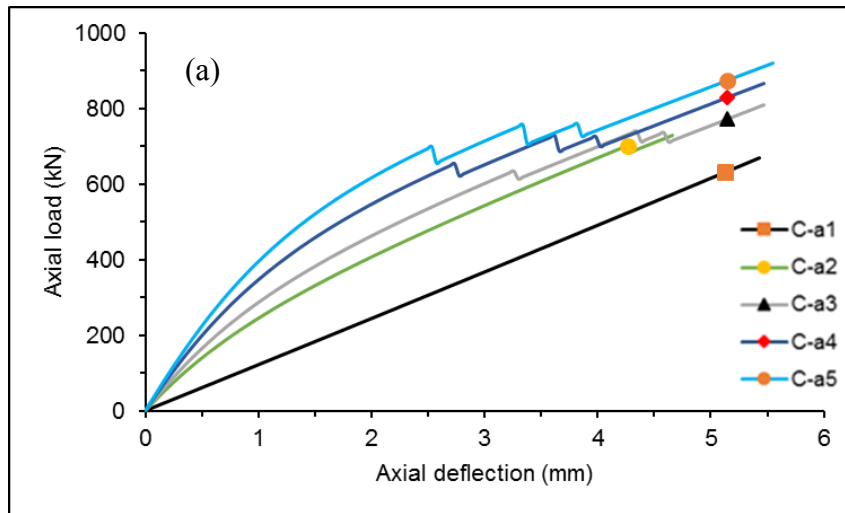
Figure 6.9 Effect of concrete strength on circular tubes (a) load-deflection curves, (b) stiffness and (c) load capacity

Table 6.19 shows the values of stiffness, load capacity and failure mode of the additional cases for filled circular tubes used to study the effect of fibre orientation. The influence of fibre orientation on the stiffness of the FRP columns is not high. A reduction in the stiffness occurs as the orientation of fibre increases towards the transverse direction. This is because the contribution of oriented fibre in boosting the axial stiffness decreases. The common failure mode is compression failure. Load capacity increases as the angle of the oriented fibre layers increases towards the transverse direction. This can be attributed to the improved FRP confinement. Figure 6.10 (a) shows the load –deformation curves of columns while Figure 6.10 (b) shows the trend of change in stiffness due to fibre orientation. Figure 6.10 (c) shows the trend of the enhancement in the capacity of columns as the angle of the fibre layers are closer to the transverse direction.

Table 6.19 Stiffness, load capacity and failure modes of C-b series

Series	Fibre orientation (Degree)	Stiffness $(\times 10^3 \text{N/mm})$	Load capacity (kN)	Failure mode*
C-b1	45	315.1	734.7	C
C-b2	60	308.8	772.8	C
C-b3	75	306.6	806.8	C
C-b4	85	304.2	838.9	C

* C: Compression failure in axial plies.
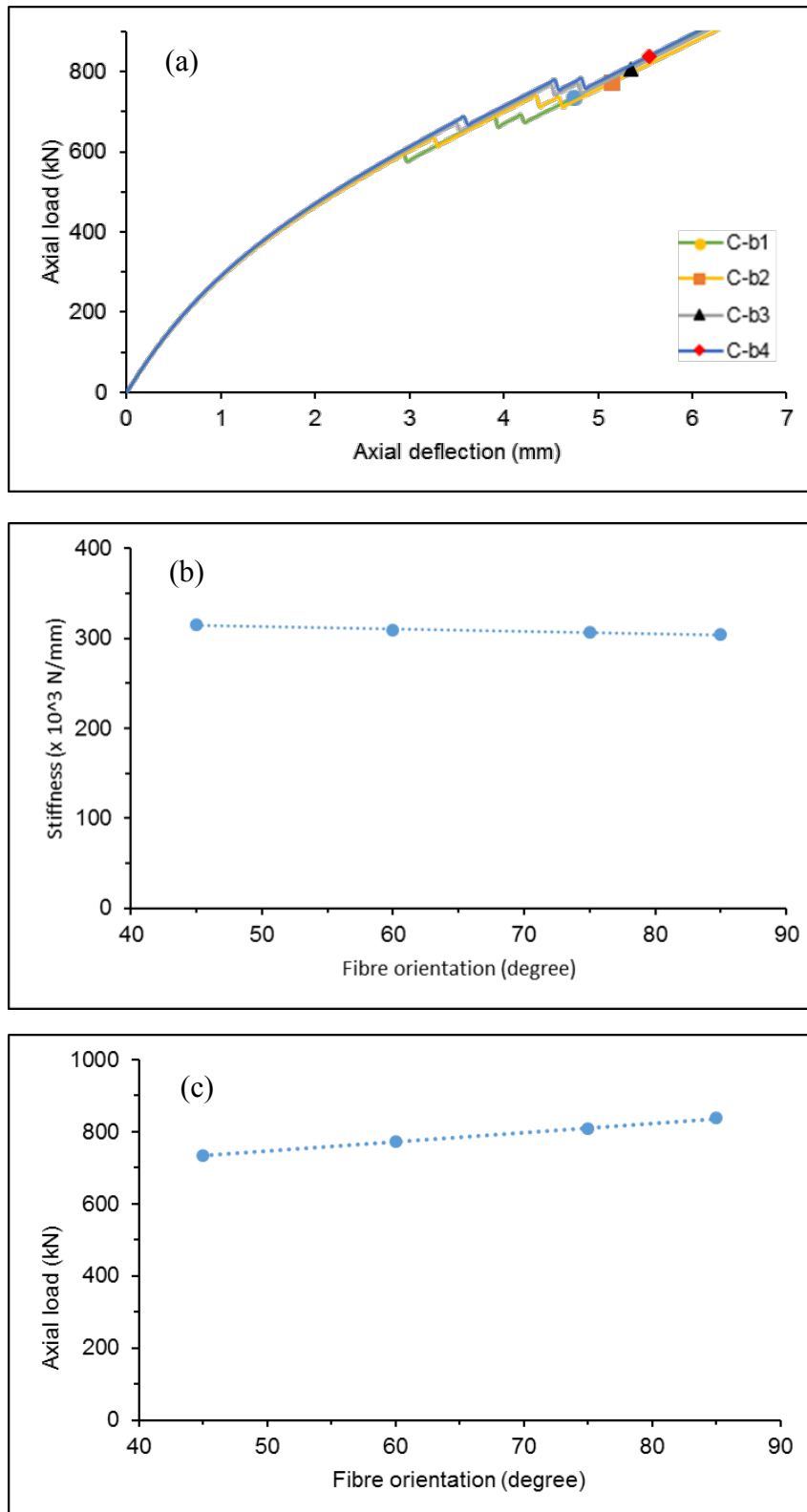
Figure 6.10 Influence of fibre orientation on filled circular tubes (a) load-deflection curves, (b) stiffness and (c) trend of load capacity

6.7 Design recommendations

According to the results of the parametric study, the axial behaviour of pultruded FRP tubes can be improved through considering the influential parameters identified in this study.

6.7.1 Design of square tubes

In case of hollow square tube where the buckling is the dominated failure mode, the results show that the wall thickness of FRP tube leads to change the failure mode from buckling failure mode to compression material failure. The width-to- thickness ratio equal to or less than 14.0 is suitable to prevent failure due to buckling for the selected type of square tube. The axial load capacity of filled square columns is positively affected by increasing the wall thickness. The stiffness of column is also improved when the wall thickness is higher than 6 mm.

Increasing fibre orientation with respect to the axial direction up to 60 degrees causes a reduction in the sensitivity of stiffness of hollow square tube. On the other hand, the load capacity is increased up to angle of 60 degrees. In case of filled columns, increasing the orientation of fibre towards the transverse direction has positive effect on the load capacity of column although it decreases the stiffness.

The longitudinal modulus of FRP tube depends on the percentage of fibre distribution in the axial and non-axial directions. Increasing the percentage of fibre in axial direction results in increasing the axial modulus and as a result, the axial stiffness of hollow pultruded FRP square tube is enhanced. The load capacity shows improvement up to the 70% content where it remains constant until percentage of axial fibre of 80 %. The percentage of the axial fibre layer has a positive effect on both the stiffness and load capacity of filled FRP columns.

Increasing compressive strength of concrete filler produces an improvement in the stiffness and load capacity of specific FRP column noting that the degree of improvement decreases as the compressive strength of concrete increases. Concrete filler with 30 MPa compressive strength or higher makes significant improvement in the axial behaviour of filled square tubes.

As the design of pultruded FRP compression member includes determining the deflection for the serviceability limit state and stresses for the ultimate limit state, the parameters that are affected positively on the stiffness should be considered in design geometry and fibre structure of FRP tube. In case of hollow square columns, increase values of wall thickness and percentage of axial fibre with keeping the angle of non-axial fibre layer equal or less than 45 degree results in increasing trend for stiffness. The improvement in the stiffness means that the pultruded FRP column reaches to the design limit of deflection at higher load level. Also, the ultimate stresses (flexural and local buckling stresses) improves since the axial stiffness is increased. For filled columns, improving properties of filler and percentage of axial fibre with keeping fibre orientation at 45 degrees or less leads to increase the stiffness. Moreover, the value of width -to- thickness ratio of 14 or less changes the failure mode from buckling to compression failure. As a result, the load capacity of column increases and the longer lengths of FRP compression members can be used in structures.

6.7.2 Design of circular tubes

Compression material failure is the predominant failure mode of hollow circular tubes in the current study. Generally, the stiffness and load capacity of hollow and filled circular column increase when the wall thickness of FRP tube increases up to 8.6 mm.

Although the load capacity of hollow circular tubes is increased as the orientation of fibre increases with respect to the axial direction, the sensitivity of stiffness of FRP columns to this parameter decreases. This is because the contribution of non-axial fibre layer in providing the axial modulus reduces. The load capacity of filled circular columns increases significantly when the angle of the oriented fibre layer is higher than 60 degrees.

Increasing the percentage of axial fibre up to 80% lead to boost the stiffness of hollow circular tube but it shows no improvement in stiffness of filled column when the percentage is higher than 70 %. The load capacity of hollow and filled circular tubes is improved as the percentage of axial fibre increases.

It can be seen from this study that improved performance can be obtained for hollow and filled circular columns if the most influential parameters are changed as appropriate.

According to the considered values of this study, keeping the diameter-to-thickness ratio of 14.8 or less provides a compression material failure for circular hollow columns. This can be attributed to improving the stiffness of FRP tube due to increase the wall thickness. However, increasing axial fibre develops the stiffness while increase the fibre orientation higher than 45 degree causes a reduction. Therefore, the load that the axial deflection of hollow circular columns reaches the design limit is improved. Filler properties is the main factor that improves the stiffness of filled circular columns. However, the wall thickness, percentage of axial fibre and orientation of fibre layer have a positive impacts on the stiffness and load capacity. The positive effects of all parameters on the stiffness and load capacity should be considered to enhance the axial behaviour of pultruded FRP columns. This will contribute effectively in spreading the usage of FRP compression members in diverse applications of civil engineering.

6.8 Conclusions

The lamina method was used to carry out a parametric study to examine the effect of different parameters on the axial behaviour of hollow and filled square and circular pultruded GFRP tubes. Parameters considered are wall thickness, percentage of fibre distribution in axial and non-axial directions, fibre orientation of FRP tube, and compressive strength of the concrete. Based on the FEM and statistical analysis, the following conclusions can be drawn:

- The stiffness and load capacity of hollow square tubes are improve when the wall thickness increases. This is because the axial stiffness of columns improves due to increase cross-sectional area of the tube. Moreover, the failure mode changes from the buckling to compression failure mode. For the selected type of square tube, the wall thickness of around 6.75 mm is the limit of which failure mode may occur. Although, the load capacity of filled columns is

increased in range of wall thickness of 5.2 mm to 7.8 mm, the wall thickness of 6.4 is the increasing point of stiffness sensitivity.

- The reduction in sensitivity of stiffness and the improvement in the load capacity of hollow square tube due to increase fibre orientation is occurred up to angle of 60 degree. The fibre orientation impacts positively on the load capacity of filled columns since effects of the FRP confinement gets better as the angle of oriented fibre layers increases with respect to the axial direction. On the other hand, increase fibre orientation impacts negatively on the sensitivity of stiffness of filled columns.

- The stiffness of hollow and filled square columns are improved by increasing the percentage of axial fibre. On the other hand, the positive effects of axial fibre percentage on the load capacity of hollow tubes is continued up to 70% while it is in increasing trend of filled columns.

- The compressive strength of filler material is the main factor that increases the stiffness of filled square columns while the load capacity shows an increasing trend when the compressive strength of filler being larger than 32 MPa.

- The results of the parametric study show that the stiffness and load capacity of hollow and filled circular columns are better as the wall thickness of the FRP tube increases.

- Increase fibre orientation leads to improve the load capacity of hollow circular tubes combined with decreasing the sensitivity of stiffness. In filled columns, the load capacity is improved significantly when the angle of oriented fibre layers being larger than 60 degree.

- The results of hollow circular columns show that increasing the percentage of axial fibre results in improvements in their stiffness and load capacity. The same trend of increasing can be shown in the behaviour of filled columns with exception that the stiffness remain constant when the percentage of axial fibre being larger than 70%. Furthermore, the results of filled circular tubes show that the stiffness and load capacity are getting enhancement as the compressive strength of filler improves.

References

Barbero, E & Tomblin, J 1994, 'A phenomenological design equation for FRP columns with interaction between local and global buckling', Thin-Walled Structures, vol. 18, no. 2, pp. 117-31.

Barbero, EJ & Raftoyiannis, IG 1993, 'Local buckling of FRP beams and columns', Journal of materials in civil engineering, vol. 5, no. 3, pp. 339-55.

Barbero, EJ & Turk, M 2000, 'Experimental investigation of beam-column behavior of pultruded structural shapes', Journal of reinforced plastics and composites, vol. 19, no. 3, pp. 249-65.

Cardoso, DC, Harries, KA & Batista, EdM 2014, 'Compressive strength equation for GFRP square tube columns', Composites Part B: Engineering, vol. 59, pp. 1-11.

Chitawadagi, MV, Narasimhan, MC & Kulkarni, S 2010, 'Axial capacity of rectangular concrete-filled steel tube columns–DOE approach', Construction and Building Materials, vol. 24, no. 4, pp. 585-95.

Correia, M, Nunes, F, Correia, J & Silvestre, N 2012, 'Buckling behavior and failure of hybrid fiber-reinforced polymer pultruded short columns', Journal of Composites for Construction, vol. 17, no. 4, pp. 463-75.

Ferdous, W, Manalo, A & Aravinthan, T 2017, 'Bond behaviour of composite sandwich panel and epoxy polymer matrix: Taguchi design of experiments and theoretical predictions', Construction and Building Materials, vol. 145, pp. 76-87.

Godat, A, Légeron, F, Gagné, V & Marmion, B 2013, 'Use of FRP pultruded members for electricity transmission towers', Composite Structures, vol. 105, pp. 408-21.

Hashem, ZA & Yuan, RL 2001, 'Short vs. long column behavior of pultruded glass-fiber reinforced polymer composites', Construction and Building Materials, vol. 15, no. 8, pp. 369-78.

Hassan, NK & Mosallam, AS 2004, 'Buckling and ultimate failure of thin-walled pultruded composite columns', Polymers and Polymer Composites, vol. 12, no. 6, pp. 469-81.

Li, F, Zhao, Q, Chen, L & Shao, G 2014, 'Experimental and theoretical research on the compression performance of CFRP sheet confined GFRP short pipe', ScientificWorldJournal, vol. 2014, p. 109692.

Nunes, F, Correia, JR & Silvestre, N 2016, 'Structural behaviour of hybrid FRP pultruded columns. Part 1: Experimental study', Composite Structures, vol. 139, pp. 291-303.

Ozbay, E, Oztas, A, Baykasoglu, A & Ozbebek, H 2009, 'Investigating mix proportions of high strength self compacting concrete by using Taguchi method', Construction and Building Materials, vol. 23, no. 2, pp. 694-702.

Puente, I, Insausti, A & Azkune, M 2006, 'Buckling of GFRP columns: An empirical approach to design', Journal of Composites for Construction, vol. 10, no. 6, pp. 529-37.

Qian, P, Feng, P & Ye, L 2008, 'Experimental study on GFRP pipes under axial compression', frontiers of architecture and civil engineering in china, vol. 2, no. 1, pp. 73-8.

Qiao, P, Davalos, JF & Wang, J 2001, 'Local buckling of composite FRP shapes by discrete plate analysis', Journal of Structural Engineering, vol. 127, no. 3, pp. 245-55.

Türkmen, İ, Gül, R & Çelik, C 2008, 'A Taguchi approach for investigation of some physical properties of concrete produced from mineral admixtures', Building and Environment, vol. 43, no. 6, pp. 1127-37.

Vincent, T & Ozbakkaloglu, T 2013, 'Influence of concrete strength and confinement method on axial compressive behavior of FRP confined high- and ultra high-strength concrete', Composites Part B: Engineering, vol. 50, pp. 413-28.

Zureick, A & Scott, D 1997, 'Short-term behavior and design of fiber-reinforced polymeric slender members under axial compression', Journal of Composites for Construction, vol. 1, no. 4, pp. 140-9.

Chapter 7:

Conclusions and Recommendations

The demand to use new materials in the construction industry has been increasing with the growth in requirements towards the quality of new buildings. The properties of the fibre reinforced polymer (FRP) materials, such as high strength, stiffness-to-weight ratio, resistance to corrosion and lightweight characteristics, make these materials a good alternative to the traditional materials such as concrete and steel used in construction. Pultruded FRP profiles have been used as structural column members in the construction industry. However, the low stiffness and buckling issues prevent pultruded columns from using their complete strength capacity.

The above issue has been researched in the previous studies in two ways. The first one is refining the accuracy of the prediction models of axial load capacity and the second one is searching for new methods to enhance the performance of FRP columns through strengthening the low axial stiffness of pultruded FRP sections. This can be done either by replacing the fibre layer of low stiffness with fibre of high stiffness, or by confining the transverse direction of the FRP profile with FRP sheet.

The current research explored the effect of potential variables in the behaviour of pultruded FRP tube columns. Furthermore, it investigated the improvement in the stiffness, load carrying capacity and energy absorption capacity of the filled tubes compared with the hollow tubes.

In addressing the goals and objectives of this study, the following four phases were conducted:

1. Investigating the effect of fibre orientation and its layup on the mechanical properties of the pultruded FRP tube and investigating the mechanical properties and stress-strain relationships of different types of filler;
2. Investigating the contribution of various types of filler material on the axial performance of square and circular filled pultruded FRP tubes ;

3. Developing a simulation method to predict the behaviour of hollow and filled columns by using finite element program STRAND7 and validating the developed method using experimental results;

4. Conducting a parametric study to evalute the impact of a range of different parameters such as FRP wall thickness, fibre orientation, laminate structure and compressive strength of the filler on the axial behaviour of FRP tubes and providing design recommendations.

7.1 Effects of orientation of the fibre layers and their layup on mechanical properties of GFRP tube and characterisation of filler material

First part of this study experimentally investigated how the fibre orientation and its layup influence on the mechanical properties of the pultruded FRP tubes. Burnout, tensile, compressive and shear tests were conducted. The compressive behaviour of different types of filler was investigated in the second part. Four types of normal concrete and three types of perlite lightweight concrete were considered in the pilot study before selecting two types of normal concrete and two types of perlite concrete to move forward with the full scale testing. Based on the results, the following conclusions were drawn:

- In addition to the properties of the constituent material, the fibre orientation and its layup have a significant impact on the mechanical properties of pultruded FRP tubes.

- The high tensile properties can be obtained by increasing the concentration of fibres in the axial direction and decreasing the angle of the non-axial fibre layer with respect to the axial direction.

- Increase in the fibre content of axial and non-axial fibre layers leads to improvement in the compressive strength and modulus. The angle of the non-axial fibre layers has an important effect as it governs how the axial fibre layers are supported against micro-buckling.

- The shear strength and modulus depend on the concentration of fibres in the axial direction and diagonal tensile field of shear forces. The results are also influenced by the shear strength of resin.

- Better mechanical properties of pultruded FRP profiles can be gained based on the stacking sequence of fibre layers and their fibre content. This improvement impacts positively on the structural performance of pultruded FRP profiles in various civil engineering applications.

- The lateral strain of perlite concrete is lower than that of normal concrete for a similar compressive strength. This indicates that the FRP confinement of perlite concrete is less effective compared with normal concrete. Moreover, the post peak behaviour of perlite concrete shows a more ductile behaviour compared with normal concrete. This can substantially influence the post peak behaviour of FRP tubes filled with perlite based filler.

7.2 Behaviour of hollow and filled pultruded FRP tubes

The axail behaviour of short pultruded FRP tubes was studied and compared with results of coupon tests. Moreover, the effects of different types of fillers on the stiffness, peak load capacity, post peak behaviour, failure modes and energy absorption capacity of the pultruded FRP tube columns were investigated in this study. Two types of normal concrete and two types of the lightweight perlite concrete were used in filling two different types of pultruded FRP tubes; square and circular sections.

The conclusions of this study are summarised below:

- The compressive behaviour of hollow FRP tubes is linear up to the peak load which it depends on the wall thickness, percentage of axial fibre layer and angle of the oriented fibre layer with respect to the axial direction. Decreasing the angle results in high contribution of orined fibre layer to resist the loading.

- Increase length-to lateral dimension ratio (L/D) of square tubes from 1 to 5 changes the failure mode from buckling bulge to local buckling where sides buckled either inside or/ and outside. On the other hand, the failure mode of circular tubes does not change even with increased L/D ratio.

- The stiffness of the filled columns improves as the modulus of the infill concrete increases. Using a filler with a modulus of 30 GPa leads to increase the stiffness of square and circular tubes by at least 77% and 45 % respectively. On the other hand, the stiffness of hollow square columns is affected positively when the wall thickness increases while decreasing the angle of oriented fibre layers with respect to the axial direction improves the stiffness of hollow circular columns.

- The peak load capacity of filled pultruded FRP tube columns is increased as the properties of the filler improves and the angle of the oriented fibre layer increases with respect to the axial direction. The high contribution of the non-axial fibre layer is obtained when its fibre content increases and their orientation increases with respect to the axial direction.The post-peak behaviour of FRP tubes is changed from a rapid drop in the load capacity for hollow columns to a gradual decrease in the filled columns. The ability of the filled columns to sustain loading after reaching the peak load is affected by the properties of filler and the transverse resistance of FRP tube. All the columns filled with perlite show the gradual reduction in strength compared to those filled with normal concrete. When the transverse resistance of FRP square tube is adequate, the post peak behaviour of columns filled with normal showed a slow reduction in strength.

- Both the plate slenderness ratio (width-to-thickness) and global slenderness (L/r) ratio have an influence on the axial behaviour of the hollow pultruded square tube columns. In those with similar (L/r) ratio, the axial behaviour is controlled by the plate slenderness ratio.

- The modes of failure of square tubes are changed due to filling with concrete from either local buckling to crushing at the end. This is followed by splitting at the corner and around the perimeter of the tube or from splitting at mid-height followed by buckling to crushing, followed by corner splitting at one end of the column. The failure modes of circular FRP tube have also changed from circumference splitting at one end of the hollow column to crushing at one or both ends followed by longitudinal splitting of the filled column.

- The energy absorption capacity of hollow pultruded FRP tubes is improved when the wall thickness and fibre orientation increase. The degree of

improvement of filled pultrude FRP tubes depends on filler properties and fibre orientation of the pultruded FRP tube. Columns filled with perlite concrete show improved energy absorption capacity, although the perlite concrete strength is lower or equal to strength of normal concrete.

7.3 Numerical investigation of hollow and filled FRP tubes

This section describes the finite element analysis using the software program STRAND 7. Mechanical properties of FRP material and stress-strain relationship of the confined concrete obtained before were used to simulate the concrete behaviour inside the finite element program. Both the lamina and plate methods were considered in the simulation.

The results in terms of the load-axial deflection curves, peak load and failure modes were checked with results of the experimental results to ensure the level of the simulation accuracy. The following primary conclusions can be drawn from the study:

- The load-deflection curves of lamina and plate methods that were used in defining FRP material in the finite element analysis are in a good agreement with experimental curves. Moreover, the computational time of plate method is longer than that of lamina method.
- The results of peak load capacity using the lamina method of filled pultruded FRP tubes reveal a better agreement with the experimental results. The maximum error is around 5.14% and 5.8 % for those that were filled with perlite and normal concrete respectively. However, in case of using plate method, they were 10.8 % and 6.0 % respectively.
- Depending on the availability of the material properties, both the lamina and plate methods can be used to model pultruded FRP tube and to simulate the failure modes. The analysis-oriented model of confined concrete can be improved for the perlite filler by using the density ratio of the lightweight to normal concrete as a reduction factor.
- Although the post-peak response is not available because of software limitations in representing the degradation of the FRP stiffness after failure, the

predicted values of the peak load, based on the failure criteria, provide a safe approach to assess the capacity of filled FRP columns for civil engineering applications.

- The applicability to do further research into investigating effects of various parameters on the axial behaviour of the filled pultruded FRP tubes was reinforced as the accuracy of the finite element simulation was validated.

7.4 Influence of different parameters on the performance of pultruded FRP columns

The finite element simulation model was used to investigate the axial performance of both hollow and filled pultruded FRP columns, which was modified by changing the wall thickness of the FRP tube, percentage of fibre distribution, fibre orientation and compressive strength of concrete infill. The lamina method for defining properties of FRP tubes in the finite element software was considered. In total, four parameters were used and three levels of variations were considered in each parameter.

Based on the results, the following conclusions were drawn:

- The stiffness and load capacity of hollow square and circular FRP tubes increase as the wall thickness increases. The failure mode of hollow square tubes changes to be compression failure rather than buckling when the walls of FRP is thicker while the failure modes of hollow circular FRP tubes is due compression failure. The load capacity of filled FRP columns is also increased.
- The sensitivity of stiffness of the hollow square tube is decreased when the fibre orientation increases but it increases as the percentage of axial fibre increases. The improvement in load capacity is continued up to 60 degree of fibre orientation and 70 % of axial fibre. In filled square tube, the influence on the stiffness and load capacity is positive with exception that the sensitivity of stiffness decrease as the angle of oriented fibre increases. The behaviour of hollow circular tube reflects the same trend of filled square tubes while the positive effect is for the load capacity of filled circular tubes.
- The stiffness of filled square tube is increased as the compressive strength of filler concrete improves. On the other hand, the significant improvement in the

load capacity is observed when the compressive strength of filler being larger than 32 MPa. For circular tubes, the prediction behaviour show that the stiffness and load capacity are getting enhancement as the compressive strength of filler improves.

- The optimum level of load capacity of filled square and circular columns can be obtained by a combination of maximum wall thickness of the FRP tube with keeping 20% of fibre oriented at angle of 75 degree with a 50MPa filler.

7.5 Contributions of the study

This study has contributed to the growing area of research of the pultruded FRP tubes by exploring four parameters fibre orientation and their layup, properties of filler material, finite element simulation to the axial behaviour of pultruded FRP tube columns and effects of different parameters.

1. The influence of the orientation of the fibre layers and their layup on the mechanical properties of the pultruded fibre reinforced polymer tubes has been studied by comparing the mechanical properties of the different pultruded FRP tubes.

2. In-depth understanding of compressive behaviour of hollow and filled pultruded FRP tubes was achieved. Different types of concrete infill were used to explain how the properties of concrete and pultruded FRP tubes govern the axial behaviour of an innovative structural column member. The findings contribute to the use of pultruded FRP-concrete column application in civil engineering.

3. Finite element analysis provides a method for predicting the behaviour of hollow and filled tubes under axial loads. This analysis uses the lamina and plate methods and delivers the applicability to modify the structure and orientation of pultruded fibre layers in order to optimise the performance of the FRP column. This method could assist designers and engineers to check and design FRP structural columns with confidence.

4. Finally, the parametric study brings a deeper understanding of the effects of other parameters on the axial compressive behaviour of the pultruded FRP tube columns, which were not explored experimentally to propose design

recommendation for safe usage of pultruded FR-concrete column. The effects of wall thickness of FRP tube, fibre orientation, percentage of axial fibre and compressive strength of filler on the stiffness, load capacity and failure modes were explained.

7.6 Recommendation for future research

The research work that has been accomplished in this study for improving the axial behaviour of the pultruded fibre reinforced polymer tube columns is comprehensive and covered a range of parameters.

Several achievements have been gained in terms of deep understanding of the axial compressive behaviour of both the hollow and filled columns, and the finite element simulation. Further research in related areas still needs to be conducted.

Below is the list of areas that need more research to widespread use of pultruded FRP tubes as structural column members in civil engineering applications:

1. Since the experimental results indicate the effect of the fibre orientation and its layup on the mechanical properties of the pultruded fibre reinforced polymer tube, it is worth to investigate and compile guidelines for obtaining optimum mechanical properties.
2. Experimental and numerical investigation on the axial behaviour of slender pultruded FRP tube columns filled with concrete since the stiffness, load capacity and energy absorption are affected positively by the properties of filler.
3. While filling provides improvement in the axial behaviour of pultruded FRP columns, investigation of the behaviour of filled pultruded FRP tube columns under combined axial load and bending moment is important to study the structural behaviour under combined actions and to spread the use of pultruded FRP tubes in different applications of civil engineering.
4. Since the improvement in the axial behaviour depends on properties of pultruded FRP tube, investigation of the axial behaviour of the hollow and

filled PFRP tube columns fabricated with hybrid laminate structure is vital to optimise the level of improvement.

5. Investigation of the mode failure of circular tubes through studying effects of diameter-to-wall thickness ratio. This will provide a guideline for the possible failure modes of hollow circular columns and how can be aware to avoid the worse mode

List of references

Abdulraheem, MS 2018, 'Experimental investigation of fire effects on ductility and stiffness of reinforced reactive powder concrete columns under axial compression', *Journal of Building Engineering*, vol. 20, pp. 750-61.

Abdulraheem, MS 2018, 'Experimental investigation of fire effects on ductility and stiffness of reinforced reactive powder concrete columns under axial compression', *Journal of Building Engineering*, vol. 20, pp. 750-61.

Al-saadi, AU, Aravinthan, T & Lokuge, W 2018, 'Structural applications of Fibre Reinforced Polymer (FRP) composite tubes: a review of columns members', *Composite Structures*, vol. 204, pp. 513-24.

AS1012.9 2014, *Methods of testing concrete*, Methods 9:Compressive strength tests-Concrete,mortar and grout specimens., Sydney, Australia.

AS1012.17 1997, *Methods of testing concrete*, Determination of the static chord modulus of elasticity and Poisson's ratio of concrete specimens, Australia.

Ascione, L, Caron, J-F, Godonou, P, van IJselmuijden, K, Knippers, J, Mottram, T, Oppe, M, Gantriis Sorensen, M, Taby, J & Tromp, L 2016, Prospect for new guidance in the design of FRP: Support to the implementation, harmonization and further development of the Eurocodes, Publications Office of the European Union.

ASTM:D5379 2012, *Standard test method for shear properties of composite materials by the V-Notched Beam method* United States.

Bai, Y & Keller, T 2009, 'Shear failure of pultruded fiber-reinforced polymer composites under axial compression', *Journal of Composites for Construction*, vol. 13, no. 3, pp. 234-42.

Bank, LC 2006, Composites for construction: Structural design with FRP materials, John Wiley & Sons.

Barbero, E & Tomblin, J 1994, 'A phenomenological design equation for FRP columns with interaction between local and global buckling', *Thin-Walled Structures*, vol. 18, no. 2, pp. 117-31.

Barbero, EJ 2017, Introduction to composite materials design, Third edn, CRC Press, Boca Raton, Fla.

Barbero, EJ & Raftoyiannis, IG 1993, 'Local buckling of FRP beams and columns', *Journal of materials in civil engineering*, vol. 5, no. 3, pp. 339-55.

Barbero, EJ & Turk, M 2000, 'Experimental investigation of beam-column behavior of pultruded structural shapes', *Journal of reinforced plastics and composites*, vol. 19, no. 3, pp. 249-65.

Becque, J, Patnaik, AK & Rizkalla, SH 2003, 'Analytical models for concrete confined with FRP tubes', *Journal of Composites for Construction*, vol. 7, no. 1, pp. 31-8.

Beddiar, A, Zitoune, R, Collombet, F, Grunevald, YH, Abadlia, MT & Bourahla, N 2014, 'Compressive behaviour of concrete elements confined with GFRP-prefabricated bonded shells', *European Journal of Environmental and Civil Engineering*, vol. 19, no. 1, pp. 65-80.

Bhowmik, T, Tan, KH & Balendra, T 2017, 'Lateral load-displacement response of low strength CFRP-confined capsule-shaped columns', *Engineering Structures*, vol. 150, pp. 64-75.

Bossio, A, Monetta, T, Bellucci, F, Lignola, GP & Prota, A 2015, 'Modeling of concrete cracking due to corrosion process of reinforcement bars', *Cement and Concrete Research*, vol. 71, pp. 78-92.

Cao, Q, Tao, J, Wu, Z & Ma, ZJ 2017, 'Behavior of FRP-steel confined concrete tubular columns made of expansive self-consolidating concrete under axial compression', *Journal of Composites for Construction*, vol. 21, no. 5.

Cardoso, DC, Harries, KA & Batista, EdM 2014a, 'Compressive strength equation for GFRP square tube columns', *Composites Part B: Engineering*, vol. 59, pp. 1-11.

Cardoso, DC, Harries, KA & Batista, EdM 2014b, 'Closed-form equations for compressive local buckling of pultruded thin-walled sections', *Thin-Walled Structures*, vol. 79, pp. 16-22.

Carrion, JE, Hjelmstad, KD & LaFave, JM 2005, 'Finite element study of composite cuff connections for pultruded box sections', *Composite Structures*, vol. 70, no. 2, pp. 153-69.

Chang, W-S 2015, 'Repair and reinforcement of timber columns and shear walls–A review', *Construction and Building Materials*, vol. 97, pp. 14-24.

Chitawadagi, MV, Narasimhan, MC & Kulkarni, S 2010, 'Axial capacity of rectangular concrete-filled steel tube columns–DOE approach', *Construction and Building Materials*, vol. 24, no. 4, pp. 585-95.

Correia, M, Nunes, F, Correia, J & Silvestre, N 2012, 'Buckling behavior and failure of hybrid fiber-reinforced polymer pultruded short columns', *Journal of Composites for Construction*, vol. 17, no. 4, pp. 463-75.

D695, A 2010, *Standard Test Method for Compressive Properties of Rigid Plastics*, United States.

Daniel, IM & Ishai, O 2006, *Engineering mechanics of composite materials*, 2nd ed. edn, Oxford University Press, New York.

Deng, J, Zheng, Y, Wang, Y, Liu, T & Li, H 2017, 'Study on axial compressive capacity of frp-confined concrete-filled steel tubes and its comparisons with other composite structural systems', *International Journal of Polymer Science*, vol. 2017.

Deskovic, N, Triantafillou, TC & Meier, U 1995, 'Innovative design of FRP combined with concrete: short-term behavior', *Journal of Structural Engineering*, vol. 121, no. 7, pp. 1069-78.

Ellobody, E, Young, B & Lam, D 2006, 'Behaviour of normal and high strength concrete-filled compact steel tube circular stub columns', *Journal of Constructional Steel Research*, vol. 62, no. 7, pp. 706-15.

Fam, A & Rizkalla, SH 2001, 'Behavior of axially loaded concrete-filled circular FRP tubes', *ACI Structural Journal*, vol. 98, no. 3, pp. 280-9.

Fam, A, Flisak, B & Rizkalla, S 2003, 'Experimental and analytical modeling of concrete-filled FRP tubes subjected to combined bending and axial loads', *ACI Struct. J*, vol. 100, no. 4, pp. 499-509.

Fam, A, Schnerch, D & Rizkalla, S 2005, 'Rectangular filament-wound glass fiber reinforced polymer tubes filled with concrete under flexural and axial loading: experimental investigation', *Journal of Composites for Construction*, vol. 9, no. 1, pp. 25-33.

Fam, AZ & Rizkalla, SH 2000, 'Concrete-filled FRP tubes for flexural and axial compression members', *Proceedings of ACMBS-3, Ottawa, Canada*, pp. 315-22.

Fanggi, BL & Ozbakkaloglu, T 2015, 'Behavior of hollow and concrete-filled FRP-HSC and FRP-HSC-steel composite columns subjected to concentric compression', *Advances in Structural Engineering*, vol. 18, no. 5, pp. 715-38.

Ferdous, W, Manalo, A & Aravinthan, T 2017, 'Bond behaviour of composite sandwich panel and epoxy polymer matrix: Taguchi design of experiments and theoretical predictions', *Construction and Building Materials*, vol. 145, pp. 76-87.

Fitzwilliam, J & Bisby, LA 2010, 'Slenderness effects on circular CFRP confined reinforced concrete columns', *Journal of Composites for Construction*, vol. 14, no. 3, pp. 280-8.

Friberg, E & Olsson, J 2014, *Application of fibre reinforced polymer materials in road bridges–General requirements and design considerations*, Gothenburg: Chalmers University of Technology, Department of Civil and ….

Gand, AK, Chan, T-M & Mottram, JT 2013, 'Civil and structural engineering applications, recent trends, research and developments on pultruded fiber reinforced polymer closed sections: a review', *Frontiers of Structural and Civil Engineering*, vol. 7, no. 3, pp. 227-44.

Gangarao, HV & Blandford, MM 2014, 'Critical buckling strength prediction of pultruded glass fiber reinforced polymeric composite columns', *Journal of Composite Materials*, vol. 48, no. 29, pp. 3685-702.

Gao, C, Huang, L, Yan, L, Ma, G & Xu, L 2015, 'Compressive behavior of CFFT with inner steel wire mesh', *Composite Structures*, vol. 133, pp. 322-30.

Godat, A, Légeron, F, Gagné, V & Marmion, B 2013, 'Use of FRP pultruded members for electricity transmission towers', *Composite Structures*, vol. 105, pp. 408-21.

Guades, E, Aravinthan, T & Islam, MM 2014, 'Characterisation of the mechanical properties of pultruded fibre-reinforced polymer tube', *Materials & Design*, vol. 63, pp. 305-15.

Hadi, MN, Pham, TM & Lei, X 2012, 'New method of strengthening reinforced concrete square columns by circularizing and wrapping with fiber-reinforced polymer or steel straps', *Journal of Composites for Construction*, vol. 17, no. 2, pp. 229-38.

Haghinejada, A & Nematzadeh, M 2016, 'Three-Dimensional Finite Element Analysis of Compressive Behavior of Circular Steel Tube-Confined Concrete Stub Columns by New Confinement Relationships', *Latin American Journal of Solids and Structures*, vol. 13, no. 5, pp. 916-44.

Han, H, Taheri, F & Pegg, N 2011, 'Crushing behaviors and energy absorption efficiency of hybrid pultruded and ±45° braided tubes', *Mechanics of Advanced Materials and Structures*, vol. 18, no. 4, pp. 287-300.

Hansen, LZ & Nielsen, MP 2005, 'Stability of masonry columns'.

Hansson, C, Poursaee, A & Jaffer, S 2007, 'Corrosion of reinforcing bars in concrete', *R&D Serial*, no. 3013.

Hany, NF, Hantouche, EG & Harajli, MH 2016, 'Finite element modeling of FRP-confined concrete using modified concrete damaged plasticity', *Engineering Structures*, vol. 125, pp. 1-14.

Hashem, ZA & Yuan, RL 2001, 'Short vs. long column behavior of pultruded glass-fiber reinforced polymer composites', *Construction and Building Materials*, vol. 15, no. 8, pp. 369-78.

Hassan, NK & Mosallam, AS 2004, 'Buckling and ultimate failure of thin-walled pultruded composite columns', *Polymers and Polymer Composites*, vol. 12, no. 6, pp. 469-81.

Hollaway, L 2010, 'A review of the present and future utilisation of FRP composites in the civil infrastructure with reference to their important in-service properties', *Construction and Building Materials*, vol. 24, no. 12, pp. 2419-45.

Hong, W-K & Kim, H-C 2004, 'Behavior of concrete columns confined by carbon composite tubes', *Canadian Journal of Civil Engineering*, vol. 31, no. 2, pp. 178-88.

Hu, H-T, Huang, C-S, Wu, M-H & Wu, Y-M 2003, 'Nonlinear Analysis of Axially Loaded Concrete-Filled Tube Columns with Confinement Effect', *Journal of Structural Engineering*, vol. 129, no. 10, pp. 1322-9.

Hu, YM, Yu, T & Teng, JG 2011, 'FRP-confined circular concrete-filled thin steel tubes under axial compression', *Journal of Composites for Construction*, vol. 15, no. 5, pp. 850-60.

ISO-527-4 1997, *Plastics-Determination of tensile properties*, Part4: Test conditions for isotropic and orthotropic fibre -reinforced plastic composites,European Committee for Standardization, Brussels, Belgium.

ISO-1172 1996, *Textile-glass-reinforced plastics-Prepregs,moulding compounds and laminates-Determination of the textile-glass and mineral-filler content-Calcination methods*, Geneve,Switzerland.

Jedidi, M, Benjeddou, O & Soussi, C 2015, 'Effect of Expanded Perlite Aggregate Dosage on Properties of Lightweight Concrete', *Jordan Journal of Civil Engineering*, vol. 9, no. 3, pp. 278-91.

Jiang, J-F & Wu, Y-F 2012, 'Identification of material parameters for Drucker–Prager plasticity model for FRP confined circular concrete columns', *International Journal of Solids and Structures*, vol. 49, no. 3, pp. 445-56.

Jiang, T & Teng, J 2012, 'Behavior and design of slender FRP-confined circular RC columns', *Journal of Composites for Construction*, vol. 17, no. 4, pp. 443-53.

Karakoç, MB & Demirboga, R 2010, 'HSC with expanded perlite aggregate at wet and dry curing conditions', *Journal of materials in civil engineering*, vol. 22, no. 12, pp. 1252-9.

Kim, H, Lee, KH, Lee, YH & Lee, J 2012, 'Axial behavior of concrete-filled carbon fiber-reinforced polymer composite columns', *The Structural Design of Tall and Special Buildings*, vol. 21, no. 3, pp. 178-93.

Koksal, H, Doran, B & Turgay, T 2009, 'A practical approach for modeling FRP wrapped concrete columns', *Construction and Building Materials*, vol. 23, no. 3, pp. 1429-37.

Kollár, LP 2002, 'Buckling of unidirectionally loaded composite plates with one free and one rotationally restrained unloaded edge', *Journal of Structural Engineering*, vol. 128, no. 9, pp. 1202-11.

Kollár, LP 2003, 'Local buckling of fiber reinforced plastic composite structural members with open and closed cross sections', *Journal of Structural Engineering*, vol. 129, no. 11, pp. 1503-13.

Kollár, LP & Springer, GS 2003, Mechanics of Composite Structures, Cambridge University Press, New York, UNITED STATES, <http://ebookcentral.proquest.com/lib/usq/detail.action?docID=217667>.

Lam, L & Teng, JG 2003, 'Design-oriented stress–strain model for FRP-confined concrete', *Construction and Building Materials*, vol. 17, no. 6-7, pp. 471-89.

Lanzón, M & García-Ruiz, P 2008, 'Lightweight cement mortars: Advantages and inconveniences of expanded perlite and its influence on fresh and hardened state and durability', *Construction and Building Materials*, vol. 22, no. 8, pp. 1798-806.

Lee, LS & Jain, R 2009, *The role of FRP composites in a sustainable world*, Springer, 1618-954X.

Li, F, Zhao, Q, Chen, L & Shao, G 2014, 'Experimental and theoretical research on the compression performance of CFRP sheet confined GFRP short pipe', *ScientificWorldJournal*, vol. 2014, p. 109692.

Lim, JC & Ozbakkloglu, T 2014, 'Factors influencing hoop rupture strains of FRP-confined concrete', in *Applied Mechanics and Materials*, Trans Tech Publ, pp. 949-53.

Lim, JC & Ozbakkaloglu, T 2014a, 'Stress–strain model for normal-and light-weight concretes under uniaxial and triaxial compression', *Construction and Building Materials*, vol. 71, pp. 492-509.

Lim, JC & Ozbakkaloglu, T 2014b, 'Unified stress-strain model for FRP and actively confined normal-strength and high-strength concrete', *Journal of Composites for Construction*, vol. 19, no. 4, p. 04014072.

Lim, JC & Ozbakkaloglu, T 2014c, 'Lateral strain-to-axial strain relationship of confined concrete', *Journal of Structural Engineering*, vol. 141, no. 5, p. 04014141.

Lima, MM, Doh, JH, Hadi, MN & Miller, D 2016, 'The effects of CFRP orientation on the strengthening of reinforced concrete structures', *The Structural Design of Tall and Special Buildings*, vol. 25, no. 15, pp. 759-84.

Lin, G & Teng, JG 2017, 'Three-Dimensional finite-element analysis of FRP-Confined circular concrete columns under eccentric loading', *Journal of Composites for Construction*, vol. 21, no. 4.

Liu, X, Nanni, A & Silva, PF 2005, 'Rehabilitation of compression steel members using FRP pipes filled with non-expansive and expansive light-weight concrete', *Advances in Structural Engineering*, vol. 8, no. 2, pp. 129-42.

Lokuge, W & Karunasena, W 2016, 'Ductility enhancement of geopolymer concrete columns using fibre-reinforced polymer confinement', *Journal of Composite Materials*, vol. 50, no. 14, pp. 1887-96.

Motoc, DL, Bou, SF & Gimeno, RB 2015, 'Effects of fibre orientation and content on the mechanical, dynamic mechanical and thermal expansion properties of multi-layered glass/carbon fibre-reinforced polymer composites', *Journal of Composite Materials*, vol. 49, no. 10, pp. 1211-21.

Mirmiran, A, Shahawy, M & Beitleman, T 2001, 'Slenderness limit for hybrid FRP-concrete columns', *Journal of Composites for Construction*, vol. 5, no. 1, pp. 26-34.

Mirmiran, A, Shahawy, M, Samaan, M, Echary, HE, Mastrapa, JC & Pico, O 1998, 'Effect of column parameters on FRP-confined concrete', *Journal of Composites for Construction*, vol. 2, no. 4, pp. 175-85.

Module7: Strength and Failure Theories 2014, <http://nptel.ac.in/courses/105108124/pdf/Lecture_Notes/LNm7.pdf>.

Mohamed, HM & Masmoudi, R 2010, 'Axial load capacity of concrete-filled FRP tube columns: Experimental versus theoretical predictions', *Journal of Composites for Construction*, vol. 14, no. 2, pp. 231-43.

Mortazavi, AA, Pilakoutas, K & Son, KS 2003, 'RC column strengthening by lateral pre-tensioning of FRP', *Construction and Building Materials*, vol. 17, no. 6, pp. 491-7.

'Nonlinear solver', 2008, *News.St7*, December, pp. 3-10, <http://www.strand7.com/News.St7/Issue%206/News.St7%206-2008.pdf>.

Nunes, F, Correia, JR & Silvestre, N 2016, 'Structural behaviour of hybrid FRP pultruded columns. Part 1: Experimental study', *Composite Structures*, vol. 139, pp. 291-303.

Ozbakkaloglu, T 2013, 'Compressive behavior of concrete-filled FRP tube columns: Assessment of critical column parameters', *Engineering Structures*, vol. 51, pp. 188-99.

Ozbakkaloglu, T 2015, 'A novel FRP–dual-grade concrete–steel composite column system', *Thin-Walled Structures*, vol. 96, pp. 295-306.

Ozbakkaloglu, T & Zhang, W 2012, 'Investigation of key column parameters on compressive behavior of concrete-filled FRP tubes', *Applied Mechanics and Materials*, vol. 256-259, pp. 779-83.

Ozbakkaloglu, T & Xie, T 2016, 'Geopolymer concrete-filled FRP tubes: Behavior of circular and square columns under axial compression', *Composites Part B: Engineering*, vol. 96, pp. 215-30.

Ozbakkaloglu, T, Lim, JC & Vincent, T 2013, 'FRP-confined concrete in circular sections: Review and assessment of stress–strain models', *Engineering Structures*, vol. 49, pp. 1068-88.

Ozbay, E, Oztas, A, Baykasoglu, A & Ozbebek, H 2009, 'Investigating mix proportions of high strength self compacting concrete by using Taguchi method', *Construction and Building Materials*, vol. 23, no. 2, pp. 694-702.

Pan, Y, Guo, R, Li, H, Tang, H & Huang, J 2017, 'Analysis-oriented stress–strain model for FRP-confined concrete with preload', *Composite Structures*, vol. 166, pp. 57-67.

Pantelides, CP, Yan, Z & Reaveley, LD 2004, *Shape modification of rectangular columns confined with FRP composites*.

Park, J-W, Yeom, H-J & Yoo, J-H 2013, 'Axial loading tests and FEM analysis of slender square hollow section (SHS) stub columns strengthened with carbon fiber reinforced polymers', *International Journal of Steel Structures*, vol. 13, no. 4, pp. 731-43.

Pessiki, S, Harries, KA, Kestner, JT, Sause, R & Ricles, JM 2001, 'Axial behavior of reinforced concrete columns confined with FRP jackets', *Journal of Composites for Construction*, vol. 5, no. 4, pp. 237-45.

Popovics, S 1973, 'A numerical approach to the complete stress-strain curve of concrete', *Cement and Concrete Research*, vol. 3, no. 5, pp. 583-99.

Puente, I, Insausti, A & Azkune, M 2006, 'Buckling of GFRP columns: An empirical approach to design', *Journal of Composites for Construction*, vol. 10, no. 6, pp. 529-37.

Qasrawi, Y, Heffernan, PJ & Fam, A 2015, 'Performance of concrete-filled FRP tubes under field close-in blast loading', *Journal of Composites for Construction*, vol. 19, no. 4, p. 04014067.

Qian, P, Feng, P & Ye, L 2008, 'Experimental study on GFRP pipes under axial compression', *frontiers of architecture and civil engineering in china*, vol. 2, no. 1, pp. 73-8.

Qiao, P & Shan, L 2005, 'Explicit local buckling analysis and design of fiber–reinforced plastic composite structural shapes', *Composite Structures*, vol. 70, no. 4, pp. 468-83.

Qiao, P, Davalos, JF & Wang, J 2001, 'Local buckling of composite FRP shapes by discrete plate analysis', *Journal of Structural Engineering*, vol. 127, no. 3, pp. 245-55.

Ragheb, WF 2017, 'Development of closed-form equations for estimating the elastic local buckling capacity of pultruded FRP structural shapes', *Journal of Composites for Construction*, vol. 21, no. 4, p. 04017015.

Rocca, S, Galati, N & Nanni, A 2008, 'Review of design guidelines for FRP confinement of reinforced concrete columns of noncircular cross sections', *Journal of Composites for Construction*, vol. 12, no. 1, pp. 80-92.

Rousakis, TC, Karabinis, AI, Kiousis, PD & Tepfers, R 2008, 'Analytical modelling of plastic behaviour of uniformly FRP confined concrete members', *Composites Part B: Engineering*, vol. 39, no. 7, pp. 1104-13.

Sengul, O, Azizi, S, Karaosmanoglu, F & Tasdemir, MA 2011, 'Effect of expanded perlite on the mechanical properties and thermal conductivity of lightweight concrete', *Energy and Buildings*, vol. 43, no. 2, pp. 671-6.

Sheikh, SA & Khoury, SS 1993, 'Confined concrete columns with stubs', *ACI Structural Journal*, vol. 90, pp. 414-.

Siddiqui, NA, Alsayed, SH, Al-Salloum, YA, Iqbal, RA & Abbas, H 2014, 'Experimental investigation of slender circular RC columns strengthened with FRP composites', *Construction and Building Materials*, vol. 69, pp. 323-34.

Strand7 Pty Ltd *ST7-1.57.10.3 Nonlinear elastic material*, Strand7 Pty Ltd, <http://www.strand7.com/webnotes/search/?q=st7-1.57.10.3&all=>.

Talaeitaba, SB, Halabian, M & Ebrahim Torki, M 2015, 'Nonlinear behavior of FRP-reinforced concrete-filled double-skin tubular columns using finite element analysis', *Thin-Walled Structures*, vol. 95, pp. 389-407.

Teng, J & Lam, L 2004, 'Behavior and modeling of fiber reinforced polymer-confined concrete', *Journal of Structural Engineering*, vol. 130, no. 11, pp. 1713-23.

Teng, J & Hu, Y 2007, 'Behaviour of FRP-jacketed circular steel tubes and cylindrical shells under axial compression', *Construction and Building Materials*, vol. 21, no. 4, pp. 827-38.

Teng, J, Yu, T, Wong, YL & Dong, SL 2007, 'Hybrid FRP–concrete–steel tubular columns: Concept and behavior', *Construction and Building Materials*, vol. 21, no. 4, pp. 846-54.

Teng, J, Huang, Y, Lam, L & Ye, L 2007, 'Theoretical model for fiber-reinforced polymer-confined concrete', *Journal of Composites for Construction*, vol. 11, no. 2, pp. 201-10.

Teng, J, Jiang, T, Lam, L & Luo, Y 2009, 'Refinement of a design-oriented stress–strain model for FRP-confined concrete', *Journal of Composites for Construction*, vol. 13, no. 4, pp. 269-78.

Teng, J, Xiao, Q, Yu, T & Lam, L 2015, 'Three-dimensional finite element analysis of reinforced concrete columns with FRP and/or steel confinement', *Engineering Structures*, vol. 97, pp. 15-28.

Topçu, İB & Işıkdağ, B 2008, 'Effect of expanded perlite aggregate on the properties of lightweight concrete', *Journal of materials processing technology*, vol. 204, no. 1, pp. 34-8.

Türkmen, İ & Kantarcı, A 2007, 'Effects of expanded perlite aggregate and different curing conditions on the physical and mechanical properties of self-compacting concrete', *Building and Environment*, vol. 42, no. 6, pp. 2378-83.

Türkmen, İ, Gül, R & Çelik, C 2008, 'A Taguchi approach for investigation of some physical properties of concrete produced from mineral admixtures', *Building and Environment*, vol. 43, no. 6, pp. 1127-37.

Vincent, T & Ozbakkaloglu, T 2013a, 'Influence of fiber orientation and specimen end condition on axial compressive behavior of FRP-confined concrete', *Construction and Building Materials*, vol. 47, pp. 814-26.

Vincent, T & Ozbakkaloglu, T 2013b, 'Influence of concrete strength and confinement method on axial compressive behavior of FRP confined high- and ultra high-strength concrete', *Composites Part B: Engineering*, vol. 50, pp. 413-28.

Vincent, T & Ozbakkaloglu, T 2015a, 'Compressive behavior of prestressed high-strength concrete-filled aramid FRP tube columns: experimental observations', *Journal of Composites for Construction*, vol. 19, no. 6, p. 04015003.

Vincent, T & Ozbakkaloglu, T 2015b, 'Influence of slenderness on stress-strain behavior of concrete-filled FRP tubes: experimental study', *Journal of Composites for Construction*, vol. 19, no. 1, p. 04014029.

Wang, J, Feng, P, Hao, T & Yue, Q 2017, 'Axial compressive behavior of seawater coral aggregate concrete-filled FRP tubes', *Construction and Building Materials*, vol. 147, pp. 272-85.

Wang, L, Liu, W, Fang, Y, Wan, L & Huo, R 2016, 'Axial crush behavior and energy absorption capability of foam-filled GFRP tubes manufactured through vacuum assisted resin infusion process', *Thin-Walled Structures*, vol. 98, pp. 263-73.

Wang, W, Sheikh, MN, Hadi, MNS, Gao, D & Chen, G 2017, 'Behaviour of concrete-encased concrete-filled FRP tube (CCFT) columns under axial compression', *Engineering Structures*, vol. 147, pp. 256-68.

Wang, Y, Feng, J, Wu, J & Hu, D 2016, 'Effects of fiber orientation and wall thickness on energy absorption characteristics of carbon-reinforced composite tubes under different loading conditions', *Composite Structures*, vol. 153, pp. 356-68.

Xie, T & Ozbakkaloglu, T 2015, 'Behavior of steel fiber-reinforced high-strength concrete-filled FRP tube columns under axial compression', *Engineering Structures*, vol. 90, pp. 158-71.

Xie, T & Ozbakkaloglu, T 2016, 'Behavior of recycled aggregate concrete-filled basalt and carbon FRP tubes', *Construction and Building Materials*, vol. 105, pp. 132-43.

Xue, B & Gong, J 2016, 'Study on steel reinforced concrete-filled GFRP tubular column under compression', *Thin-Walled Structures*, vol. 106, pp. 1-8.

Yan, Z, Pantelides, CP & Reaveley, LD 2007, 'Posttensioned FRP composite shells for concrete confinement', *Journal of Composites for Construction*, vol. 11, no. 1, pp. 81-90.

Youssf, O, Hassanli, R & Mills, JE 2017, 'Retrofitting square columns using FRP-confined crumb rubber concrete to improve confinement efficiency', *Construction and Building Materials*, vol. 153, pp. 146-56.

Youssf, O, ElGawady, MA, Mills, JE & Ma, X 2014, 'Finite element modelling and dilation of FRP-confined concrete columns', *Engineering Structures*, vol. 79, pp. 70-85.

Yu, T & Teng, JG 2011, 'Design of Concrete-Filled FRP Tubular Columns: Provisions in the Chinese Technical Code for Infrastructure Application of FRP Composites', *Journal of Composites for Construction*, vol. 15, no. 3, pp. 451-61.

Yu, T & Teng, J 2012, 'Behavior of hybrid FRP-concrete-steel double-skin tubular columns with a square outer tube and a circular inner tube subjected to axial compression', *Journal of Composites for Construction*, vol. 17, no. 2, pp. 271-9.

Yu, T, Teng, J & Wong, Y 2009, 'Stress-strain behavior of concrete in hybrid FRP-concrete-steel double-skin tubular columns', *Journal of Structural Engineering*, vol. 136, no. 4, pp. 379-89.

Yu, T, Fang, X & Teng, J-G 2013, 'FRP-confined self-compacting concrete under axial compression', *Journal of materials in civil engineering*, vol. 26, no. 11, p. 04014082.

Yu, T, Teng, J, Wong, Y & Dong, S 2010, 'Finite element modeling of confined concrete-II: Plastic-damage model', *Engineering Structures*, vol. 32, no. 3, pp. 680-91.

Zeng, JJ, Guo, YC, Gao, WY, Li, JZ & Xie, JH 2017, 'Behavior of partially and fully FRP-confined circularized square columns under axial compression', *Construction and Building Materials*, vol. 152, pp. 319-32.

Zhang, B, Teng, JG & Yu, T 2015, 'Experimental behavior of hybrid FRP–concrete–steel double-skin tubular columns under combined axial compression and cyclic lateral loading', *Engineering Structures*, vol. 99, pp. 214-31.

Zhang, B, Teng, J & Yu, T 2017, 'Compressive behavior of double-skin tubular columns with high-strength concrete and a filament-wound FRP tube', *Journal of Composites for Construction*, vol. 21, no. 5, p. 04017029.

Zhang, S, Caprani, C & Heidarpour, A 2018, 'Influence of fibre orientation on pultruded GFRP material properties', *Composite Structures*, vol. 204, pp. 368-77.

Zhang, Y, Feng, P, Bai, Y & Ye, L 2012, 'Morter- filled FRP tubes strengthening axially compresses steel members', in *6th International Conference on FRP Composites in Civil Engineering*: *Proceedings of the 6th International Conference on FRP Composites in Civil Engineering* Rome; Italy, pp. 1-6.

Zhao, J, Yu, T & Teng, J 2014, 'Stress-strain behavior of FRP-confined recycled aggregate concrete', *Journal of Composites for Construction*, vol. 19, no. 3, p. 04014054.

Zhou, Y, Liu, X, Xing, F, Cui, H & Sui, L 2016, 'Axial compressive behavior of FRP-confined lightweight aggregate concrete: An experimental study and stress-strain relation model', *Construction and Building Materials*, vol. 119, pp. 1-15.

Zhou, Y, Liu, X, Xing, F, Li, D, Wang, Y & Sui, L 2017, 'Behavior and modeling of FRP-concrete-steel double-skin tubular columns made of full lightweight aggregate concrete', *Construction and Building Materials*, vol. 139, pp. 52-63.

Zhu, L, Ma, L, Bai, Y, Li, S, Song, Q, Wei, Y, Zhang, L, Zhang, Z & Sha, X 2016, 'Large diameter concrete-filled high strength steel tubular stub columns under compression', *Thin-Walled Structures*, vol. 108, pp. 12-9.

Zureick, A & Scott, D 1997, 'Short-term behavior and design of fiber-reinforced polymeric slender members under axial compression', *Journal of Composites for Construction*, vol. 1, no. 4, pp. 140-9.

Appendix A: Conference Presentations

A.1 Conference Paper I:
Investigation on filled pultruded FRP tubes for civil infrastructure.

Al-saadi, A.U., Aravinthan, T., Lokuge, W. (2018). Investigation on filled pultruded FRP tubes for civil infrastructure. *Proceeding of the 11th Asian- Australasian Conference on Composite Materials. 29th July- 1st August, Cairns, Australia.*

Abstract. The main reason for the limited use of pultruded fibre reinforced polymer (PFRP) profiles in column applications in the construction industry is the buckling failure and the rapid drop in the load carrying capacity after reaching the peak value. One way to overcome this shortage is using concrete as a filler material to increase the stiffness and the strength of a given FRP column and to enhance the buckling resistance.

The aim of this study is to investigate how the concrete infill can improve the load carrying capacity and modify the failure mode of the pultruded FRP tube columns to ensure their safe and effective use. Different sections of PFRP tube sections were filled using normal and lightweight concrete. The results of square and circular PFRP tube show that the load carrying capacity is increased due to filling with concrete when the hoop stiffness of the PFRP tube is adequate. All the filled columns failed in a more ductile manner compared with the hollow PFRP sections. The findings would make a contribution to the field of PFRP-concrete column applications in the civil engineering as it provides an approach to enhance the axial behaviour of the PFRP columns.

A.2   Conference Paper II:

Influence of concrete modulus on the axial behaviour of pultruded fibre reinforced polymer tube columns.

Abstract. The use of hollow Pultruded Fibre Reinforced Polymer (PFRP) tubes in column applications is limited due to the instability conditions related to buckling. The low axial stiffness and slenderness ratio are the main parameters that govern their axial compressive behaviour. Filling PFRP tubes with concrete results in an enhancement in the axial stiffness while providing a support to the walls of the PFRP tube against buckling.

In this research, the modulus of elasticity of concrete and fibre orientation of PFRP are selected as experimental variables to be investigated. In order to cover a range of concrete modulus between 5 and 30 GPa, two types of both normal and lightweight perlite concrete are selected. The height of the columns is selected to ensure a slenderness ratio (length/lateral dimension) of 5. The experimental results show that the load carrying capacity of filled PFRP tubes is improved when the concrete modulus increases. A change in the modes of failure is also observed due to the concrete filler; end crushing and longitudinal corner splitting instead of local buckling for square hollow PFRP columns. It is concluded that the axial behaviour is substantially improved by having a composite hybrid profile with appropriate concrete filled PFRP in columns. Such enhancement would pave the way for the use of innovative structural profile in civil infrastructure.

A.3 Conference Paper III:
Numerical investigation on hollow pultruded fibre reinforced polymer tube columns.

Abstract. As the axial behaviour of hollow pultruded fibre reinforced polymer (PFRP) profiles is governed by the instability conditions due to the local and global buckling, the determination of the safe load carrying capacity of FRP columns is vital. The compressive performance of PFRP tube depends on many factors such as fibre type, fibre content, and orientation of fibre layers, cross-section, thickness and height of the column member.

In this study, concentric compressive testing was conducted using PFRP short columns. Based on the fibre orientation and thickness, the samples were divided into two groups of tubes in a square shape and two groups in a circular shape. The height of columns is designed to keep the slenderness ratio (length/lateral dimension) of 5. The axial behaviour of FRP columns was simulated using STRAND7 finite element software package. The laminate method was followed to define the mechanical properties of the FRP material. Failure was investigated by using the Tsai-Wu failure criterion.

The experimental results show that the failure mode of the hollow square tube was either local buckling or corner splitting at the mid-height followed by buckling. Although both types of circular tubes failed in a similar way by crushing one end with high noise, followed by separation of the crushed end into strips, the stiffness and the load capacity of PFRP column was higher for the profiles with fibres oriented close to the axial direction. The numerical results are in close agreement with the peak value of the experimental results. This can be extended to study the effects of all factors that influence the axial behaviour of PFRP columns numerically.

Appendix B: Pilot Study of Concrete Infill

Different concrete mixes were conducted as a first step for identifying properties of concrete filler material, which are meet the main objective of this research. Concrete cylinders of four types of normal concrete were prepared and tested based on the AS 10212.9 (2014) standard in addition to three mixes of perlite concrete with varied content of perlite aggregate. The trial mixes of normal concrete were prepared using low, medium and high premix concrete while three percentages of perlite content were followed in preparing mixes of perlite concrete. The concrete modulus was calculated based on the AS 1012.17-1997 standard by using the compressometer to measure the longitudinal strain of cylinder. The summary of the test results can be shown in Tables B.1 to Tables B. 7.

Table B.1 Results of compressive test of the normal concrete (P-N1)

Specimen No.	f_c' (MPa)	Modulus (GPa)	Unit weight (kg/m^3)
1	27.0	-	2175
2	24.6	-	2160
3	26.9	31.2	2182
4	26.0	28.4	2168
Average	26.1	29.8	2171
SD	1.10	1.98	9.52

Table B.2 Results of compressive test of the normal concrete (P-N2)

Specimen No.	f_c' (MPa)	Modulus (GPa)	Unit weight (kg/m^3)
1	11.3	-	2140
2	11.7	-	2148
3	9.4	19.50	2150
4	12.8	19.40	2141
Average	11.3	19.45	2145
SD	1.40	0.07	4.79

Table B.3 Results of compressive test of the normal concrete (P-N3)

Specimen No.	f_c' (MPa)	Modulus (GPa)	Unit weight (kg/m³)
1	24.3	-	2215
2	22.9	-	2194
3	23.6	24.3	2233
4	22.7	24.3	2199
Average	23.4	24.3	2210
SD	0.73	0.00	17.4

Table B.4 Results of compressive test of the normal concrete (P-N4)

Specimen No.	f_c' (MPa)	Modulus (GPa)	Unit weight (kg/m³)
1	50.5	-	2247
2	55.9	-	2271
3	51.1	32.4	2248
4	54.0	32.5	2255
Average	52.9	32.55	2256
SD	2.52	0.07	11.2

Table B.5 Results of compressive test of the perlite concrete (P-P1)

Specimen No.	f_c' (MPa)	Modulus (GPa)	Unit weight (kg/m³)
1	12.6	-	1659
2	13.7	-	1674
3	10.4	13.00	1659
4	10.2	12.90	1670
Average	11.8	12.95	1666
SD	1.71	0.07	8.05

Table B.6 Results of compressive test of the perlite concrete (P-P2)

Specimen No.	f_c' (MPa)	Modulus (GPa)	Unit weight (kg/m^3)
1	5.2	-	1483
2	5.9	-	1465
3	7.0	10.7	1495
4	5.9	9.1	1466
Average	6.0	9.9	1477
SD	0.75	1.13	14.7

Table B.7 Results of compressive test of the perlite concrete (P-P3)

Specimen No.	f_c' (MPa)	Modulus (GPa)	Unit weight (kg/m^3)
1	2.4	-	1250
2	2.5	-	1212
3	2.1	4.7	1219
4	2.5	4.3	1206
Average	2.4	4.5	1222
SD	0.17	0.28	19.5

Appendix C: Results of the Material Tests

The results of the entire material tests of pultruded fibre reinforced polymer tubes and concrete infill materials, which were discussed in Chapter 3, are presented here. The equations used in determining in calculation the specific mass, glass fibre content, peak stress, elastic modulus are presented in this appendix.

C.1 Burnout test

The dimensions of the coupon specimens and results of the burnout test according to ISO 1172 (1996) standard can be seen in Tables C.1 to C.4. Equations C.1 and C.2 were used to calculate the specific mass ρ and fibre content M_f respectively.

$$\rho = \frac{m_0}{V_S} \qquad \text{C.1}$$
$$M_f = (m_3 - m_1)/(m_2 - m_1) \qquad \text{C.2}$$

Where m_0 and V_S are the dry weight and volume of the coupon specimen, m_1 is the initial mass of the dry crucible, m_2 is the initial mass of the dry crucible plus dried coupon specimens and m_3 is the final mass of the crucible plus residue after calcination.

Table C.1 Results of burnout test of pultruded FRP square tube S1

Specimen No.	Width (mm)	Length (mm)	Thickness (mm)	Specific mass (g/cm^3)	Fibre content (%)
1	29.81	19.92	5.32	1.992	79.51
2	29.75	19.56	5.15	1.935	77.70
3	29.74	19.53	5.19	1.902	74.77
Average				1.943	77.32
SD				0.045	2.394

Table C.2 Results of burnout test of pultruded FRP square tube S2

Specimen No.	Width (mm)	Length (mm)	Thickness (mm)	Specific mass (g/cm³)	Fibre content (%)
1	30.25	20.06	6.46	2.001	72.15
2	29.70	19.57	6.49	2.017	72.20
3	29.67	19.69	6.37	2.004	72.23
Average				2.007	72.20
SD				0.009	0.042

Table C.3 Results of burnout test of pultruded FRP circular tube C1

Specimen No.	Width (mm)	Length (mm)	Thickness (mm)	Specific mass (g/cm³)	Fibre content (%)
1	29.82	20.04	5.95	2.091	80.08
2	29.68	19.97	5.80	2.015	78.57
3	29.72	20.34	5.98	2.069	79.82
Average				2.058	79.49
SD				0.039	0.806

Table C.4 Results of burnout test of pultruded FRP circular tube C2

Specimen No.	Width (mm)	Length (mm)	Thickness (mm)	Specific mass (g/cm³)	Fibre content (%)
1	29.56	20.39	5.99	2.056	77.90
2	29.61	19.64	6.04	2.118	78.19
3	29.74	19.70	6.02	2.072	78.84
Average				2.082	78.31
SD				0.032	0.482

The calculation of the fibre volume fraction using the results of the burnout test (fibre weight fraction was done based of the following equations:

$$F_V^f = \frac{F_W^f}{F_W^f + (1 - F_W^f)\frac{\rho_f}{\rho_m}} \qquad \text{C.3}$$

Where F_V^f and F_W^f are the volume and weight fibre fraction ratios respectively while ρ_f and ρ_m are the density of the fibre and matrix respectively.

216

C.2   Tensile test

The tensile test of coupon specimens of all pultruded FRP tubes was carried out based on the ISO 527-4 (1997). Tables C.5 to C.8 present results of the coupon specimens. The equations that were used to calculate the tensile stress σ_t, elastic modulus E_t and Poisson's ratio v are:

$$\sigma_t = \frac{F}{A} \qquad\qquad \text{C.4}$$
$$E_t = (\Delta\sigma)/(\Delta\varepsilon) \qquad\qquad \text{C.5}$$
$$v = \frac{\varepsilon_t}{\varepsilon_l} \qquad\qquad \text{C.6}$$

Where F and A are the measured force and cross-sectional area of the specimens respectively. $\Delta\sigma$ and $\Delta\varepsilon$ are the stress and strain variations of the linear part of stress-strain curve respectively. ε_t is the transverse strain value while ε_l is the longitudinal strain value.

Table C.5 Results of tensile test of pultruded FRP square tube S1

Specimen No.	Peak stress (MPa)	Modulus (GPa)	Poisson's ratio	Strain at peak (micro)
1	917.92	43.200	-	23236.9
2	969.16	42.000	-	23757.8
3	966.26	-	0.332	-
4	933.75	-	0.326	-
5	976.79	-	0.305	-
Average	952.78	42.600	0.321	23497.4
SD	25.514	0.849	0.023	368.3

Table C.6 Results of tensile test of pultruded FRP square tube S2

Specimen No.	Peak stress (MPa)	Modulus (GPa)	Poisson ratio	Strain at peak (micro)
1	554.19	-	0.194	-
2	522.17	35.600	-	14481.6
3	553.07	-	0.229	-
4	498.93	36.500	-	13811.3
5	472.97	-	0.265	-
Average	520.27	36.050	0.229	14146.4
SD	35.081	0.636	0.035	474.0

Table C.7 Results of tensile test of pultruded FRP circular tube C1

Specimen No.	Peak stress (MPa)	Modulus (GPa)	Poisson ratio	Strain at peak (micro)
1	511.76	37.900	-	13169.4
2	470.38	-	0.329	-
3	441.88	-	0.364	-
4	438.99	-	-	-
5	493.04	42.900	-	10604.1
Average	471.21	40.400	0.347	11886.7
SD	31.700	3.536	0.025	1813.9

Table C.8 Results of tensile test of pultruded FRP circular tube C2

Specimen No.	Peak stress (MPa)	Modulus (GPa)	Poisson ratio	Strain at peak (micro)
1	479.84	28.200	-	17178.1
2	461.45	-	0.221	-
3	406.93	25.300	-	15420.0
4	378.03	-	0.241	-
5	373.20	-	0.234	-
Average	419.89	26.750	0.232	16299.1
SD	48.529	2.051	0.010	1243.2

C.3 Compressive test

The compressive test of coupon specimens of all pultruded FRP tubes was carried out based on the ASTM D 695 (2010). Tables C.9 to C.12 present results of the coupon specimens. The equations that were used to calculate the compressive stress σ_c and elastic modulus E_c are:

$$\sigma_c = \frac{F_c}{A} \qquad\qquad\qquad C.7$$
$$E_c = (\Delta\sigma)/(\Delta\varepsilon) \qquad\qquad\qquad C.8$$

Where F_c and A are the measured compressive force and cross-sectional area of the specimens respectively. $\Delta\sigma$ and $\Delta\varepsilon$ are the stress and strain variations of the linear part of stress-strain curve respectively.

Table C.9 Results of compressive test of pultruded FRP square tube S1

Specimen No.	Peak stress (MPa)	Modulus (GPa)	Strain at peak (micro)
1	537.65	49.500	12149.8
2	522.16	-	-
3	516.18	-	-
4	521.18	-	-
5	531.40	-	-
Average	525.71	49.500	12149.8
SD	8.643	-	-

Table C.10 Results of compressive test of pultruded FRP square tube S2

Specimen No.	Peak stress (MPa)	Modulus (GPa)	Strain at peak (micro)
1	445.99	45.800	11987.9
2	492.71	41.500	10937.0
3	493.06	-	-
4	550.03	-	-
5	549.25	-	-
Average	506.21	43.650	11462.4
SD	44.028	3.040	743.1

Table C.11 Results of compressive test of pultruded FRP circular tube C1

Specimen No.	Peak stress (MPa)	Modulus (GPa)	Strain at peak (micro)
1	329.71	46.100	6461.4
2	433.77	52.600	8095.6
3	345.90	-	-
4	340.19	-	-
5	378.29	-	-
Average	365.57	49.350	7278.5
SD	42.220	4.596	1155.5

Table C.12 Results of compressive test of pultruded FRP circular tube C2

Specimen No.	Peak stress (MPa)	Modulus (GPa)	Strain at peak (micro)
1	489.14	32.400	15674.1
2	351.70	35.400	11289.2
3	426.02	-	-
4	389.76	-	-
5	381.70	-	-
Average	407.66	33.900	13481.7
SD	52.684	2.121	3100.6

C.4 Shear test

The shear test of coupon specimens of all pultruded FRP tubes was carried out based on the ASTM D5379/D5379M (2012). Tables C.13 and C.14 present results of the coupon specimens. The equations that were used to calculate the shear strain γ_{sh}, shear stress τ_{sh} and elastic modulus G_{sh} are:

$$\gamma_{sh} = |\varepsilon_{+45}| + |\varepsilon_{-45}| \qquad\qquad \text{C.9}$$

$$\tau_{sh} = \frac{F_{sh}}{A_{sh}} \qquad\qquad \text{C.10}$$

$$G_{sh} = \Delta\tau / \Delta\gamma_{sh} \qquad\qquad \text{C.11}$$

Where ε_{+45} and ε_{-45} are the shear strain from the strain gauges at +45 and -45. F_{sh} and A_{sh} are the applied force and cross-sectional area between the notches of the specimens respectively. $\Delta\tau$ and $\Delta\gamma$ are the difference in applied shear stress between the two strain points and $\Delta\gamma_{sh}$ the difference between the two strain points (normally 0.004) respectively. The typical load-displacement of shear specimens are displayed in Figures C.1 and C.2.

Table C.13 Results of shear test of pultruded FRP square tube S1

Specimen No.	Width (mm)	Thickness (mm)	Load (N)	Peak stress (MPa)	Modulus (GPa)
1	10.37	5.23	5885.91	108.53	3.757
2	10.77	5.17	5448.45	97.85	-
3	10.42	5.10	5013.00	94.33	-
4	10.43	5.10	5569.00	104.69	-
5	10.35	5.12	5273.00	99.51	-
Average				101.0	3.757
SD				5.632	-

Table C.14 Results of shear test of pultruded FRP square tube S2

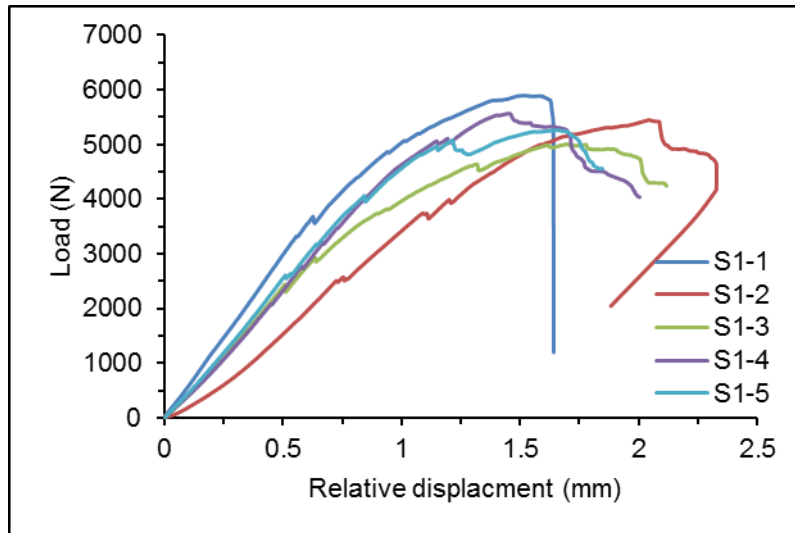| Specimen No.	Width (mm)	Thickness (mm)	Load (N)	Peak stress (MPa)	Modulus (GPa)
1	10.78	6.31	4656.43	68.45	6.405
2	10.50	6.33	4959.62	74.62	6.980
3	10.57	6.24	4915.00	74.52	-
4	10.53	6.24	4572.00	69.58	-
5	10.51	6.23	4194.00	64.05	-
Average				70.25	6.690
SD				4.455	0.407

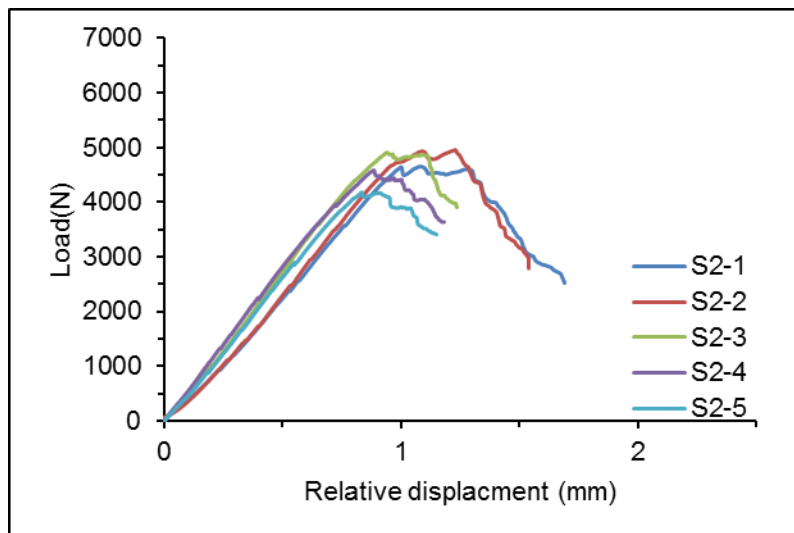Figure C.1 Load-displacement curves of shear specimens of square tube S1

Figure C.2 Load-displacement curves of shear specimens of square tube S2

C.5 Compressive strength test of concrete

The compressive strength of the different types of the concrete infill was determined based on the AS 10212.9 (2014) standard. The measured data on the axial load was used to calculate the concrete strength, which it was adopted in addition to the axial and transverse strain values in calculating the concrete modulus and Poisson's ratio. Tables C.15 to C.18 show the summary of test results of concrete cylinders.

Table C.15 Results of compressive test of the perlite concrete (P1)

Specimen No.	$f_c^`$ (MPa)	Modulus (GPa)	Poisson's ratio	Unit weight (kg/m^3)
1	4.06	4.8	0.22	1272
2	4.54	5.1	0.11	1263
3	4.81	-	-	1315
4	4.35	-	-	1251
5	4.73	-	-	1253
Average	4.50	4.9	0.17	1271
SD	0.30	0.20	0.08	26.2

Table C.16 Results of compressive test of the perlite concrete (P2)

Specimen No.	$f_c^`$ (MPa)	Modulus (GPa)	Poisson's ratio	Unit weight (kg/m^3)
1	11.4	7.7	0.26	1786
2	11.5	-	-	1759
3	9.2	5.7	0.10	1759
4	10.0	-	-	1737
5	10.0	-	-	1761
Average	10.4	6.7	0.18	1760
SD	1.0	1.4	0.10	17.3

Table C.17 Results of compressive test of the normal concrete (N1)

Specimen No.	$f_c^`$ (MPa)	Modulus (GPa)	Poisson's ratio	Unit weight (kg/m^3)
1	11.3	-	-	2103
2	10.6	-	-	2128
3	12.0	17.5	0.25	2143
4	10.9	-	-	2108
5	11.2	-	-	2112
6	11.0	16.5	0.21	2109
Average	11.2	17.0	0.23	2117
SD	0.5	0.7	0.03	15.4

Table C.18 Results of compressive test of the normal concrete (N2)

Specimen No.	$f_c^`$ (MPa)	Modulus (GPa)	Poisson's ratio	Unit weight (kg/m^3)
1	-	-	-	2156
2	30.1	-	-	2194
3	30.3	29.2	0.24	2162
4	35.9	31.6	0.18	2167
5	35.0	-	-	2165
Average	33.0	30.4	0.21	2169
SD	3.06	1.7	0.04	14.7